Integration of *In Silico* and *In Vitro* ADMET Properties in Lead Identification and Optimization of Compounds for the Treatment of Parasitic Diseases

Roslyn Thelingwani

Thesis Presented for the degree of

DOCTOR OF PHILOSOPHY

in the Department of Chemistry

University of Cape Town
August 2012

Supervisors

Professor Kelly Chibale

Department of Chemistry, University of Cape Town

Professor Collen Masimirembwa

Department of DMPK & BAC, African Institute of Biomedical Science and Technology, Harare

Department of Clinical Pharmacology, University of Cape Town

Professor Peter Smith

Department of Clinical Pharmacology, University of Cape Town

TABLE OF CONTENTS

ACKNOWLEDGEMENTS

Kelly Chibale who gave me the opportunity to work in his group and for his supervision. Your patience is also greatly appreciated.

Collen Masimirembwa, you have been a great source of inspiration. Thank you for taking care of all the chemistry in my life!

Peter Smith, thank you for the guidance and the training.

My colleagues at AiBST and Cape Town, you made this journey easier. Thank you for the advice, constructive criticism in lab meetings and the help with experiments.

My son Tafadzwa, you may be too young to understand this now but you gave mummy a new sense of purpose.

Cecil you have been awesome. God bless you my brother for taking care of the scientist's crazy needs. You are the only one who could wait for me till midnight to finish an experiment!

My family for the love and encouragement. You have also been a source of pressure tjo! like my grandmother would proudly introduce me to her friends as Dr Thelingwani. What choice did I have other than finishing this!

To everyone I have worked and collaborated with thank you very much.

ABSTRACT

Introduction

Parasitic infections are the major causes of illness and death in tropical regions especially in Africa. The main parasitic diseases include leishmaniasis, filariasis, malaria, river blindness, Chagas disease and schistosomiasis. With the absence of vaccines, treatment relies mainly on chemotherapy hence the need for efficacious and safe medicines. Many of the medicines currently used have low efficacy and cause side effects. Some are also being lost to drug resistance. To address the inadequacy of treatment options for infectious diseases, a number of initiatives have been started to promote drug discovery and development in Africa. In parallel they have been collaboration between African institutions and leading pharmaceutical companies as well as other relevant R & D organizations. This has led to the need to modernize African approaches to drug discovery and development with respect to the integration of medicinal chemistry, pharmacology and pharmacokinetics as reflected in the processes of Absorption, Distribution, Metabolism, Excretion and Toxicity (ADMET). However, scientific and technological expertise in pharmacokinetics for drug discovery is under developed in Africa.

Objectives

The first objective of this work was to set up *in silico* and *in vitro* methods for the evaluation of the major determinants of pharmacokinetic properties of drugs. The processes that determine a compound's pharmacokinetics are solubility and permeability (which determine compound absorption), protein binding (which determine volume of distribution), and metabolism (which determine compound clearance). Absorption and metabolism, in turn determine a compound's bioavailability. The second objective was to apply these *in silico* and *in vitro* assays set up in the characterization of chemical entities in different scenarios of drug discovery, development and optimal clinical use of medicines in Africa against parasitic infections. ADMET assays were applied in the characterization of synthetic hybrid molecules with anti-malarial activity to guide the choice and molecular design of lead compounds with good pharmacokinetic and pharmacodynamic (PK/PD) properties. In the herbal medicine/ natural products driven drug discovery setting, which is one of the most common approaches in Africa, the aim was to apply the ADMET assays in the characterization of Frutinone A, a natural product from a herbal extract with broad spectrum anti-microbial activity. The third aim was to apply the ADMET tools in the rationalization of pharmacokinetic liabilities of thiabendazole, an anti-helminthic drug in clinical use with a view to improve its safe clinical use. Successful demonstration of the utility of these ADME assays in these commonly used models of drug discovery and development in Africa would add value to the increasing effort to find safe and effective therapies against parasitic diseases.

Methods
Setting up of *in silico* and *in vitro* ADME assays was bench marked against leading pharmaceutical industry standards. Physicochemical properties were determined using *in silico* predictions and *in vitro* assays. For solubility, the turbidimetric method was used. Lipophilicity and purity determination were conducted using the reverse phase HPLC method. Screening for inhibition was performed using recombinant enzymes and known diagnostic inhibitors as controls. Mechanism and mode of inhibition studies were determined using the same system. Metabolism and clearance of the compounds were determined in human liver microsomes and cryopreserved hepatocytes. Metabolites, possible routes of metabolism and the enzymes involved in metabolism were also determined. *In silico*, the interaction of the various enzymes with the enzyme active site were simulated using docking software including GOLD, GLUE, FlexX and AutoDock.

Results
In silico and *in vitro* ADME platforms for the determination of compound purity, solubility, lipophilicity (logP and LogD), ionisability (pKa), permeability, protein binding, metabolic stability, metabolite identification, reaction phenotyping, and enzyme inhibition based drug-drug interactions were successfully setup in this study. These methods were then applied various scenarios of drug discovery.

In the medicinal chemistry driven drug discovery approach, ADMET characterization was conducted on two new chemical series from our laboratory with demonstrated anti-malarial activity. The artemisinin-chloroquine hybrid chemical series demonstrated good metabolic stability predictive of good bioavailability. The compounds where, however, potent inhibitors of CYP3A4 and CYP2D6, and were predicted to pose the risk drug-drug interactions if given together with other drugs, which rely on the enzymes for elimination. Most of the compounds inhibited via the non-competitive mode, which is difficult to simulate using docking methods. For the 3,4-HPO-4-amino-7-chloroquinolinyl hybrid chemical series, metabolic clearance was predicted to be moderate in hepatocytes and human liver microsomes.

In the herbal products/natural products driven drug discovery approach, Frutinone A, which is a component of abroad-spectrum herbal extract demonstrated potent CYP1A2 inhibition and moderately inhibited CYPs 3A4, 2D6, 2C9 and 2C19. CYP1A2 inhibition was characterized by an IC_{50} of 0.56μM. Inhibition was differential showing mixed (K_i = 0.48μM) and competitive (K_i = 0.31μM) inhibition with CEC and ER respectively. Two binding sites, one for inhibitors and the other for substrates were identified *in silico*. Hepatic clearance was predicted to be low (7.17ml/min/kg), with reaction phenotyping studies indicating no clearance by the enzymes tested.

In the rational use of medicines approach, the ADMET assays were applied to thiabendazole, an anthelminthic drug, which was shown to be a potent inhibitor against CYP1A2. The compound was a potent reversible and mechanism- based inhibitor with inhibition characterized by an IC_{50} of 0.83μM

and a K_I of 1.4μM. Drug-drug interaction (DDI) simulation studies using SimCyp showed good predictions for competitive inhibition. However, predictions for mechanism-based inhibition (MBI)-based DDI were not in agreement with clinical observations.

Conclusion

This work has led to the successful setting up of an ADMET platform capable of supporting drug discovery projects in Africa. The work demonstrated the application ADMET in various scenarios of drug discovery, development and optimal clinical use of medicines in Africa.

ABBREVIATIONS

5OH-TBZ	5hydroxy-thiabendazole
ADME	Absorption, Distribution, Metabolism and Excretion
ADMET	Absorption, Distribution, Metabolism, Excretion and Toxicity
API	Active Pharmaceutical Ingredient
BBB	Blood-Brain Barrier
BFC	7-benzyloxy-4-(trifluromethyl)-coumarin
CEC	3-cyano-7-ethoxycoumarin
CHC	3-cyano-7-hydroxycoumarin
CYP	Cytochrome P450
DAD	Diode Array Detector
DBF	Dibenzylfluorescein
DDI	Drug-drug interactions
DMSO	Dimethylsulfoxide
ER	Endoplasmic reticulum
GSH	Glutathione
HAT	Human African Trypanosomiasis
HAMC	7-hydroxy-4-(aminomethyl)-coumarin
HFC	7-hydroxy-4-trifluoromethylcoumarin
IVIVE	*In Vitro-In Vivo* Extrapolation
HPLC	High Pressure Liquid Chromatography
HTS	High Throughput Screening
LC/MS	Liquid chromatography/ mass spectrometry
LDH	Lactate Dehydrogenase
MAMC	7-Methoxy-4-(aminomethyl)-coumarin
MBI	Mechanism Based Inhibitor/Inhibition
MFC	7-methoxy-4-trifluoromethylcoumarin
MIC	Metabolic Intermediate Complex
MS	Mass Spectrometry
NADPH	β-Nicotinamide Adenine Dinucleotide 2′-Phosphate
NCE	New Chemical Entity
PB	Protein Binding
P*f*CRT	*Plasmodium falciparum* Chloroquine Resistance Transporter
P-gp	P-glycoprotein

PK	Pharmacokinetics
PK/PD	Pharmacokinetics and Pharmacodynamic
PPP	Public-Private Partnerships
R&D	Research and Development
ROI	Return on investment
SAR	Structure Activity Relationships
spp	Species
TBZ	Thiabendazole
WHO	World Health Organization

LIST OF TABLES

LIST OF FIGURES

LIST OF PUBLICATIONS

***In Vitro* and *in Silico* Identification and Characterization of Thiabendazole as a Mechanism-Based Inhibitor of CYP1A2 and Simulation of Possible Pharmacokinetic Drug-Drug Interactions**

Roslyn S. Thelingwani, Simbarashe P. Zvada, Hugues Dolgos, Anna-Lena B. Ungell, and Collen M. Masimirembwa

Drug Metab Dispos. 2009 37(6): page number 1286-1294. PMID:19299526

ABSTRACT

Thiabendazole (TBZ) and its major metabolite 5-hydroxythiabendazole (5OH-TBZ) were screened for potential time-dependent inhibition (TDI) against CYP1A2. Screen assays were carried out in the absence and presence of NADPH. TDI was observed with both compounds, with k_{inact} and K_I values of 0.08 and 0.02min^{-1} and 1.4 and 63.3μM for TBZ and 5OH-TBZ, respectively. Enzyme inactivation was time-, concentration-, and NADPH-dependent. Inactivation by TBZ was irreversible by dialysis and oxidation by potassium ferricyanide, and there was no protection by glutathione. 5OH-TBZ was a weak TDI of CYP1A2, and enzyme activity was recovered by dialysis. IC_{50} determination of TBZ and 5OH-TBZ showed both compounds to be potent inhibitors, with IC_{50} values of 0.83 and13.05μM, respectively. IC_{50} shift studies also demonstrated that TBZ was a TDI of CYP1A2. In silico methods identified the thiazole group as a TDI fragment and predicted it as the site of metabolism. The observation pointed to epoxidation of the thiazole and the benzyl rings of TBZ as possible routes of metabolism and mechanisms of TDI. Drug-drug interaction (DDI) simulation studies using SimCyp showed good predictions for competitive inhibition. However, predictions for mechanism-based inhibition (MBI)-based DDI were not in agreement with clinical observations. There was no TBZ accumulation upon chronic administration of the drug. The *in vitro* MBI findings might therefore not be capturing the *in vivo* situation in which the proposed bioactivation route is minor. This might be the case for TBZ in which, in vivo, UDP glucuronosyltransferases and sulfanotransferase metabolize and eliminate the 5OH-TBZ.

Potent inhibition of CYP1A2 by Frutinone A, an active ingredient of the broad spectrum antimicrobial herbal extract from *P. fruticosa*

Roslyn S. Thelingwani, Kariema Dhansay, Peter Smith, Kelly Chibale, and Collen M. Masimirembwa

Xenobiotica. 2012 Apr 25. [Epub ahead of print]. PMID: 22533317

ABSTRACT

Frutinone is an active ingredient extracted from the lipophilic fraction of the *Polygala Fruticosa* demonstrating various antibacterial and fungal properties. The aim of this study was to characterize its metabolism in an effort to understand metabolism based drug-herb interactions. *In vitro* metabolic clearance and metabolite identification studies were done using cryopreserved hepatocytes. Reaction phenotyping and inhibition studies were done using human liver microsomes and recombinant cytochrome P450s (CYPs). Frutinone A-CYP1A2 interactions were rationalized using docking simulations. Hepatic clearance was predicted to be low (7.17 ml/min/kg), with reaction phenotyping studies indicating no clearance by the enzymes tested. Frutinone was identified as a potent inhibitor of CYP1A2 with moderate effects on CYP2C19, 2C9, 2D6 and 3A4. CYP1A2 inhibition was reversible and characterized by an IC_{50} of 0.56μM. Inhibition was differential showing mixed (K_i= 0.48 μM) and competitive (K_i= 0.31 μM) inhibition with 3-cyano-7-ethoxycoumarin and ethoxyresorufin, respectively. Two binding sites, one for inhibitors and the other for substrates were identified in silico. The potent CYP1A2 inhibition by Frutinone A could be predictive of the potential drug-herb interaction risk in the use of herbal extracts from *P. fruticosa*. The data suggest future pharmacological research on this chromocoumarin should take metabolic properties into account.

Application of in silico, *in vitro* and *in vivo* ADMET/PK platforms in drug discovery.

Collen Masimirembwa and **Roslyn Thelingwani**

In Drug Discovery Africa: Impacts of Genomics, Natural Products, Traditional Medicines, Insights into Medicinal Chemistry, and Technology Platforms in Pursuit of New Drugs. Springer 2012. Edited by Kelly Chibale, Mike Davies-Coleman and Collen Masimirembwa

ABSTRACT

Drug discovery is a risky and expensive business fraught with high attrition rates. The healthcare benefits and financial rewards that can be realized if successful have, however, ensured the relevance and continued growth of the pharmaceutical industry. The major reasons for high attrition rates during drug discovery include lack of efficacy, toxicity, inadequate pharmacokinetics (PK), and market forces; factors which can be complexly interrelated. PK has been shown to affect the efficacy and safety of new chemical entities (NCEs). The pharmaceutical industry responded by frontloading the characterization of the processes that determine the PK of compounds, that is, absorption, distribution, metabolism and excretion (ADME). The ADME data is being used to guide medicinal chemists in the design of molecules with favourable disease specific PK properties. In late stages of drug discovery, the preclinical ADME data is being used to predict human PK and safety of NCEs. As African research scientists initiate drug discovery activities, integration of PK, in the traditionally medicinal chemistry and disease pharmacology driven efforts, is important towards ensuring increased chances of discovering good candidate drugs (CD). We have therefore setup in silico, in vitro and in vivo ADMET platforms, which various African drug discovery scientists can access. Drugs for non-communicable disease fail more from lack of efficacy than poor PK whereas drugs for infectious disease fail more from poor PK than from lack of efficacy. Drug discovery efforts in Africa are also mainly based on natural products for which little is known or can be inferred from the PK of conventional synthetic drugs. These factors point to the need of promoting the sciences and technologies of PK research at many African institutions.

Manuscripts in Preparation.

1. Thelingwani et al., Identification of ADME/PK liabilities in artemisinin-chloroquinoline hybrids

2. Thelingwani et al., Identification of ADME/PK liabilities in 3,4-HPO-4-amino-7-chloroquinolinyl hybrids

1 INTRODUCTION

Modern pharmaceutical industry aims to integrate pharmacology, medicinal chemistry and ADME/PK in the drug discovery and development value chain. This is an approach applied by major R&D-based pharmaceutical companies in developed countries. In Africa the picture is different with drug discovery still in its infancy and still conducted in non-integrated approaches by small academic research groups, which are either pharmacology or medicinal chemistry driven. A few groups have begun working on establishing ADME/PK platforms to support the increasing drug discovery initiatives on the continent.

Drug discovery in Africa has traditionally been driven by herbal and/or traditional medicines as well as natural products chemistry with limited expertise in synthetic medicinal chemistry and ADME/PK. In pharmacology, discovery efforts in Africa largely involve the use of cell cultures and animal disease models. There is comparatively limited work on molecular-target based drug discovery. With challenges such as drug resistance, drug-drug interactions and suboptimal PK properties resulting in treatment failures being faced in the treatment of many parasitic infections, there is any urgent need to come up with new medicines.

This thesis therefore explores the integration of ADME/PK in herbal/natural products and in synthetic medicinal chemistry-driven drug discovery as well as the optimal clinical use of drugs already on the market for the treatment of infectious parasitic diseases. Various biochemical assays and *in silico* tools

will be setup and employed towards the identification of ADME/PK liabilities, molecular and kinetic data, which will be used in the future design and synthesis of safer analogues or guide the design of safer dosing regimens.

1.1. Parasitic infections

Infections with parasites are important causes of morbidity worldwide, ranking among the top killers according to the WHO reports (World Health Organisation, 2004). It is estimated that over half of the world's population suffers from parasitic diseases which include malaria, leishmaniasis, African trypanosomiasis, Chagas disease, protozoal diarrhea, schistosomiasis, river blindness and lymphatic filariasis (Watkins, 2003). Low-income countries are the hardest hit especially in Africa where they are the major causes of death. Of the parasitic infections malaria is the deadliest with the WHO reporting 216 million cases in 2010 (World Health Organisation, 2011). The main parasitic diseases, causal agents and epidemiology are shown in Table 1.1.

1.1.1 Challenges with drugs available for treatment

Many of the drugs used to treat parasitic infections are decades old, with many of them having been discovered using empirical methods or initially targeted for other diseases or veterinary use. Therefore many of the drugs on the market have many challenges including low efficacy, severe side effects and drug resistance. If many of them were to be evaluated for efficacy and safety using current regulatory standards, they would not pass the drug discovery and development requirements.

Table 1.1: Main parasitic diseases
(Table adapted from Renslo et.al (Renslo and McKerrow, 2006)).

Disease	Organism	Burden	Therapy needs
Malaria	*Plasmodium spp*	Estimated 216 million reported cases with 655 000 deaths in 2010 (World Health Organisation, 2011)	Drugs circumventing drug resistance
Leishmaniasis	*Leishmania spp*	Estimated 1.6 million new cases annually (World Health Organisation, 2006)	Safe, orally bioavailable drugs, especially for the visceral form of the disease
Trypanosomiasis	*T. Brucei* (African Trypanosomiasis) *T. Cruzi* (Chagas Disease)	50-70000 estimated cases in 2006 (World Health Organisation, 2006) 20 million estimated to be infected in 2009 (World Health Organisation, 2010b)	Safe and orally bioavailable drugs especially for the chronic disease phase
Schistosomiasis	*Schistosoma spp*	> 200 million existing infections (Renslo and McKerrow, 2006)	Backup drugs in case they is resistance to praziquantel

The choice of effective medicines for treating parasitic infections is very limited due to reasons indicated above. For example, praziquantel is the only drug available for treatment of schistosomiasis which is effective against all three species affecting humans (Fenwick *et al.*, 2003). The two other drugs, oxamniquine and metrifonate are effective against *S. mansoni* and *S. haematobium* respectively (Caffrey, 2007). However the drugs are not in use anymore. The structure of the drugs is shown in Fig 1.1.

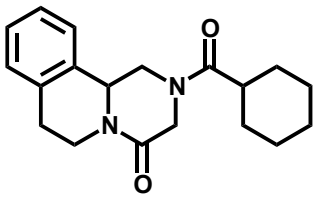

praziquantel

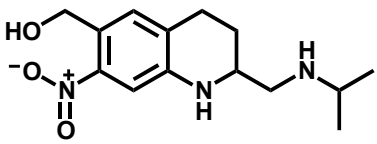

oxamniquine

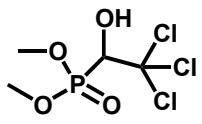

metrifonate

Figure 1.1: Chemical structures of the common antischistosomal drugs

Drug resistance to many of the many of the traditional drugs has also been one of the major challenges associated with antiparasitics (Fig 1.2).

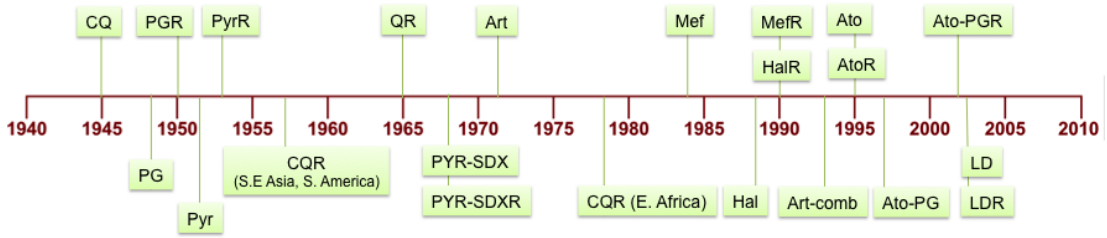

Adapted from Hyde (Hyde, 2005)

Figure 1.2: Dates of introduction of antimalarials and observations of treatment failure: *Q - quinine, Pyr – pyrimethamine, SDX – sulfadoxine, CQ-chloroquine, Mef –mefloquine, ato – atovaquone, PG - proguanil combination, Art – artemisinin and derivatives, Hal – halofantrine, LD – LapDap (chlorproguanil–dapsone).*

This has seen the loss of clinical usefulness of most drugs. Resistance to melarsoprol, diminazene and isometamidium (Fig 1.3) by trypanosomes has been reported (Delespaux and de Koning, 2007). *P. falciparum* resistance has been recorded in all the current antimalarials including the recommended artemisinins (Dondorp *et al.*, 2011; Dondorp *et al.*, 2009; Noedl *et al.*, 2008).

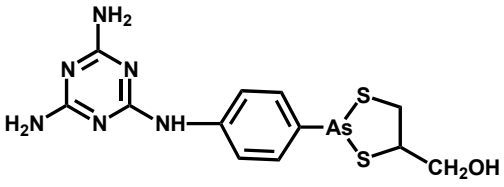

melarsoprol

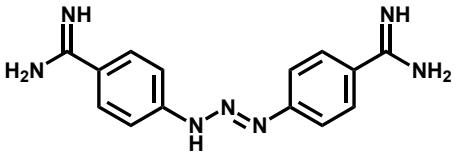

isomentamidium

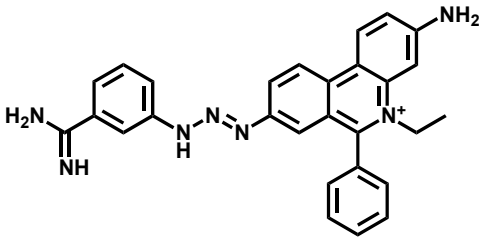

diminazene

Figure 1.3: Drugs where resistance has been shown in the treatment of HAT

Some treatments are associated with severe side effects. For example in the treatment of malaria and HAT several drugs have been associated with side effects. In malaria the use of amodiaquine, quinine and halofantrine is limited because of toxicity. Amodiaquine is effective against drug resistant malaria but its use is limited because long-term exposure is associated with agranulocytosis (Rouveix *et al.*, 1989) and hepatitis (Larrey *et al.*, 1986). Examples are of drugs associated with side effects are shown in Fig 1.4.

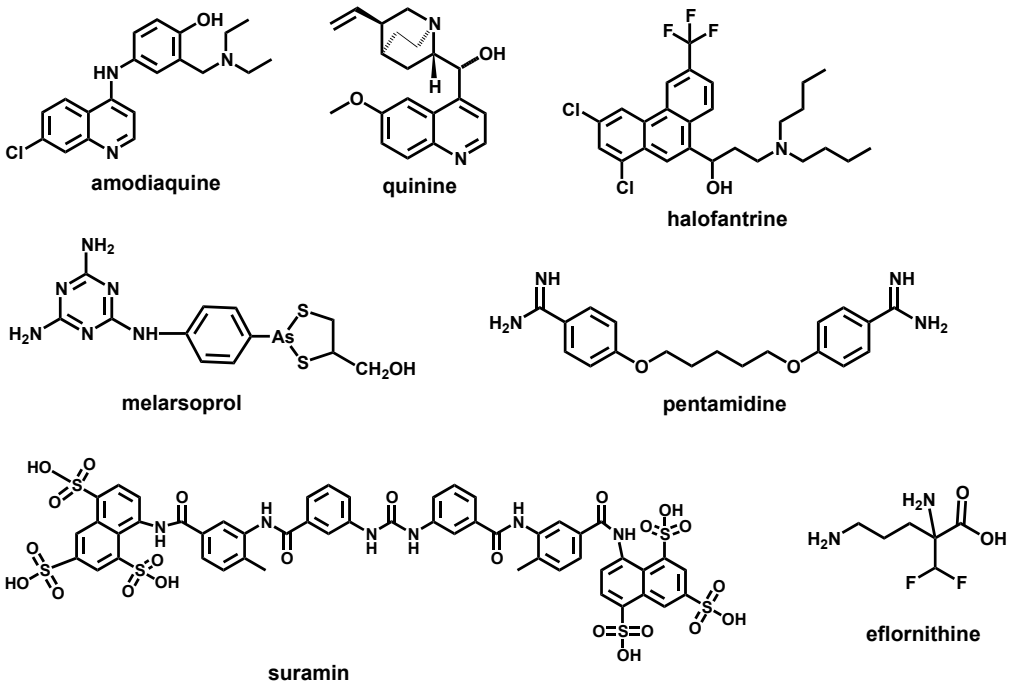

Figure 1.4: Examples of drugs associated with side effects in the treatment of malaria and HAT. Drugs associated with side effects in malaria treatment are amodiaquine, quinine and halofantrine with melarsoprol, pentamidine, suramin and eflornithine associated with side effects in HAT treatment

Long term exposure to halofantrine is associated with cardiac dysrhythmias (Sowunmi *et al.*, 1998)and quinine with predisposition to blackwater fever(Bruce-Chwatt, 1987). The treatment of HAT with melasoprolol, suramin, pentamidine and eflornithine is associated with severe side effects which range from immediate side effects such as shock and vomiting to severe

ones such as kidney damage to reactive encephalopathy(Fairlamb, 2003).

In general, the current antiparasitic drugs are characterized by large and complex dose regimens, prolonged administration for successful treatment, and possess various modes of toxicity (Table 1.2). Many of the drugs are used in combination to increase efficacy and reduce emergence of drug resistance. No PK/PD rationalization and optimization was done in the choice of combination drugs hence the sometimes complex empirical dosing regimens.

1.1.2 Burden of parasitic diseases in relation to drug discovery

Many parasitic diseases are found mainly in the tropics, which lie in some of the poorest regions of the World. In Africa the burden mainly comes from diseases such as malaria, trypanosomiasis, leishmaniasis and protozoal diarrhoea. For most of the diseases, there are no vaccines, leaving chemotherapy to be the only effective way of treating and controlling the diseases. The development and discovery of drugs for curing parasitic diseases is not market driven because the bulk of the people living in endemic areas cannot afford to pay for their treatments. With the cost of producing one drug being estimated at $1.8 billion (Paul et al., 2010), coming up with new medicines is extremely challenging. Some drugs are also not able to recover their production cost due to tough competition on the market (Lombardino and Lowe, 2004). This makes this area unappealing to pharmaceutical companies, which need a return on investment (ROI) for sustainable R&D for new medicines.

Table1.2: Dosing regimen and safety issues associated with selected antiparasitic drugs.

Disease	Drug	Dosing Regimen	Toxicity	References
Malaria	Amodiaquine	10mg/kg/day once a day for 3 days (fixed dose with artesunate)	Linked to agranulocytosis and hepatotoxicity. Unsafe for prophylaxis	(World Health Organisation, 2010a)
	Quinine	20mg/kg salt intravenously over 4hrs in cases of severe malaria 10mg/kg orally every 8hrs	Hyperinsulinaemic hypoglycaemia, predisposition to blackwater fever, ototoxicity.	(Taylor and White, 2004; Krishna and White, 1996)
HAT	Eflornithine	100-400mg/kg bodyweight at 6hr intervals for 14 days	Vomiting, nausea, diarrhea, nausea, thrombocytopenia, convulsions and leucopenia. Severity increases with treatment duration	(Burri and Brun, 2003; Na-Bangchang *et al.*, 2004)
	Pentamidine	4mg/kg bodyweight at 24h intervals for 7 days	Hypoglycaemia, injection site pain, diarrhoea, nausea, vomiting	(Delespaux and de Koning, 2007; Nok, 2003)
Leishmaniasis	Amphotericin B	1 mg/kg on alternate days × 15 doses in 30 days intravenously	Nephrotoxicity and acute reactions after IV infusion including high fever, chills, vomiting and drowsiness	(Berman, 2005; Croft *et al.*, 2005)
Onchocerciasis	Diethylcarbamazine	2-3mg/kg of body weight 3 times a day	Visual impairment, cellular cytotoxicity as a result of immune factors, inflammatory reactions, itching and swelling of the face	(Van Laethem and Lopes, 1996)

1.1.3 Efforts in promotion of drug discovery for parasitic infections

1.1.3.1 Public-private partnerships

The formation of public-private partnerships (PPP), which operate on a non-profit basis, has been one of the approaches used to promote the discovery of drugs for parasitic and infectious diseases in resource poor nations. The aim is to spread the cost and risk for drug development among international networks, pharmaceutical companies, academic institutions and non-governmental organizations. Drugs developed in the networks are distributed at cost price. Examples of successes so far include the registration of the artesunate-amodiaquine combination therapy for malaria by the Drugs for Neglected Diseases initiative (DNDi) (http://dndi.org/portfolio/asaq.html). Other examples include Coartem® a fixed dose combination of artesunate and lumefantrine by the Medicines for Malaria Venture (MMV) (http://www.mmv.org/).

1.1.3.2 Drug repositioning

In this approach new uses for existing approved drugs are examined. Since the drugs will have been approved, they will have undergone the various required evaluations for safety. This results in big reductions in costs and research and development time. An example where this approach has been widely used is in antimalarials and some examples are shown in Fig 1.5. Antibiotics including clindamycin, doxycycline, tetracycline and sulfonamides (Nzila *et al.*, 2011) have been found to be effective. Withdrawn drugs can also be reoptimised for use. An example is piperaquine, which was withdrawn in the in the 1980s due to resistance. However it was later rediscovered and

found to be a suitable drug for use in artemisinin based combination therapies (Davis *et al.*, 2005). Combined with dihydroartemisinin, it has become one of the WHO recommended artemisinin based combination therapies for malaria treatment (World Health Organisation, 2010a).

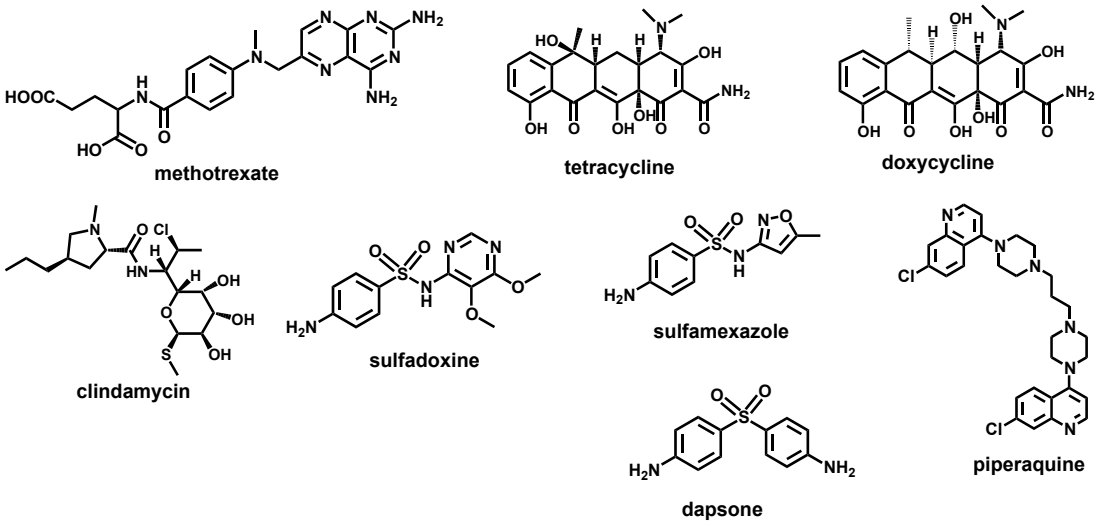

Figure 1.5: Repositioned drugs in the treatment of malaria. The compounds include the antibacterial sulphonamides sulfadoxine, dapsone and sulfamexazole, the long acting antibacterials doxycycline, clindamycin and tetracycline, the 4-aminoquinoline piperaquine and the anticancer drug methotrexate

1.1.3.3 Novel approaches with existing drugs

Drugs may be reintroduced after a period of non-use. This approach is used in cases where a drug has been stopped because of resistance. The hope will be that re-expansion of drug non-resistant parasites will have occurred. This approach was successfully applied in Malawi where chloroquine was reintroduced after 10 years of non-use and showed effectiveness (Laufer et al., 2010). To delay the reoccurrence of resistance, the drug is used as part of a combination. Other drugs may also be combined with newer ones to offer an effective solution and to delay resistance to the newer drug. Combinations

can also be made with older drugs. However current recommended combinations in malaria chemotherapy are the ACTs.

1.2. Overview of the drug discovery process

The drug discovery process is a long, multidisciplinary (Fig 1.6), costly and risky business that requires careful planning and good communication between researchers. The process begins with the identification of the medical need, a process that requires formation of a research team. A working hypothesis is formulated and novel compounds are synthesized and tested against a validated molecular target, whole organism or cell culture.

Further preclinical studies conducted either *in vitro, in silico and/*or *in vivo*. Data from the studies then determines whether a compound will pass as a preclinical candidate and go though the whole process up to clinical trials and final approval. Considering the lengthy, risky and costly nature of the process many considerations have to be made early in the discovery stages to ensure candidates proceeding to the next stages carry minimum risk in terms of liabilities either physicochemical or pharmacokinetic.

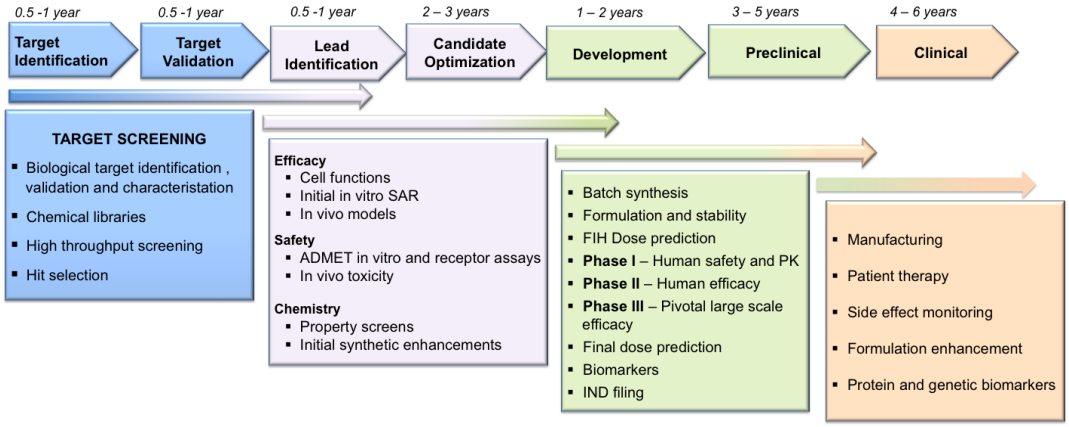

Figure 1.6: Overview of the drug discovery process. *Adapted from Kerns and Li (Kerns and Li, 2008)*

1.2.1. Integrated approaches to drug discovery

Although the drug discovery process is often depicted as a linear process, (Fig 1.6) a lot of the screening and assays are carried out in parallel. This enables decisions to be made based on assessment of activity and liabilities each series carry. The integrated approach is exemplified in Fig 1.7, which depict the workflow for a series of new chemical entities with antimalarial activity in the discovery stage.

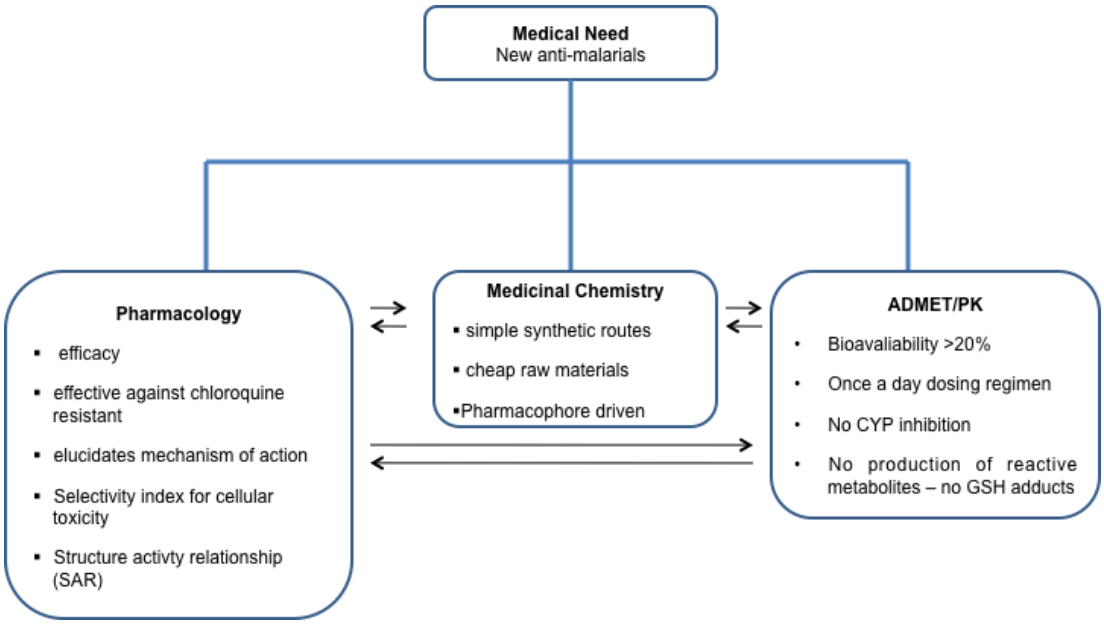

Figure 1.7: The parallel and integrated approach to lead identification for compounds with anti-malarial activities.

The aim for pharmacology is to quickly identify compounds with efficacy especially in resistant strains of the disease, determine cytotoxicity and elucidate the likely mechanism of action. The aim of medicinal chemistry is to determine cheap no-complicated routes of synthesis. From pharmacological and chemical data, structure activity relationships (SAR) can be quickly determined. Liabilities such as toxicity, non-optimal physicochemical and pharmacokinetic profiles are determined in the ADMET screens. The data

from all the screens is ultimately be used to improve on analogues of newly synthesized series of compounds.

The integrated approach has also been used *in silico* where various methods broadly categorized into ligand based, protein based and ligand-protein interactions are used. The methods are used to investigate the interaction of compounds with the enzyme active site, and can be used in combination, hence the integrated approach. Data from the different methods is combined in an effort to probe various questions under investigation. The interlinking of the various methods is depicted in Fig 1.8.

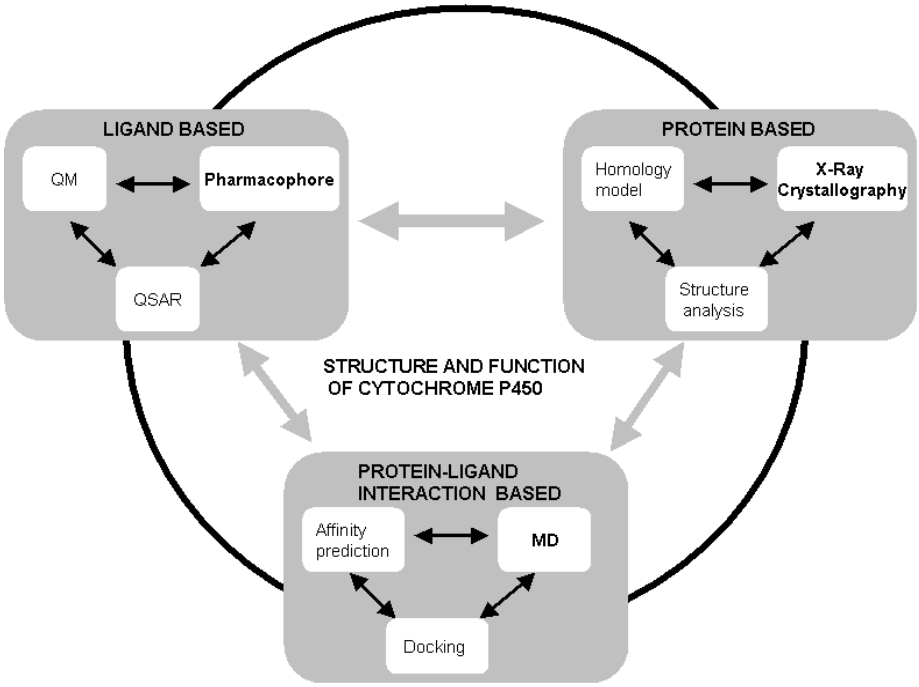

Figure 1.8: An integrated approach to molecular modeling. Relationships between the major groups and within each category are indicated by the arrows (De Graaf *et al.*, 2005)

Various software packages are available for *in silico* predictions with many new packages being developed and improvements to existing ones being

made. The *in silico* methods are being used to understand drug-receptor interactions in pharmacology and drug-enzyme/transporter interaction in pharmacokinetics towards the design of efficacious and safer analogues.

1.3. Target screening

Target screening involves the identification of a potential drug and the understanding of its role in the disease process. It also involves the studies of the mechanism of action. Various approaches have been used to identify drug targets including whole parasite screening and molecular target screening.

1.3.1. Whole parasite screening

In this approach, diverse compounds are screened on whole parasites. This has been successfully done for parasites such as *P. falciparum*, *T. brucei* and *T. cruzi*, which are easy to maintain in culture. For parasites that are difficult to maintain in continuous culture for example leishmania, transgenic cell lines are used. The lines incorporate reporter constructs such as β-lactamase, luciferase and green fluorescent protein which identify bioactive compounds in either axenic or intra-cellular cultures (Sereno *et al.*, 2007). The gene transcripts have also been used on parasites that grow well in culture for easy detection of antiparasitic activity.

To enable fast detection of antiparasitic activity some of the assays are now high throughput making it easy to screen chemical libraries of thousands of compounds. This is performed with standardized assays, and detection is by colorimetric methods coupled with the use of radioactive or fluorescent dyes.

An example is the use of the fluorescent active cell sorting in combination with YOYO-1 which is a nuclear dye in high throughput screening (HTS) for *P. falciparum* (Weisman *et al.*, 2006).

The use of HTS assays is limited to centers, which are well funded. Many research groups still use traditional methods such as lactate dehydrogenase (LDH) assay for antiplasmodial activity which are less sensitive for activity screening (Makler and Hinrichs, 1993; Makler et al., 1993). The method generates optical density values at various concentrations of the drug as raw data after addition of Malstat reagent and the nitrotetrazolium salt in phenazine ethosulfate (NBT/PES). Other methods include the ^{3}H-hypoxanthine incorporation assay, staining with giemsa and counting under the microscope and flow cytometry (Fidock et al., 2004).

1.3.2. Molecular target screening

Molecular targets screening is conducted using parasite genomes in an effort to identify gene products unique to parasites. This has been made possible by the availability sequences of whole parasite genomes combined with good bioinformatic and genome mining tools. Resistant parasites can also be generated in silico creating a drug that targets many variants of the molecular target. This is an approach that was used in the synthesis of spiroindolone NITD609 (Fig 1.9) (Rottmann et al., 2010), a compound which represents a new class of antimalarials which act by inhibiting protein synthesis. Parasite drug targets once identified are validated using chemical or genetic methods such as gene expression profiling and RNA interference (Pink *et al.*, 2005).

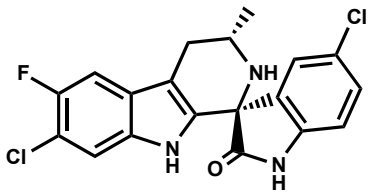

Figure 1.9: Structure of spiroindolone NITD609

1.3.3. *In vivo* screening

In vivo screens are also performed in model animals infected with parasites and various new chemical entities (NCEs) are screened by dosing the animal. Antiplasmodial activity screening is done mostly in rodent parasite models, which include *P.berghei, P. yoelii, P. chabaudi* and *P. vinckei*. This is because plasmodium species, which affect humans, are unable to infect non-primates except for one rodent model which can be infected by *P. falciparum* (Angulo-Barturen et al., 2008). The models have been shown to predict outcomes in humans sufficiently provided the closest model is used (Langhorne et al., 2011).

1.4. Medicinal chemistry strategies in antiparasitic drug discovery

Many strategies have been employed in the design and discovery of new chemical entities (NCEs) with antiparasitic activity. The aim is to obtain molecules with better profiles compared to existing ones. Due to drug resistance to many of the traditionally used antiparasitic drugs, there is an urgent need for new medicines. Some of the approaches currently being used in medicinal chemistry include use of known pharmacophores to create better analogues and use of resistance reversal agents to restore drug efficacy.

1.4.1. Improvements to known drugs and compounds classes

Improvements to drugs and known classes of compounds are made to address liabilities inherent in the parent drugs such as toxicity. Amodiaquine is a good example where analogues with better toxicity profiles are being synthesized. Amodiaquine is used to cure acute malaria. The biotransformation of amodiaquine however, leads to the formation of a quinoneimine intermediate, which is conjugated, with protein thiols resulting hepatotoxicity and agranulocytosis (Larrey et al., 1986; Rouveix et al., 1989).

It has been shown that isoquine an isomer of amodiaquine does not form the quinoneimine metabolite (O'Neill *et al.*, 2003). This approach circumvented the toxicity while at the same time retaining activity. An analogue with fluoro group replacing the 4-hydroxyl group of 4-hydroxyanilino nucleus was synthesized (Fig 1.10). The addition of the fluorine increases the oxidation potential reducing the in vivo oxidation of the molecule to the quinoneimine hence a good toxicity profile (O'Neill *et al.*, 2009).Unfortunately isoquine still failed in clinical trials due to toxicity (O'Neill *et al.*, 2009) indicating the possible existence of other bioactivation pathways resulting in drug toxicity.

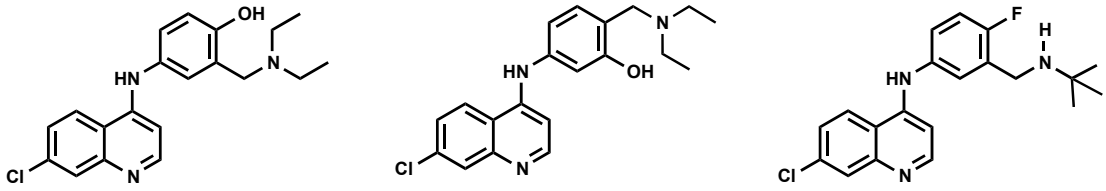

Figure 1.10: Structures of amodiaquine, isoquine and the fluoro analogue

Chloroquine had been an ideal drug of choice in treatment for malaria because of its good safety profile, oral bioavailability and low cost. Efforts have been made to synthesize analogues of chloroquine, which have better activity and can be used to treat resistant plasmodium strains. One approach has been to vary the length of the alkyl side chain. Structure activity relationships have shown analogues, which have shorter and longer side chains than chloroquine to have activity against resistant strains of *P. falciparum*(De et al., 1996). Other analogues have been synthesized in-cooperating transition metals(Biot *et al.*, 1997; Ajibade and Kolawole, 2008)and have been shown to be stable and to have a good safety profile making them suitable for use in combination with other drugs (Sa´nchez-Delgado *et al.*, 1996; Navarro *et al.*, 1997; Biot *et al.*, 1997)

1.4.2. Resistance reversers

Resistance by parasites to drugs is a major challenge in treatment where it has rendered many drugs ineffective. Some drugs such as chloroquine have been the mainstay of treatment and have been drugs of choice for many years because they are cheap, safe and generally have a good safety profile. However many of the drugs are being lost globally. The global distribution of resistance to chloroquine and sulfadoxine–pyrimethamine is shown (Fig 1.11).

In malaria treatment, chloroquine is thought to work by inhibiting the formation of hemozoin from heme. Accumulation of heme in the cell will therefore cause heme-induced cell death since heme is toxic to the plasmodium parasite. Resistance to chloroquine is linked to a point mutation on the gene coding for

the parasite's digestive membrane protein called *Plasmodium falciparum* chloroquine resistance transporter (PfCRT)(Fidock *et al.*, 2000). The mutations result in the change of a charged amino acid to an uncharged one, which allows efflux of charged chloroquine. An example is the change from positively charged lysine (K) or arginine (R) to neutral isoleucine (I) which results in the K76T and R371I mutations. This efflux reduces the concentrations of chloroquine in the food vacuole resulting decreased drug access to the heme target. However the drug target is not altered in the process (Fitch, 1969) and still remains vulnerable if the right concentrations are reached again.

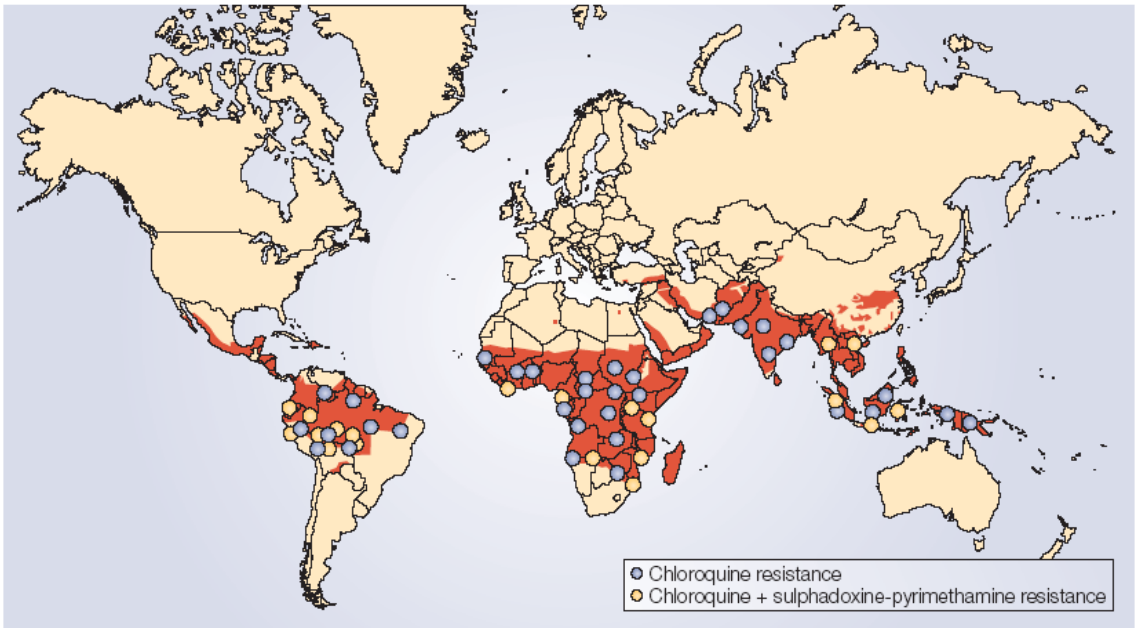

Figure 1.11: The global distribution of drug resistant malaria
Areas where *Plasmodium falciparum* resistance to the most commonly used antimalarial drugs, chloroquine and sulfadoxine-pyrimethamine are circled (Fidock *et al.*, 2004)

To prevent the pumping out of the drug, chemosensitizers have been used. These are drugs that bind to the membrane of *Pf*CTR preventing chloroquine

from being effluxed out. Verapamil and imipramine are examples of such drugs (van Schalkwyk and Egan, 2006).The clinical use of these agents however has been very difficult as concentrations required to achieve the reversal are high, causing toxicity. Attempts have therefore been made to incorporate moieties, which promote resistance reversal to known pharmacophores, which are known to have activity against parasite strains. An example is substituted acridone chemosensitizers (Kelly et al., 2007), which were made from tricyclic xanthones (Fig 1.12) which had been demonstrated to have antimalarial activity (Kelly et al., 2007).

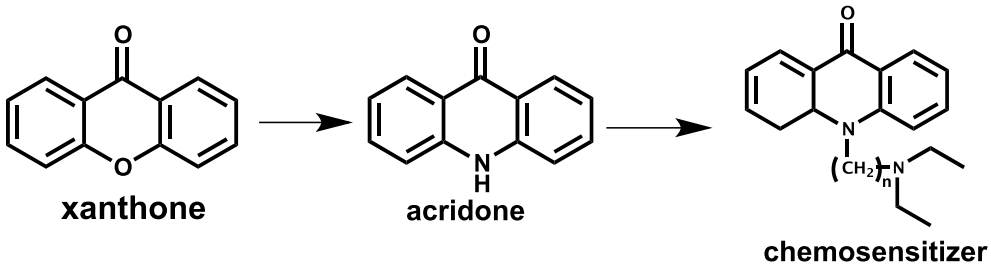

Figure 1.12: Design pathway of acridone chemosensitizers
The acridone chemosensitizers were designed with an alkyl side chain with tertiary amines at the terminal position. The acridone chemosensitizers were shown to enhance the activity of other antimalarials such as chloroquine (Kelly *et al.*, 2007)

1.4.3. Molecular hybridization

Molecular hybridization is a method where single entities containing two drugs/pharmacophoric units derived from bioactive molecules are linked together by a covalent linker (Walsh and Bell, 2009). The approach takes advantage of good properties of one drug e.g. the transport mechanism of one pharmacophoric unit can enhance the access of the other to the drug target.

The advantages of the molecular hybridization approach include potentially reduced costs and improved patient compliance. The reduced cost is in terms of quality control, production and logistics as the drug will now just be considered as one active pharmaceutical ingredient (API) instead of two. The disadvantage of the method is that it requires a fixed ratio of the two pharmacophores; hence they have to have the same magnitude of activity. Also the covalent linkage can lead to undesirable changes to the parent activity, safety and pharmacokinetic profile.

Many hybrid drugs have been explored to date. The first hybrids to be successfully synthesized were the trioxaquines, which comprised of chloroquine and synthetic endoperoxide cores (Fig 1.13). The hybrids (**a** and **b**) were shown to have good antimalarial activity and this was attributed to the secondary amines in the linker which led to accumulation of compounds in the parasite food vacuole (Dechy-Cabaret et al., 2004). Compound **b** was selected as an antimalarial drug candidate (Coslédan *et al.*, 2008).

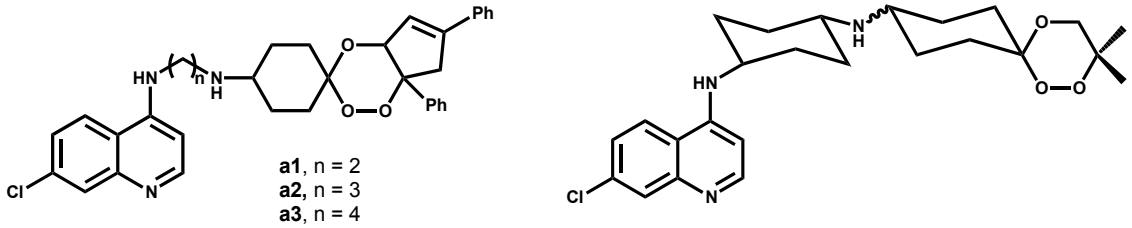

Figure 1.13: Representative structures of trioxaquine hybrids

Further studies into the trioxaquine hybrids led to the synthesis of analogues which incorporated moieties such as ferrocene (Bellot et al., 2010) (Fig 1.14).

Although the trioxaferrocene analogue had comparable activity to **a** (Fig 1.13) it was still inferior compared to **b.**

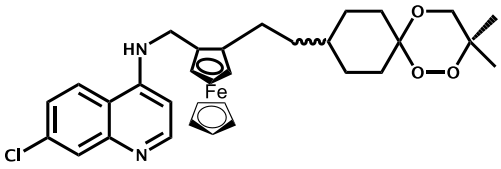

Figure 1.14: Trioxaferrocene hybrid incorporating the ferrocene moiety

Other hybrids have been synthesized from trioxolanes (Vennerstrom et al., 2004), tetraoxaquines (Opsenica *et al.*, 2008) and dioxane scaffold, based on ascaridole (Opsenica et al., 2007). The approach has also been further used to make hybrid prodrugs which release an active group once inside the parasite in the presence of iron (O'Neill et al., 2004). Other groups have hybridized artemisinin and 1,4-naphthoquinone derivatives with good antimalarial activity (Feng *et al.*, 2011). Although the hybrids are cytotoxic against mammalian cell lines they have potential to be optimized and represent a new class of effective antimalarials.

1.4.4. Exploration of natural products

This strategy benefits from knowledge of medicinal plants among natives of parasite disease endemic regions. Natural products represent a source of potential new pharmacophore because of the diverse array of chemicals they present. The chemical diversity is high among plants, which use them as defense against parasitic infections. This has inspired medicinal chemists to identify and synthesize some of these compounds and/or their analogues. Artemisinin and quinine are examples of drugs from natural products.

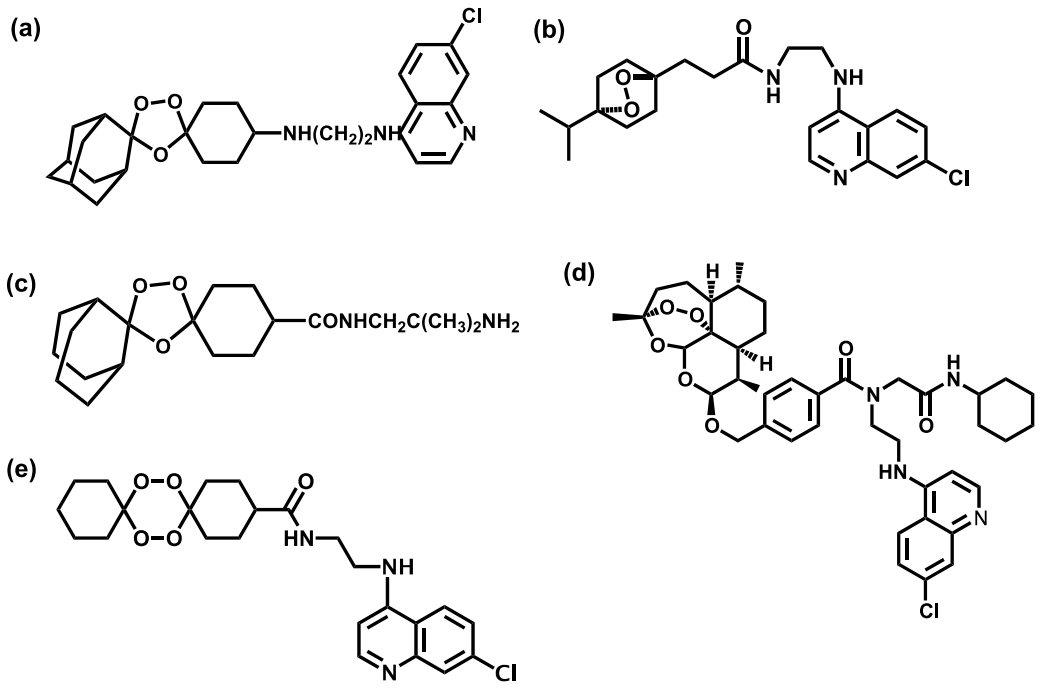

Figure 1.15: Hybrid antimalarials. The compounds include (a) trioxalaquines, (b)combination of 4-aminoquinoline with a dioxane scaffold, based in ascaridole, (c)trioxolanes, (d)artemisinin-chloroquinoline hybrids and (e) tetraoxalaquines.

The challenge with this approach is the chemical qualitative and quantitative variations associated with seasonal changes and geographical location, making it sometimes challenging to standardize herbal medicines. Activity has also been shown to be lower in some natural products when the active ingredient is isolated as compared to the crude extract, which is believed to be a cocktail of many interacting substances (Rasoanaivo et al., 2011).

The established natural product antimalarial drugs include quinine, an alkaloid isolated from the bark of the cinchona tree, artemisinin, an endoperoxide sesquiterpene lactone from Artemisia annua *sp* and lapachol, a prenylated naphthoquinone from *tabebua sp* (Fig 1.16). Lapachol provided the main pharmacophore that was used in the development of atovaquone. Natural products have also been investigated in the treatment of Leishmania (Polonio

and Efferth, 2008) and HAT(Hoet *et al.*, 2004) where drugs in current use are either toxic or are being lost to resistance.

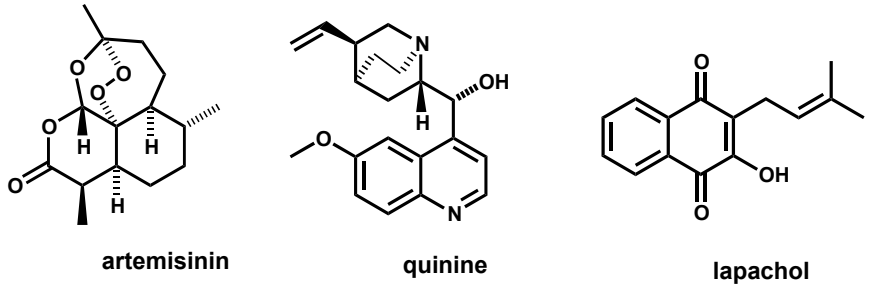

Figure 1.16: Isolated natural products with pharmacophores that have been used in the synthesis of antimalarial drugs

1.5. Property and Physicochemical screening

Structural properties of compounds offer a fast way of evaluating the drug likeliness of new chemical entities. Physicochemical properties on the other hand are affected by the various structural properties. This makes the structural properties very useful for predicting physicochemical properties without even measuring them.

1.5.1. Structural properties

Structural properties that are widely used include molecular weight (MW), polar surface area (PSA), hydrogen bonding (HB), lipophilicity (logP), shape and ionisability (pK_a). It is from these properties that rules and guidelines have emerged and are widely used as guidelines for design and synthesis of new molecules with potentially desired properties.

1.5.1.1. MW

High molecular weight has been shown to cause a decline in bioavailability as it affects the fraction absorbed (F_a)(Varma *et al.*, 2010). On the other hand high molecular weight has been linked to increase in lipophilicity hence better interaction with target site such as enzyme active sites. This has been associated with increased activity in general but some studies have indicated that high molecular weight does not necessarily result in high activity (Oprea, 2002a). This is demonstrated in Fig 1.17, which shows the relationship between the MW and activity. Other disease target classes have also been shown to favour low molecular weight compounds, for example CNS drugs (Pajouhesh and Lenz, 2005).

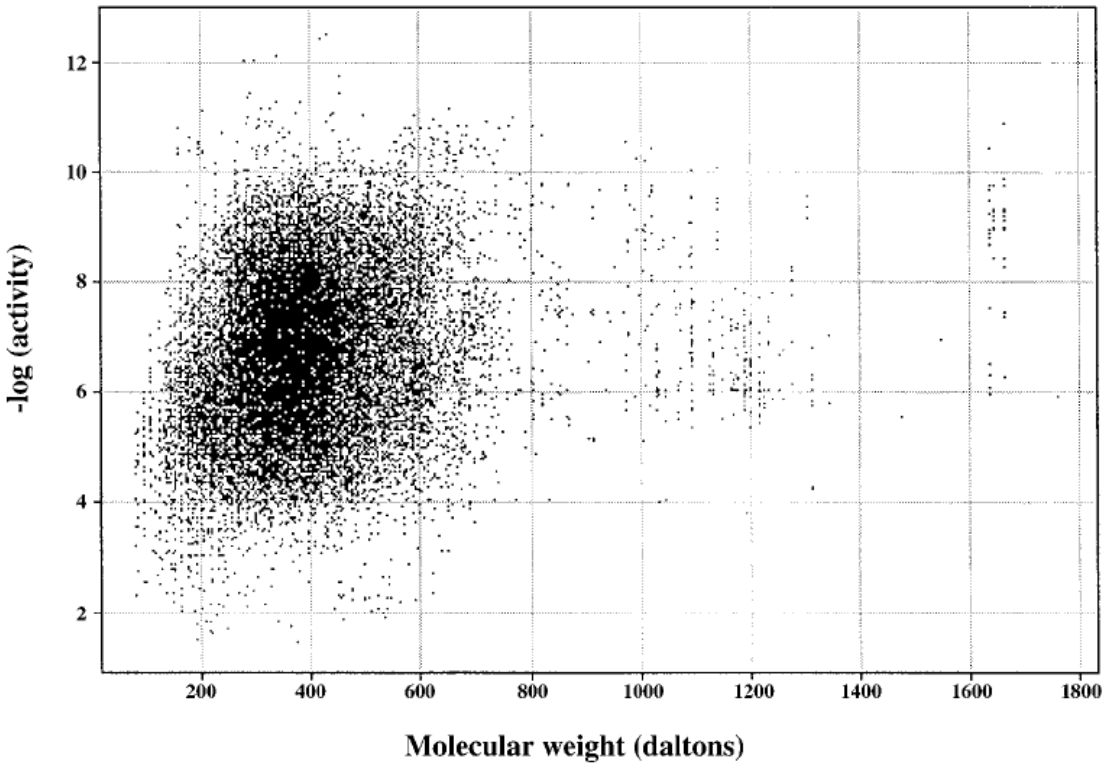

Figure 1.17: The relationship between molecular weight (MW) and activity (Oprea, 2002a)

1.5.1.2. Hydrogen bonding and the polar surface area

Hydrogen bonding is a major determinant of permeability as the shedding of hydrogen bonded water molecules facilitates the diffusion through the membrane. Therefore, the higher the hydrogen bonding, the more unfavorable the permeability process becomes. This has been demonstrated with peptides, which are compounds with high hydrogen bond forming potential, and they have been shown to have minimal distribution through the BBB (Pardridge, 1998) and low intestinal absorption (Chan and Stewart, 1996).

Hydrogen bonding is a major determinant of permeability as the shedding of hydrogen bonded water molecules facilitates the diffusion through the membrane. Therefore, the higher the hydrogen bonding, the more unfavorable the permeability process becomes. This has been demonstrated with peptides, which are compounds with high hydrogen forming potential, and they have been shown to have minimal distribution through the BBB (Pardridge, 1998) and low intestinal absorption (Chan and Stewart, 1996).

The hydrogen bonding potential of a drug is measured by the polar surface area (PSA), which is defined as a sum of surfaces of polar atoms (usually oxygens, nitrogens) and their attached hydrogens. PSA is a useful parameter in predicting drug transport properties and has been widely used to investigate blood-brain barrier penetration (BBB) (Feng, 2002) and to predict absorption of drugs (Clark, 1999; Palm et al., 1997). PSA has been shown to be sufficient for determining molecules likely to exhibit poor intestinal

absorption (Fig 1.18a). Intestinal absorption decreases with an increase in the number of hydrogen bonds (Fig 1.18b).

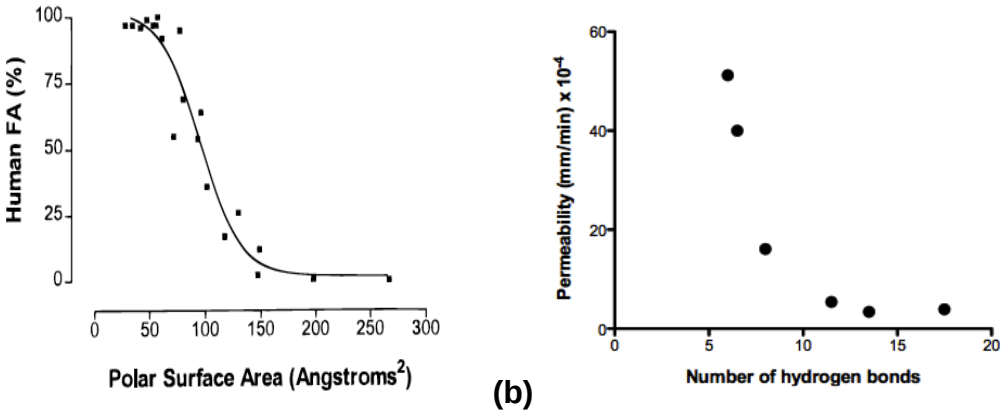

Figure 1.18: The correlation between the polar surface area and intestinal absorption: The amount of compounds absorbed has been demonstrated to decrease with an increase in the polar surface area (a) (Clark, 1999; Palm *et al.*, 1997). This has been further shown in a study done with renin inhibitors (b) (Chan and Stewart, 1996)

1.5.1.3. Lipophilicity

Lipophilicity is the tendency of a compound to partition into a nonpolar lipid matrix versus an aqueous matrix (Kerns and Di, 2008b). It is a very important parameter affecting ADME, toxicity, protein binding and permeability and has been used as a predictor in many *in silico* models. The partition between the aqueous phase and the organic phase when all the compounds are in neutral form is expressed using the relationship

$$LogP = log\left(\frac{[compound_{organic}]}{[compound_{aqueous}]}\right)$$

When the partition is measured at known pH lipophilicity is expressed as the distribution coefficient (Log_D) which is calculated using the relationship;

$$LogD_{pH_x} = log\left(\frac{[compound_{organic}]}{[compound_{aqueous}]}\right)$$

Many methods have been used to measure lipophilicity, but the main ones are the shake-flask, reverse-phase HPLC and capillary electrophoresis. In the shake flask method, compounds are dissolved in dimethylsulfoxide (DMSO) and added to a plate containing a mixture of octanol and buffer. The mixture is agitated and the amount of compound in each phase determined. The reverse phase HPLC method utilizes the partitioning between the aqueous mobile phase and the stationery phase. The lipophilicity of standards, which have known lipophilicity and retention times, is used to calculate the lipophilicity of the unknowns.

The capillary electrophoresis method utilizes microemulsion electrokinetic chromatography, where the affinity for the microemulsion phase is used to estimate LogD (Poole *et al.*, 2000). The greater the affinity the compound has to the stationary phase, the longer time it will take to elute. The LogD is estimated in the same manner as the reverse HPLC methods where a series of standards are used. Various software have also been used to estimated lipophilicity with many chemical drawing software (e.g. CHEMDRAW, ACD and Marvin Beans) incorporating software to calculate lipophilicity.

1.5.1.4. pKa

The pKa is an indication of a compound's ionisability. It is therefore an important factor in determining the physicochemical behavior of compounds at

various pHs. The pKa is defined as the negative log of the ionization constant K_a where, for the ionization of an acid;

$$\mathbf{HA \Leftrightarrow H^+ + A^-}$$

$$pK_a = -log\left(\frac{[H^+] \times [A^-]}{[HA]}\right)$$

From this equation the Henderson-Hasselbach equation, which shows the relationship between pKa and pH, can be derived.

$$pH = pK_a + \log\left(\frac{[A^-]}{[HA]}\right)$$

The Henderson-Hasselbach equation is useful in calculating the concentration of ionic and neutral species if the pKa is known.

Ionized compounds are more soluble in aqueous media than neutral ones as they are more polar. The reverse is true for permeability where ionized compounds are less permeable than neutral ones. Since the pKa determines the degree of ionization it is a major determinant of solubility and permeability. In turn the balance between permeability and solubility is therefore essential for orally absorbed compounds and should be noted when modifications on synthetic compounds are to be made.

Many methods have been utilized in the determination of pKa both experimentally and *in silico*. There has been a variety of software for the prediction of pKa which include MOKA (www.moldiscovery.com), advanced chemistry development (ACD) pKa database (www.acdlabs.com) and some of the software has been added to structure drawing software such as Marvin (www.chemaxon.com). Various experimental methods can also be used with

some being high throughput methods suitable for screening large compound libraries.

The method that is termed the 'gold standard' is the pH-metric method (Avdeef, 1993) where the compound is dissolved in water and titrated with an acid or base mixture of a known molarity. A pH electrode measures the change in molarity. The pKa is measured at the inflection point of the curve. The method has been incorporated in instruments and commercialized for example the Sirius GLpKa instrument (www.sirius-analytical.com). Variations have also been made where UV has been used to monitor the changes in pH, for example in the Sirius spectral gradient analysis method (www.sirius-analytical.com). The spectral gradient method utilizes an HPLC pump and the absorption changes with pH are measured using a diode array detector (DAD). Another method is capillary electrophoresis, which is based on the electrophoretic mobility of a compound in neutral and ionized form in different buffers (Cleveland Jr *et al.*, 1993). The mobility increases with ionization therefore the pKa is obtained by plotting pH against mobility.

1.5.2. Rules based on structural properties

Many rules have been formulated around structural properties with some being used as a standard for rapid property profiling. The most common rule is the Lipinski rule of 5 which is used as a quick predictor of oral absorption and permeability (Lipinski *et al.*, 2001). The rule states that poor absorption is likely when the molecular weight is greater than 500, logP is greater than 5 and if there are more than 5 and 10 hydrogen bond donors and acceptors

respectively. Additions to these rules were proposed by Veber, who added ≤10 rotatable bonds and ≤ 140 $Å^2$ PSA as essential for good absorption (Veber *et al.*, 2002).

Uptake of drugs in the brain has also been shown to be affected by physicochemical properties with a set of rules being defined for a drug to be active in the central nervous system (CNS) like(Pardridge, 1995). The rules states that the MW should be less than 500, LogD should be between 1 and 4, and the PSA should be between 60 and 90 $Å^2$. These guidelines have been generally accepted, and further studies have been done to verify the usefulness of the rules in estimating the BBB crossing of compounds (van de Waterbeemd *et al.*, 1998). The CNS compounds clustered around the MW, LogD and PSA cutoff (Fig 1.19). Although a significant number of non-CNS drugs clustered in the same space, the rules are still very useful for guiding the synthesis of CNS like drugs and also for avoiding them.

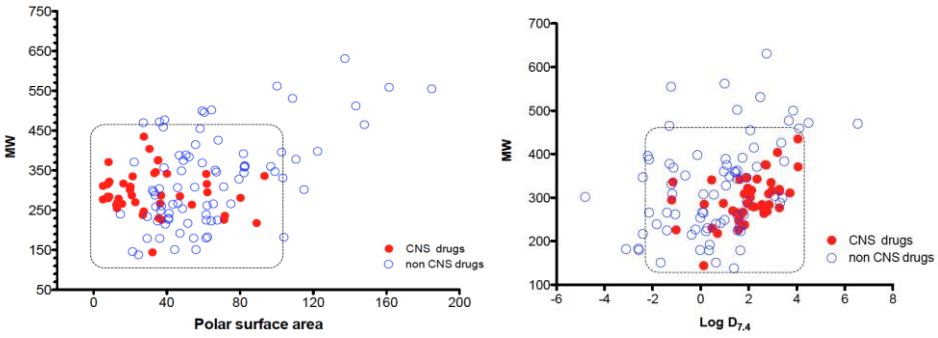

Figure 1.19: Effect of structural properties on blood-brain barrier crossing ability: The influence of size (MW), lipophilicity (LogD7.4) and polar surface area on the ability of compounds to cross the blood-brain barrier (van de Waterbeemd et al., 1998).

Rules have also been defined to guide in the identification of lead like compounds. The rule of 3 where the molecular weight has to be between 350

and 450, the calculated LogP between 3.5 and 4.5, and the LogD to be between -1 and 4 was formulated for lead-like compounds (Oprea, 2002a; Oprea, 2002b). Further computational studies led to a set of further properties being added as guide to identifying lead like compounds (Hann and Oprea, 2004). In these revised rules the Mw ≤ 460, hydrogen bond donors ≤ 5, hydrogen acceptors ≤ 9, rings ≤ 4, rotatable bonds ≤ 10, log of water solubility (LogSw) ≤ -5 and the log P to be -4 ≤ Log P ≤ 4.2.

1.5.3. Physicochemical properties

The most commonly used physicochemical properties are integrity/stability, permeability, solubility, protein binding and volume of distribution. Screening for physicochemical properties is an important aspect of drug discovery as it provides information that is used to design, select and optimize leads with the highest chances of success. The screens are a valuable tool to medicinal chemists because they can be correlated to structure and are the main determinants of ADME. Poor physicochemical properties have also been linked to long development time line and high resource demands mainly due to difficult formulation development, stability and dissolution studies (Kerns and Di, 2008b).

1.5.3.1. Integrity

Integrity screens seek to verify the identity and purity of the compound. Many APIs are produced by organic chemical synthesis, a process that leaves behind various components including residual solvents and various organic and inorganic impurities. It is therefore important to remove these impurities,

as many of the experiments that are performed on the compound will assume the correct identity and purity of the compound. It also provides confidence in SAR data. Purity checks can be done using high performance liquid chromatography (HPLC). However for the verification of the compound structure more sensitive methods such as liquid chromatography-mass spectrometry (LC-MS) and nuclear magnetic reasonance (NMR) are used.

1.5.3.2. Permeability

Permeability is the velocity of a molecule as it passes through a membrane barrier. Permeability experiments are important in drug discovery as compounds often meet membrane barriers in living systems. The major barriers are the gastrointestinal epithelial cells and the blood-brain barrier (BBB). Various methods by which molecules cross the barrier have been described as illustrated in Fig 1.20. Methods to estimate permeability have been described with the parallel artificial membrane assay and the monolayer transport assays being the most commonly used.

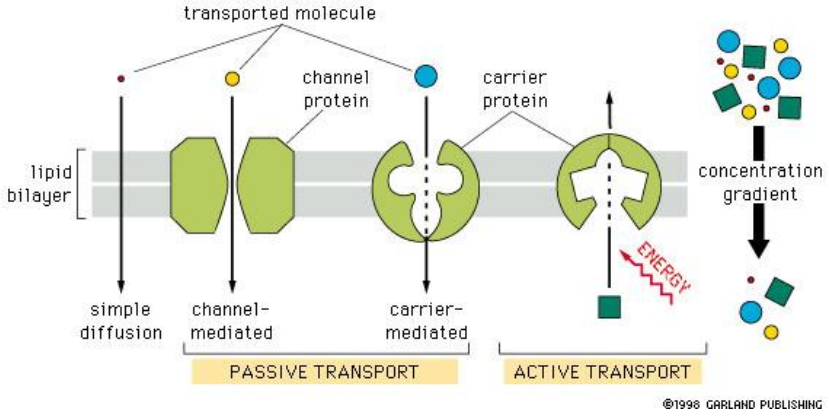

Figure 1.20: Mechanism of transport across cell membrane
Simple (passive) diffusion is the most important mechanism for drugs and it involves movement by Brownian motion across the bilayer. Transport also occurs by active uptake where compounds bind to transmembrane proteins using ATP as a source of energy. Molecules may also enter cells via paracellular transport where they pass through channels between epithelial cells.

1.5.3.2.1. Parallel artificial membrane assay

The parallel artificial membrane assay (PAMPA) (Kansy *et al.*, 1998) effectively measures permeability assuming the mode of transport across the cell membrane is passive diffusion. The system utilizes lipids such as lecithin diluted in organic solvent such as dodecane to mimic lipids in the bilayer of the cell membrane. The assay is performed as illustrated in Fig 1.21.

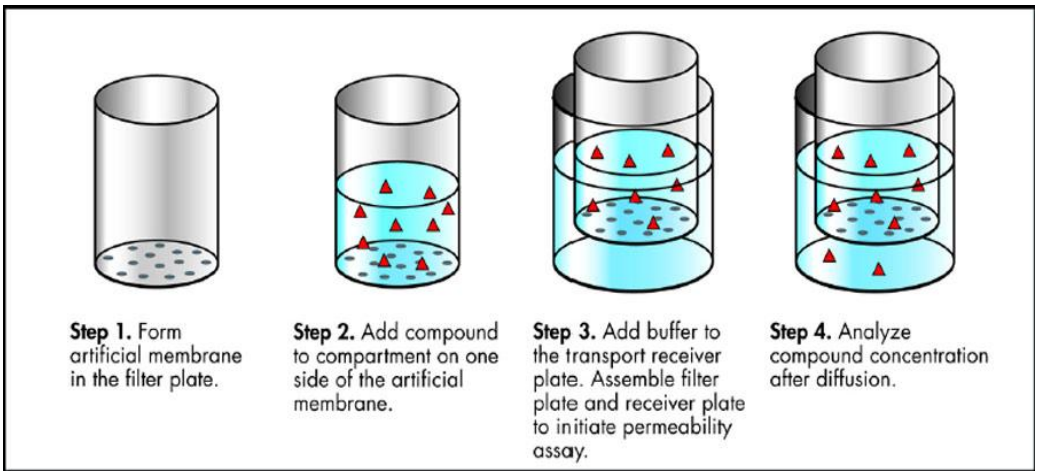

Figure 1.21: Representation of the parallel artificial membrane assay.

The method offers a rapid way of screening compounds and is suitable for high throughput screening. Concentration of compound is then measured from both the acceptor and donor well after an incubation period (5hrs – overnight) and the permeability calculated. Permeability is then calculated using the relationship below:

$$P_{app} = \frac{-\ln [\, 1 - C_A / C_{equilibrium} \,]}{S * (1 / V_D + 1 / V_A) * t}$$

Where C_D = final drug concentration in donor well (μM); C_A =final drug concentration in acceptor well (μM); V_D = volume of drug solution added into the donor well (ml); V_A = volume of buffer added into the acceptor well (ml); $C_{equilibrium}$ = $(C_D * V_D + C_A * V_A) / (V_D + V_A)$; S = membrane area ($cm^2$) and t = incubation time (s)

1.5.3.2.2. Cell monolayer transport

This method utilizes cell lines and takes into account the effects of other mechanisms such as active transport and the effect of transporters. Common cell lines used in this assay include the CaCO-2 (Artursson *et al.*, 2001) and the MDCK (Irvine *et al.*, 1999) cells. The experimental setup is illustrated in Fig 1.22.

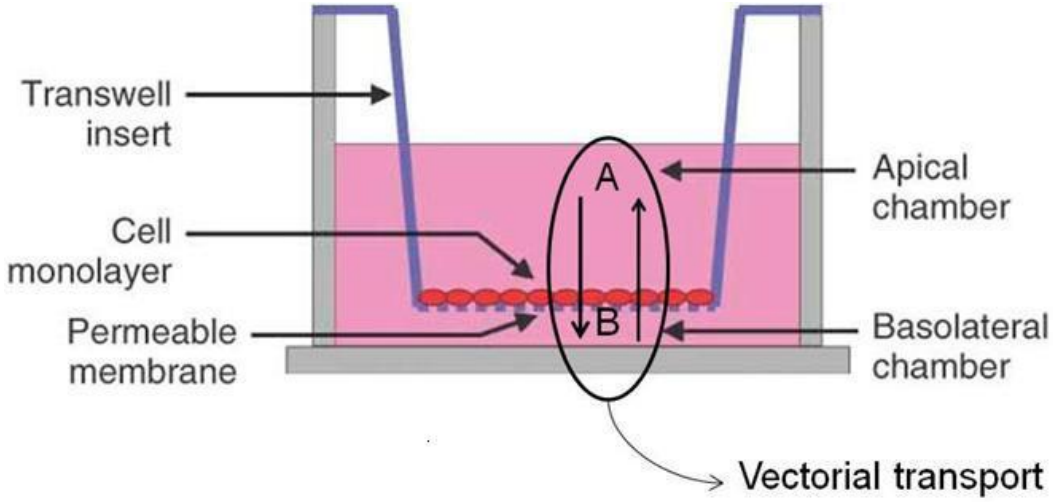

Figure 1.22: Setup for the cell monolayer transport assay. Transport of test compounds can be measured in the A-B as well as the B-A direction. Effect of test compounds on transporters expressed by the cells as they grow can also be investigated.

CaCo-2 cells express efflux transporters such as P-glycoprotein and uptake transporters on the apical side. Permeability experiments are then done by measuring the apical to basolateral transport and basolateral to apical transport. Inhibitors can be incorporated to evaluate their effect on transporters. Permeability and inhibition of transporters by antiparasitic drugs have been investigated (Hayeshi *et al.*, 2006), with a number of the compounds including natural products being shown to be inhibitors of P-glycoprotein.

1.5.3.3. Solubility

Solubility affects absorption hence an important parameter for orally administered drugs. Parameters affecting solubility include pKa, lipophilicity, molecular weight, hydrogen bond formation and size. Poor solubility may necessitate novel formulations, which lead to increases in costs and delays during drug development. Besides being important for the achievement of good oral bioavailability, solubility experiments give a guide for the concentrations that can be used for *in vitro* assays. Poor solubility may lead to misleading data where, for example, a compound may be determined as non-inhibiting where in actual fact the compound will have precipitated and was not available to the enzyme.

The choice of solubility determination experiments is usually governed by the amount of compound available and the experimental factors that need to be controlled. The type of assay needed for the discovery stage may differ to the requirements for the development or clinical stage, and the decisions are governed by a number of factors as illustrates in Fig 1.23.

Thermodynamic and kinetic solubility assays are used to measure solubility. Kinetic solubility assays measure the fastest precipitating species of the compound. The compounds are dissolved in organic solvent, usually DMSO, and then a small volume is added to aqueous buffer. The onset of precipitation is measured by the change in absorbance (Avdeef, 2007) or nephelometry (Bevan and Lloyd, 2000). The solubility assays can be adapted to suit the changes in the gastrointestinal tract by varying the pH of the buffer.

Kinetic assays are suitable for the discovery phase as there are many compounds to evaluate. The method also requires small amounts of compound. The assay however has low sensitivity making it difficult to rank compounds below 20μM (Teng-Man Chen *et al.*, 2002).

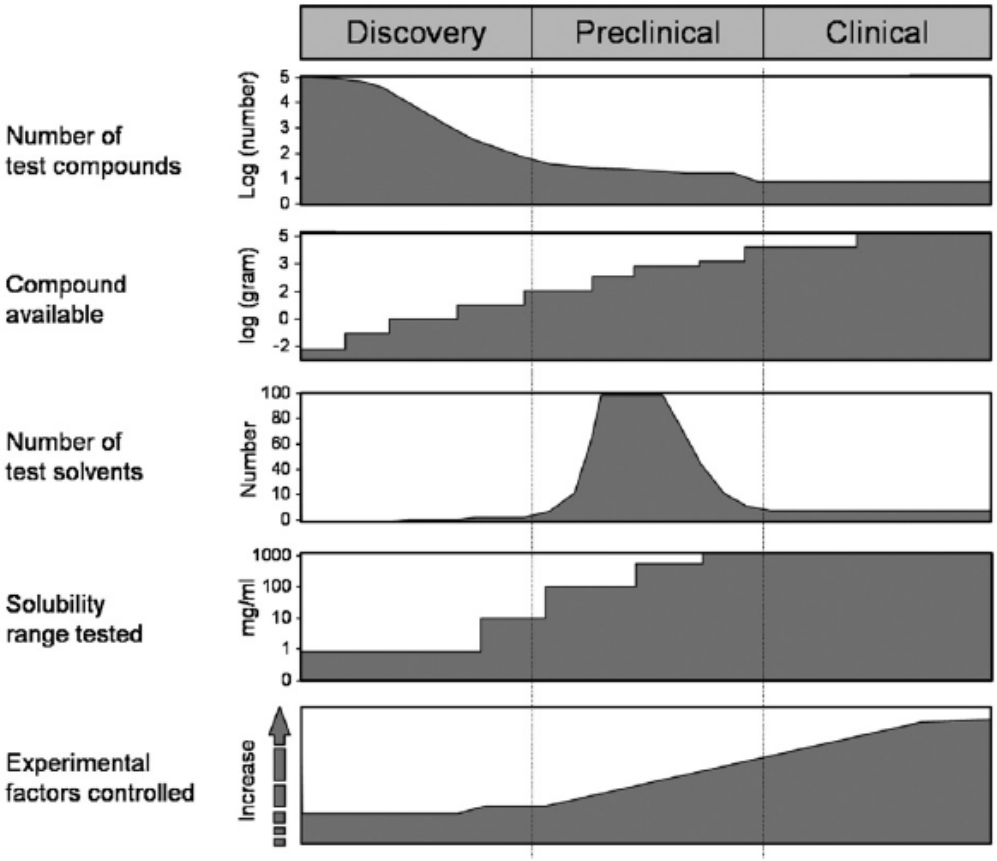

Figure 1.23: Considerations for the setup of solubility assays in drug development: The number of compounds that need to be screened and the quantity of drug available governs the choice of assay. Solubility range and number of experimental factors to be controlled increase as the drug candidate moves along the drug discovery pipeline. The number of solvents used increases in the preclinical stage to provide the necessary data to facilitate formulation. Adapted from Alsenz and Kansy (Alsenz and Kansy, 2007)

Thermodynamic assays measure the saturation of a compound in equilibrium with excess undissolved solid at the end of the dissolution process (Bard *et al.*, 2008). Two methods are commonly used to measure thermodynamic

solubility, namely the shake flask and the pH-metric method. In the shake flask method the solubility is measured by adding solid crystalline solid compound in a vial and adding solvent. The vial is shaken for 24-75 hours under controlled temperature. The undissolved material is then removed by filtration and concentration of compound measured by LS-MS.

The pH-metric method utilizes the pKa of the compound to determine the intrinsic solubility. Known volumes of acid or base are added to a solution of test compound. The pH change produces a titration curve and the pKa shift is used to calculate solubility using the relationship below:

$$Log\ S_0 = Log\ \left(\frac{C}{2}\right) - \left(pK_a^{app} - pK_a\right)$$

Where S_0 is the intrinsic solubility, C is the concentration of compound, pK_a^{app} is the shifted pKa and pKa is the actual measures pKa of compound (Avdeef, 2007)

Thermodynamic solubility measurements are used mainly in development where large amounts of the compound will have been synthesized. It is also an expensive method but it provides better quality data, which can be used to make models for solubility prediction. Apart from the in vitro methods, various software have also been used to measure solubility including Volsurf (Cruciani *et al.*, 2000), AlogPs (www.vcclab.org) and QikProp (www.schrondinger.org).

1.6. Pharmacokinetic screening

Pharmacokinetics is the study of the time course of a drug and metabolite levels in different fluids, tissues and excreta of the body, and the

mathematical relationships required to develop models to interpret such data (Gibaldi and Perrier, 1975). It is a process that describes the fate of a drug from the time it is taken to the time of elimination as illustrated in Fig 1.24. The process involves absorption, distribution, metabolism and excretion ADME. Toxicity can also be added to the process hence ADMET.

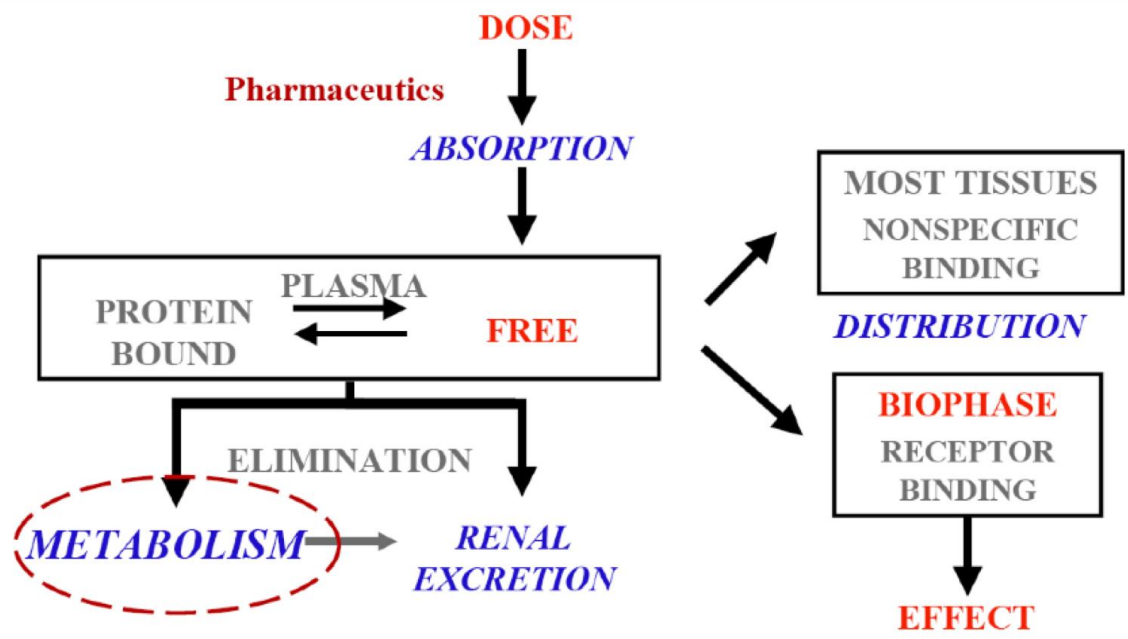

Figure 1.24: The fate of a drug. The drug is absorbed from the site of administration into the blood stream where it is carried to site of action. Many drugs are carried to the liver where metabolism occurs. The drug is changed to more soluble products, which are excreted in urine.

Knowledge of the ADME process will determine how much and how often a certain drug will need to be given to obtain the right therapeutic effect. Concentrations above the therapeutic window may lead to toxic effects and those below may lead to under treatment. The time course for a drug given either orally (p.o.) or intravenously (i.v.) is illustrated in Fig 1.25. The effect of each process is discussed in further detail.

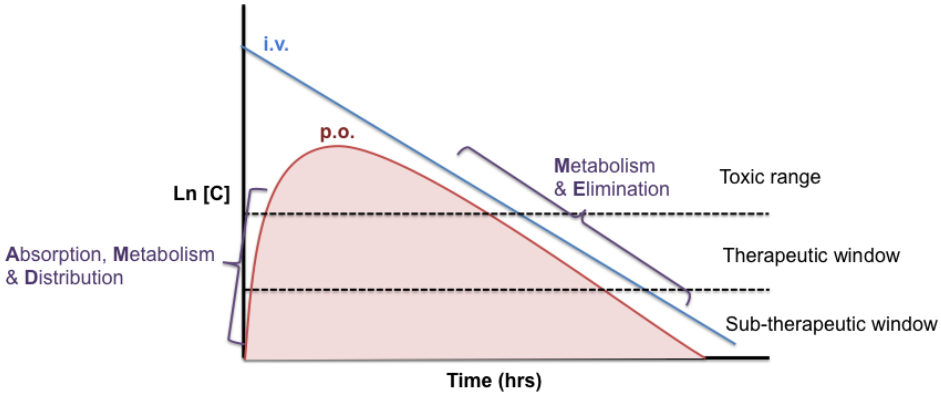

Figure 1.25: Pharmacokinetic profile following p.o and i.v dose.

ADME/PK is one of the main causes of drug failure in the late phases of drug discovery. It was the leading cause of drug failure in the 1990s before PK and ADME screens were developed accounting for up to 40% of drug attrition. The introduction of screening platforms saw a drop in the attrition rate to less than 10% (Fig 1.26)

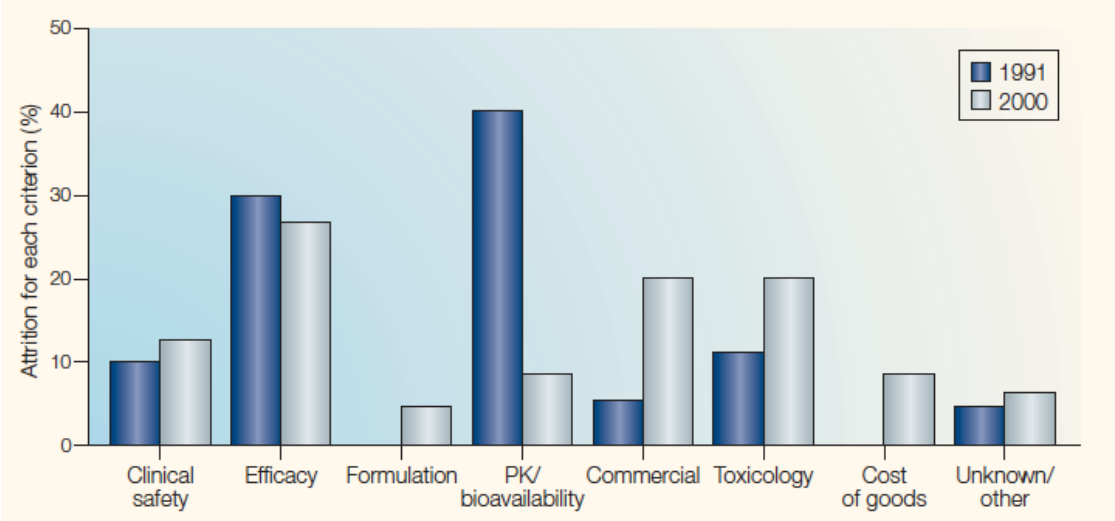

Figure 1.26: Major causes of drug attrition 1991-2000 (Kola and Landis, 2004): With the development of ADME/PK screens poor efficacy, toxicity, and commercial factors are now the leading causes of drug failure.

1.6.1. Absorption

Absorption is the major determinant of bioavailability in orally administered compounds. It is a fundamental property for orally administered drugs as they rely on the absorption in the GI tract and also need to overcome other barriers to get to their sites of action. Many of the drugs are absorbed via the passive diffusion route and the major parameters that affect this are the acid/base character, lipophilicity, solubility and permeability.

The solubility and the lipophilicity are two opposing properties. Highly lipophilic compounds will have low solubility but good permeability across lipid membranes. However for compounds to cross the membrane they have to be in solution requiring lipophilicity to be low. Therefore compounds possessing a good balance of the two have higher chances of achieving high oral bioavailability.

The acid base character as determined by the pKa determines the charge state of the molecule in solution at a particular pH and the site at which most the drug is absorbed. Many drug products are absorbed in their unionized forms. The GI has various pHs depending on the site and the state i.e. whether it is the fasted or fed state as illustrated in Fig 1.26. The ileum and the jejunum offer the greatest area for absorption and it is at these two sites that many drug products are absorbed (Avdeef, 2001) within a pH range of 4.5 -8.0. Also many weak acids are absorbed in the stomach and weak bases in the small intestine.

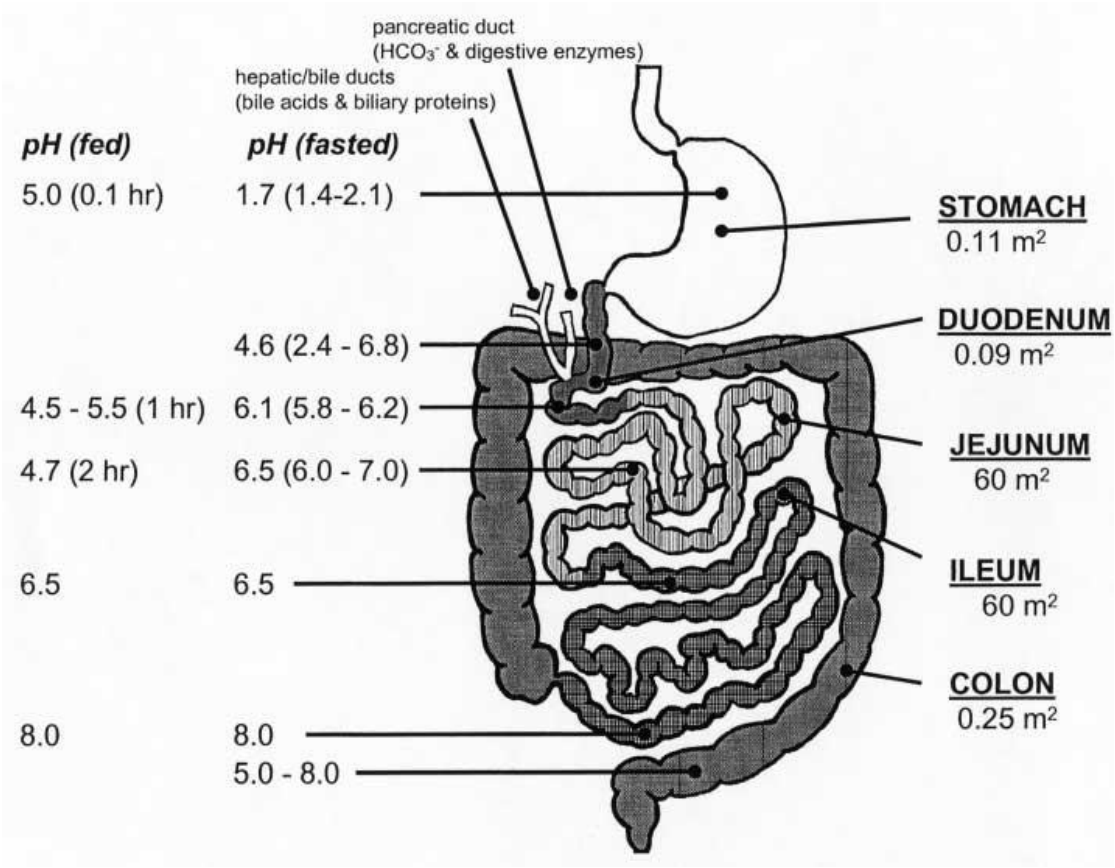

Figure 1.27: Physical properties of the GI tract (Avdeef, 2001).

In vitro, absorption is measured using cell lines such as the CaCO-2 and MDCK. These are models that take into account the role of transporters. Many drugs have been shown to be substrates or inhibitors of P-glycoprotein (P-gp). The role of P-gp has been well studied and it has been shown to inhibit the transport of some compounds across membranes (Burton *et al.*, 2002). Metabolism has also been shown to have a role in the absorption of drugs (Burton *et al.*, 2002).

1.6.2. Metabolism

Metabolism involves the enzymatic conversion from one chemical entity to another. This process is the body's defense mechanism against chemical

insults and is therefore regarded as a detoxification mechanism. It facilitates the excretion of drugs by converting them from lipid soluble non-polar compounds to more polar compounds. Metabolism mainly occurs in the liver with the cytochrome P450 (CYP) being the most important enzymes in the biotransformation of most drugs.

1.6.2.1. Major classes of drug metabolizing enzymes

The drug metabolizing enzymes are a diverse group of proteins responsible for metabolizing xenobiotic compounds. Xenobiotics include drugs, environmental pollutants and endogenous compounds such as steroids and prostaglandins (Guengerich, 1995). The enzymes are grouped as Phase I and Phase II enzymes. The CYP3A family is the largest contributor to drug metabolism in the Phase I enzymes accounting for up to 50% of metabolism of current drugs on the market and UGTs are the most important phase II in terms of metabolism (Fig 1.28). The other enzymes in each class are also shown with their contribution depicted by the size of each section in the chart.

Phase I reactions are mainly performed in the liver and they often make xenobiotics more accessible to phase II reactions. Some phase II reactions can occur directly without first undergoing phase I reactions. The endoplasmic reticulum (ER) and the cytosol are the most important subcellular organelles containing the drug metabolizing enzymes in the hepatocytes. The phase I oxidative enzymes are almost exclusively localized in the ER together with the phase II enzyme, glucuronosyl transferase. Other phase II enzymes including glutathione-S-transferase are predominantly found in the cytoplasm.

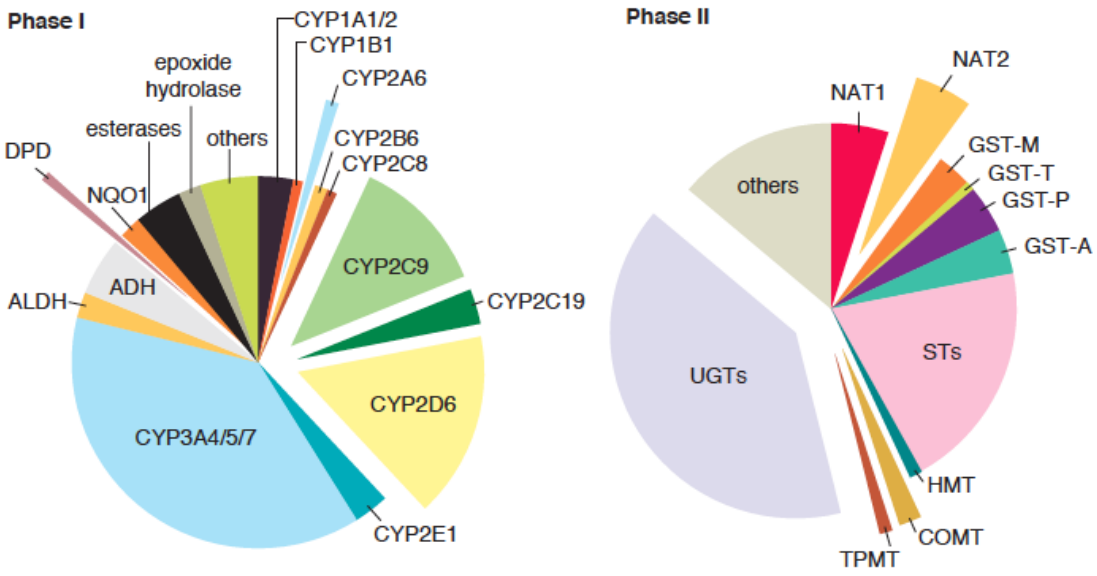

Figure 1.28: The major classes of drug metabolizing enzymes and their relative contribution to drug metabolism (Evans and Relling, 1999).*(ADH, alcohol dehydrogenase; ALDH, aldehyde dehydrogenase; CYP, cytochrome P450; DPD, dihydropyrimidine dehydrogenase; NQO1, NADPH: quinone oxidoreductase or DT diaphorase; COMT, catechol O-methyltransferase; GST, glutathione S-transferase; HMT, histamine methyltransferase; NAT, N-acetyl-transferase; STs, sulfotransferases; TPMT, thiopurine methyltransferase; UGTs, Uridine 5'-diphospho-glucuronosyltransferase).*

1.6.2.2. Sources of drug metabolizing enzymes for metabolism studies

1.6.2.2.1. Subcellular fractions

The liver is the richest source of drug metabolizing enzymes. Other sources include the skin, blood and gut wall. Homogenizing the liver and subjecting it to different centrifugation speeds results in different enzymes sources illustrated in Fig 1.29. The main advantage of the enzyme subfractions is in the ease of preparation for most of them, reproducible nature, capacity for long term storage at -80^{0}C and ample characterization of incubation conditions. They are, therefore, ideally suited for enzyme-substrate interaction studies.

Microsomes are the most used source of enzymes and contain the major membrane bound enzymes including CYPs, FMOs and UGTs. They are particularly useful when comparing results before and after the addition of specific CYP inhibitors, enhancers and antibodies. Microsomes can also be made from pooled liver samples. This takes into account interindividual variability making them a useful in vitro study model (Venkatakrishnan et al., 2003).

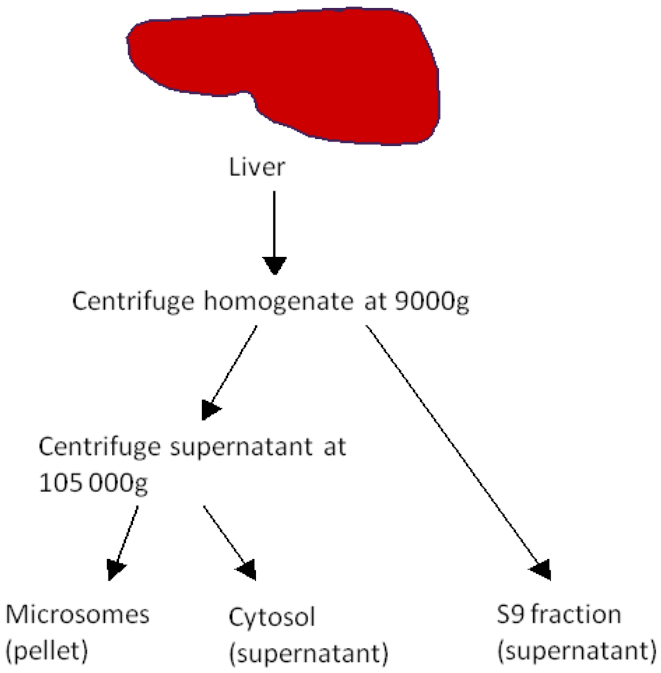

Figure 1.29: Preparation of drug metabolizing enzyme containing subcellular fractions

Hepatocytes and liver slices are prepared from fresh tissue. Their main advantage is that they mimic the *in vivo* enzyme environment as compared to all the other cell fractions. They represent a complete system taking into account the role of transporters. However they are expensive and long-term storage is problematic. The other cell fractions include the cytosol, which mainly contains the phase II enzymes.

1.6.2.2.2. Recombinant enzymes

A variety of systems have been used to express drug-metabolizing enzymes including E. coli, insect cells, yeast and human embryonic cells. Much of the effort has gone into the CYPs because of their predominant role in drug metabolism. The first expression systems to be used were the yeast and the human lymphoblastoid cells (Crespi *et al.*, 1991), but the commercially competent enzymes are the *E. coli* and baculovirus infected insect cells expressed because of the high expression in these systems (Waterman, 1994). Some of the common expression systems for drug metabolizing enzymes are summarized in Table 1.3.

Table 1.3: Expression systems for recombinant drug metabolizing enzymes

Enzyme	Enzyme source	Comment
CYP	Human lymphoblastoid cells	Low expression levels
	Yeast	CYP alone or CYP/reductase
	Baculovirus infected insect cells	CYP alone or CYP/reductase
	E.Coli	CYP alone or CYP/reductase; N-terminal modifications
UGT	COS cells	Low expression levels
	Human Embryonic Kidney (HK293) cells	Highest expression of active protein
	Baculovirus-infected Insect Cells	Expression of active protein at a level less than 1mg/liter
	E. coli	Expression of aglycone or UDPGA binding domains as fusion proteins
ST	Baculovirus-infected Insect Cells	Very high activity levels, purification unnecessary
	E. coli	High level expression of soluble, active proteins
NAT	*E. coli*	High level expression of soluble, active proteins
GST	*E. coli*	High level expression of soluble, active proteins

1.6.2.3. Scope of drug metabolism

Drug metabolism can lead to a variety of outcomes depending on the type of chemical exposure, route of metabolism and the enzyme that is involved. Drugs can be given as prodrugs, which are inactive but are changed to the active form of the drug after biotransformation. An example is the antimalarial proguanil which is relatively inactive but is metabolized to the active cycloguanil by CYP3A family and CYP2C19 (Fig 1.30) (Lu *et al.*, 2000; Birkett *et al.*, 1994).

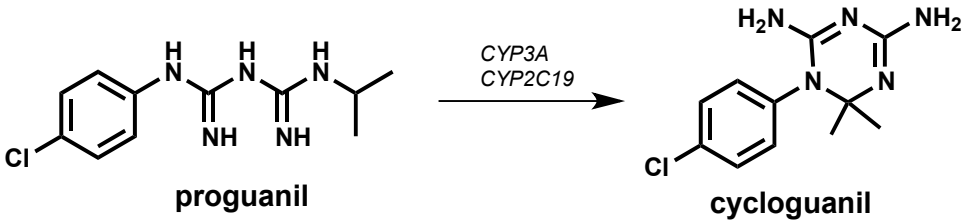

Figure 1.30: CYP3A and CYP2C19 biotransformation of proguanil to cycloguanil

An active drug can also be metabolized to an inactive metabolite. For example, the broad-spectrum anthelmintic drug praziquantel, which is metabolized by CYP3A4 to 4-hydroxypraziquantel (Fig 1.31) (Meier and Blaschke, 2001; Masimirembwa and Hasler, 1994).

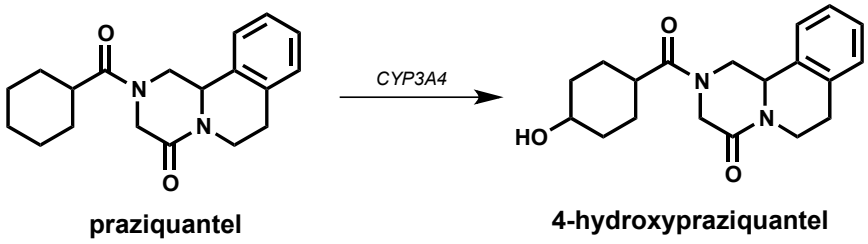

Figure 1.31: CYP3A4mediated biotransformation of praziquantel to 4-hydroxypraziquantel

Metabolism may also result in the formation of toxic metabolism from otherwise safe compounds. An example is the metabolism of paracetamol and amodiaquine. The two compounds are both metabolized to quinoneimine metabolites (Fig 1.32), which have toxic effects. At high concentrations, paracetamol is metabolized by several CYP isoforms including CYPs 2E1, 1A2, 2A6, 3A4 and CYP2D6 (Dong *et al.*, 2000; Laine *et al.*, 2009) to the reactive paracetamol quinoneimine which is associated with hepatic injury.

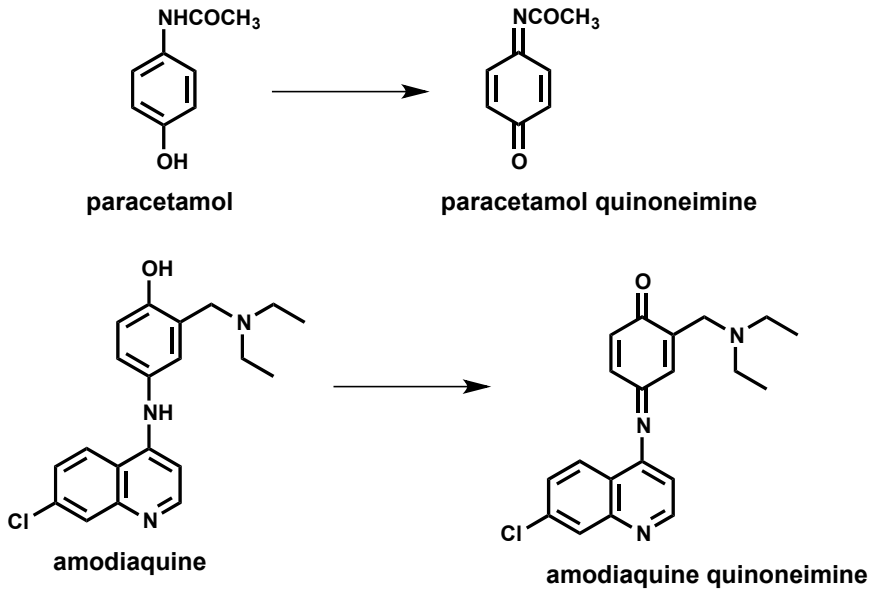

Figure 1.32: Bioactivation of paracetamol and amodiaquine to reactive quinoneimine intermediates associated with toxicity

CYPs have also been associated with bioactivation of xenobiotics such as aflatoxin B1 to carcinogenic aflatoxin B1-8-9-epoxide (Fig 1.33).

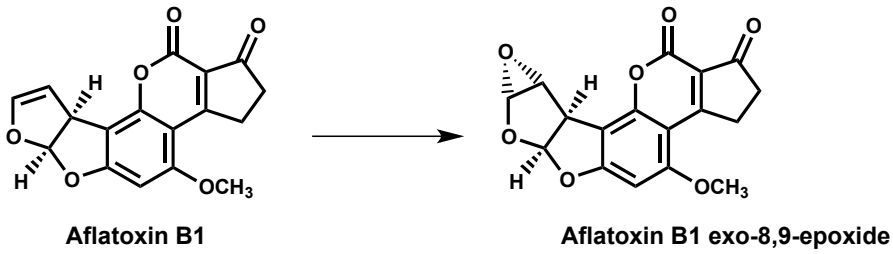

Figure 1.33: Bioactivation of aflatoxin B1 to the carcinogenic aflatoxin B1 exo-8.9-epoxide

1.6.2.4. Assays for evaluating drug metabolism

The most commonly used assays to evaluate drug metabolism are hepatic-based systems. The common assays that are performed are metabolic stability, reaction phenotyping and metabolite profiling which are discussed in detail in the following sections.

1.6.2.4.1. Metabolic stability

Screening for metabolic stability gives an estimation of the susceptibility of a compound to biotransformation. The disappearance of a compound from reaction media containing drug metabolizing enzymes is expressed as the half life ($t_{1/2}$) and intrinsic clearance (CL_{int}). These parameters are then used to calculate secondary pharmacokinetic values such as the hepatic clearance (CL_H), bioavailability and *in vivo* $t_{1/2}$. Hepatocytes and microsomes are the commonly used systems for doing metabolic stability assays as they have a good representation of drug metabolizing enzymes with hepatocytes taking into account phase II enzymes and the role of transporters. Measurements of drug concentrations are conducted using the mass spectrometer.

Several models have been used to extrapolate *in vitro* data to *in vivo* including the well stirred, parallel tube and dispersion models (Houston and Carlile, 1997). Various scaling factors have also been used and they differ depending on the animal model that is being used. Commonly used scaling factors for humans take into account the body weight for an average man (70kg), liver weight (1680g) and number of hepatocytes (117.5 million cells) or microsomes (38.2 mg) per gram liver (Barter *et al.*, 2007; Wilson *et al.*, 2003).

The assay and calculations are performed assuming that the liver is the main organ of clearance, the major elimination pathway is oxidative metabolism, there is no inactivation of the enzyme or non specific binding, and the concentration of the test compound is below the Michaelis-Menten constant (K_m). It is also assumed the rate of metabolism and the activity of the metabolizing enzymes *in vitro* is the same as the *in vivo* situation.

Various *in silico* methods have been used to estimate metabolic stability. Metasite® (Cruciani *et al.*, 2005) predicts sites of metabolic instability and can be useful in structure design where it can be used to determine if planned substructure modifications will be liable to metabolism. VolSurf has been used to predict CYP3A4 stability (Crivori *et al.*, 2004). Other software packages that have been used include KnowItAll (www.biorad.com), ADMENSA (www.inpharmatica.com) and Meteor (www.ihasalimited.org).

1.6.2.4.2. Metabolite profiling

Metabolite profiling involves the incubation of drug candidate with hepatic enzymes followed by identification of major metabolites on mass spectrometer. This allows the identification of major routes of metabolism providing information as to whether modifications need to be made or not. It also allows the selection of animal models to use. Ideal models will be the ones that form metabolites similar to those generated with human in vitro systems. Identification of major metabolites of a lead can allow their synthesis and testing for activity. There are compounds that are active together with their metabolites. Artemisinin is one such example, which has a number of

active metabolites including artesunate and dihydroartemisinin both of which have been registered as effective antimalarials. *In silico* software such as Metasite® are useful in predicting the likely metabolites that can be formed from a compound by various CYPs.

1.6.3. Metabolism based toxicity

Toxicity is responsible for the failure of many drugs and withdrawal of drugs after approval (Fig 1.26). The main causes of drug toxicity include drug-drug interactions and bioactivation into reactive metabolites which bind to proteins and form adducts which are recognized as foreign by the body. Many of the causes of toxicity are metabolism based. Common drug-drug interactions that result in toxicity include induction, inhibition and formation of toxic metabolites.

1.6.3.1. Inhibitory drug-drug interactions

Inhibitory drug-drug interactions have been recognized as one important cause of pharmacokinetic toxicity. The inhibition of metabolism of a co-administered drug may lead to higher plasma concentrations of the other than intended. Many cases of interaction of antiparasitic drugs with drug metabolizing enzymes via different mechanisms have been documented. Inhibition may be reversible, quasi irreversible or non-reversible.

1.6.3.1.1. Reversible inhibition

Reversible inhibition results when inhibitors bind to the enzyme via non-covalent interactions such as hydrogen bonds, hydrophobic interactions and ionic bonds. The inhibitors do not undergo chemical modification and can be

removed by dialysis. Reversible inhibition is further divided into competitive, uncompetitive, non-competitive and mixed modes.

Competitive inhibition is the commonest type of interaction found among therapeutic drugs. In this type of inhibition, the inhibitor has an affinity for the substrate-binding site and therefore competes with the substrate for access to the binding site. However increasing the concentration of the substrate will out-compete the inhibitor hence minimize its effect. Examples of antiparasitic drugs that have been found to be competitive inhibitors include chloroquine, oxamniquine and primaquine (Fig 1.34), which have been shown to be competitive inhibitors of CYP2D6 *in vitro* (Masimirembwa *et al.*, 1995). Chloroquine has also been demonstrated to be a significant inhibitor of CYP2D6 in healthy individuals (Simooya *et al.*, 1998).

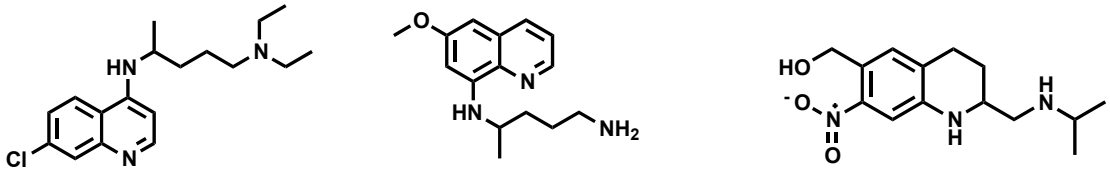

Figure 1.34: Examples of antiparasitic drugs that have been shown to be competitive inhibitors of CYP2D6

Non-competitive inhibitors bind to both the enzyme and the enzyme-substrate complex resulting in reduced activity. This type of inhibition is not affected by increasing the substrate concentration. An example of a non-competitive inhibitor is isoniazid inhibiting phenytoin oxidation. It has been shown to be a potent inhibitor of CYP2C19 and CYP3A *in vitro* (Zeruesenay et al., 2001). *In vivo* it has been shown to be a non-competitive inhibitor of phenytoin oxidation resulting in the accumulation of the drug (Kutt, 1975). Phenytoin oxidation is

saturable at therapeutic doses leading to accumulation of the drug if any minor metabolic interference occurs and the effect is felt more in slow acetylators of isoniazid (Kutt, 1975).

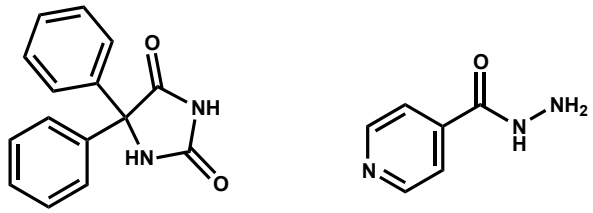

phenytoin isoniazid

Figure 1.35: Structure of phenytoin and isoniazid

Uncompetitive inhibitor binds only to the substrate-enzyme complex preventing the formation of product. This occurs at sites other than the binding site causing the conformation of the enzyme to change. This type of interaction is rare among therapeutic drugs. The differences in the types of inhibition are summarized in Table 1.4.

Drug-herb interactions via inhibitory mechanisms are also very common (Chavez *et al.*, 2006; Fugh-Berman and Ernst, 2001; Izzo, 2005). Inhibition by various forms of St John's Wort have been reported (Chaudhary and Willett, 2006; Obach, 2000).

Table 1.4: Differences between the types of reversible inhibition

	Competitive	Non-competitive	Uncompetitive
Binding site on enzyme	Specifically at the catalytic site, where it competes with substrate for binding in a dynamic equilibrium- like process. Inhibition is reversible by substrate	Binds E or ES complex other than at the catalytic site. Substrate binding unaltered, but ESI complex cannot form products. Inhibition cannot be reversed by substrate.	Binds only to ES complexes at locations other than the catalytic site. Substrate binding modifies enzyme structure, making inhibitor-binding site available. Inhibition cannot be reversed by substrate.
Kinetic effect	V_{max} is unchanged; K_m, as, Defined by [S] required for ½, Maximal activity, is increased	K_m appears unaltered; V_{max} is decreased proportionately to inhibitor concentration.	Apparent V_{max} decreased; K_m, as defined by [S] required for 1/2 maximal activity, is decreased
Lineweaver -Burk plot	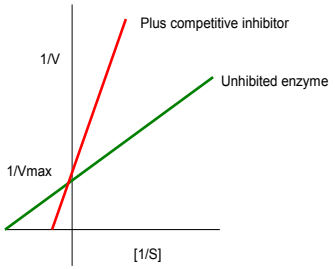	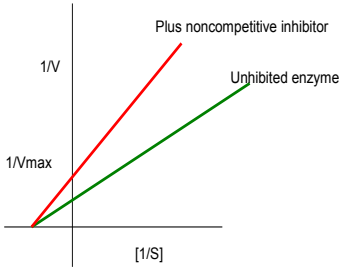	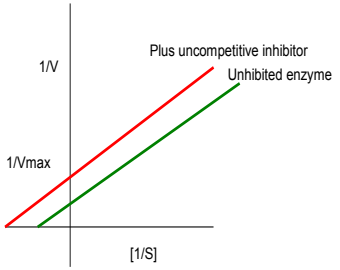
Reaction scheme	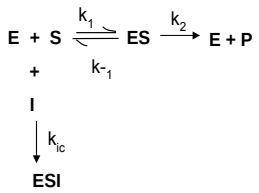	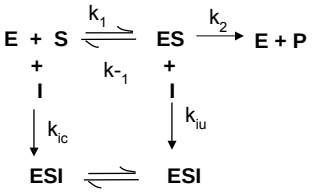	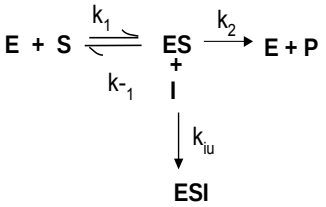
Michaelis –Menten equation	$v_o = \frac{Vmax[S]}{Km\,(1+1/K_i) + [S]}$	$v_o = \frac{Vmax[S]}{Km\,(1+1/K_i) + [S]}$	$v_o = \frac{Vmax[S]}{Km\,(1+1/K_i) + [S]\,(1+1/k_i)}$

1.6.3.1.2. Irreversible inhibition

This type of inhibition cannot be reversed by dialysis, gel filtration or dilution and is more profound than reversible inhibition. Irreversible inhibition is characterized by time and concentration dependence, with slow onset of effects. Irreversible inhibitors are usually good drugs with high specificity for target enzyme, a characteristic that has made them very useful in elucidating enzyme mechanism and in mapping the active site. Irreversible inhibition is divided into two main groups: quasi-irreversible and mechanism based inhibition.

Quasi-irreversible inhibition involves the formation of metabolic intermediates with the heme iron by strong ligation leaving the enzyme in a non-functional inactive state. Binding is not covalent as in mechanism-based inhibition and in some cases it may be reversed. Restoration of catalytic activity may or may not require the synthesis of new protein. This type of reaction is common with drugs that undergo activation by CYPs and form inhibitory complexes e.g. methyldioxybenzenes, alkylamines, macrolide antibiotics e.g. troleandomycin and erythromycin, and hydrazines (Lin and Lu, 1998). Some of the structures are shown in Fig 1.36.

The activity of the enzyme can be restored depending on the compound by incubating the MI complexes with lipophilic compounds or potassium ferricyanide which can displace the MI from the active site. Although this is very easy to do *in vitro,* it is not the case i*n vivo* where the MI complexes tend to be more stable (Lin and Lu, 1998). *In vitro* the displacement can be

determinined by measuring the activity of the enzyme after incubation with compounds that can displace the MI from the active site.

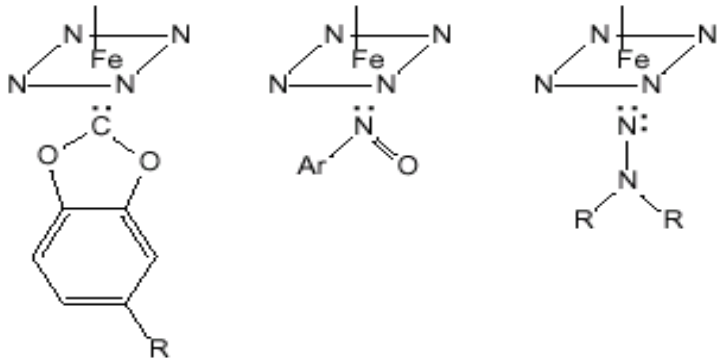

Figure 1.36: Structures thought to form metabolite intermediate (MI) complexes after bioactivation with CYP. Methlenedioxyphenyl compounds which form carbene iron complex (left); alkylamines which form nitrosoiron complexes (middle); and 1.1 dialkylhydrazines which form nitrene iron complex (right) (Lin and Lu, 1998).

Mechanism based inhibition is defined as inactivation of cytochromes P450 (CYPs) by metabolic products that form heme or protein adducts (Silverman, 1988). The compounds that are transformed to reactive species and prior to release from the active site cause inactivation of the enzyme are known as mechanism based or suicide inhibitors (Fontana *et al.*, 2005). There are features that are characteristic of MBI *in vitro* including time-, concentration-, and NADPH dependency, non-prevention by glutathione and free radical scavengers, non reversal by dialysis and protein washing, reduction of P450 content, 1:1 stoichiometric reaction and inactivation following pseudo first order kinetics. Various substructures on drugs have also been associated with this type of inhibition including thiophenes and epoxides (Fontana *et al.*, 2005)

1.6.3.1.3. Inductive drug-drug interactions

This is when a drug accelerates the metabolism of a coadminstered drug by inducing corresponding metabolic pathways. This results in the reduction in efficacy of the affected drug due to lowered plasma levels. An example of a drug which has this kind of effect is rifampicin which is used as part of a regimen in the treatment of tuberculosis. Coadminstration of rifampicin with oral contraceptives has been shown to result in menstrual disturbances and unplanned pregnancies (Daniels *et al.*, 1984). It has also been shown to increase metabolism of cyclosporin in patients resulting in transplant rejection due to low concentrations of the immunosupressive agent (Moddry *et al.*, 1985). In both cases rifampicin induces CYP3A which is responsible for metabolism of the cyclosporin and oral contraceptives. Quinine, primaquine and albendazole have also been shown to cause induction of CYP1A1/2 in HepG2 cells (Bapiro *et al.*, 2002).

1.6.3.1.4. Drug-herb interactions

Herbal medicines are widely used the world over, with 80% estimated to be used in developing countries. Coadminstration of herbs and conventional medicines poses the risk of drug-herb interactions with some having clinical significance. The role of a number of herbs in altering the ADME process has been shown (Zhou *et al.*, 2003). The inductive interaction of St John's Wort with CYPs has been well studied with hyperforin being identified as the causal agent among the various components(Moore *et al.*, 2000).

1.6.3.2. Assays for evaluating metabolism based drug toxicity

There are many *in vitro* assays for predicting toxicity with subsequent extrapolations made to *in vivo* outcomes. This is because there is a clear understanding of the mechanisms of drug-drug/herb interactions. Common assays include the inhibition screen assays, pathway identification and induction screen assays.

Inhibition has also been shown to cause clinically significant interactions between herbs and conventional medicines, Grapefruit juice has been shown to increase oral bioavailability of many conventional drugs including terfenadine, midazolam and verapamil and this has been linked to inhibition of CYP3A4 (Fuhr, 1998). Methysticin and dihydromethysticin, which are components of Kava have been shown to be mechanism based inhibitors of CYPs (Mathews *et al.*, 2002). Other interactions with transporters and enzymes together with the potential adverse effects have been reviewed (Zhang *et al.*, 2012).

1.6.3.2.1. Inhibition assays

Inhibition assays are performed to evaluate whether a drug has potential to inhibit drug metabolising enzymes. The drug metabolising enzyme marker substrate drug is incubated with enzymes systems e.g. human liver microsomes (HLM), hepatocytes or recombinant enzymes. Measurements of the metabolic rate in the presence and absence of drug will enable the estimation of the inhibitory potential of a test compound. The mechanism of inhibition can also be determined. The results from these assays are

expressed as IC_{50} or K_i where the IC_{50} is the concentration of drug required to cause 50% reduction in activity and K_i which is the dissociation constant for inhibitor binding.

1.6.3.2.2. Pathway identification and reaction phenotyping

Experiments are performed to elucidate the metabolic pathways important in the metabolism of candidate drugs. Metabolites and enzymes involved are identified. The candidate drug is incubated in HLM or hepatocytes in the presence of diagnostic inhibitors to identify the likely enzymes involved. Incubations are also performed in a panel of recombinant enzymes which are derived from cells engineered to express specific CYP isoforms.

1.6.3.2.3. Enzyme induction assays

Experiments are performed in enzymes that are known to be inducible for example CYPs 1A2, 2A6, 2B6, 2C9 and 3A4. Hepatocytes are cultured in the presence of the candidate drug and the messenger RNA levels or enzyme activity measured. Reporter cell lines such as the human hepatoma cell line integrated with either the CYP3A4 enhancer region and a luciferase reporter gene or the CYP3A4-luciferase construct and the human pregnane X receptor (PXR) (Raucy *et al.*, 2002)have also been developed and used as rapid screening assays.

1.6.4. Distribution

Distribution is the reversible transfer of drug from and to the site of measurement. The major pharmacokinetic determinants of distribution include

the volume of distribution (V_d), fraction unbound in blood (f_u), fraction unbound in tissue (f_{uT}) and the blood plasma ratio (B/P).

1.6.4.1. Volume of distribution

The volume of distribution gives an indication of how widely a compound is distributed in the body representing the apparent volume in which the compound is dissolved. It is calculated using the relationship below:

$$V_d = (V_{blood} + V_{tissue}).\left(\frac{f_{u,blood}}{f_{u,tissue}}\right)$$

where f_u, blood is the fraction of compound unbound in blood, f_u, tissue is the fraction of compound unbound in tissue. V_{blood} and V_{tissue} is the volume in blood and volume in tissue respectively.

Plasma protein bound and hydrophilic compounds tend to be restricted into the blood stream hence their V_d is close to the V_{blood} (70ml/Kg). Moderately lipophilic and protein bound compounds distribute evenly in tissue and blood hence volume is close to that of body water which is the same as blood volume. Lipophilic drugs on the other hand bind to tissue components and have very low blood concentrations resulting in high V_d values which exceed body water volume. An example of such as drug is the antimalarial chloroquine, which has a V_d of 235 L/Kg because it is highly lipid soluble therefore it binds outside the serum for example in melanin containing cells (Krishna and White, 1996). The drug therefore is extensively distributed into body tissues, including the placenta and breast milk.

1.6.4.2. Protein binding

The binding of drugs to serum or plasma proteins is a saturable process, which occurs via various interactions including hydrogen bonding, van der Waals and electrostatic interactions. It is important to measure protein binding (PB) as it directly correlates to V_d where high plasma PB implies more drug is present in the central blood compartment. Low PB means more drug is free to partition into tissue therefore high V_d. The two plasma proteins that are mostly responsible for binding drug molecules are human serum albumin (HSA) and AGP.

Protein binding has an effect on the PK and exposure to the therapeutic target. Bound drug cannot permeate through cell membranes and is therefore not available for metabolism or excretion. The distribution of the drug is also limited including brain permeation. Besides binding to the protein, drugs can also be bound to red blood cells. It is therefore important to measure the blood/plasma partitioning to know where the bulk of the drug will be. In many PK studies blood is centrifuged and red blood cells removed. This means drug bound to RBCs will not be quantitated. Two techniques are widely used to measure protein binding including ultrafiltration and dialysis.

2 AIMS AND OBJECTIVES

2.1 Aim

To determine ADME/PK properties of new synthetic chemical entities and herb/natural products to guide the molecular design of better analogues and to evaluate the ADMET/PK of anti-parasitic drugs on the market to optimize their safe use.

2.2 Objectives

I. To setup the first pharmaceutical industry standard *in silico* and *in vitro* ADMET platform to support drug discovery and development in Africa

II. To use molecular and kinetics data obtained from biochemical assays and *in silico* computational methods in the identification of ADME/PK liabilities of novel artemisinins and quinoline hybrid new chemical entities with antimalarial activities

III. To determine the molecular mechanism of CYP1A2 inhibition by thiabendazole towards understanding the nature and extent of drug-drug interactions between thiabendazole and CYP1A2 substrate drugs.

IV. To explore the risk of drug-herb interaction by evaluating the ADMET/PK of the natural product, Frutinone A, which is found in herbal extracts used for the treatment of a broad range of infectious diseases.

3 MATERIALS AND METHODS

3.1 Materials

3.1.1. Chemicals and Biologics

Bactosomes from E. coli co-expressing human NADPH-P450 reductase and the individual CYPs (CYPs 1A2, 2C9, 2C19, 2D6 and 3A4) were obtained from CYPEX (CYPEX, Dundee, UK). Human Liver microsomes (HLM) were obtained from BD GenTest (Ellisville, MO). Cryopreserved hepatocytes were obtained from In vitro Technologies (Baltimore, MD, USA). Substrates for the fluorescence-based plate assays including 3-Cyano-7-ethoxycoumarin (CEC), 7-benzyloxy-4-trifluoromethylcoumarin (BFC), 7-methoxy-4-trifluoromethylcoumarin (MFC), and MAMC were obtained from BD GenTest Corporation (Ellisville, MO).

Inhibitors for the CYP assays including sulfaphenazole, ketoconazole, quinidine, α-naphthoflavone, troleandomycin, ticlopidine, erythromycin and paroxetin were obtained from Sigma Chemical Co. (St. Louis, MO). Furafylline, tienilic acid, 1'hydroxybufuralol and bufuralol, were obtained from BD GENETEST Corporation (Ellisville, MO). Fluvoxamine was obtained from Tocris Bioscience (Ellisville, MO).Frutinone A was a generous gift from the Department of Clinical Pharmacology, University of Cape Town.

Reagents and consumables for the fluorescence-based assays including Tris, ACN, β-Nicotinamide adenine dinucleotide 2′-phosphate reduced tetrasodium salt (NADPH), potassium phosphate monobasic, potassium phosphate dibasic, NaOH and black coaster plates were obtained from Sigma Chemical

Co. (St. Louis, MO).Thiabendazole, artemisinin, artesunate, dihydroartemisinin, ivermectin, praziquantel, pyrimethamine, quinine, tinidazole, albendazole, cycloguanil, primaquine, proguanil, amodiaquine, monodesethylamodiaquine, chloroquine, dethylcarbamazine, pyrantel, suramin, 4-chlorophemybiguanide, metoprolol, propanolol, testosterone and niclosamide were obtained from Sigma Chemical Co. (St. Louis, MO).

L-glutathione reduced, potassium ferricyanide, 1640 RPMI media, HEPES, chloroquine, Cremophor, Amar Blue, Eagles Minimum Essential Medium, Bovine foetal calf serum (FCS), Phosphate buffered saline and ethanol were obtained from Sigma Chemical Co. (St. Louis, MO). All other reagents were of reagent grade. All other reagents were of the highest obtainable grade.

3.1.2. Equipment and Software

For in silico predictions, Metasite, Moka, and Volsurf academic licenses were obtained from Molecular Discovery (Molecular discoveries Ltd, Pinner, Middlesex, UK, www.moldiscovery.com). Other software including Autodock (http://autodock.scripps.edu/resources/adt),GOLD (www.ccdc.cam.ac.uk)GLUE (Molecular discoveries Ltd, Pinner, Middlesex, UK, www.moldiscovery.com) and FlexX (www.biosolveit.de)were obtained as either open sources or accessed through collaborative licenses. Key analytical equipment used in this study include, Agilent HP1100 HPLC (Agilent systems, Santa Clara, CA, USA), Waters Quattro and QTof LC-MS/MS machines (Waters, Milford, MA, USA), and the Victor^2 multilabel readers (Wallac, Turku, Finland).

3.2 Methods

3.2.1 PART I: Setting up of the ADME PK platform

The various biochemical and analytical methods were set up in preparation for the screening of the various compounds in the study. A set of marker reactions was used to determine the activity of the enzymes. The formation of metabolite was used to follow enzyme activity. Some of the literature methods were adapted to suit our setting and validations were done to ensure experiments were optimal for the various studies performed.

3.2.1.1 Fluorescence- based plate assays

The assays use chromogenic substrates, which result in the formation of fluorescent metabolites. Measuring the formation of fluorescent metabolite at appropriate wavelength was used to follow the activity of the enzyme. The marker reactions used in this study are summarized in Table 3.1.

3.2.1.1.1 Optimization of assay conditions

Assay conditions were optimized with respect to enzyme concentration, incubation time and substrate concentration. Conditions reported by the enzyme manufacturer for the assays were used as a starting point (www.cypex.com) and other reported generic methods (Crespi *et al.*, 1997; Masimirembwa *et al.*, 1999).

Table 3.1: Marker reactions and detection wavelengths for the fluorescence based plate assays

Marker reaction	Substrate	Metabolite	Metabolite Detection Wavelength (nm)	
			Excitation	Emission
CYP1A2 mediated CEC O-deethylation	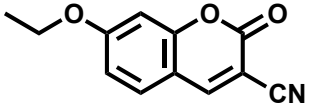 CEC	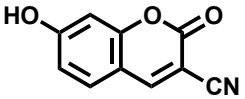 CHC	405	460
CYP2C19/ 2C9 mediated MFC O-demethylation	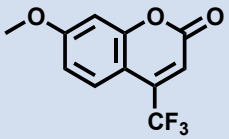 MFC	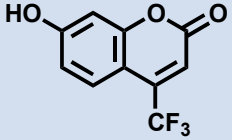 HFC	405	535
CYP2D6 mediated MAMC O-demethylation	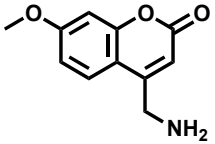 MAMC	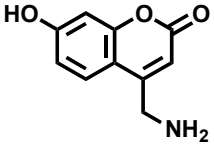 HAMC	390	460
CYP3A4 mediated BFC O-debenzylation	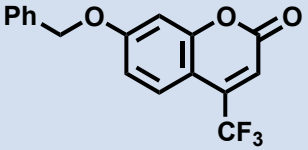 BFC	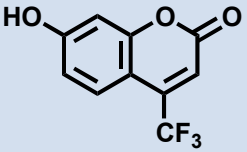 HFC	405	535

CEC, 3-cyano-7-ethoxycoumarin; **CHC**, 3-cyano-7-hydroxycoumarin; **MFC**, 7-methoxy-4-(trifluoromethyl)-coumarin; **HFC**, 7-hydroxy-4-(trifluoromethyl)-coumarin; **BFC**, 7-benzyloxy-4-(trifluromethyl)-coumarin, **MAMC**, 7-Methoxy-4-(aminomethyl)-coumarin; **HAMC**, 7-hydroxy-4-(aminomethyl)-coumarin.

3.2.1.1.1.1 Linearity with enzyme concentration

The assay was performed using generic conditions for fluorescent assays (Crespi *et al.*, 1997) in 96 well black coaster plates (Corning Incorporation, Corning, NY). The substrate concentration used was a quarter of the reported Km in literature. Varying concentrations of enzyme (0-50pmol/ml) were incubated with substrate and 0.1M phosphate buffer pH 7.4. Preincubation was then performed to warm the incubation mixture to 37^0C prior to reaction initiation. The reaction was initiated by addition of 10µl of 20mM NADPH (16mM for CYP2D6). This was followed by 15min incubation in a shaking incubator. Termination of the reaction was by addition of an ice-cold solution of 80% ACN in 5mM Tris. Fluorescence of the metabolites was measured at appropriate wavelength (Table 3.1) using the Wallac Victor^2 multilabel counter (Wallac, Turku, Finland).

3.2.1.1.1.2 Linearity with incubation time

The assay was performed using optimised enzyme concentrations above. Enzyme, substrate and 0.1M phosphate buffer pH7.4 were incubated at varying incubation time ranging between 0 and 1hr. All the other conditions and metabolite detection were as above.

3.2.1.1.1.3 Km determination

The assay was performed using the optimal incubation time and enzyme concentration obtained above. Varying concentrations of substrate in the range of 1 – 200µM were used. Reaction conditions and analysis were as

described above. Km calculations were then performed using SIGMA PLOT Enzyme kinetics module (SYSTAT Software Inc, Richmond, CA).

3.2.1.1.2 Setup of the inhibition assay

The assay was performed using marker reactions and known diagnostic inhibitors for the various CYP isoforms (Table 3.1). The structures of the various inhibitors and the concentrations used in the assay are shown in Table 3.2.

Table 3.2: Experimental conditions for the inhibition assay

CYP	Inhibitor	Structure	Concentration (μM)	
			Low	High
1A2	α-naphthoflavone	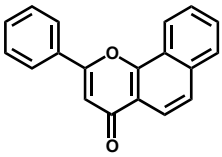	0.01	0.1
2C9	Sulfaphenazole	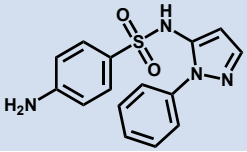	0.1	1
2C19	Ticlopidine	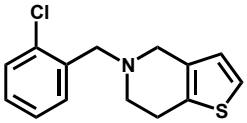	1	10
2D6	Quinidine	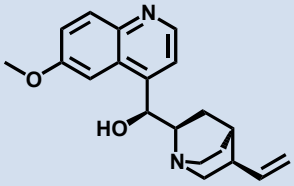	0.01	0.1
3A4	Ketoconazole	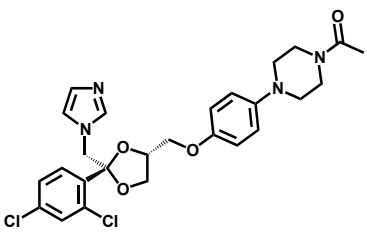	0.1	1

The assay was performed using previously optimized conditions as summarized in Table 3.3.

Table 3.3: Experimental conditions for the reversible inhibition assay

CYP	Enzyme (pmol/ml)	Substrate	[Substrate] (µM)
1A2	2.5	CEC	3
2C19	10	MFC	85
2C9	25	MFC	85
2D6	30	MAMC	15
3A4	10	BFC	13

The inhibitors were incubated with substrate, enzyme and 0.1M phosphate buffer pH7.4. The plate was preincubated for 10min to warm the mixture to 37^0C. Addition of 10µl 1mM NADPH (0.8mM for CYP2D6) was used to initiate the reaction. This was followed by incubation for 15 min at 37^0C. The reaction was terminated by addition of ice-cold 80% ACN in 5mM Tris solution. Formation of fluorescent metabolite was followed at the appropriate wavelength (Table 3.1). The remaining activity was expressed as:

Equation 3.1

$$\%\ remaining\ activity = \frac{inhibited\ \ response}{uninhibited\ response} \times 100$$

3.2.1.1.3 IC_{50} assay

Determining the $IC_{50,}$ values of the diagnostic inhibitors and comparing them to previously reported literature values validated the reversible inhibition assay. Varying concentrations of the inhibitors were incubated with substrate, enzyme and 0.1M phosphate buffer as described for the reversible inhibition

assay. The choice of inhibitor range to use was guided by reported literature IC_{50}s. The ranges were as follows: α-naphthoflavone 0-1μM, quinidine and ketoconazole 0-2μM, ticlopidine 0-100μM and sulfaphenazole 0-12μM. The amount formed at each inhibitor concentration relative to the control (% remaining activity) was plotted against the concentration of the inhibitor. The data was the analysed by non-linear regression and calculated using the IC_{50} model in GraphPad Prism version 5 **(**GraphPad Prism; GraphPad Software, San Diego, CA).

3.2.1.1.4 Setup of the time dependent inhibition assay

The time-dependent inhibition assays was performed using the conditions optimised for the reversible assay as a starting point. The method was adapted to our setting from published methods (Atkinson *et al.*, 2005; Polasek *et al.*, 2006). The assay was conducted in 2 stages namely the inactivation and the activity assay (Fig 3.1).

The reaction mixtures for both the inactivation and activity assays were preincubated to 37^0C prior to reaction initiation. In both assays the reaction was initiated by the addition of 10μl 20mM NADPH (16mM for CYP1A2) and incubation done for 15min. The experimental parameters are summarised in Table 3.4. The buffer was at 0.1M final concentrations and the test compounds were at 1 and 20μM. The reaction was terminated by addition of ice cold 80% ACN in 5mM Tris. Measurement of the formation of fluorescent metabolite was done as described for the reversible inhibition assay.

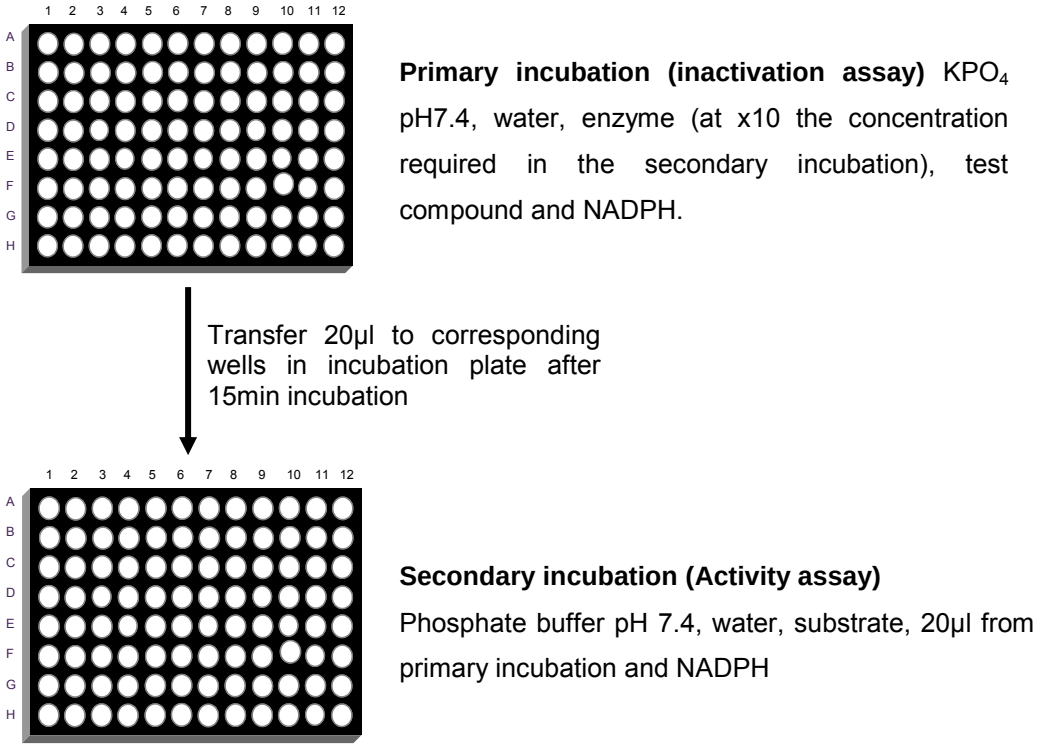

Figure 3.1: Outline for time-dependent inhibition assay

3.2.1.1.5 Calculation of the normalized ratio

In the screen assay, the effect of each inhibitor on the activity of the enzyme was expressed as the normalized ratio calculated as shown in the equation below. The classification was based on the method by Atkinson (Atkinson *et al.*, 2005).

Equation 3.2

$$Normalised\ Ratio = \frac{(R + I^{NADPH})/(R - I^{NADPH})}{(R + I^{no\ NADPH})/(R - I^{no\ NADPH})}$$

where $R + I^{NADPH}$ is the rate of reaction when incubation is performed in the presence of both inhibitor and NADPH, $R - I^{NADPH}$ is the rate of reaction when incubation is performed in the presence of NADPH but in the absence of inhibitor, $R+ I^{no\ NADPH}$ is the rate of reaction when incubation is performed in the presence of inhibitor but in the absence of NADPH, and $R – I^{no\ NADPH}$ is the rate of reaction when incubation is performed in the absence of both inhibitor and NADPH.

Table 3.4: Experimental conditions for the time-dependent inhibition screen assay

CYP	[a][Enzyme] (pmol/ml)	Substrate	[b][Substrate] (µM)	Positive control	Negative control
1A2	25	CEC	12	Furafylline (0.01 and 0.1µM)	Fluvoxamine (0.1 and 1µM)
2C19	100	MFC	*250	Ticlopidine (1 and 10µM)	Sulfaphenazole (0.1 and 1µM)
2C9	250	MFC	*250	Tienilic acid (0.1 and 1µM)	Sulfaphenazole (0.1 and 1µM)
2D6	300	MAMC	60	Paroxetine (0.1 and 1µM)	Quinidine (0.01 and 0.1µM)
3A4	100	BFC	*13	Troleandomycin (0.1 and 1µM)	Ketoconazole (0.01 and 0.1µM)

[a] the enzyme amount in the preincubation mix (10x required in second incubation)

[b] substrate concentration at 4x the Km (to reduce the effect of reversible inhibition)

* Substrate not at 10x the concentration because of solubility limitations

Compounds with a normalized ratio below 0.7 were classified as TDI, those with normalized ratio above 0.9 as non-TDI, and those with a normalized ratio lying between 0.7 and 0.9 fell in the grey zone in which their status cannot be clearly defined.

3.2.1.1.6 Validation of the TDI assay

The two stage time-time dependent assay was validated using known and non-time dependent inhibitors from literature. The compounds chosen for the validation are summarised in Table 3.5. The assay and detection of the formation of the fluorescent substrate was as described above. Validation was done for CYPs 1A2, 2C9, 2C19 and 3A4.

Table 3.5: Validation compounds for the TDI assay

CYP	Strong TDI	Weak TDI	Non-TDI
1A2	Furafylline, bergamottin, resveratrol	Tacrine, ticlopidine, carbamazepine,	Fluvoxamine, α-naphthoflavone
2C9	Tienilic acid, hydrastine and fluoxetine	Methimazole, silibinin, cimetidine, fluvoxamine	Sulfaphenazole
2C19	Ticlopidine, cimetidine	Methimazole	Omeprazole
3A4	Troleandomycin, erythromycin	-	Ketoconazole

3.2.1.2 CYP2D6 inhibition screen assays

The assay was performed because signal to noise ratio for the fluorescence-based plate assay was very low making analysis difficult. The CYP2D6 mediated bufuralol hydroxylation to 1'hydroxy bufuralol was used as a marker reaction. The reaction is shown in Fig 3.2.

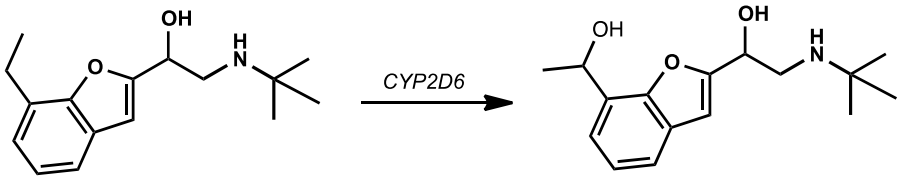

bufuralol 1' hydroxy-bufuralol

Figure 3.2: CYP2D6 mediated bufuralol hydroxylation.

3.2.1.2.1 Inhibition assay

The assay was set up in a similar manner to the fluorescent assay except the substrate used was bufuralol at 5µM final concentration. The reaction was initiated with a 10µl solution of 20mM NADPH. Termination of the reaction was by one volume of ice-cold ACN. The solution was left at -20^{0}C for 1hour to precipitate the protein. This was followed by centrifugation at 13000rpm for 15min at 4^{0}C. The supernatant was collected and analyzed by LC/MS.

3.2.1.2.2 TDI assay

In the inactivation assay CYP2D6 (60pmol/200µl) was incubated with quinidine (0.01 and 0.1µM) in 0.1M phosphate buffer pH7.4. The incubation mixture was warmed at 37^{0}C for 10min. This was followed by addition of 10µl 1mM NADPH to initiate the reaction. Further incubation was performed for 15min. An aliquot was transferred to prewarmed plate at 37^{0}C containing substrate (25µM bufuralol) in 0.1M phosphate buffer pH 7.4. A fresh solution of 10µl 20mM NADPH was added to the mix to initiate the reaction. Further incubation for 15min was done and the reaction was terminated with ice-cold ACN. The solution was left at 20^{0}C for 1hour to precipitate the protein. This was followed by centrifugation at 13000rpm for 15min at 4^{0}C. The supernatant was collected and analyzed by LC/MS.

3.2.1.3 Bioanalysis of 1'hydroxybufuralol

The metabolite (1'hydroxybufuralol) was analysed by LC/MS. Prior to analysis the compound was optimised on LC-MS. A 1µM solution was prepared from the 1'hydroxybufuralol standard and used for the subsequent optimisations. MS conditions were optimised with respect to the cone voltage and the collision energy. The compound was then analysed using the optimised conditions. Bioanalysis was performed on a Waters Quattro (Waters, Milford, MA, USA) with ESI interface. The chromatographic system was an Agilent 1100 HPLC system, using an C18 column (2.1 x 30 mm, 1.8µm). The mobile phases consisted of water and acetonitrile acidified with 0.1% formic acid at 50:50. The flow rate was 0.2ml/min. 1'hydroxy-bufuralol was analysed in +ESI mode where the capillary voltage was 3.5kV, Collision energy was 16 and the cone voltage 25V.

3.2.1.4 Determination of metabolic clearance

The intrinsic clearance (CL_{int}) was determined in human liver microsomes and cryopreserved hepatocytes. Bioanalysis was by HPLC and LC/MS/MS. Extrapolations were done from the determined in vitro clearance to in vivo using scaling factors to determine the hepatic clearance (CL_H) (Barter *et al.*, 2007; Wilson *et al.*, 2003).

3.2.1.4.1 Metabolic stability in HLM assay for analysis by HPLC

The assay was set up using four controls: midazolam, verapamil, diltiazem and tolbutamide as the rapid, fast, intermediate and slow clearance controls (Obach, 1999). The compounds (10µM) were incubated with enzyme

(2mg/ml) and 0.1M phosphate buffer pH 7.4. The reaction was initiated by addition of 1mM NADPH. At varying points (0, 5, 10,15, 20 and 30min) an aliquot was taken and the reaction stopped by addition of ice cold ACN. Extraction was done twice by a double volume of ACN followed by centrifugation at 10000g for 15 minutes at 4^0C. The supernatant was collected and dried under a gentle stream of nitrogen. Residue was reconstituted in mobile phase and analysed by HPLC. Bioanalysis was performed on an Agilent 1100 HPLC system using a Zorbax C18 (4.6 x 150mm ID, 5µm) for chromatographic separation. The mobile phase consisted of **A.** 10mm ammonium acetate acidified with 0.1% TFA and **B.** ACN. An isocratic run was the performed for 15min at a flow rate of 1ml/min. The injection volume was 0.1ml. Detection was by DAD at 214, 254, 230, 286 and 250nm. The disappearance of compound from media was used as a measure of the rate of metabolism.

3.2.1.4.2 Metabolic stability in HLM assay for analysis by LC/MS

The assay was set up using four controls: midazolam, verapamil, diltiazem and tolbutamide as the rapid, fast, intermediate and slow clearance controls(Obach, 1999).The test compounds (1µM) were mixed with HLM (1 mg/ml, BD Bioscience, San José, CA, USA) and phosphate buffer (0.1 M, pH 7.4). After 10 min preincubation at 37°C, the reaction was initiated with the addition of NADPH (1mM). At 0, 5, 15 and 45 min aliquots were taken and quenched 1:1 with a solution of 100% acetonitrile and 0.8% formic acid. The samples were centrifuged at 2737g for 20 min at 4°C and the supernatant was diluted 1:1 in water prior analysis. Bioanalysis was performed on a

Waters TQD (Waters, Milford, MA, USA) with ESI interface. The chromatographic system was a Waters Acquity UPLC system (Waters, Milford, MA, USA) using an Acquity UPLC HSS T3 C18 column (2.1 x 30 mm, 1.8µm). The mobile phases consisted of water and acetonitrile acidified with 0.2% formic acid and the gradient was 4-95% acetonitrile in 1.6 min at a flow rate of 1 ml/min. The compounds were analysed in ES+ mode using conditions in Table 3.6.

3.2.1.4.3 Metabolic stability assay in hepatocytes for LC/MS analysis

The assay was performed using generic incubation conditions with respect to substrate concentration (1µM), incubation time (0-60min) and enzyme concentration (1 x 10^6 cells/ml) (Masimirembwa *et al.*, 2003; Masimirembwa *et al.*, 2001; Thompson, 2000). The substrate concentration was assumed to be much lower than the likely Km of most compounds. Bioanalytical analysis was performed using generic ultra pressure liquid chromatography (UPLC) MS/MS method with a limit of quantitation of at least 0.2µM was used.

The incubations were performed in duplicate in 96-well plates at 37^0C and 5% CO_2/95% O_2 in a Cytomat 2C15 incubator. Test compounds (1µM) were mixed with hepatocytes at a concentration of 1million cells/ml (In Vitro Technologies, Baltimore, MD, USA) and HEPES (25 mM)/l-glutamine (2mM) supplemented William's E medium (Sigma-Aldrich, St Louis, MO, USA). After 0, 15, 30, 45 and 60 min, the incubations were quenched with three volumes of stop solution containing acetonitrile and 0.8% formic acid. In order to assure sufficient precipitation the samples were kept at -20^0C for 20min

before centrifuged at 4^0C at 3220g for 20 min. Prior analysis the supernatant was diluted 1:1 in water.

Table 3.6: Tuning parameters and MRM transitions for metabolic stability control compounds

Compound	Ionization Mode	MRM transitions	Capillary Voltage (kV)	Cone Voltage (CV)	Collision Energy (CE)
Midazolam	+ESI	326.35 > 291.35	3.5	35	25
Verapamil	+ESI	455.71 > 165.23	3.5	30	25
Diltiazem	+ESI	415.52 > 178.09	3.5	35	18
Tolbutamide	-ESI	269.01 > 105.32	3.5	35	30

3.2.1.4.4 Data analysis

The disappearance of compound from media was used as a measure of the metabolism of the compound. The response was log transformed and plotted against the incubation time. The slope of the resulting line (k) was used to determine the in vitro half-life ($T_{1/2}$) using the relationship:

Equation 3.3

$$\boldsymbol{k = \frac{ln\,2}{T_{1/2}}}$$

The *in vitro* apparent intrinsic clearance (CL_{int}) was then calculated using the following relationship for HLM

Equation 3.4

$$CL_{int} = \frac{ln\,2 \times volume\ of\ incubation\ (\mu l)}{T_{1/2} \times amount\ of\ enzyme\ (mg)}$$

and the following relationship in hepatocytes

Equation 3.5

$$\boldsymbol{CL_{int} = \frac{ln\,2 \times volume\ of\ incubation\ (\mu l)}{T_{1/2} \times number\ of\ hepatocytes\ (1 \times 10^6\ cells)}}$$

The CL_{int} was scaled to the whole liver using various scaling factors. The body weight of an average man was taken to be 70 kg, liver weight as 1680g and number of hepatocytes in 1g liver to be 117.5 million cells or microsomes (38.2 mg) per gram live(Barter *et al.*, 2007; Wilson *et al.*, 2003). Using these factors the apparent clearance ($CL_{int,\ app}$) was calculated using:

Equation 3.6

$$CL_{int,app} = \frac{CL_{int} \times HPGL \times Liver\ Weight}{1000 \times Body\ weight}$$

where CL_{int} = *in vitro* clearance and HPGL = hepatocytes per gram liver. In the case of HLM the relationship is as follows:

Equation 3.7

$$CL_{int,app} = \frac{CL_{int} \times MPGL \times Liver\ Weight}{Body\ weight}$$

To estimate the hepatic clearance (CL_H) due to metabolism, the well-stirred model was used. The well-stirred model was chosen against other models such as the parallel tube and the dispersion models because of its simplicity and the fact that very small differences in predicted values by the three models have been observed (Houston and Carlile, 1997). The hepatic clearance was expressed as:

Equation 3.8

$$CL_H = \frac{Q_H \times CL_H}{Q_H \times CL_H}$$

where Q_H is the hepatic blood flow and the CL_{int} is clearance scaled to the whole liver, and reflects the actual metabolic capacity of the enzyme system. The fraction bound in hepatocytes and in blood was not taken into account.

3.2.1.5 Metabolite identification

The assay was performed using the same conditions, as the intrinsic clearance in hepatocytes except the substrate concentration was 4μM and incubation time was120 min. The metabolite profile was obtained from MSE data generated on a Waters Synapt HDMS mass spectrometer (Waters, Milford, MA, USA) operating under positive electrospray ionization (ESI) conditions in V-mode. A generic method with two scan functions was used as follows: m/z 80–1000, cone voltage 25V and 0.1s scan time, the trap collision

energy (CE) in function 1 was 6V and in function 2 an energy ramp of 15–45V was used, the transfer cell CE was 12V. Dynamic range enhancement (DRE) were utilized and data was collected in centroid. Leucine-Enkephaline was used as a lock mass (m/z 556.2771) for internal calibration at a concentration of 250 pmol/µl and a flow rate of 40 µl/min.

Chromatographic separation of metabolites was performed on a Waters Acquity UPLC system (Waters, Milford, MA, USA) using an Acquity UPLC BEH C18 column (2.1 x 50 mm, 1.7µm). The mobile phases consisted of **A**. H_2O/0.1% formic acid and **B**: acetonitrile and the gradient was as 5–65% **B** in 6 min at a flow rate of 750 µl/min. The Metabolynx™ software (Waters, Milford, MA, USA) was used for processing and analysis of the data.

3.2.2 PART II: Identification of ADME/PK liabilities of 3,4-HPO-4-AMINO-7-chloroquinolinyl hybrid compounds with antimalarial activity

3.2.2.1 Structures of the 3,4-HPO-4-amino-7-chloroquinolinyl hybrids

The structures of the synthesized 3,4-HPO-4-amino-7-chloroquinolinyl hybrids are summarized in Table 3.7.

Table 3.7: Structures of 3,4-HPO-4-amino-7-chloroquinolinyl hybrids with antimalarial activity

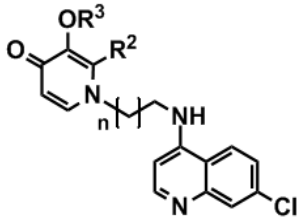

Compound	R^2	R^3	n
3-Benzylated analogues			
3.1a	Me	Bn	1
3.2a	Et	Bn	1
3.1b	Me	Bn	2
3.2b	Et	Bn	2
3.1c	Me	Bn	3
3.2c	Et	Bn	3
3.1d	Me	Bn	5
3.2d	Et	Bn	5
3.2d.2HCl	Et	Bn	5
Deprotected analogues			
3.1e	Me	H	1
3.2e	Et	H	1
3.1f	Me	H	2
3.2f	Et	H	2
3.1g	Me	H	3
3.2g	Et	H	3
3.1h	Me	H	5
3.2h	Et	H	5
3-Methoxy analogues			
3.3a	Me	Me	3
3.3b	Et	Me	3
3.4a	Me	Me	5
3.4b	Et	Me	5

3.2.2.2 Biological assays

3.2.2.2.1 Antiplasmodial screening *in vitro*

Efficacy screening was done using the sensitive (D10 and 3D7) and resistant (W2 and K1) *P. falciparum* strains. The strains were maintained in continuous culture according to the method of Trager and Jensen (Trager and Jensen, 1976). In brief the cultures were maintained in 1640 RPMI media supplemented with 25mM HEPES, 0.23% sodium bicarbonate and albumax II. Synchronization was achieved by sorbitol treatment to leave only the ring stage parasitized cells.

Efficacy screening was done with an initial ring stage parasitemia of 0.8-1.5% at 3% hematocrit. Parasite viability was determined using the parasite lactate dehydrogenase assay according to published methods with chloroquine as the reference drug. The IC_{50} was determined using non-linear regression model in GraphPad (GraphPad Software, San Diego, CA). The phiβ-Haematin inhibition assay was done as described by Ncozaki and Egan (Ncokazi and Egan, 2005).

3.2.2.2.2 Cytotoxicity studies in the KB cell line

The KB cell line, which is derived from human carcinoma of the nasopharynx, was used. The cultures were maintained as monolayers in RPMI 1640 supplemented with 10% HIF at 37^0C under an atmosphere of 5%CO_2/ 95% air mixture. The assay was conducted under the same conditions. On day 1 the cells were harvested, counted, washed in serum free media (2000rpm for 10 minutes at 4^0C) and resuspended in fresh medium at a concentration of 4 x

10^4 ml^{-1}. A 100µl was added to wells in a 96 well plate and incubated overnight to allow cells to adhere. A 10-fold serial dilution of the test compounds starting at 600µg/ml in media was performed across the plate on day 2. Plate was incubated for 72hrs and on day 5 microscopic assessments were made. Alamar blue was then added to each well and the plate incubated for 4hrs after which fluorescence was measure at Ex/Em 530/580. IC_{50} values were then calculated using non-linear regression analysis.

3.2.2.3 Physicochemical screens

3.2.2.3.1 Rule based predictions

The likelihood of the compounds to be drugs and to have good oral absorption was predicted using Lipinski's rule of 5 (Lipinski *et al.*, 2001) and Veber rules (Veber *et al.*, 2002). Potential of the newly synthesized compounds to be lead like was predicted following a set of rules by Oprea ((Hann and Oprea, 2004; Oprea, 2002a; Oprea, 2002b; Oprea *et al.*, 2001). The potential for the drugs to cross the BBB and act CNS drugs was predicted using rules suggested by Pardridge (Pardridge, 1995) and multivariate analysis in VolSurf (Crivori *et al.*, 2000). The various physicochemical properties (clogP, hydrogen bond donors and acceptors) were calculated using the chemaxon property calculator in Marvin Sketch (www.chemaxon.com).

3.2.2.3.2 Purity determination

Compounds were tested for purity using reverse phase HPLC method adapted from literature (de Aquino Ribeiro *et al.*, 2007; Patel *et al.*, 2004; Xie *et al.*, 2007). An Agilent/HP 1100 series LC system (Hewlett Packard, CA,

USA) consisting of a G1311A Quaternary Pumps, a G1322A degasser and G1315A diode array detector was used. Chromatographic separation was achieved on a Zorbax (C18, 4.6 x 150mm I.D, particle size, 5µm). The mobile phase consisted of 5% ACN in 0.1% trifluoroacetic acid **(A)** and 95% ACN in trifluoroacetic acid **(B).** The conditions for gradient solvent elution were 10-25% B in 0-0.5min, 25-90% B in 0.5-5.5min, 90% B in 7-10min and 10% B in 10-15min at a flow rate of 1ml/min. Detection was at 214nm at room temperature. Injection volume was 100µl. Run time was 15min at ambient temperature. Testosterone was run as a control compound. The purity was determined using the relationship:

Equation 3.9

$$Purity = \frac{Area\ of\ compound\ peak}{total\ area\ of\ all\ detected\ peaks}$$

The total area of detected peaks excluded the solvent front

3.2.2.3.3 Lipophilicity determination

Lipophilicity was determined using reverse phase method, which utilizes the capacity factor as a predictor for lipophilicity. The same HPLC system used for determining purity above was used in this assay. Samples were dissolved in 50% ACN. Chromatographic separation was achieved on a Zorbax (C18, 4.6 x 150mm I.D, particle size, 5µm).The mobile phase consisted of 5% ACN in 10mM ammonium acetate **(A)** and 95% ACN in 10mM ammonium acetate **(B).** The conditions for gradient solvent elution were 0% B in 0-2 min, 0-100% B in 2-17min, 100% B in 17-20min and 0% B in 20-22min at a flow rate of 1ml/min. Detection was at 214nm at room temperature. Injection volume was 100µl. Run time was 22min at ambient temperature. Four reference

compounds with accurately determined k´ values and known literature $LogD_{7.4}$ ranging from -0.15 and 5.22 were used for calibration.

3.2.2.3.4 Determination of aqueous solubility

Aqueous solubility was determined using the turbidimetric method. Stock concentrations were prepared in DMSO and diluted in buffer (0.01M phosphate buffered saline pH 7.4) prior to analysis. This was followed by a 2hr incubation at 37^0C. Precipitate formation was followed at 595nm. To avoid false positives, compounds were diluted in solvent (100%) DMSO treated in the same way as the test compounds. Compounds were assayed at concentrations ranging between 0 and 100µM. Paracetamol and niclosamide were used as the soluble and non-soluble controls respectively. *In silico* predictions were done in Volsurf (Cruciani *et al.*, 2000) and AlogPs (www.vcclab.org).

3.2.2.4 *In vitro* ADME experiments

3.2.2.4.1 Determination of CL_{int} and metabolite identification

The CL_{int} was determined in HLM and hepatocytes. The assay was performed as described for the relevant metabolic stability assays in section 3.2.1.4. Data analysis was performed as described in the same section. LC-MS conditions for the hybrids were as summarized in Table 3.8. Midazolam, verapamil, diltiazem and tolbutamide were used as the rapid, fast, intermediate and slow control compounds. Metabolites were identified as previously described (3.2.1.5).

Table 3.8: LC/MS parameters for 3,4-HPO-4-amino-7-chloroquinolinyl hybrids with antimalarial activity(complete this table).

Compound	Ionization mode	Capillary Voltage (kV)	m/z	CV	**Mobile phase (A:B)
3.1a	+ESI	3.5	420.14	30	50:50
3.2a	+ESI	3.5	434.16	30	60:40
3.1b	+ESI	3.5	434.16	30	60:40
3.2b	+ESI	3.5	478.17	30	60:40
3.1c	+ESI	3.5	448.17	35	60:40
3.2c	+ESI	3.5	462.19	35	60:40
3.1d	+ESI	3.5	476.20	35	60:40
3.2d	+ESI	3.5	414.19	35	60:40
3.1h	+ESI	3.5	293.10	28	50:50
3.4a	+ESI	3.5	372.63	30	50:50
3.4b	+ESI	3.5	414.30	30	50:50

*** CV** – Cone Voltage
** **A** - ACN acidified with 0.1% formic acid and **B -** water acidified with 0.1% ACN

3.2.2.4.2 Inhibition screen assay and IC_{50} determination

Inhibition screen assay was performed in recombinant CYPs 1A2, 2C9, 2C19 and 3A4 in 96 well black microtiter plates (Corning Incorporated, Corning, NY) using the inhibition assay previously described (3.2.1.1.2). For the compounds that significantly inhibited (greater than 20% inhibition), the IC_{50} was determined using the reversible IC_{50} assay (3.2.1.1.3). All test compounds were tested at 3 and 20μM for the inhibition screen assay. For the IC_{50} determination the ranges used for all the test compounds was 0-50μM. For CYP2D6 the bufuralol to hydroxybufuralol marker reaction was used to follow enzyme activity. The inhibition and the IC_{50} assays were performed as described in section 3.2.1.2.

3.2.2.4.3 TDI fluorescence-based screen assay

The assay was only performed in CYP3A4. The experiment was conducted using the two-stage TDI screen assay as earlier described. Ketoconazole and troleandomycin were used as negative and positive controls respectively. Conditions for the assay were as in Table 3.4. All the test compounds were assayed at 1 and 20μM. Data was analyzed as described for TDI above.

3.2.2.4.4 Mechanism of inhibition

The assay was an adaptation of the reversible inhibition assay. CYP3A4 was chosen for this study as it showed the greatest susceptibility to inhibition. The difference was in the variation of the inhibitor concentration as well as the substrate concentrations. The substrate concentration was at 0.25, 0.5, 1, 2, 5, and 10x the Km value, and the inhibitor concentration at 0, 0.5, 1 and 2x the IC50 value. The activity at varying substrate concentration was plotted against the activity expressed relative to the control. Plots were made for each inhibitor concentration. The data was fitted using non-linear regression analysis in Sigma Plot software (SYSTAT Software Inc., Richmond, CA) into each of the equation for the different modes of inhibition i.e. competitive, non-competitive, uncompetitive and mixed inhibition models. The model with the best fit was taken to be the mode of inhibition and the K_i, Km and V_{max} calculated.

3.2.3 PART III: Identification of ADME/PK liabilities in artemisinin-chloroquinoline hybrids

3.2.3.1 Structures of the artemisinin-chloroquinoline hybrids

The artemisinin-chloroquinoline hybrids had already been shown to demonstrate potent antiplasmodial activity in both CSR and CQS strains of *P. falciparum* (Feng et al., 2011).Two compounds, **3.9** and **3.10** were chosen for this study together with intermediates and building blocks arising from their synthesis. Artemisinin, dihydroartemisinin and chloroquine were used as controls. The structures are shown in Fig 3.3. Activity for the compounds is summarized in Table 3.9.

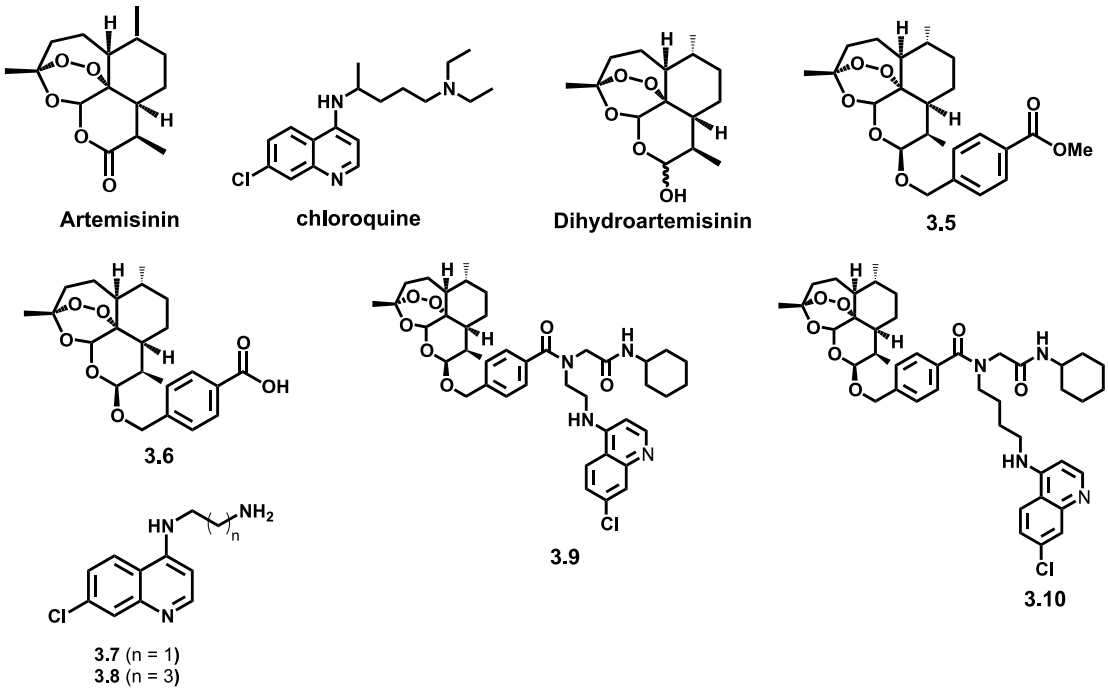

Figure 3.3: Structure of artemisinin-chloroquinoline hybrids, their intermediates, artemisinin, dihydroartemisinin and chloroquine

Table 3.9: *In vitro* efficacy screening of artemisinin-chloroquinoline hybrids and their intermediates

Adapted from Feng (Feng *et al.*, 2011)

Compound	n	D10 IC_{50} (μM)	K1 IC_{50} (μM)	[a]RI	HeLa IC_{50} (μM)	[c]TI	[d]βHIA IC_{50} (equiv)
Artemisinin	-	0.023 ± 0.0014	0.014 ± 0.0037	0.61	[b]ND	-	0.66 ± 0.1
Dihydroartemisinin	-	0.004	0.003	0.75	[b]ND	-	[b]ND
Chloroquine	-	0.020 ± 0.0033	0.219 ± 0.0023	11	8.54	39	1.91 ± 0.3
3.2	-	0.006	0.006	1	[b]ND	-	[b]ND
3.3	-	1.37	2.56	1.87	[b]ND	-	[b]ND
3.4	-	2.15	2.74	1.27	[b]ND	-	[b]ND
3.5	1	0.026 ± 0.014	0.023 ± 0.0014	0.88	0.286	12	0.045 ± 0.04
3.6	3	0.035 ± 0.014	0.021 ± 0.0014	0.60	0.169	8	0.031 ± 0.01

[a]**RI**, Resistance Index; [b]**ND**, Not Determined; [c]**TI**, Therapeutic Index; [d]**βHIA**, β-Haematin Inhibition Assay

3.2.3.2 Metabolic stability in human liver microsomes and hepatocytes

The assay was performed in both human liver microsomes and hepatocytes. Assay conditions, bioanalysis and data analysis were as described for metabolic stability assays in previous sections. The LS/MS conditions used for the artemisinin-chloroquinoline hybrids, artemisinin, chloroquine and dihydroartemisinin are summarized in Table 3.10. Metabolites were identified as described earlier.

3.2.3.3 Reaction phenotyping

All incubations were conducted in duplicate in a final volume of 200µl. Screening was done using recombinant CYPs 1A1, 1A2, 1B1, 2B6, 2C8, 2C9, 2C19, 2D6,2E1, 3A5, 3A4 and human liver microsomes (HLM).Compounds were incubated with appropriate concentrations of recombinant enzyme or HLM and potassium phosphate buffer pH 7.4. All the CYPs were at 10 pmol per 200µl and HLM were at 1mg/ml. Reactions were initiated by addition of 10µl 1mM NADPH. The mixture was incubated for 30 min at 37^0C. All reactions were terminated by addition of ice-cold acetonitrile. Another sample where the reaction was terminated at 0 min was used as a control. The samples were vortexed and centrifuged at 13400 rpm at 4^0C. The supernatant was then collected for LC-MS analysis. Metabolism was signified by loss of compound from the reaction media. The loss of the compound from media was determined using the relationship:

Equation 3.10

$$\%\ Lost\ compound = \left(1 - \frac{area\ at\ T_{30min}}{area\ at\ T_{0min}}\right) \times\ 100$$

Table 3.10: Tuning parameters and chromatographic conditions for the artemisinin-chloroquinoline hybrid drugs and control compounds

Compound	m/z	Ionization Mode	Capillary Voltage (kV)	Cone Voltage (V)	Mobile phase
Artemisinin	*300.05	+ESI	3.5	15	10mM NH_4COOH: ACN acidified with 0.1% formic acid (20:80)
DHA	*285	+ESI	3.5	15	10mM NH_4COOH: ACN acidified with 0.1% formic acid (20:80)
Chloroquine	320.71	+ESI	3.5	30	10mM NH_4COOH: ACN acidified with 0.1% formic acid (35:65)
3.9	761.58	+ESI	3.5	30	Water acidified with formic acid: ACN acidified with 0.1% formic acid (20:80)
3.10	790.75	+ESI	3.5	35	Water acidified with formic acid: ACN acidified with 0.1% formic acid (20:80)

* NH_4 adducts

3.2.3.4 Inhibition assays

The compounds were screened for inhibition using the previously described assay (section 3.2.1.1.2 and 3.2.1.1.3). IC_{50} determination was done for compounds showing potent inhibition in CYP3A4.

3.2.4 PART IV: Molecular Mechanism of CYP1A2 inhibition by TBZ

3.2.4.1 Screening antiparasitic drugs for TDI

Antiparasitic drugs had been previously screened for inhibition against the five major CYP isoforms (CYP1A2, 2C19, 2C9, 2D6 and 3A4) from our previous studies (Bapiro *et al.*, 2005). To continue the work the antiparasitic drugs were screened for TDI as some of the compounds had already shown potent inhibition against some of the CYPs. Twenty-one compounds were screened using the 2-stage TDI assay. Screens were done for CYP1A2, CYP2C9 and CYP3A4. The structures of the screened compounds are shown in Fig 3.4. Thiabendazole (**TBZ**) was chosen as the compound do further studies on. Its metabolite 5-hydroxy-TBZ (**5OH-TBZ**) was also screened for TDI. All the subsequent assays were performed on CYP1A2, the enzyme TBZ significantly inhibited.

3.2.4.2 IC_{50} determination

The assay was conducted in a similar way to the TDI screen assay except that the concentration of inhibitor was varied. **TBZ** and its metabolite **5OH-TBZ** were preincubated at varying concentrations ranging from 0 - 40μM with 25pmol/ml of recombinant CYP1A2 in 0.1M KPO_4 pH 7.4. The assay was performed in the presence and absence of NADPH. The activity assay was then performed with high CEC concentration (12μM) to minimise the contribution of reversible inhibition. Reaction termination and measurement of CEC was conducted in the same way as the TDI screen. The data was analysed by non-linear regression and fitted into GraphPad as described earlier.

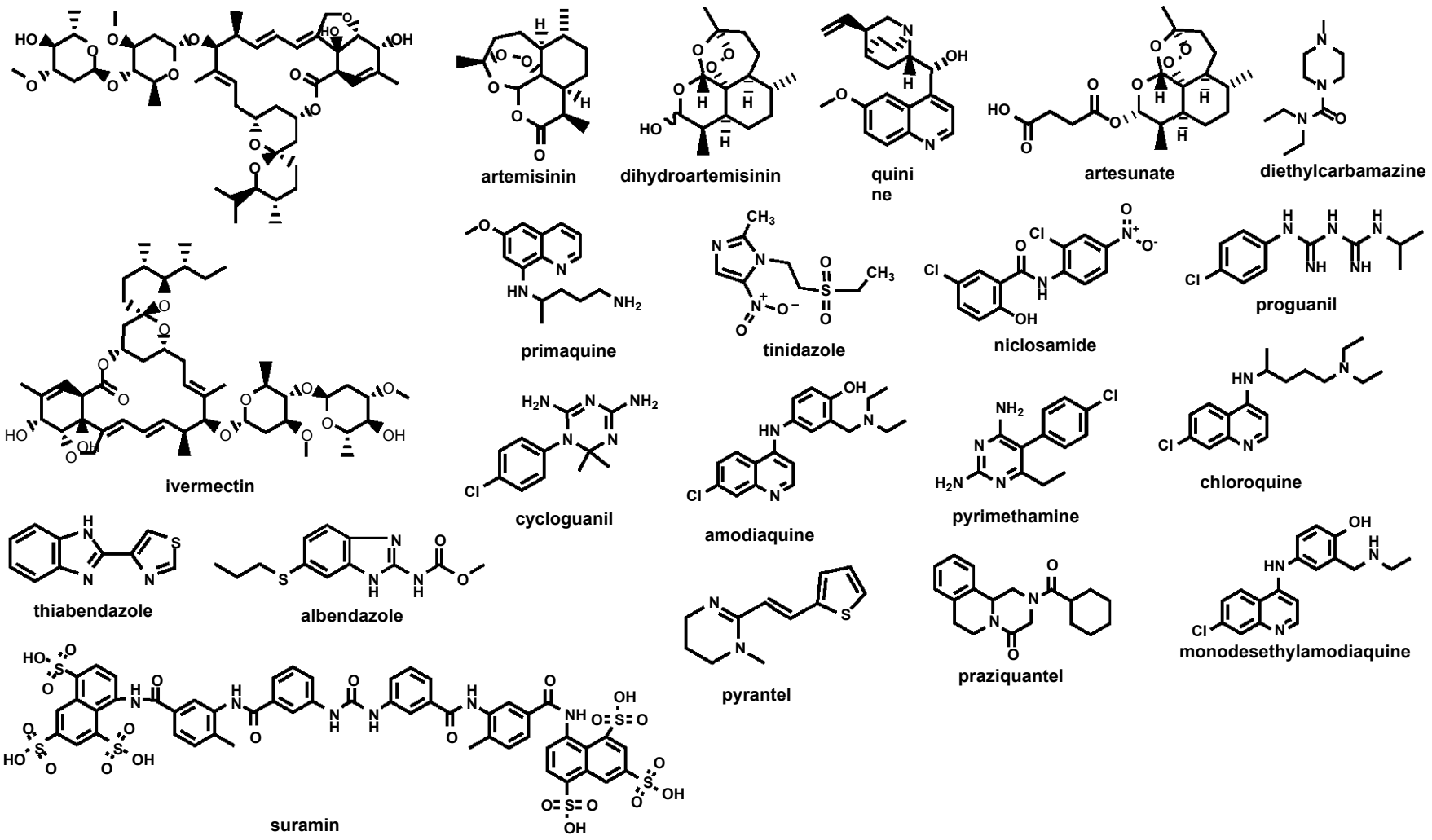

Figure 3.4: Structures of antiparasitic drugs screened for time-dependent inhibition

3.2.4.3 Kinetics of CYP1A2 inhibition by TBZ and 5OH-TBZ

The two-step incubation method was used to characterise the time- and concentration-dependent inhibition of **TBZ**. In the inactivation assay varying concentrations of **TBZ** (0-20µM) and **5OH-TBZ** (0 -200µM) were incubated with CYP1A2 (25pmol/ml) in 0.1M KPO_4 pH 7.4. The reaction was initiated by addition of 10µl 20mM NADPH. At selected preincubation times an aliquot of the preincubation mix (1:10 dilution) was taken and added to the activity assay plate. Incubation was done for 15min at 37^0C. The reaction was terminated by addition of ice-cold 80% ACN in 5mM Tris solution. The activity was followed by measuring the formation of CEC.

3.2.4.4 Mechanism of TDI

Various experiments were conducted to determine if **TBZ** and its metabolite were MBI of CYP1A2. The assays conducted were the IC_{50} shift, electrophile trapping by glutathione (GSH), oxidation by potassium ferricyanide (K_3FeCN_6) and dialysis.

3.2.4.4.1 IC_{50} shift

Two assays were conducted to determine the IC_{50} shift. The first assay was the competitive inhibition assay where the inactivation step was omitted. **TBZ** and **5OH-TBZ** were incubated with substrate at Km concentration (CEC at 3µM) in 0.1M KPO_4 pH 7.4. In the second experiment the IC_{50} was determined using the TDI IC_{50} assay, which was conducted in a similar way as above (3.2.2.2). In both experiments the reaction was initiated by addition

of 10µl 20mM NAPDH followed by 15min incubation. Analysis of fluorescent metabolite was as described for the fluorescent-based plate assays.

3.2.4.4.2 Effect of glutathione on the inactivation of CYP1A2 by TBZ

The time-dependent inactivation of CYP1A2 by **TBZ** was investigated in the presence of 5mM GSH. The GSH was added together with **TBZ** (1 and 20µM) in the inactivation assay both in the presence and absence of NADPH. The activity assay was then performed and the enzyme activity followed by measuring the formation of CHC. Control activities were determined in the absence of **TBZ**.

3.2.4.4.3 Effect of K_3FeCN_6 on the inactivation of CYP1A2 by TBZ

The assay was performed to determine whether the catalytic function of recombinant CYP1A2 could be restored after oxidation by K_3FeCN_6 (2mM in 0.1M KPO_4 pH 7.4). The combined effect of K_3FeCN_6 and GSH was also investigated and in this case GSH was added in the inactivation assay. The experiment was divided into three parts: the inactivation assay, restoration of activity assay and the activity assay. An aliquot (50µl) was taken from the inactivation assay after 10min and added to the activity restoration assay plate, which had 50µl K_3FeCN_6 (0.1M KPO_4 pH 7.4 for the controls). After a further 10min incubation, another 10µl aliquot was taken and added to the activity assay plate. The activity plate consisted of fresh 0.1M KPO_4 pH 7.4, 1mM NAPDH and 12µM CEC. The reaction was then terminated by addition of an ice-cold 80% ACN in 5mM Tris solution. The activity was followed by measuring the formation of CHC.

3.2.4.4.4 Effect of dialysis

The 2-step assay was adapted to determine the effect of dialysis. In the inactivation assay 25pmol/ml CYP1A2 was incubated with NADPH and either 1µM furafylline, 20µM fluvoxamine, 20µ **TBZ**, 20µM **5OH-TBZ** or 0.2 DMSO (vehicle control) 0.1M KPO_4 pH 7.4. The incubation mixture was transferred to Slide-A-Lyser mini-dialysis units with molecular weight cut off of 10 000 (Pierce Chemicals, Rockford, IL). Dialysis was performed at 4^0C for 4hrs in 50mM KPO_4 pH 7.4. The dialysis buffer was changed every hour. Parallel analysis was performed with incubation mixes that were stored at 4^0C for the duration of the dialysis experiment. Samples were then analysed for activity as above.

3.2.4.5 *In silico* experiments

3.2.4.5.1 Substructure search and site of metabolism prediction

A TDI substructure search was performed before the site of metabolism prediction to identify chemical groups in TBZ that were likely to cause TDI. An in house script (Susanne Winiwater, unpublished) was used in the identification. TBZ was then submitted to Metasite version 2.7.5 (Molecular discoveries Ltd, Pinner, Middlesex, UK, www.moldiscovery.com) to predict the site(s) of metabolism. Metasite is fully automated and it considers structural complementarity between the enzyme active site and the ligand and comes up with the optimal orientation. Both the protein active site and the ligand are presented by selected distance–based descriptors using molecular interaction fields computed in GRID. The site of metabolism is described by a probability index that is a product of similarity between ligand and protein. Default

parameters were used and the top three averaged rankings with the reactivity component enabled were considered. Calculations were performed in a Linux (RedHat 8.0) operating system on a 1.8-GHz Pentium IV computer.

3.2.4.5.2 Docking studies

A crystal structure of CYP1A2 in complex with α-naphthoflavone (PDB2HI4) with a resolution of 1.95Å was used. The enzyme is a wild type except that the terminal transmembrane helical domain was removed to increase the solubility for crystallisation. The co-crystallised α-naphthoflavone was removed before docking. The structure of **TBZ** was drawn in SYBYL and converted to a 3D structure in CORINA. Two docking software were used namely GOLD and GLUE.

3.2.4.5.2.1 Docking experiments in GLUE

TBZ was docked into the active site of CYP1A2 with the crystallographic water molecules. The program maps the active site using hydrophobic, hydrogen bond donor/acceptor and electrostatic probes. Prior to the docking experiment the ligand is removed from the active site of the crystal structure. A dummy molecule incapable of accepting hydrogen bonds was added above the heme iron to inactivate the interactions between docked compound and the heme. The PDB file was modified in GREATER, which converted the PDB file format to the input required for the docking procedure (kout file). Default parameters were used for the docking procedure.

3.2.4.5.2.2 Docking experiments in GLUE

TBZ was built and energy minimized in vacuo using the conjugated gradient method, which employs MMF94s force field and charges. The genetic algorithm implemented in GOLD was then used to optimise the orientation of the ligand into the active site. During the optimisation, the ligand was considered flexible and the enzyme active site rigid. Ten dockings were allowed with an early termination if the root mean square distances were within 1.5Å for the top three solutions.

3.2.4.5.3 Prediction of drug-drug interactions

PK simulations were performed using the Simcyp population based ADME simulator version 8.1 to simulate the *in vivo* effects of **TBZ** on the elimination of itself and other CYP1A2 substrates: caffeine and theophylline. In general the simulation process involved uploading enzyme kinetic data for TBZ. The pharmacokinetics data for CYP1A2 substrate drugs were already uploaded in the Symcyp software. *In vivo* co-administration of **TBZ** with CYP1A2 was only available for caffeine and theophylline. The modelling that was performed mimicked published experimental methodology (e.g. dose, interval, duration and sample size) when **TBZ** was administered alone (Tocco *et al.*, 1966a) or in combination with theophylline (Schneider *et al.*, 1990) and caffeine (Bapiro *et al.*, 2005). A fasted virtual Caucasian population was used in all the simulations. Clinical trial sample sizes of 10 were used in all the evaluations. The oral route of drug administration was considered in this scenario for all the DDIs tested, and an additional theophylline-**TBZ** interaction was also simulated after theophylline infusion (Schneider *et al.*, 1990).

3.2.4.5.3.1 Competitive inhibition

In these simulations, **TBZ** was the competitive inhibitor, with a K_I value of 1.54μM as determined in our previous studies (Bapiro et al., 2001). The affected drugs were caffeine and theophylline given at doses used clinically. A single oral dose pharmacokinetic trial design was considered in all simulations that involved competitive CYP1A2 inhibition.

3.2.4.5.3.2 MBI

Clinical drug doses, frequency and duration of 3 days (TBZ is dosed twice daily for 3 days), were uploaded at trial design stage. The effect of **TBZ** on its own elimination was also tested after 3 days of administration. In addition, **TBZ**-theophylline interactions were simulated following published data (Schneider et al., 1990).

3.2.5 PART V: Drug-herb interaction by evaluating the ADMET/PK of the active ingredient natural product, Frutinone A

3.2.5.1 *In vitro* experiments

3.2.5.1.1 CL_{int}, metabolite identification and reaction phenotyping

The assays were performed using generic incubation conditions as described in the previous sections. For metabolic stability assay Frutinone A was run at a cone voltage of 30 in positive electrospray mode. All the other conditions were as described in the previous sections.

3.2.5.1.2 Inhibition and TDI screens

All incubations were conducted in duplicate in a final volume of 200µl. The inhibition, TDI and IC_{50} and mechanism of inhibition assays were performed as previously described. For the IC_{50} screen Frutinone concentrations were as follows: 0, 0.098, 0.195, 0.391, 0.781, 1.563, 3.125, 6.25, 12.5, 25, 50 and 100µM. Inhibition and TDI screens were performed in all the 5 major CYPs. The IC_{50} screen was only performed in CYP1A2.

3.2.5.1.3 Mechanism of inhibition of CYP1A2 by Frutinone A

The experiment was performed as previously described (Part I). Differential inhibition of CYP1A2 by Frutinone A was investigated in this assay. Two substrates were used: CEC and 7-ethoxyresorufin (ER). This was done because some CYP1A2 inhibitors have been shown to exhibit different modes of inhibition based substrates used(Shimada *et al.*, 2010).

3.2.5.2 *In silico* experiments

Calculations were performed on a windows operating system on a 1.6-GHz

core duo computer. Docking experiments were performed using Autodock Vina (Trott and Olson, 2010) and FlexX (*www.biosolveit.de).* The crystal structure of CYP1A2 in complex with α-naphthoflavone (PDB2HI4) with a resolution of 1.95 Å was used (Sansen *et al.*, 2007).

3.2.5.2.1 Autodock Vina

Ligand files were prepared using Autodock tools (http://autodock.scripps.edu/resources/adt). Polar hydrogens were added to the protein and Gasteiger charges were assigned and non-polar hydrogens merged automatically. Charge of the heme, Fe, was corrected manually to 3^{+}. Automated docking was done using Autodock Vina. A grid box centered at 2.61, 18.23 and 20.35 defined the binding pocket. The dimensions of the grid were 50 Å x 50Å x 50Å and were separated by 0.375 Å. In docking all the rotatable bonds were allowed to rotate freely. After docking the results were clustered using a mean root square deviation cut-off of 2.0Å. Clusters were ranked according to the binding energies of their representative structure within each cluster. Docking results were analysed using the PyMOL molecular graphics system (DeLano, 2002).

3.2.5.2.2 FlexX

The active site was defined by the coordinates of α -naphthoflavone in the crystal structure (PDB2H14). Atoms within 6.5 Å of the complexed structures were included as part of the active site. Water molecules and metal atoms were kept in the protein description. Ligands were submitted to the program as mol. 2 files and charges were assigned and automatically distributed in

delocalised systems of the ligands. Energy minimizations of ring systems were done by CORINA_F (Molecular Networks GmbH, Erlangen, Germany http://www.mol-net.de), which is part of the software. Docking was done using default settings.

4 RESULTS

4.1 PART I: Setting up of the ADME/PK platform

4.1.1 Optimization of conditions for fluorescence-based plate assays

Reaction conditions were optimized with respect to the substrate concentration, incubation time and the enzyme concentration. A summary of the conditions chosen is shown in Table 4.1. The signal to noise ration were all above 4 except for CYP2D6.The cut-off that is required to ensure there is no interference from other components of the reaction is 2.5. The CYP2D6 was therefore set for LC/MS analysis. The linearity range for each of the optimised reaction in shown in brackets.

Table 4.1: Summary of the optimised reaction conditions for the fluorescent-based plate assays

CYP	**Enzyme** *(pmol/ml)*	**Substrate**	**Km** *(µM)*	**Time** *(min)*	**S/N**
1A2	2.5 [0-50]	CEC	3.56	15 [0-20]	14.42
2C19	10 [0-30]	MFC	86.31	15 [0-40]	8.15
2C9	25 [1-40]	MFC	52.59	15 [0-40]	7.33
2D6	30 [0-50]	MAMC	14.7	15 [0-30]	3.5
3A4	10 [0-40]	BFC	12.7	15 [0-30]	9.5

CEC, 3-cyano-7-ethoxycoumarin; **MFC**, 7-methoxy-4-trifluoromethylcoumarin; **BFC**, 7-benzyloxy-4-trifluoromethylcoumarin; **S/N**, signal to noise ratio.

4.1.2 Determination of IC_{50} for the CYP diagnostic inhibitors

IC_{50} was determined for the diagnostic inhibitors of the CYP isoforms used in this study (CYPs 1A2, 2C9, 2D6, 3A4 and 2C19). The resulting sigmoidal curves obtained in GraphPad are shown in Fig 4.1.

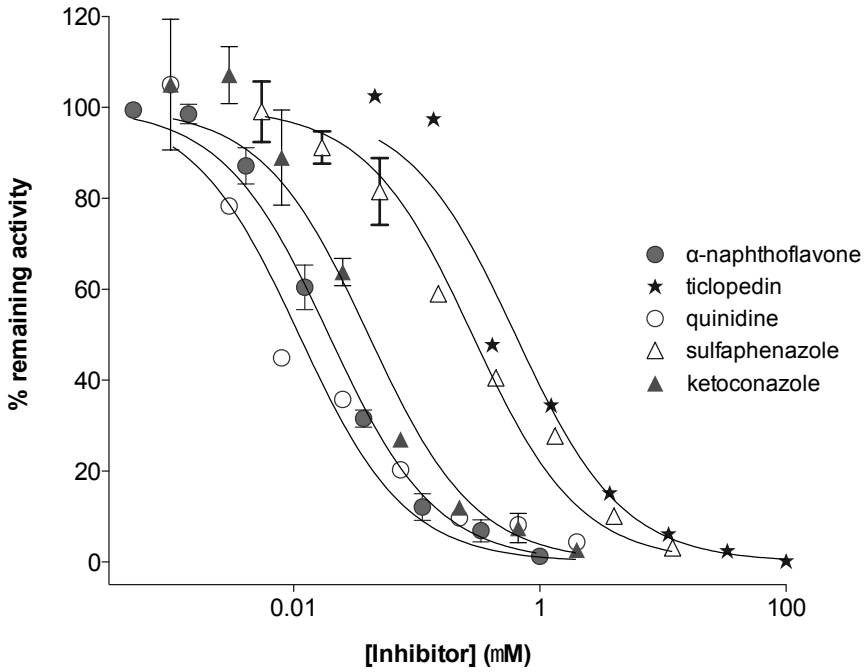

Figure 4.1: IC_{50} curves for diagnostic inhibitors of CYPs 1A2, 2C19, 2C8, 2C9, 2D6 and 3A4

The obtained values were compared to literature values as a way to validate the inhibition assay. The comparisons are summarised in Table 4.2.

Table 4.2: Summary of the optimised reaction conditions for the fluorescent-based plate assays

CYP	Inhibitor	Determined IC50 (μM)	Literature IC_{50} (μM)
1A2	α-naphthoflavone	0.020 ± 0.007	[a]0.02 -0.082
2C19	Ticlopidine	0.630 ± 0.09	[b]3.7 – 3.99
2C9	Sulfaphenazole	0.280 ± 0.06	[c]0.26 – 1.3
2D6	Quinidine	0.011 ± 0.009	[d]0.02- 0.2
3A4	Ketoconazole	0.040 ± 0.008	[e]0.03 – 0.17

[a](Ghosal *et al.*, 2003; Weaver *et al.*, 2003; Moody *et al.*, 1999; Sai *et al.*, 2000; Bu *et al.*, 2000)
[b](Donahue *et al.*, 1997; Sudsakorn *et al.*, 2007)
[c](Dierks *et al.*, 2001)
[d](Dierks et al., 2001; Weaver et al., 2003; Bu et al., 2000; Yin et al., 2000; Sai et al., 2000)
[e](Dierks *et al.*, 2001; Weaver *et al.*, 2003; Moody *et al.*, 1999; Sai *et al.*, 2000)

4.1.3 Set up and validation of the TDI assay

Known time and non-time dependent inhibitors for CYPs 1A2 2C19, 2C9, 2D6 and 3A4 were used to determine if the assay would discriminate between the two. Data from the CYP1A2 validation set is shown in Fig 4.2. All the compounds that were reported as TDI were picked by the assay except for carbamazepine and tacrine. The non-TDI behaved in an expected manner.

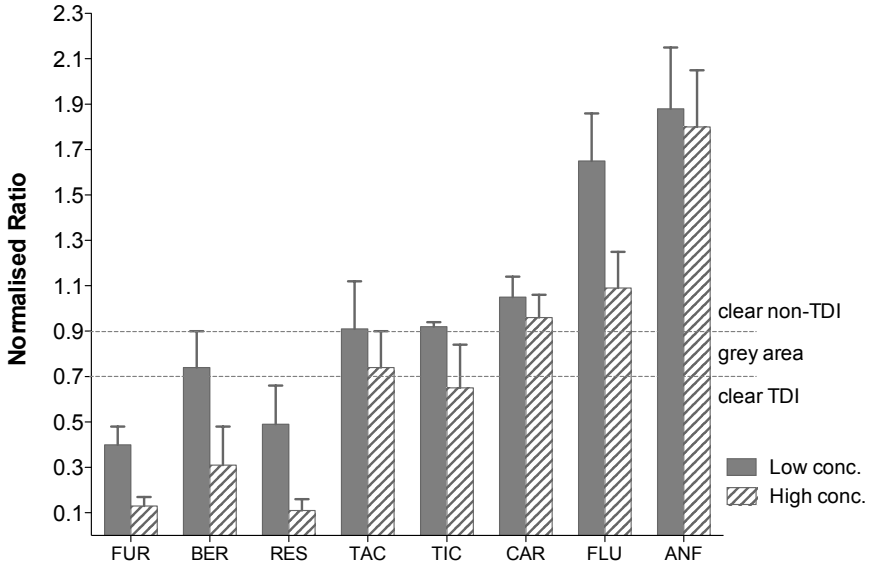

Figure 4.2: Time dependent-inhibition of CYP1A2 by various test compounds. All the compounds were at 1 and 20μM except for furafylline and ANF, which were at 0.01 and 0.1μM. The compounds were as follows: **FUR**, Furafylline, **BER**, bergamottin, **RES**, resveratrol, **TAC**, tacrine, **TIC**, ticlopidine, **CAR**, carbamazepine, **FLU**, fluvoxamine, **ANF**, α-naphthoflavone.

Validation for CYP2C9 was performed using tienilic acid, hydrastine, fluoxetine, methimazole, silibinin, cimetidine and fluvoxamine. In this assay all the compounds behaved as expected with the exception of silibinin and methimazole (Fig 4.3). All the weak time dependent inhibitors (methimazole, silibinin, cimetidine and fluvoxamine fell in the grey area.

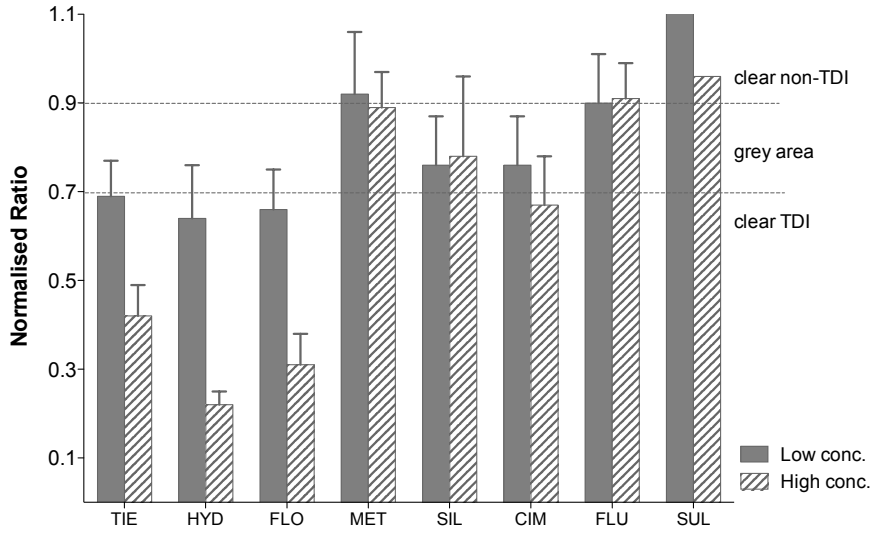

Figure 4.3: Time dependent-inhibition of CYP2C9 by various test compounds. The compounds were as follows: **TIE**, tienilic acid, **HYD**, hydrastine, **FLO**, Fluoxetine, **MET**, methimazole, **SIL**, silibinin, **CIM**, cimetidine, **FLU**, fluvoxamine, **SUL**, sulfaphenazole.

For CYP3A4 all the compounds behaved as expected. The data is summarized in Fig 4.4

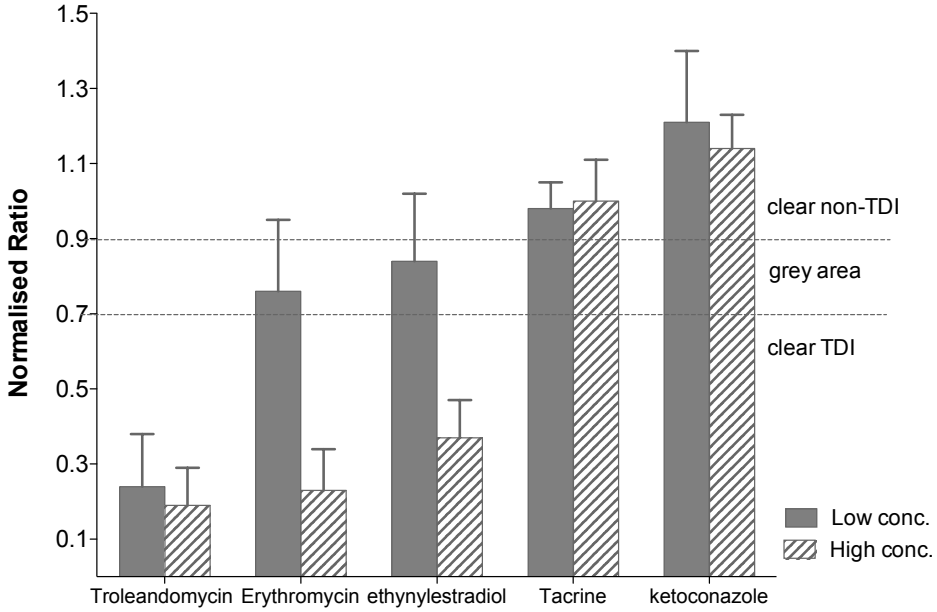

Figure 4.4: Time dependent-inhibition of CYP3A4 by various test compounds.

For the CYP2C19 validation the assay managed to pick ticlopidine and cimetidine as TDI, and omeprazole as non-TDI. However the assay failed to pick methimazole, which is a weak TDI.

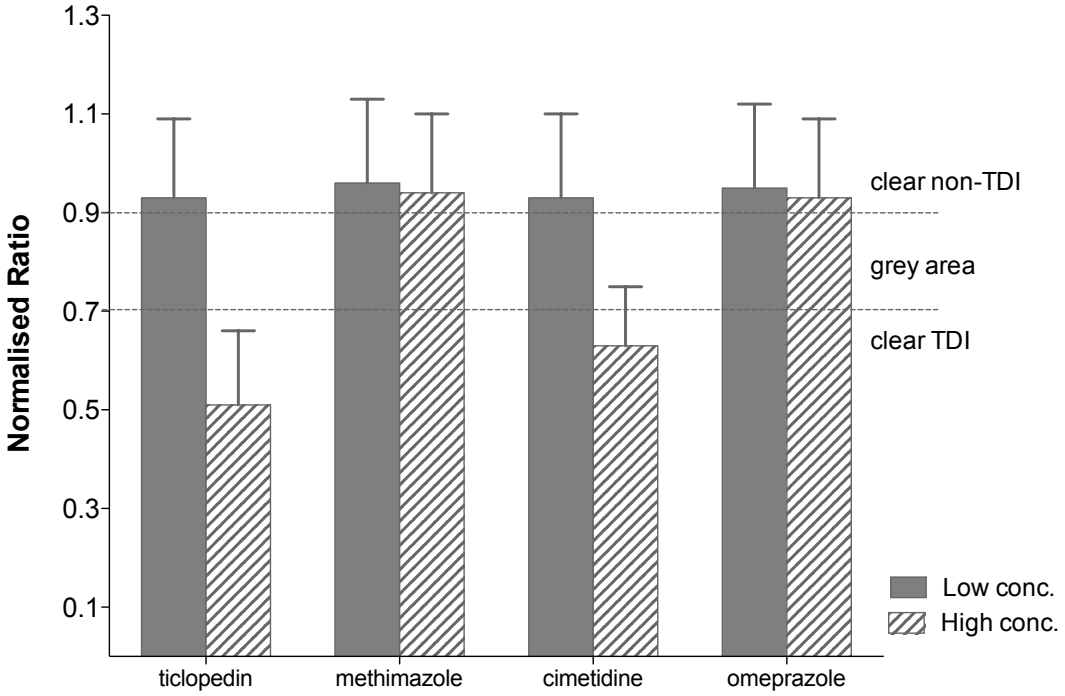

Figure 4.5: Time dependent-inhibition of CYP2C19 by various test compounds

4.1.4 CYP2D6 LC/MS based plate assay

The signal to noise ratio for CYP2D6 was poor in the fluorescence-based assays (Table 4.1) so an LC/MS method was set. 1'hydroxybufuralol was measured to follow the activity of the enzyme. The spectra of daughter ions of 1'hydroxybufuralol at 1μM run using a 50:50 ACN: water mobile phase acidified with 0.1% formic acid. The limit of detection was 0.01μM.

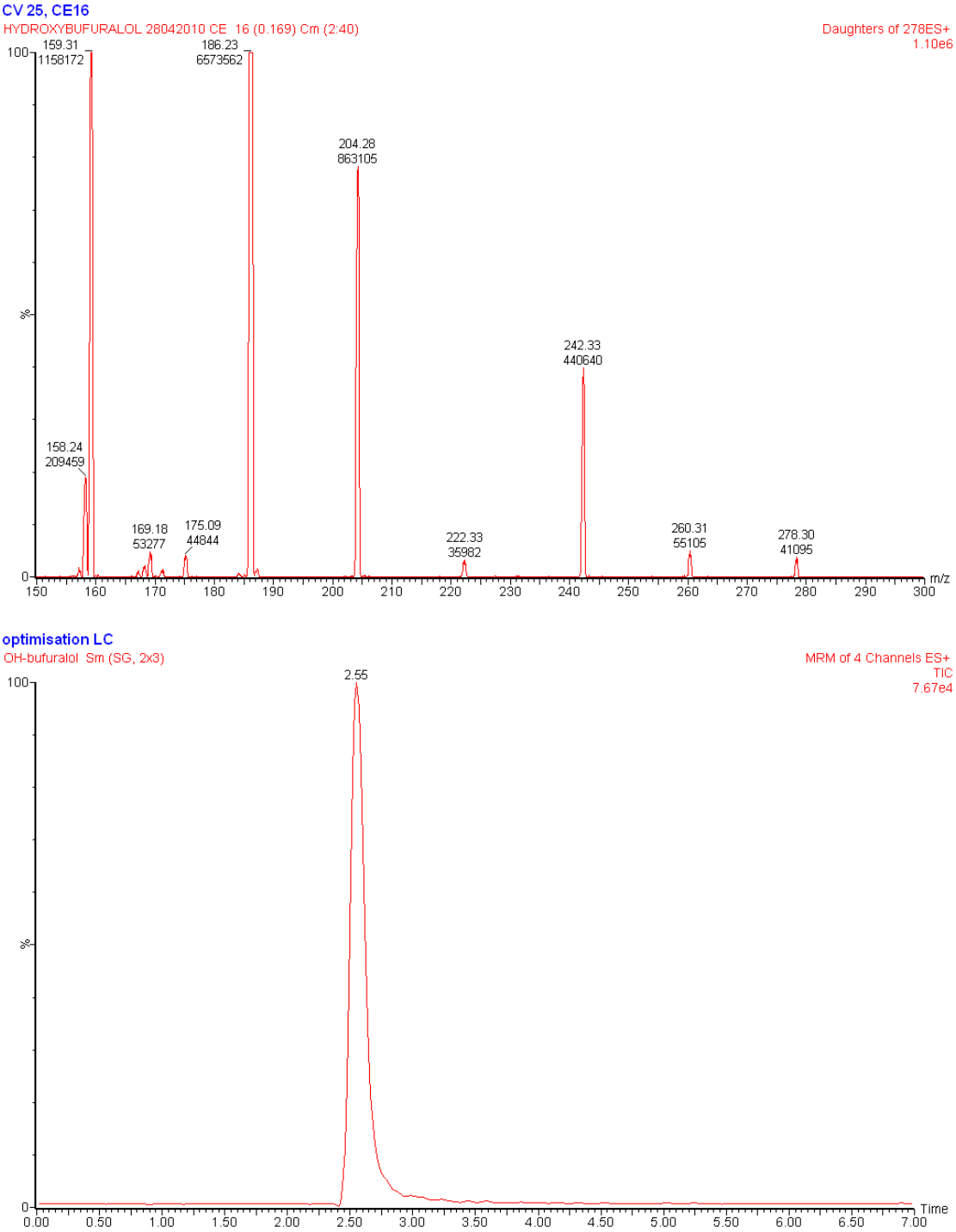

Figure 4.6: Mass spectra of daughter ions of 1'hydroxybufuralol and chromatogram for the parent ion at 0.1µM.

4.2 PART II: Identification of ADME/PK liabilities of 3,4-HPO-4-amino-7-chloroquinolinyl hybrid compounds with antiplasmodial activity.

4.2.1 *In vitro* antiplasmodial activity

The 3,4-HPO-4-amino-7-chloroquinolinyl hybrids had efficacy in both the CQR and CQS *P. falciparum* strains (Table 4.3). Some of the compounds **(3.2c**, **3.2d, 3.2d.HCl, 3.1g, 3.2g, 3.1h** and **3.3a)** had better activity compared to chloroquine, which was used as the control drug in the CQR K1 strain.

Table 4.3: Antiplasmodial activity of 3,4-HPO-4-amino-7-chloroquinolinyl hybrids

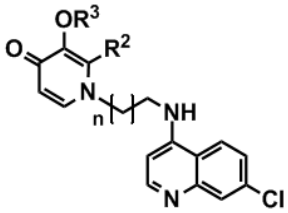

Comp.	R^2	R^3	n	Antiplasmodial Activity IC_{50} (μM)			βHIA (IC_{50}/equiv)
				3D7	K1	W2	
CQ	-	-	-	0.01	0.44	0.10	1.9
3.1a	Me	Bn	1	0.49	3.15	9.93	0.93
3.2a	Et	Bn	1	0.95	8.43	2.59	0.50
3.1b	Me	Bn	2	0.28	3.57	2.15	0.49
3.2b	Et	Bn	2	0.12	71.6	2.32	0.41
3.1c	Me	Bn	3	0.05	2.2	1.12	22.4
3.2c	Et	Bn	3	0.004	0.13	0.10	0.19
3.1d	Me	Bn	5	35.70	4.38	0.39	0.01
3.2d	Et	Bn	5	0.01	0.08	0.02	0.16
3.2d.2HCl	Et	Bn	5	0.01	0.1	ND	ND
3.1e	Me	H	1	10.80	32.6	0.28	2.9
3.2e	Et	H	1	0.40	0.89	1.24	1.1
3.1f	Me	H	2	ND	ND	ND	ND
3.2f	Et	H	2	0.12	0.38	0.54	1.3
3.1g	Me	H	3	0.03	0.07	0.08	2.7
3.2g	Et	H	3	0.05	0.27	0.16	0.98
3.1h	Me	H	5	0.390	0.16	0.07	0.18
3.2h	Et	H	5	0.08	0.61	0.09	0.49
3.3a	Me	Me	5	0.13	2.8	0.09	1.07
3.3b	Me	Me	3	0.07	0.22	0.76	0.75
3.4a	Et	Me	5	ND	ND	0.22	0.47
3.4b	Et	Me	3	ND	ND	0.21	1.71

The compounds were potent inhibitors of β-haematin formation with all the compounds having better activity compared to chloroquine except for compound **3.1e (**Table 4.3**)**. No significant differences were observed between compounds with an alkyl linker of 4 or 6 chains (**3.2c** vs. **3.4d**). All the compounds except **3.2b**, **3.2c**, **3.2d**, **3.2d.HCl** and **3.1h** were not significantly cytotoxic to mammalian cells as demonstrated by their lack of toxicity to the KB cell line (Table 4.4).

Table 4.4: Antiplasmodial activity of 3,4-HPO-4-amino-7-chloroquinolinyl hybrids

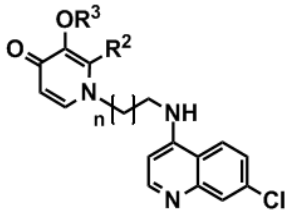

Compound	R^2	R^3	n	RI		**KB	Selectivity Indices	
				K1/3D7	*W2/3D7*	(µg/ml)	KB/3D7	KB/K1
CQ	-	-	-	48.9	10.8	10.9	3811.1	77.95
POD	-	-	-	-	-	0.0003	0.0007	ND
3.1a	Me	Bn	1	6.4	2.0	22.5	109	17
3.2a	Et	Bn	1	8.9	2.7	23.3	6.3	1.0
3.1b	Me	Bn	2	12.8	7.7	28.9	18.7	1.0
3.2b	Et	Bn	2	596	19.3	6.6	0.21	1.0
3.1c	Me	Bn	3	0.27	44.0	53.2	2331	54.7
3.2c	Et	Bn	3	32.5	25	4.16	2250	69
3.1d	Me	Bn	5	0.25	0.12	75.3	36	1.0
3.2d	Et	Bn	5	11.4	2.1	1.86	345	1.0
3.2d.2HCl	Et	Bn	5	12.5	ND	3.27	828.6	65.1
3.1e	Me	H	1	3.0	0.026	ND	ND	ND
3.2e	Et	H	1	2.2	3.1	ND	ND	ND
3.1f	Me	H	2	ND	ND	ND	ND	ND
3.2f	Et	H	2	3.2	4.5	19.5	117	1.0
3.1g	Me	H	3	0.66	2.3	66.3	5136	2201
3.2g	Et	H	3	5.4	3.2	28.3	1181	236
3.1h	Me	H	5	0.47	0.4	1.38	18	1.0
3.2h	Et	H	5	7.7	1.1	17.7	475.9	61.6
3.3a	Me	Me	5	-	-	18.6	358.5	166.4
3.3b	Me	Me	3	-	-	10.3	395	125.9
3.4a	Et	Me	5	-	-	ND	ND	ND
3.4b	Et	Me	3	-	-	ND	ND	ND

POD-podophyllotoxin, **CQ-** chloroquine

For the compounds that did not demonstrate significant cytotoxicity the profile was comparable to that of chloroquine and was better than the podophyllotoxin, which was the control drug. The 3D7 strain showed better selectivity indices for all the compounds with the exception of compound **3.2c**. However the selective indices were lower compared to chloroquine except for compounds **3.1c**, **3.2c**, **3.2g**, and **3.2d.2HCl**, which was comparable. Resistance indices were lower in all the compounds compared to chloroquine with the exception of **3.2b**, **3.2c** and **3.1c.**

4.2.2 Physicochemical profiling

4.2.2.1 Prediction of drug likeliness and oral bioavailability

All the 3,4-HPO-4-amino-7-chloroquinolinyl hybrids satisfied the Lipinski rule of 5 with the exception of **3.1c**, **3.2b, 3.1c, 3.1d**, **3.2a**, **3.2d**, and **3.2d.HCl** (Table 4.5). The compounds that failed did so by one property (cLogP). Thus these compounds still had potential to have good oral bioavailability and to be druggable. If the Veber rules for predicting good oral bioavailability are to be considered in the test compounds, all the compounds except **3.1d**, **3.2d** and **3.2d.HCl** were in the prescribed chemical space. The compounds that failed did so because they had too many rotatable bonds.

4.2.2.2 Prediction of lead likeliness and BBB penetration

According to rules by Pardridge for BBB penetration, all the 3,4-HPO-4-amino-7-chloroquinolinyl hybrid compounds were predicted to cross the blood-brain barrier.

Table 4.5: Prediction of physicochemical properties to determine the drug likeliness, oral absorption, BBB crossing potential and lead likeliness for the artemisinin-chloroquinoline and 3,4-HPO-4-amino-7-chloroquinolinyl hybrid compounds

	Predicted Physicochemical properties									Violations			
Compound	**Mw**	**HBA**	**HBD**	**cLogP**	**LogD**	**Ring count**	**Rot. bonds**	**PSA**	**LogSw**	**Lipinski**	**Veber**	**CNS like**	**Lead like**
3.1a	419.90	5	1	4.49	4.25	4	7	56.17	-5.24	1	0	1	1
3.2a	433.93	5	1	5.01	4.77	4	8	56.17	-5.37	1	0	1	1
3.1b	433.93	5	1	4.55	4.30	4	8	64.97	-5.45	0	0	1	2
3.2b	447.96	5	1	5.07	4.83	4	9	56.17	-5.60	1	0	1	2
3.1c	447.96	5	1	5.06	4.82	4	9	56.17	-5.78	1	0	1	2
3.2c	461.98	5	1	5.59	5.34	4	10	56.17	-5.89	1	0	1	4
3.1d	476.01	5	1	5.95	5.71	4	11	56.17	-6.16	1	1	1	5
3.2d	490.04	5	1	6.47	6.23	4	12	56.17	-6.29	1	1	1	5
3.2d.2HCl	490.04	5	1	6.47	6.23	4	12	56.17	-6.29	1	1	1	5
3.1e	329.78	5	2	2.65	2.41	3	4	64.97	-3.77	0	0	0	0
3.2e	343.80	5	2	3.17	2.93	3	5	56.17	-3.89	0	0	0	0
3.1f	343.80	5	2	2.71	2.47	3	5	64.97	-3.92	0	0	0	0
3.2f	329.78	5	2	2.51	2.26	3	5	64.97	-3.89	0	0	0	0
3.1g	357.83	5	2	3.23	2.98	3	6	64.97	-4.04	0	0	0	0
3.2g	371.86	5	2	3.75	3.51	3	7	64.97	-4.45	0	0	0	0
3.1h	385.89	5	2	4.11	3.87	3	8	64.97	-4.71	0	0	0	0
3.2h	399.91	5	2	4.64	4.39	3	9	64.97	-4.94	0	0	0	1
3.4a	399.91	5	1	4.23	3.10	3	7	56.17	-4.94	0	0	0	1
3.3a	371.86	5	1	3.34	3.62	3	8	56.17	-4.40	0	0	0	1
3.4b	413.94	5	1	4.75	3.99	3	8	56.17	-5.08	0	0	0	2
3.3b	385.89	5	1	3.86	4.51	3	10	56.17	-4.53	0	0	1	0

Mw, Molecular weight; **HBA**, Hydrogen bond acceptors; **HBD**, hydrogen bond donors; **cLogP**, calculated LogP; **RB**, rotatable bonds; **PSA**, polar surface area

The exception were the benzylated analogues which were either too lipophilic (**3.1a**, **3.2a,** **3.1b**, **3.2b**, **3.1c**, **3.2c**, **3.1d**, **3.2d** and **3.2d.2HCl**) or had molecular weight falling outside the desired chemical space (Table 4.5).

Predictions for 3,4-HPO-4-amino-7-chloroquinolinyl hybrid compounds in VolSurf also showed the compounds to have potential to cross the BBB. The compounds (highlighted in yellow) were projected on the plot of training compounds (black circles) (Fig 4.7). The compounds were known BBB crossing and non-crossing compounds from literature in-built in the software. In terms of lead likeliness all the other compounds were within the desired ranges with the exception of the benzylated analogues (Table 4.5), which had violations ranging from 1 to 5. The number of violations increases with increasing lipophilicity for the analogues.

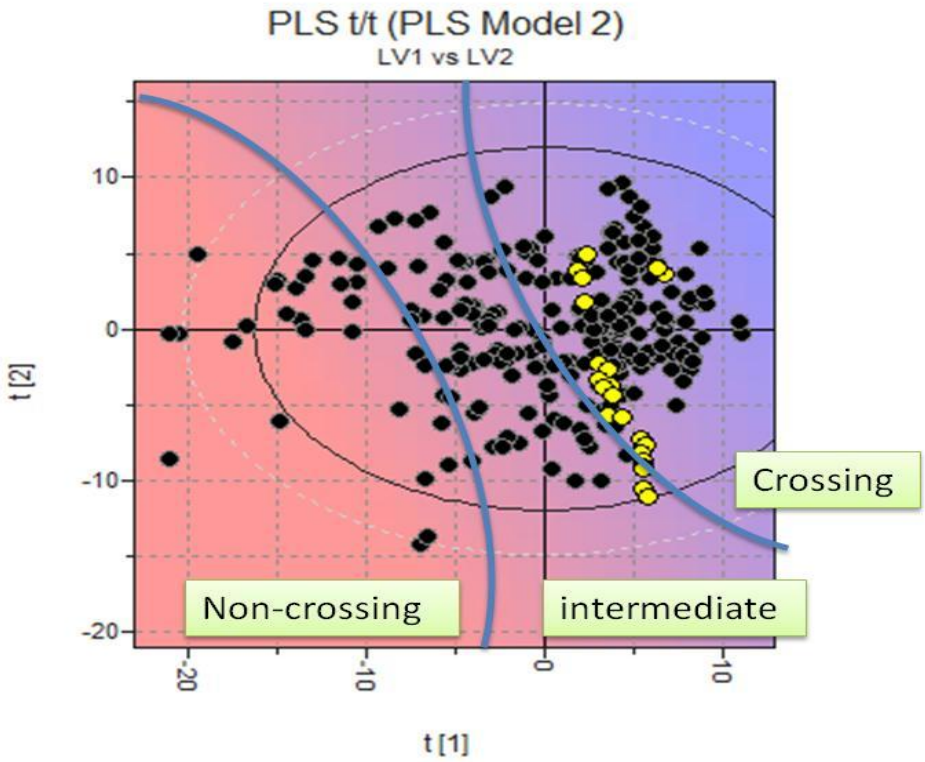

Figure 4.7: Volsurf predictions for blood brain barrier penetration by 3,4-HPO-4-amino-7-chloroquinolinyl hybrid compounds

4.2.2.3 Lipophilicity and purity determination

The purity for all the compounds was above 95%. From integrity studies there was no indication the compounds were degrading in the media even after a week. Further studies on the compounds were therefore continued with confidence. For lipophilicity determination, reference compounds with accurately determined k' and known literature $LogD_{7.4}$ were used to perform calibrations. The $LogD_{7.4}$ values ranged between -0.15 and 5.22. Representative chromatograms for the blank and reference compounds are shown in Fig 4.8.

Blank

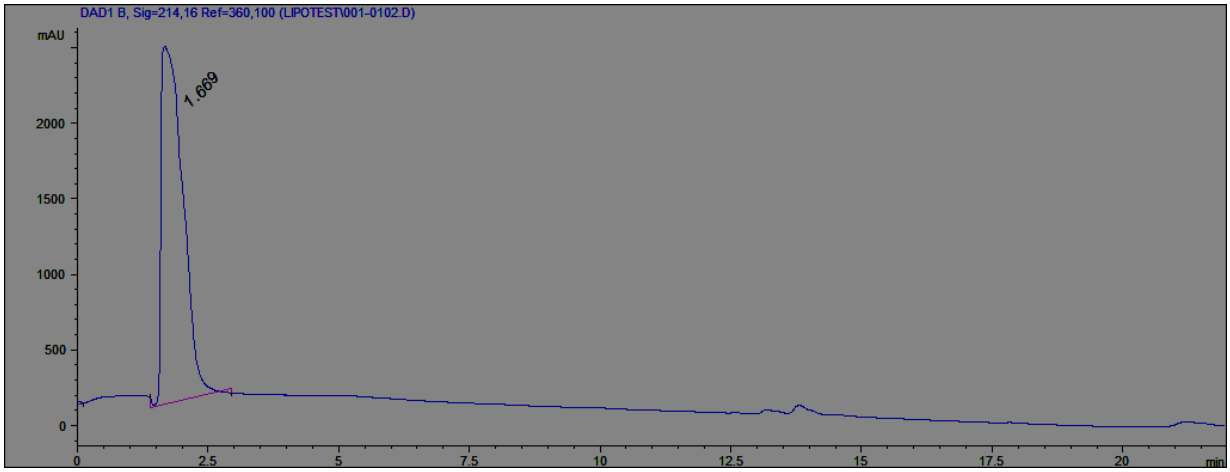

Reference compounds

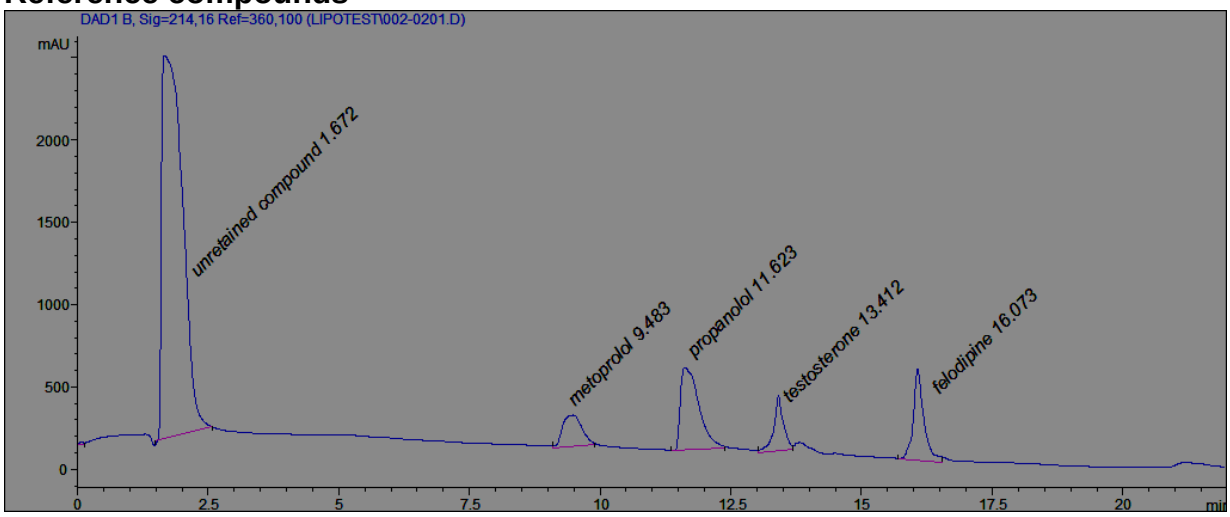

Figure 4.8: Chromatograms showing different retention capacities of the reference compounds.

The retention times were used to correct the reported k'. Corrected k' values and literature $LogD_{7.4}$ values are shown in Table 4.6.

Table 4.6: Calculated k´ and log D values for reference compounds

	Literature		Experiment		
Compound	**k´**	**$logD_{7.4}$**	**T_r (min)**	**k´**	**Estimated $logD_{7.4}$**
Metoprolol	7.8	0.02	9.48	7.64	-0.18
Propanolol	9.3	1.15	11.62	9.47	1.56
Testosterone	10.9	3.19	13.41	11.00	3.01
Felodipine	13.4	5.2	16.07	13.28	5.17

The k' was plotted against the retention time of the reference compounds and the resulting curve was used to calculate the k' for the test compounds. Another standard curve was made by plotting the retention times of the test compounds against the literature $LogD_{7.4}$ to determine the $LogD_{7.4}$ of the test compounds. A summary of the determined $LogD_{7.4}$ values is given in Table 4.7.

4.2.2.4 Solubility determination

Two compounds from the series had low solubility with the exception of **3.2g** and **3.4a**. According to cutoffs set for the turbidimetric assay all the compounds had high solubility except for compound **3.2c**, **3.1d**, **3.2d** and **3.2h** that were partially soluble (in the range 20-100μM). Compounds **3.2g** and **3.3a** were poorly soluble. If the guidelines for potential solubility issues in humans for discovery compounds are to be followed (Kerns and Di, 2008a) all the compounds had moderate solubility with the exception of compound **3.2g** and **3.4a** which were poorly soluble. The guidelines state that compounds

below 10µg/ml are poorly soluble, between 10 and 60µg/ml moderate and above 60µg/ml highly soluble.

Table 4.7: Experimentally determined $LogD_{7.4}$ of 3,4-HPO-4-amino-7-chloroquinolinyl hybrids

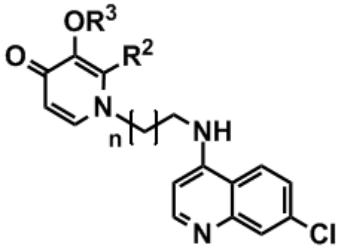

Compound	R^2	R^3	n	$LogD_{7.4}$
3.1a	Me	Bn	1	1.53
3.2a	Et	Bn	1	1.47
3.1b	Me	Bn	2	1.63
3.2b	Et	Bn	2	2.62
3.1c	Me	Bn	3	2.27
3.2c	Et	Bn	3	3.66
3.1d	Me	Bn	5	4.77
3.2d	Et	Bn	5	5.82
3.2d.2HCl	Et	Bn	5	5.82
3.1e	Me	H	1	0.26
3.2e	Et	H	1	ND
3.1f	Me	H	2	ND
3.2f	Et	H	2	ND
3.1g	Me	H	3	ND
3.2g	Et	H	3	1.27
3.1h	Me	H	5	1.30
3.2h	Et	H	5	2.40
3.3a	Me	Me	5	0.22
3.3b	Me	Me	3	1.63
3.4a	Et	Me	5	ND
3.4b	Et	Me	3	ND

As expected the deprotected compounds had higher solubility compared to the benzylated forms as the former were in salt form (Fig 4.9). The 3-methoxylated analogues exhibited low aqueous solubility when compared to corresponding benzylated analogues. However all the compounds had

solubility which allowed testing in biological assays as the highest concentration required was 20μM. There was no correlation in solubility between experimental and predicted data.

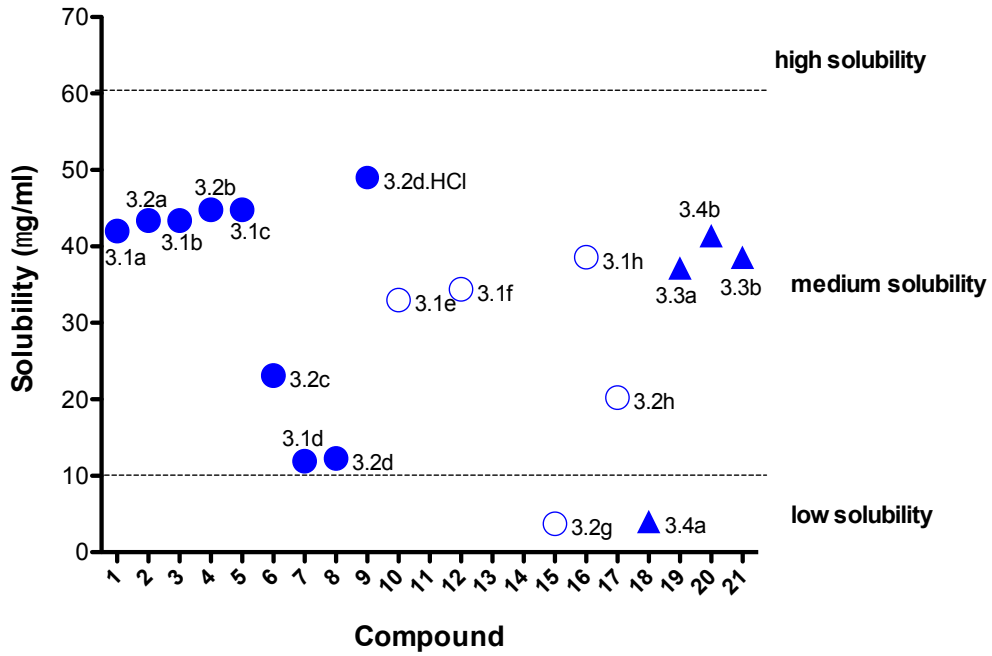

Figure 4.9: Solubility of 3,4-HPO-4-amino-7-chloroquinolinyl hybrids. The benzylated analogues are represented by filled circles, deprotected analogues by non-filled circles and the methoxy analogues by triangles

There was an increase in the lipophilicity of the compounds with increase in linker carbon chain as expected. However there was no correlation between experimentally determined lipophilicity and solubility values.

4.2.3 ADME profiling

4.2.3.1 Metabolic clearance in human liver microsomes and cryopreserved hepatocytes

Hepatic clearance (CL_H) in human liver microsomes was intermediate for all compounds except for **3.1b**, **3.1c**, **3.1d** and **3.1h,** which were low (Table 4.8) using the well-stirred model.

Table 4.8: Metabolic stability in human liver microsomes and cryopreserved hepatocytes

	Compound	Human liver microsomes				Cryopreserved hepatocytes			
		[a]$T_{1/2}$ (min)	[b]$Cl_{int,app}$ (ml/min/kg)	[c]CL_H (ml/min/kg)	% of Q_H	[a]$T_{1/2}$ (min)	[b]$Cl_{int,app}$ (ml/min/kg)	[c]CL_H (ml/min/kg)	% of Q_H
A	Midazolam	5.13	257.90	19.42	92.47	21.0	91.65	17.09	81.36
	Verapamil	10.88	121.69	17.91	85.30	-	-	-	-
	Diltiazem	33.81	39.16	13.67	65.09	-	-	-	-
	Tolbutamide	301.37	4.39	3.63	17.30	-	_	_	_
	Propanolol	-	-	-	-	50.0	38.92	13.64	64.95
	Clozapine	-	-	-	-	99.0	19.74	10.18	48.45
B	**3.1a**	34.48	7.24	5.38	25.63	67.3	29.05	12.19	58.04
	3.2a	ND	ND	ND	ND	44.4	43.99	14.21	67.69
	3.1b	96.27	2.59	2.31	10.99	54.7	35.81	13.24	63.04
	3.2b	33.49	7.45	5.50	26.19	43.3	45.12	14.33	68.24
	3.1c	49.51	5.04	4.06	19.35	20.7	94.47	17.18	81.81
	3.2c	31.36	7.96	5.77	27.48	53.2	150.02	18.42	87.72
	3.1d	72.20	3.46	2.97	14.13	30.2	64.58	15.85	75.46
	3.2d	17.77	14.04	8.41	40.07	15.4	127.18	18.02	85.83
	3.2d.HCl	21.46	11.63	7.48	35.64	22.7	86.29	16.89	80.43
C	**3.1e**	12.58	19.84	10.20	48.57	-	-	-	-
	3.2e	18.58	13.43	8.19	39.00	-	-	-	-
	3.2g	15.97	15.62	8.96	42.66	-	-	-	-
	3.1h	9.27	26.93	11.80	56.18	-	-	-	-
	3.2h	36.87	6.77	5.12	24.37	-	-	-	-
D	**3.4a**	20.82	11.99	7.63	36.34	-	-	-	-
	3.3a	19.47	12.82	7.96	37.90	73.5	26.51	11.72	55.80

[a]Elimination half-life ($T_{1/2}$) = time taken for compound to eliminated to half its original concentration; [b]Apparent clearance ($Cl_{int,\ app}$) = *in vivo* clearance scaled from in vitro clearance; [c]Hepatic blood flow (Q_H), A= controls; B= benzylated analogues, C= deprotected analogues, D = methoxy analogues

In hepatocytes, compounds **3.1c**, **3.1d, 3.2c**, **3.2d** and **3.2.HCl** were predicted to be fast with **3.1a**, **3.1a**, **3.1b**, **3.2b**, and **3.3a** being predicted to be intermediate. Predicted clearance was higher in hepatocytes compared to human liver microsomes. The ranking of the compounds into fast, slow and intermediate CL_H was based on the comparison of estimated CL_H to hepatic blood flow (Q_H) where CL_H>75% of Q_H is fast, CL_H< 25% is slow and CL_H 25-75 is intermediate.

4.2.3.2 Biotransformation in human cryopreserved hepatocytes

Given that the metabolic clearance of many of the N-alkyl-3, 4-HPO hybrids was intermediate to fast in hepatocytes, further studies to understand their biotransformation were conducted. Metabolites identified in hepatocytes were mainly as a result of N-dealkylation of the pyridinone into **M1** and a carbonyl intermediate (7-chloroquinolinyl-4-amino-aldehyde), which subsequently yields a carboxylic acid, **M5** (7-chloroquinolin-4-ylamino carboxylic acid and to a minor extend **M8** (N-alkenyl-7-chloroquinolin-4-yl-amine).

The second significant metabolic route is linear chain cleavage to give **M2** (7-chloroquinolin-4-amine) and a carbonyl intermediate which subsequently gives a carboxylate **M4** and a hydroxyl metabolite **M3** (a pyridinyl alcohol) as a minor metabolite (Fig 4.10). From mass balance estimates most of the metabolites identified accounted for the biotransformation of the compound. All the compounds analyzed cleaved to form **M1** with the exception of **3.3a**, **3.1h** and **3.2d**. Carboxylic acids resulting from the 4-aminoquinoline moiety only favoured the long chain amino acids (n ≥ 4). Hydroxylated compounds

resulted from the short chain analogues (n ≤ 2) with the exception of **M7**. Hydroxylation of the uncleaved compound was observed to a minor extent in **3.2d** and **3.3a** (Fig 4.10). The full profiles for each of the tested compounds showing the retention time and abundance of each metabolite is shown in Appendix A.

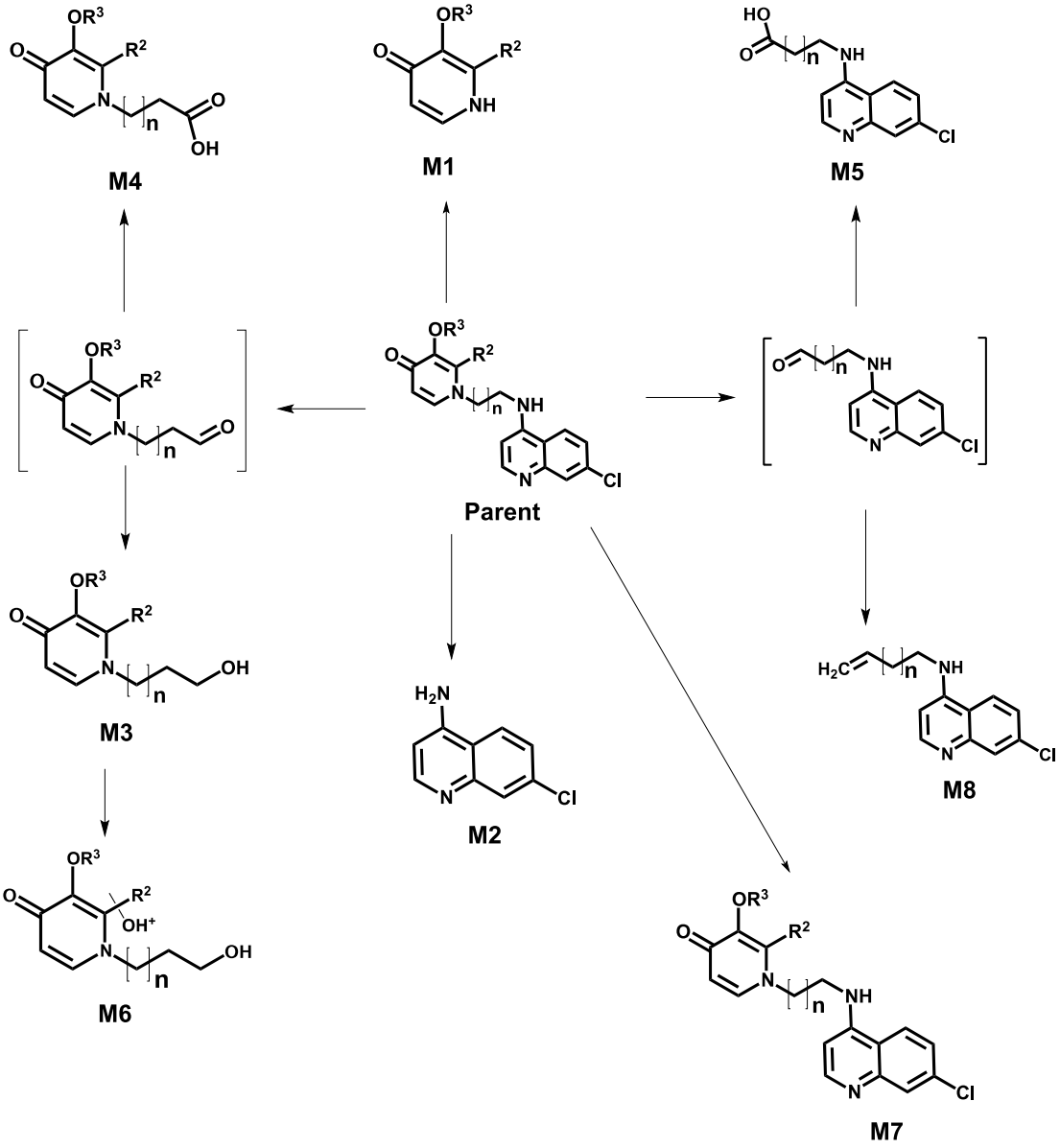

Figure 4.10: General scheme for the metabolism of selected 4-aminoquinoline-3, 4-hydroxypyridinone hybrids in human cryopreserved hepatocytes

4.2.3.3 Inhibition studies in the 5 major cytochrome P450s

4.2.3.3.1 Inhibition screens

None of the 4-aminoquinoline-3, 4-hydroxypyridinone hybrids had significant inhibitory effects on CYP2C9 and CYP2C9. In CYP1A2 the inhibition was moderate. In cases where the IC_{50} was determined in CYP1A2 (**3.1d**, **3.1e**, **3.1f**, **3.1h** and **3.2h**) the value was greater than 10μM predictive of low risk DDI. No further analysis was therefore performed in these isoforms. Potent inhibition was shown on CYP3A4 and CYP2D6 with all the compounds (Table 4.9) having IC_{50} values ranging between 1-10μM. This put the risk of DDI with substrates of the two isoforms at intermediate level. The only exception was compound **3.2b** with CYP2D6. Inhibition against CYP3A4 was driven by lipophilicity with the greatest inhibition being shown by the most lipophilic compounds. The greatest inhibition was shown by the benzylated analogues in both CYP3A4 and CYP2D6. TDI was investigated in CYP3A4 and all the compounds were negative for TDI (Fig 4.11).

4.2.3.3.2 Kinetic and mechanisms of CYP3A4 inhibition

Further analysis into the kinetics and mechanism of inhibition of the compounds by CYP3A4 indicated the compounds inhibited via a non-competitive mechanism (Table 4.9), with the exception of **3.2e, 3.2h** and **3.4a,** which demonstrated mixed type inhibition and compound **3.1f**, which demonstrated the competitive mode. The K_i values for the compounds also corresponded with the IC_{50} values in demonstrating that the compounds were potent inhibitors.

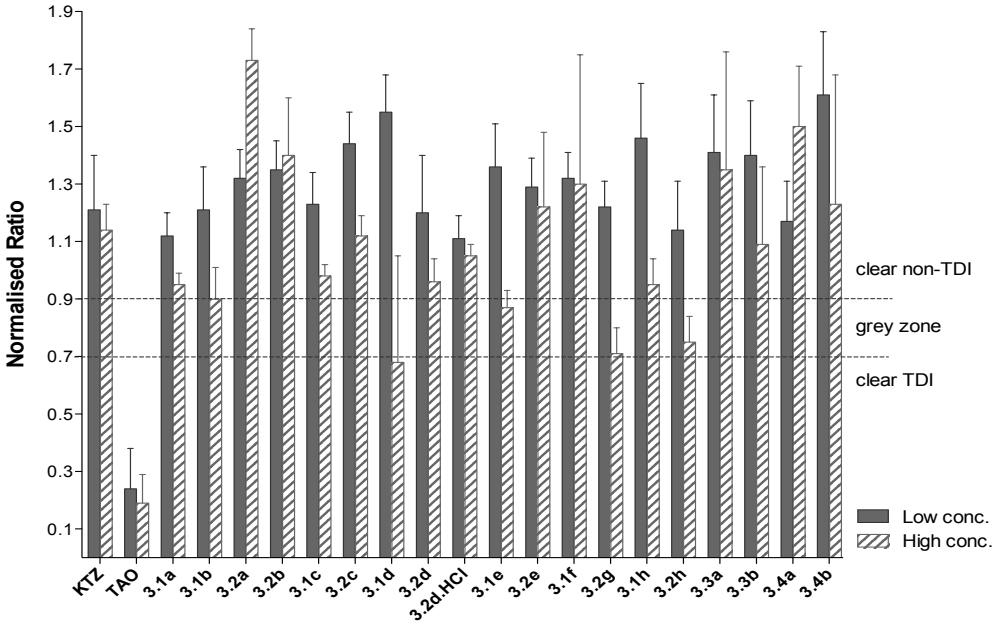

Figure 4.11: TDI in CYP3A4 by the 4-aminoquinoline-3, 4 hydroxypyridinone hybrids

Table 4.9: Inhibition of the 4-aminoquinoline-3, 4-hydroxypyridinone hybrids by the five major drug metabolizing enzymes

		Cytochrome P450 inhibition: % inhibition (IC_{50})					Kinetics of CYP3A4 inhibition	
	Compound	CYP1A2	CYP2C19	CYP2C9	CYP2D6	CYP3A4	K_i (μM)	Mode of inhibition
A	*Controls	95 (0.01)	40	65	96 (0.02)	70 (0.08)		
B	**3.1a**	13	4	12	98 (2.58)	68 (7.73)	9.66	non-competitive
	3.2a	31	17	25	98 (3.08)	84 (3.07)	70.99	non-competitive
	3.1b	17	32	43	89 (3.88)	75 (1.77)	0.36	non-competitive
	3.2b	8	43	62	4	90 (1.18)	1.14	non-competitive
	3.1c	15	31	37	85 (2.05)	87 (1.00)	1.19	non-competitive
	3.2c	15	58	5	81 (5.18)	91 (4.33)	27.59	non-competitive
	3.1d	88 (22.64)	49	36	100 (6.38)	93 (2.25)	3.73	non-competitive
	3.2d	10	61	48	89 (2.17)	92 (1.36)	0.79	non-competitive
	3.2d.2HCl	31	54	30	90 (3.44)	94 (0.29)	0.34	non-competitive
C	**3.1e**	68 (17.26)	11	8	90 (2.76)	43 (5.87)	39.60	non-competitive
	3.2e	0	0	2	97 (2.31)	32 (12.34)	0.97	mixed
	3.1f	57 (36.46)	23	26	100 (6.33)	52 (14.86)	5.42	competitive
	3.2g	33	0	24	97 (3.22)	65 (6.53)	6.70	non-competitive
	3.1h	64 (14.56)	2	1	94 (ND)	75 (4.29)	5.81	non-competitive
	3.2h	63 (38.67)	18	49	98 (8.07)	89 (4.40)	3.39	mixed
D	**3.4a**	20	3	21	92 (4.58)	46 (6.13)	3.69	mixed
	3.3a	9	0	13	84 (5.08)	64 (2.52)	4.38	non-competitive
	3.4b	9	1	20	93 (ND)	63 (12.80)	3.95	non-competitive
	3.3b	6	0	18	84 (2.32)	54 (2.15)	3.58	non-competitive

ND; not determined; IC_{50} is the concentration of inhibitor resulting 50% inhibition (in brackets); % inhibition was as determined at 20μM. *Controls for each respective CYP were as follows: CYP1A2, α-naphthoflavone at 0.1μM, CYP2C19, ticlopidine at 10μM, CYP2C9, sulphaphenazole at 1μM, CYP2D6, quinidine at 1μM and CYP3A4, ketoconazole at 1μM

4.3 PART III: Identification of ADME/PK liabilities in artemisinin-chloroquinoline hybrids

4.3.1 Determination of metabolic clearance in HLM and hepatocytes

Hepatic clearance was intermediate for the two hybrids in hepatocytes and HLM except for compound **3.9** in HLM (Table 4.10). The clearance of the compounds was higher than that for both artemisinin and chloroquine. None of the hybrids behaved the same as chloroquine. The clearance in hepatocytes was rapid in the first 15 min and then slowed down thereafter.

Table 4.10: Metabolic stability of artemisinin-chloroquinoline hybrids in HLM and hepatocytes

Compound	[a]$T_{1/2}$ (min)	[b]$Cl_{int,app}$ (ml/min/kg)	[c]CL_H (ml/min/kg)	% of Q_H
Human liver microsomes				
artemisinin	25.96	25.60	11.52	54.84
chloroquine	346.57	1.91	1.75	8.34
3.9	9.47	269.03	19.48	92.76
3.10	19.31	34.29	13.02	62.02
Cryopreserved hepatocytes				
artemisinin	-	-	-	-
chloroquine	-	-	-	-
3.9	26.46	25.03	11.42	54.37
3.10	31.90	12.66	20.75	60.31

4.3.2 Metabolite identification

Metabolites were identified in hepatocytes. The bulk of the compound remained unchanged after the 60 minutes incubation with 76% and 77% remaining for **3.9** and **3.10** respectively. Five metabolites were identified for

compound **3.9.** The metabolites were mainly products of hydroxylation (Fig 4.12).

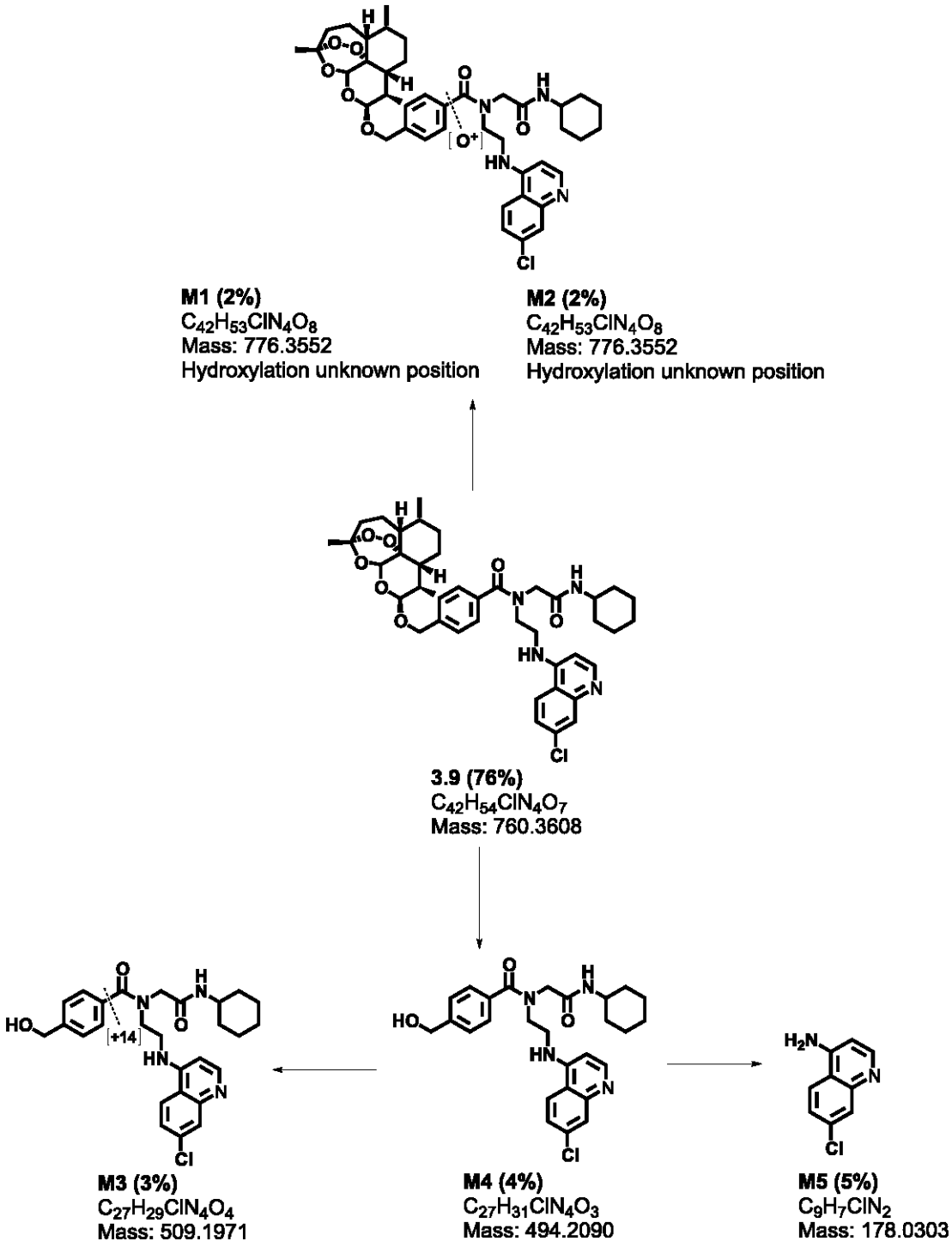

Figure 4.12: Biotransformation of compound 3.9 in hepatocytes

Two metabolites were identified for compound 3.10 (Fig 4.13). The fragment that was identified suggested the cleavage that was holding the two major building blocks on the compound that is the artemisinin and the 4-aminoquinoline core. However the data suggest most of the compound remained intact as indicated by the high percentage of the parent compound identified.

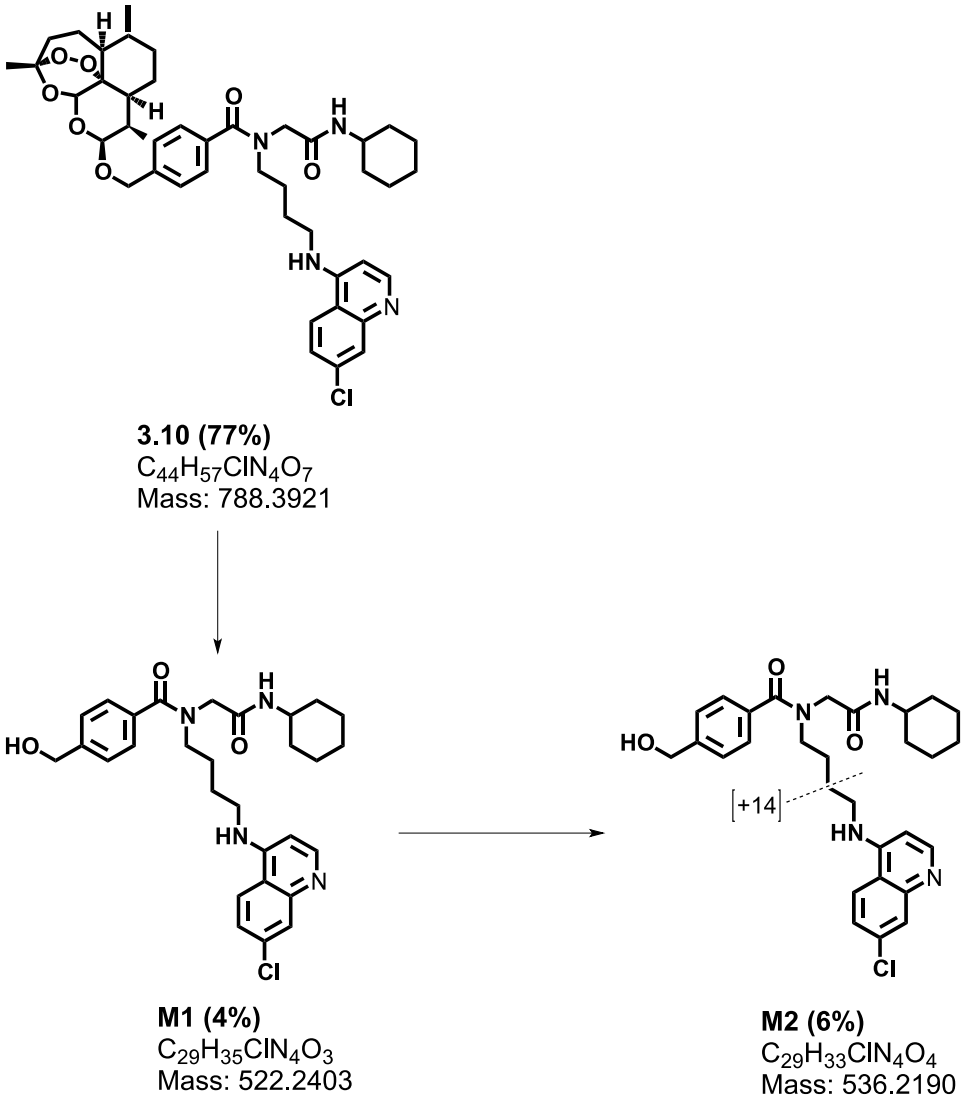

Figure 4.13: Biotransformation of compound 3.10 in hepatocytes

4.3.3 Reaction phenotyping

The enzymes responsible for metabolizing the two artemisinin-chloroquinoline hybrids were determined (Fig 4.14). There was no contribution from CYPs 2B6, 2C8 and 2E1 for both compounds. The highest contribution came from CYPs CYP2C9 and 2C19 for both compounds. Less than 20% of the compound was metabolized by the contributing enzymes except for compound **3.10** in CYPs 2C9 and 2C19.

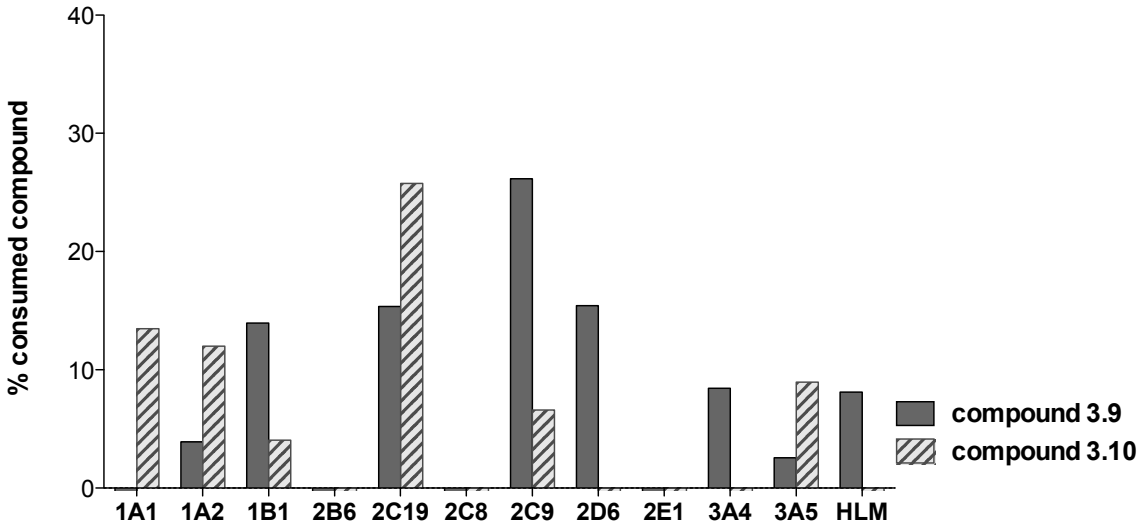

Figure 4.14: Reaction phenotyping for the artemisinin-chloroquinoline hybrids. Data for compound **3.9** is represented by the solid columns and that for compound **3.10** by checked columns**.**

4.3.4 Inhibition studies

The artemisinin-chloroquinoline hybrids and their intermediates showed significant inhibition against CYP3A4 (Fig 4.15). Inhibition in the hybrids was potent with more than 80% inhibition. The inhibition was characterized by an IC_{50} of 0.059 and 0.214μM for compounds **3.9** and **3.10** respectively (Fig 4.16)

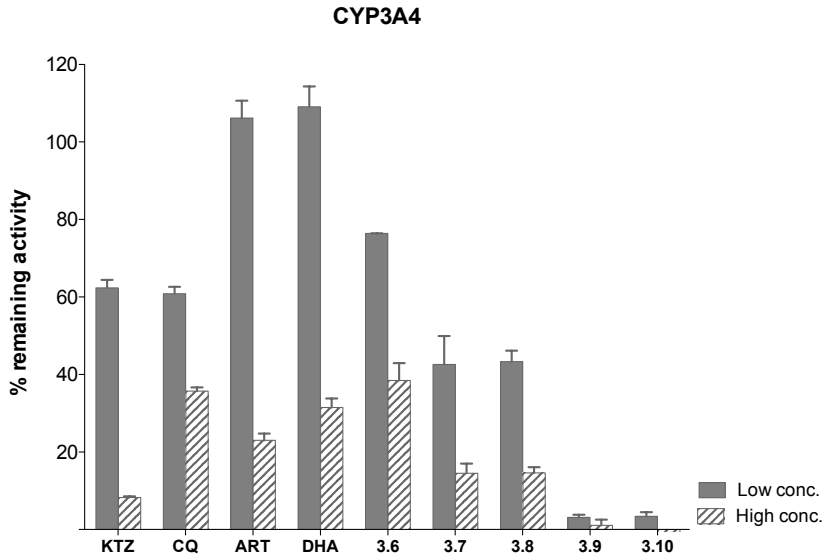

Figure 4.15: Inhibition of CYP3A4 by the artemisinin-chloroquinoline hybrids.

The inhibition of intermediates was characterized by an IC_{50} of 0.7192, 1.014 and 0.6333μM for **3.6**, **3.7** and **3.8** respectively. Inhibition for ketoconazole, which is a known potent CYP3A4 inhibitor, was 0.0023μM.

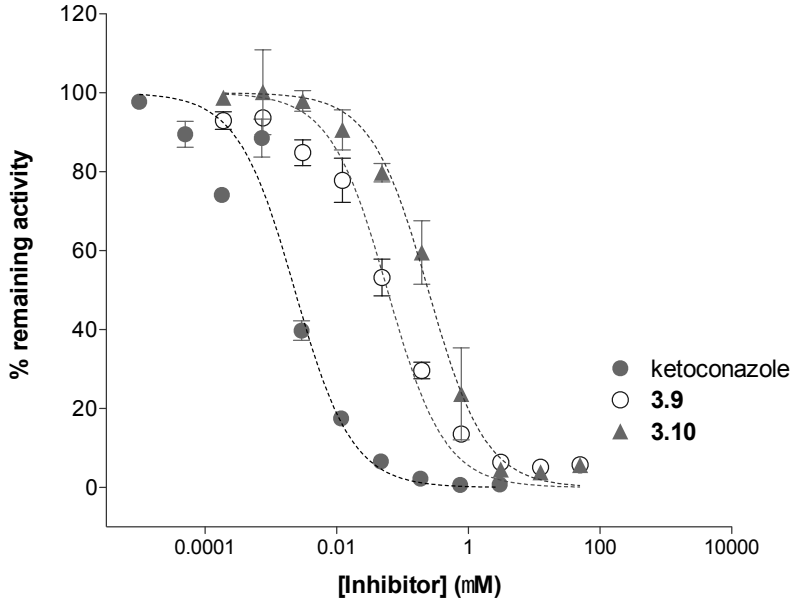

Figure 4.16: Inhibition of CYP3A4 mediated BFC metabolism by the artemisinin-chloroquinoline hybrids

The hybrids (**3.9** and **3.10**) and intermediate **3.6** also demonstrated potent inhibition against CYP2C9 and CYP2C19 (Fig 4.17). The other intermediates had moderate effects. Chloroquine, artemisinin and dihydroartemisinin (DHA) were comparable to intermediate **3.7** and **3.8.**

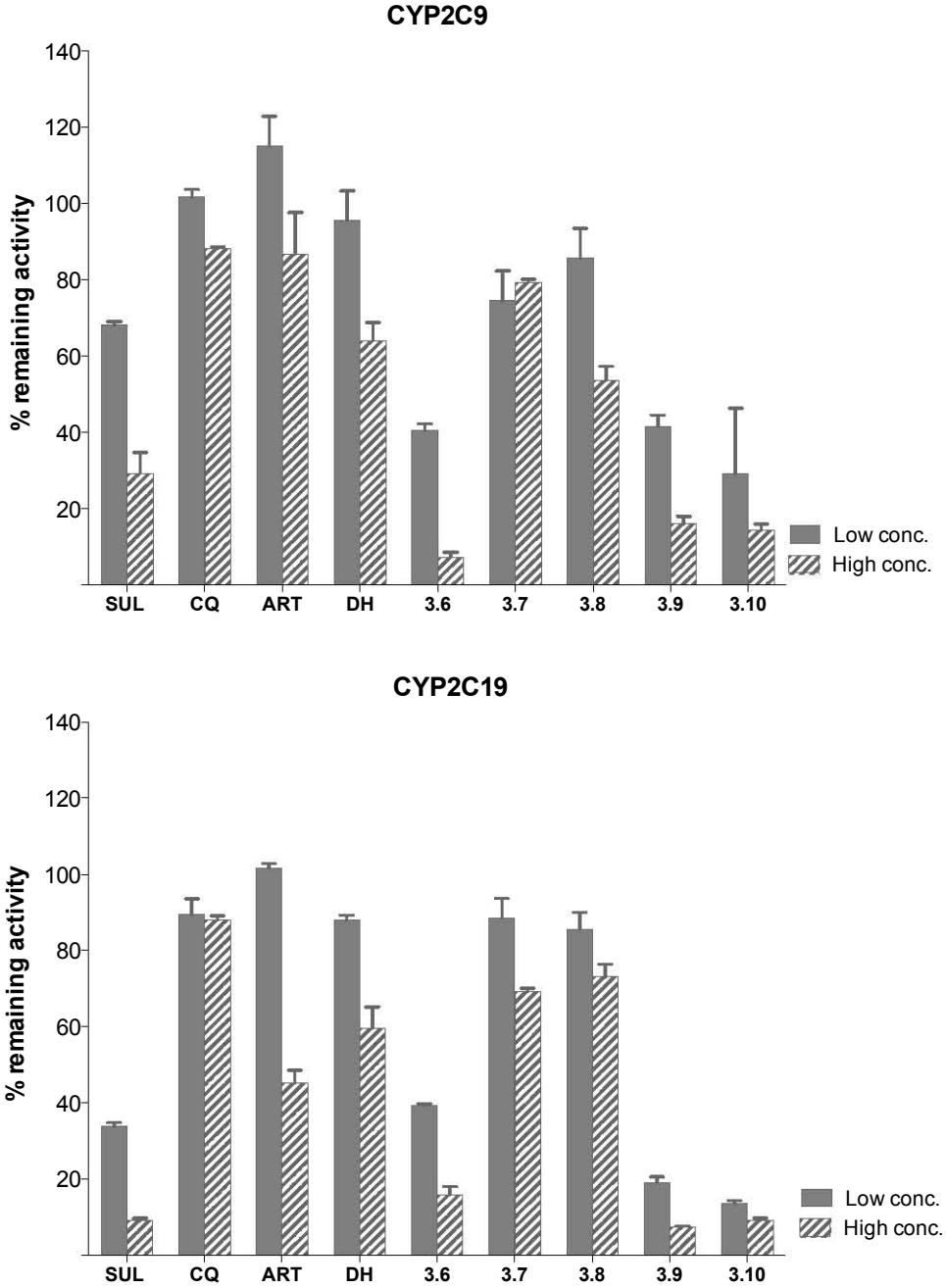

Figure 4.17: Inhibition of CYP2C9 and 2C19 by the artemisinin-chloroquinoline hybrids.

Inhibition was not significant in CYP2D6 with artemisinin and dihydroartemisinin showing no inhibition (Fig 4.18). The inhibition was moderate for the hybrids with the compounds **3.7** and **3.8** being potent against CYP1A2.

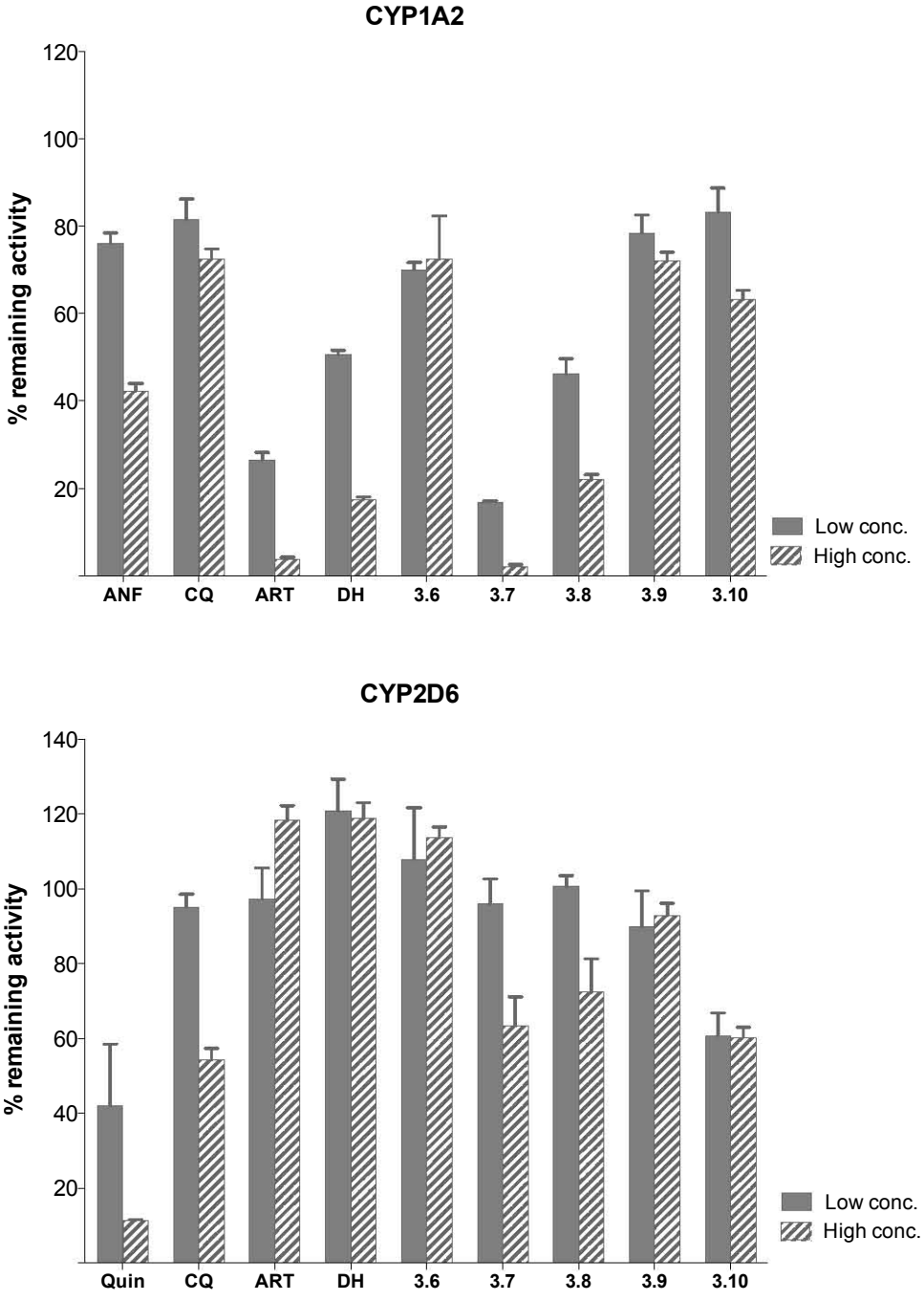

Figure 4.18: Inhibition of CYP1A2 and 2D6 by the artemisinin-chloroquinoline hybrids.

4.4 PART IV: Molecular Mechanism of CYP1A2 inhibition by TBZ

4.4.1 TDI screen of antiparasitic drugs

Parasitic drugs were screened for TDI in CYPs 1A2, 2C9 and 3A4. None of the compounds showed TDI against CYP2C9 and CYP3A4. The same was observed in CYP1A2 except for TBZ and its metabolite 5OH-TBZ which demonstrated potent inhibition and mild TDI respectively. The inhibition was potent at both low (3μM) and high concentration (20μM). The data for CYP1A2 is summarized in Fig 4.19. Compounds that were in the grey zone did not show any concentration dependence making them very unlikely to be TDI for the CYP isoforms. The negative control (α-naphthoflavone) and the positive control (furafylline) were clearly non-TDI and TDI respectively as expected. No significant loss of activity was observed in the control experiments where there was no inhibitor.

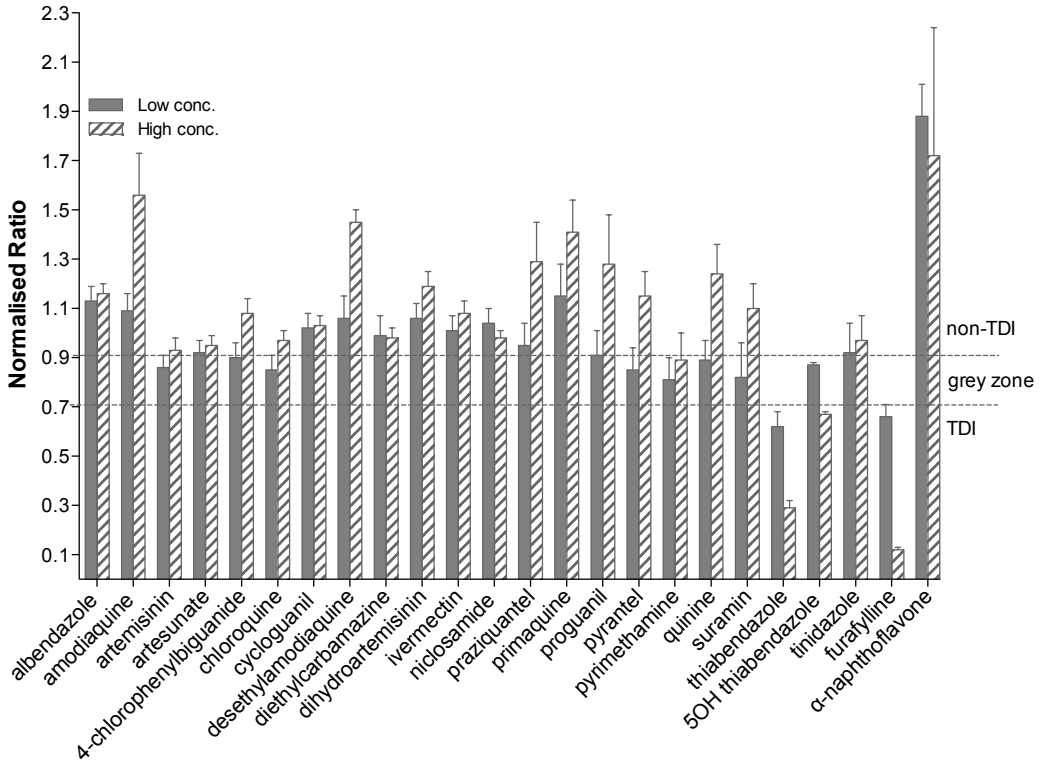

Figure 4.19: Time-dependent inhibition of CYP1A2 by antiparasitic drugs

4.4.2 IC_{50} determination

Inhibition of CYP1A2 by TBZ and 5OH-TBZwas evaluated using the activity assay to show the effects of TBZ and 5OH-TBZ via competitive inhibition. Both compounds were potent inhibitors of CYP1A2 with the inhibition characterized by an IC_{50} of 0.83 and 13.05μM respectively. The IC_{50} curves are shown in Fig 4.20.

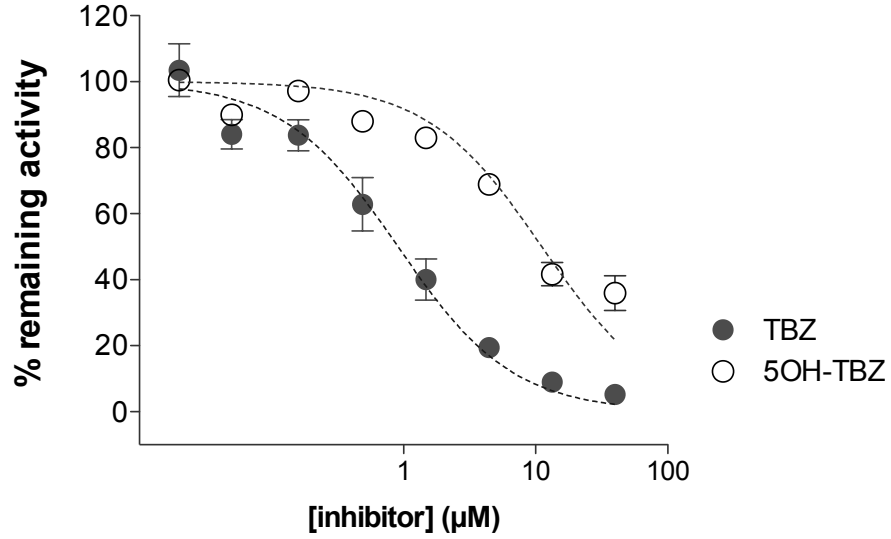

Figure 4.20: Inhibition of CYP1A2-mediated CEC metabolism by TBZ and 5OH-TBZ

4.4.3 Kinetics of CYP1A2 Inactivation by TBZ and 5OH-TBZ

Kinetics of CYP1A2 inactivation by TBZ and 5OH-TBZ were followed by measuring loss of CEC dealkylation activity. Inactivation of CYP1A2 was in a time- and concentration-dependent manner and followed pseudo-first order kinetics. The time course for the inactivation is shown in Fig. 4.21a. Nonlinear regression analysis of the time course data was then used to determine the initial rate constants for the inactivation at various concentrations of the two compounds (Fig. 4.21b). Inactivation constants k_{inact} and K_I for CYP1A2 were

determined to be 0.08 min^{-1} and 1.4μM, respectively, for TBZ and 0.02min^{-1} and 63.03μM for 5OH-TBZ respectively. At higher concentrations of TBZ, some loss of activity was observed at the zero point because of the carryover of TBZ into the inactivation assay mixture. Because 5OH-TBZ is a weak inhibitor, there were no significant changes in the activity of the enzyme at the varying time points for the lower concentrations (1.6, 3.1, and 6.3μM). However, the changes were much clearer at the higher concentrations, giving clearer slopes (Fig. 4.21a).

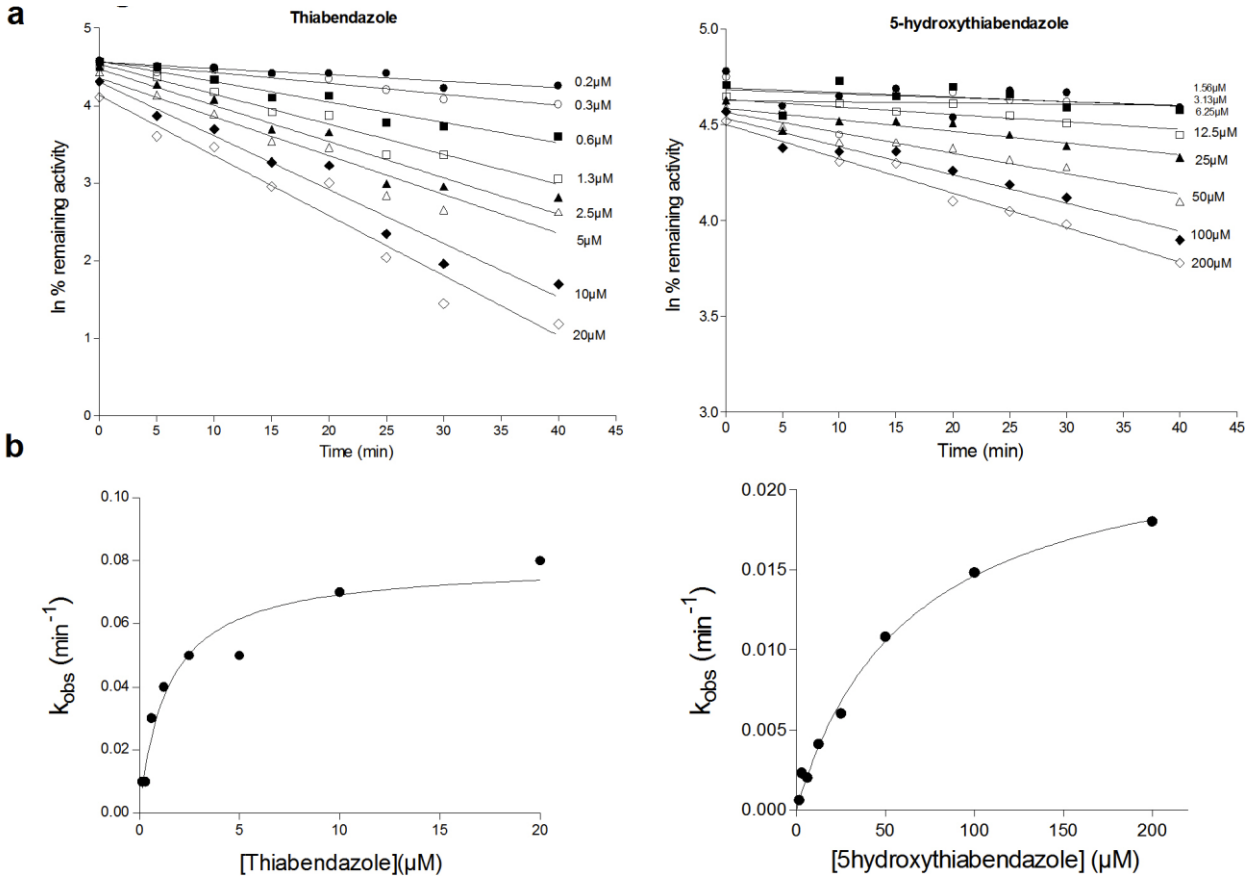

Figure 4.21: Time- and concentration-dependent inactivation of CEC dealkylation by TBZ and 5OH-TBZ.

4.4.4 Mechanism of TDI

4.4.4.1 IC_{50} shift

The two-step assay was performed for TBZ based on the fact that TDI causes a decrease in the IC_{50} value when preincubated with NADPH. Because TBZ had been shown to be a potent TDI, the assay was used to further confirm the observed result. TBZ inhibited CYP1A2 activity, with an IC_{50} value of 84.5μM when preincubation was done in the absence of NADPH. Preincubation with NADPH increased the inhibition of CYP1A2 considerably (Fig. 4.21), giving a further strong indication that TBZ is a time-dependent inhibitor of CYP1A2. The IC_{50} value was lowered to 2.8μM.

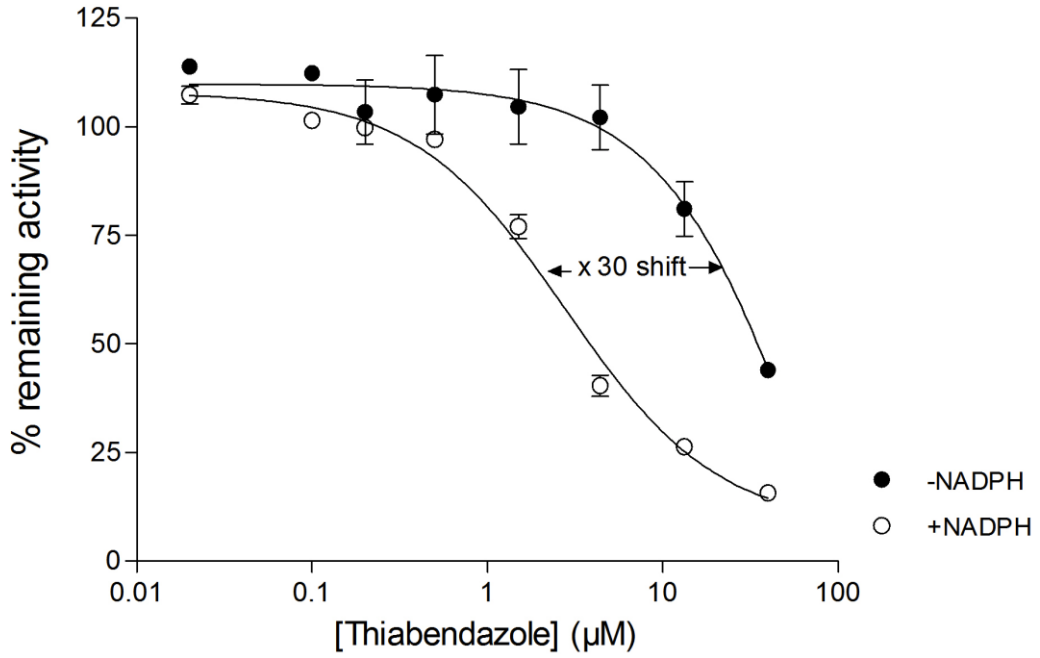

Figure 4.22: Inhibition of CYP1A2-mediated CEC metabolism by TBZ in the presence and absence of NADPH in the preincubation step.

4.4.4.2 Effect of GSH and K_3FeCN_6 on the Inactivation of CYP1A2

Protection of the enzyme inactivation by GSH and restoration of activity by oxidation by K_3FeCN_6 was investigated both in the presence and absence of NADPH. There was no significant increase in activity in the presence of GSH,

an indication that it failed to protect the enzyme from inactivation (Fig 4.23). K_3FeCN_6 was not able to restore enzyme activity, giving an indication that the inhibitor was not displaced from the enzyme. Inactivation was not significant when NADPH was absent in the preincubation step. There was no significant change when the compounds were used in combination.

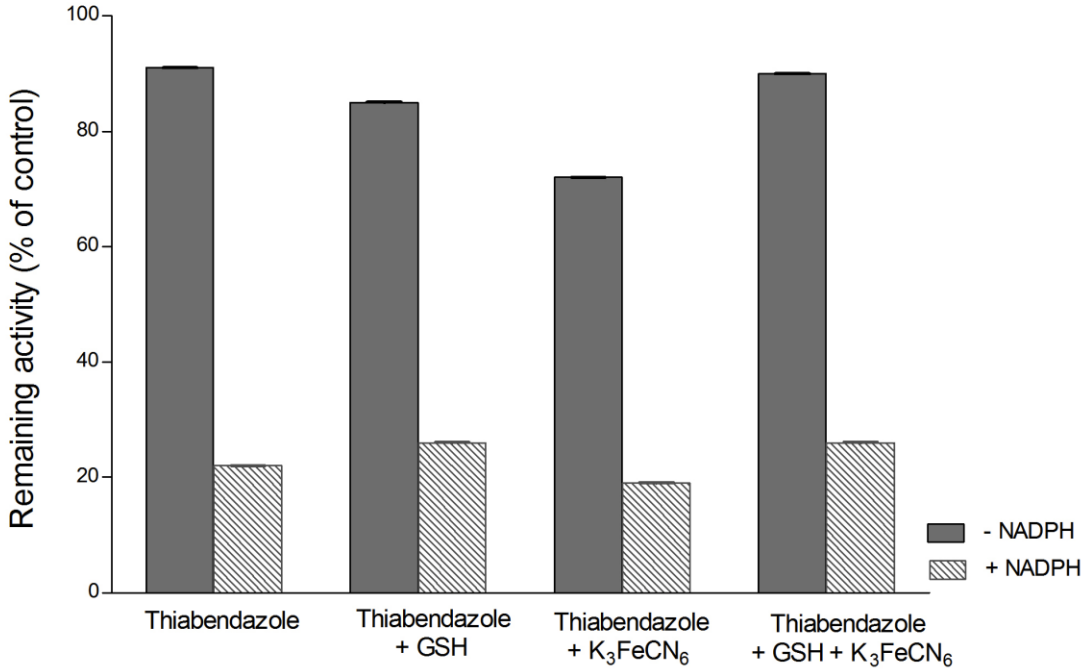

Figure 4.23: Effect of GSH and KFe_6CN_3 on the inactivation ofCYP1A2 by TBZ.

4.4.4.3 Effect of Dialysis

To determine whether the inactivation effects by TBZ and 5OH-TBZ were reversible, compounds were incubated with CYP1A2. For comparison, the experiment was also conducted with samples that were not dialyzed. As indicated in Fig 4.24, the dialysis did not affect the magnitude of inactivation by furafylline, which is a known MBI of CYP1A2. The effects of fluvoxamine were greatly reduced by dialysis, and activity was restored to 100%. It was clear that TBZ was an irreversible inhibitor, because there was no significant restoration of activity after dialysis. 5OH-TBZ was a clear reversible inhibitor.

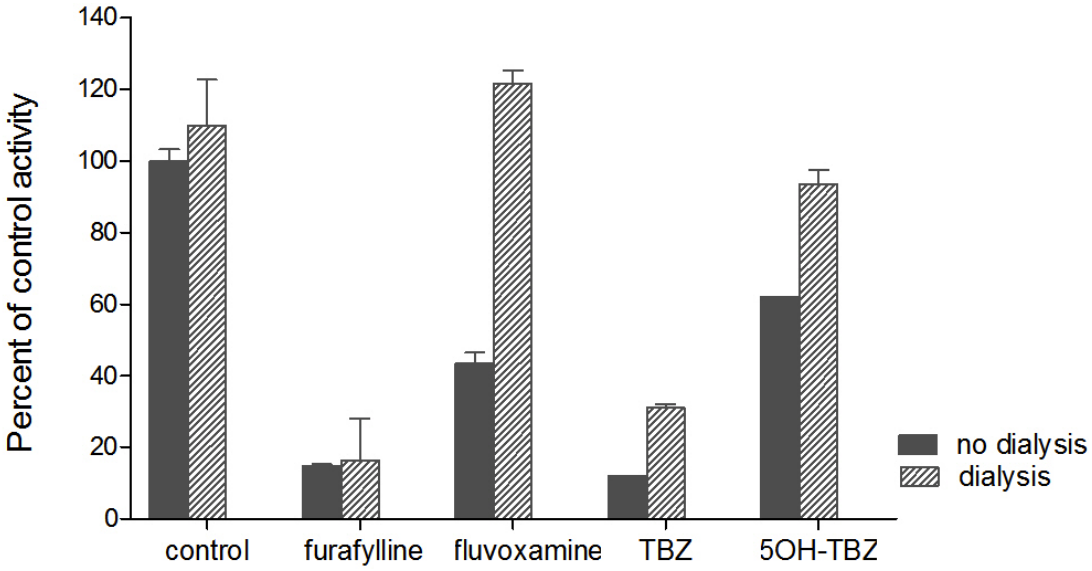

Figure 4.24: Effect of dialysis on inactivation of CYP1A2 CEC dealkylase activity by TBZ and 5OH-TBZ.

4.4.5 Substructure Search and Site of Metabolism Prediction

Based on substructures associated with TDI (Fontana *et al.*, 2005), two substructures were identified: a conjugated system and the thiazole ring (Fig. 4.25).

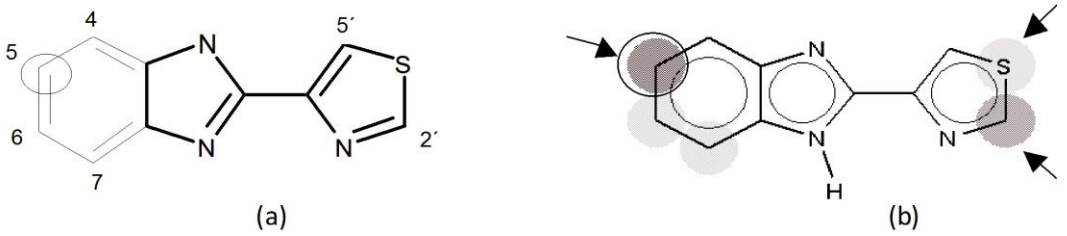

Figure 4.25: Site of metabolism prediction and substructure search in thiabendazole. Two fragments associated with TDI, the thiazole moiety and a conjugated system, were identified (a). The structure and numbering of thiabendazole are also shown, and the known hydroxylation site (from literature) is circled. The site of metabolism was then predicted using MetaSite (b). The top three sites of metabolism predicted by the program are indicated by arrows, with the position ranked first circled

These substructures have been associated with mechanism-based inhibition (MBI), where they are metabolized to reactive metabolites that bind

irreversibly to the enzyme (Fontana *et al.*, 2005). The compound was then submitted to MetaSite, which is a program that predicts the likely site of metabolism. The program has been proven to be able to predict the likely site metabolism within the top three predictions in 80% of the cases in structurally diverse compounds (Cruciani *et al.*, 2005). MetaSite predicted the 5C on the benzyl group of thiabendazole as the top ranked site of metabolism (Fig. 4.25b).

4.4.6 Docking studies

The results obtained from the docking experiments were in agreement with the site of metabolism predictions. There was one preferred orientation in all the three GOLD solutions in which the benzene ring of the compound was the closest to the heme catalytic center at an average distance of 4.5 Å in all the three solutions. One of the three docking poses is shown (Fig. 4.26).

In GLUE, eight of the 10 docking solutions were in agreement with the site of metabolism prediction. In five of the 10 solutions, the thiazole ring was toward the heme and in three the benzene was the one closest to the heme catalytic center. In two of the solutions, both predicted groups were too far away from the catalytic center for any metabolism to occur. Examples of the possible docking poses are shown (Fig 4.27). Interactions of the benzene ring or the thiazole ring of thiabendazole with phenylalanine 226 of CYP1A2 seem to be important in determining the orientation of thiabendazole in the enzyme active site.

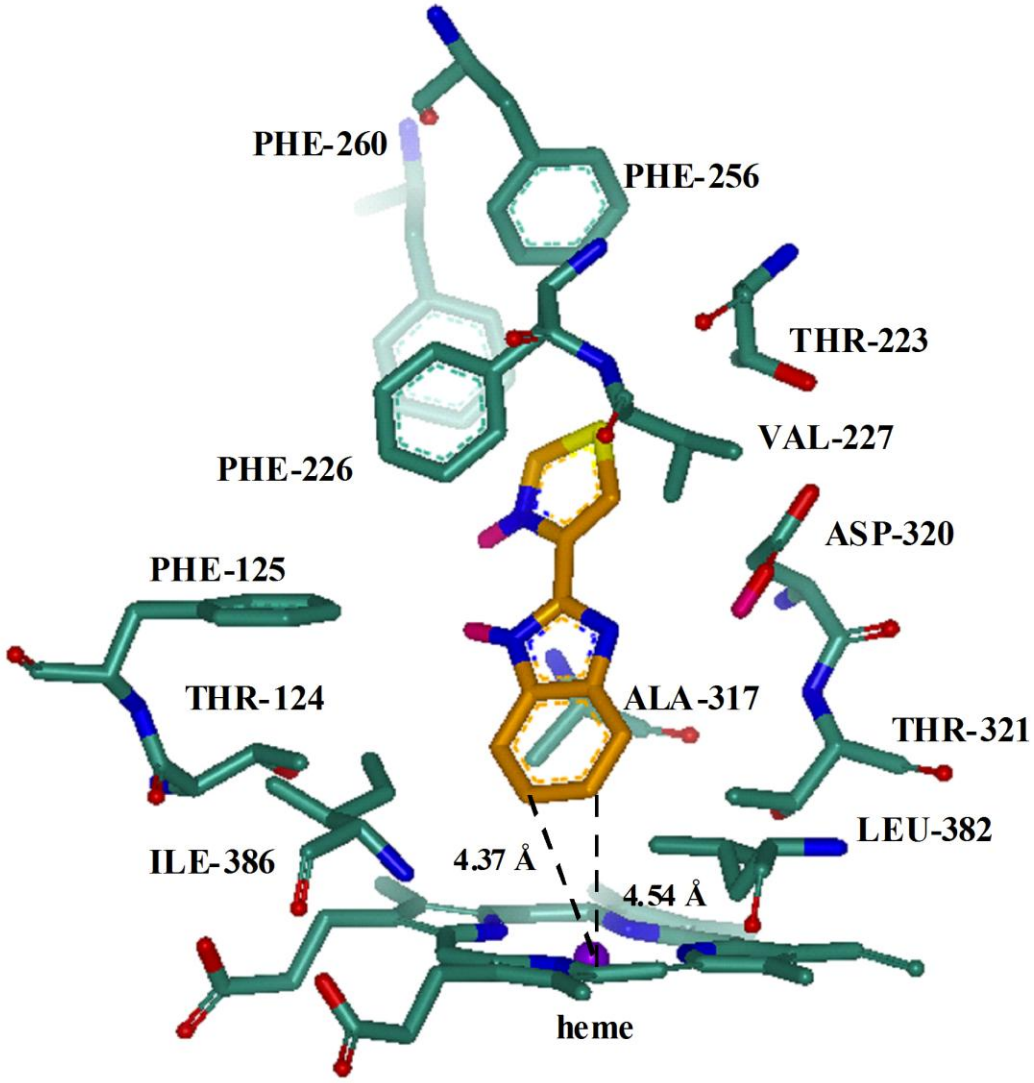

Figure 4.26: Binding of thiabendazole into the active site of CYP1A2 (PDB 2HI4). The heme prosthetic group, amino acid residues constituting the active site and thiabendazole are all depicted in sticks. Carbon atoms are colored orange in thiabendazole and green in the heme and amino acid residues. Oxygen, nitrogen, and heme iron are colored red, blue, and purple, respectively. Hydrogens and water molecules are not shown.

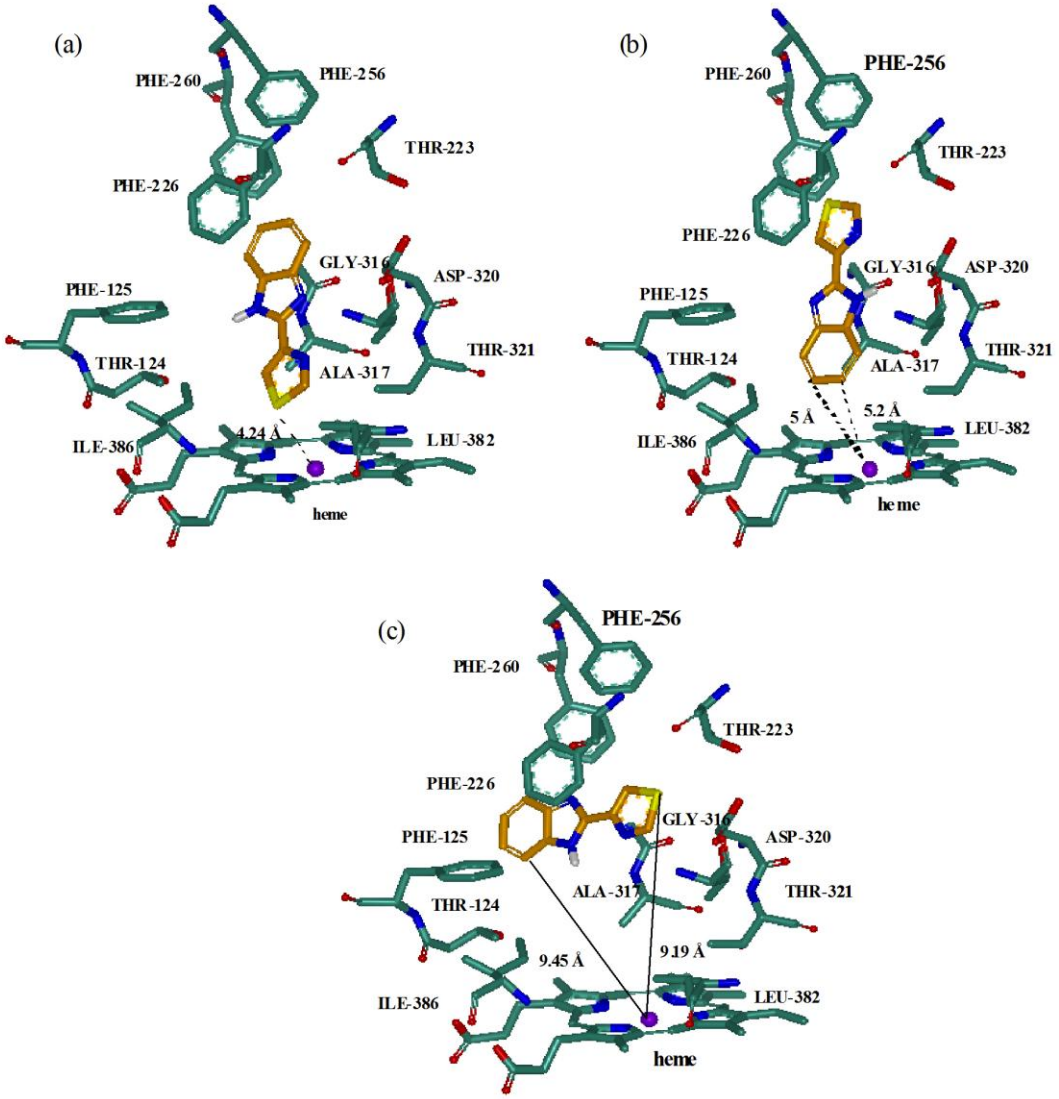

Figure 4.27: Examples of different orientations in which thiabendazole docks into the active site of CYP1A2. The color-coding is the same as described for legend Fig 4.26. In five of the top 10 ranked solutions, the thiazole group was the group closest to the heme (b); in three solutions, the benzene ring in which hydroxylation occurs was closest (a); and in two solutions, both groups were further away (c). Interactions of the benzene or thiazole moiety of thiabendazole with phenylalanine 226 ofCYP1A2 seems to be important in determining the orientation of thiabendazole in the enzyme active site.

4.4.7 DDI Pharmacokinetic Simulations

The simulated DDI interactions involving TBZ as a competitive and as an irreversible inhibitor of CYP1A2 are summarized in Table 4.11. The MBI effects were significantly more profound compared with the competitive

effects for the CYP1A2substrate tested.

Table 4.11: Prediction of DDI between TBZ and other CYP1A2 substrates

Combination	Mechanism	Predicted Mean AUC -Fold Increase	Observed Clinical DDI -Fold Increase in AUC
TBZ/TBZ	MBI	22.51	1.0
TBZ/caffeine	Competitive	1.23	1.60
	MBI	11.40	-
TBZ/ theophylline	Competitive	1.56	2.91
	MBI	5.65	-

4.5 PART V: Drug-herb interaction by evaluating the ADMET/PK of the active ingredient natural product, Frutinone A

4.5.1 Determination of intrinsic clearance and metabolite identification

The hepatic clearance (CL_H) of the compound was predicted to be low (Figure 4.28) with a calculated in vitro $T_{1/2}$ of 179.55 min and *in vitro* clearance 3.86 µl/min/million cells at 1µM of Frutinone A.

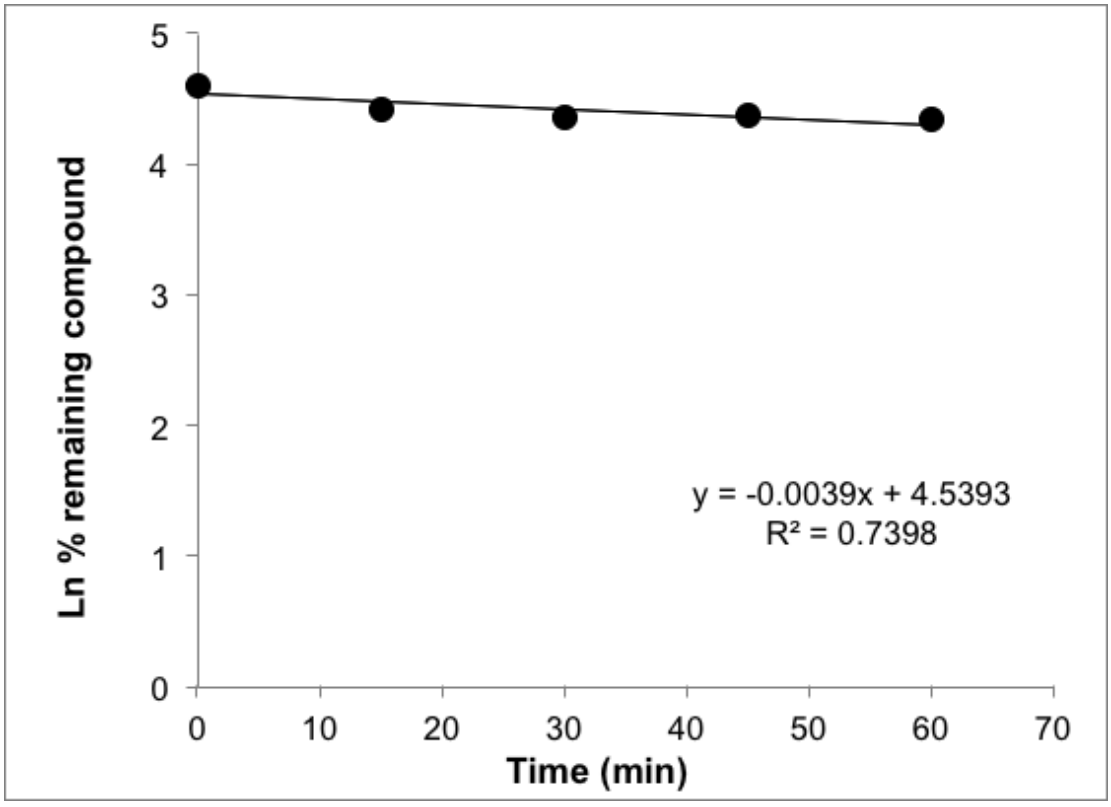

Figure 4.28: Rate of metabolism of Frutinone A in cryopreserved hepatocytes. Metabolism was measured by the disappearance of Frutinone A from media containing human cryopreserved hepatocytes. The data was linearized to enable calculation of the half-life using the slope of the line

Calculations were means of two replicates. Estimated whole liver clearance was 10.89ml/min/kg. Hepatic clearance was estimated using the well-stirred model and was predicted to be 7.17 ml/min/kg. Binding of the compound to

plasma protein and hepatocytes was not taken into account when the calculations were done. The value predicted for hepatic clearance was calculated to be about 30% of the blood flow (Q_H = 21 ml/min/kg). One minor by product (4%) postulated to have resulted from lactone ring opening and enzymatic or non-enzymatic aqueous hydrolysis was identified (Figures 4.29).

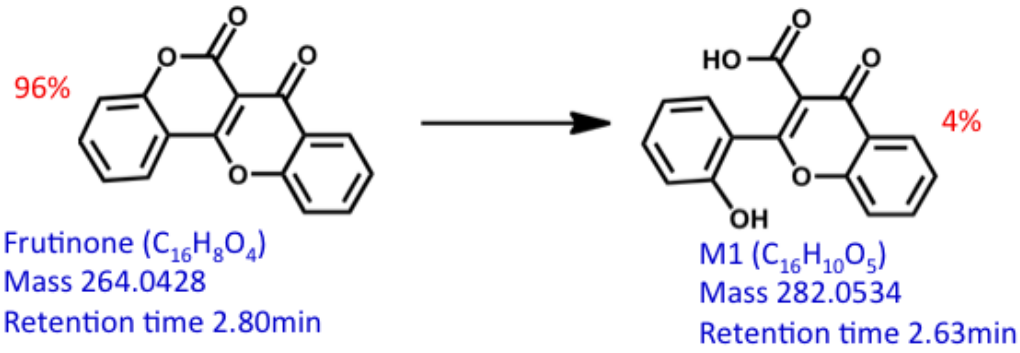

Figure 4.29: Proposed hydrolysis pathway for Frutinone A in cryopreserved human hepatocytes. The hydrolysis byproduct was identified using LC-MS and Metabolynx™ software and was postulated to be a result of enzymatic- or non-enzymatic-mediated lactone ring opening via hydrolysis.

Up to 96% of the parent compound remained in the incubation. The parent had a mass of 264.04 and retention time 2.80min. The by-product on the other hand had a mass of 282.05 and retention time of 2.63min.Spectra for the Frutinone and the by-product are shown in Fig 4.30.

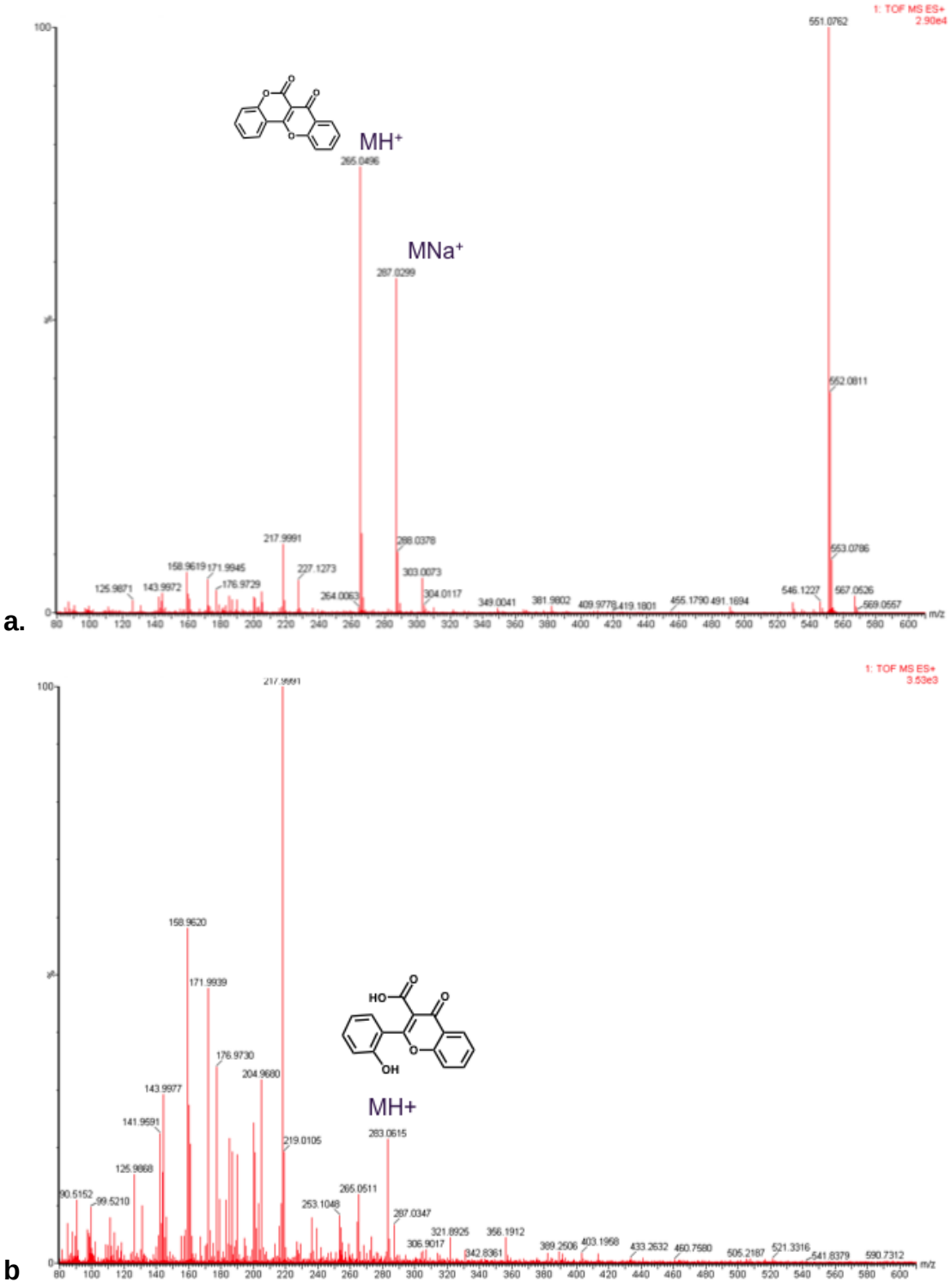

Figure 4.30: MS spectra of protonated ions of Frutinone A (m/z 265.0496) and its minor by-product M1 (m/z 283.0534). Frutinone A was incubated in cryopreserved hepatocytes for 0 and 120 min. Spectra were obtained from scans made on the sample at 0 min where no reaction was expected to have occurred (a) and after 120 min (b), to enable identification of any metabolites.

4.5.2 Reaction phenotyping

The compound was tested for metabolism by any of the 11 CYPs and HLM. There was slight metabolism observed with CYP1A1, 1B1, 2C8, 2C9 and HLM (Table 4.12). No metabolism was observed with the rest of the CYPs including CYP1A2.

Table 4.12: Disappearance of Frutinone A from media in incubations with various enzymes

Enzyme	% lost compound
CYP1A1	28.53 ± 0.56
CYP1A2	0.00 ± 0.02
CYP1B1	15.68± 0.41
CYP2B6	0.95± 0.63
CYP2C19	0.00 ± 0.04
CYP2C8	26.41± 0.53
CYP2C9	25.93± 0.56
CYP2D6	0.00 ± 0.00
CYP2E1	0. 00 ± 0.01
CYP3A4	0.00 ± 0.01
CYP3A5	0.00 ± 0.02
HLM	6.76 ± 0.37

The amount of compound lost in the media relative to the control was determined and used to estimate the metabolism of the compound as described under materials and methods. The results are an average of two replicates

4.5.3 Reversible and time-dependent inhibition screens on the effect of Frutinone A on the major CYPs

The effect of Frutinone A on the five major CYP isoforms (CYP1A2, 2C9, 2C19, 2D6 and 3A4) was investigated. The compound inhibited all the five isoforms. Potent inhibition was shown with CYP1A2 with moderate effects on CYPs 2C9, 2C19, 2D6 and 3A4 (Table 4.13). TDI screening was conducted on CYP1A2 using CEC O-deethylation as a marker reaction.

Table 4.13: Effect of Frutinone A on the activity of the five major CYP isoforms

Enzyme	Compound	% Remaining activity (low conc)	% remaining activity (high conc)
CYP1A2	α-naphthoflavone	53.87 ± 6.56	16.29 ± 4.05
	Frutinone A	11.77 ± 1.90	7.45 ± 1.78
CYP2C19	Ticlopidine	53.29 ± 0.03	16.84 ± 0.15
	Frutinone A	79.17 ± 0.34	51.52 ± 1.05
CYP2C9	Sulfaphenazole	71.24 ± 5.12	30.28 ± 2.25
	Frutinone A	73.79 ± 12.98	62.04 ± 12.13
CYP2D6	Quinidine	42.00 ± 6.46	9.57 ± 0.90
	Frutinone A	100.76 ± 8.71	64.36 ± 1.41
CYP3A4	Ketoconazole	83.27 ± 7.10	20.13 ± 0.77
	Frutinone A	81.97 ± 1.65	41.16 ± 4.58

There was no TDI observed when Frutinone A was preincubated with NADPH (Figure 4.31). There was also no concentration dependence making it unlikely that this compound would be a time-dependent inhibitor of CYP1A2.

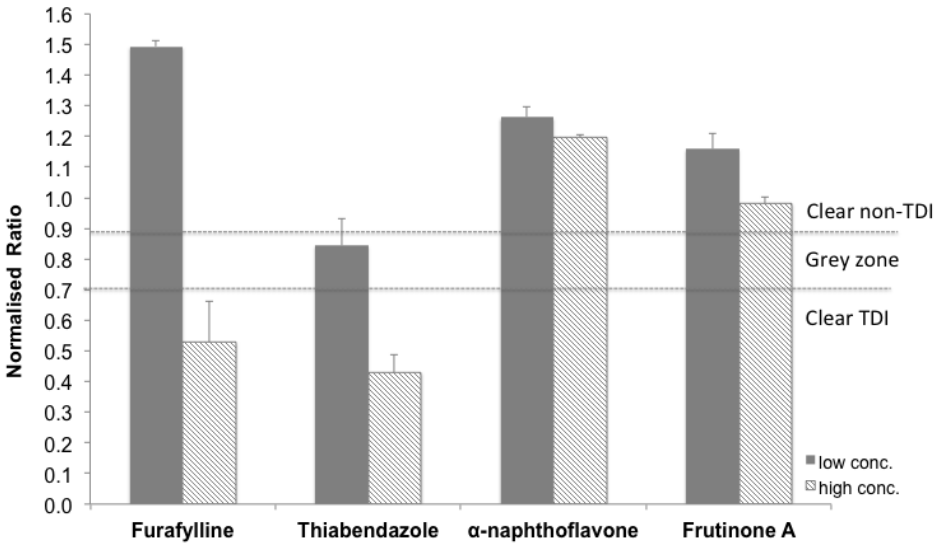

Figure 4.31: Time-dependent inhibition (TDI) effects of Frutinone A on CYP1A2 activity. Frutinone A was incubated in human liver microsomes both in the presence and absence of NADPH. Furafylline and thiabendazole were used as positive control TDI inhibitors and α-naphthoflavone CYP1A2 was used as a negative control non-TDI inhibitor. Frutinone A and thiabendazole were evaluated at 1 and 20μM, and furafylline and α-naphthoflavone at 0.01 and 0.1 μM.

4.5.4 Effect of Frutinone A on CYP1A2 mediated CEC O–deethylation and ethoxyresorufin O -deethylation

Further investigations were carried out on CYP1A2 as the greatest inhibition had been seen with this enzyme. Frutinone A inhibited CYP1A2 with an IC_{50} value of 0.56μM (Figure 4.32).

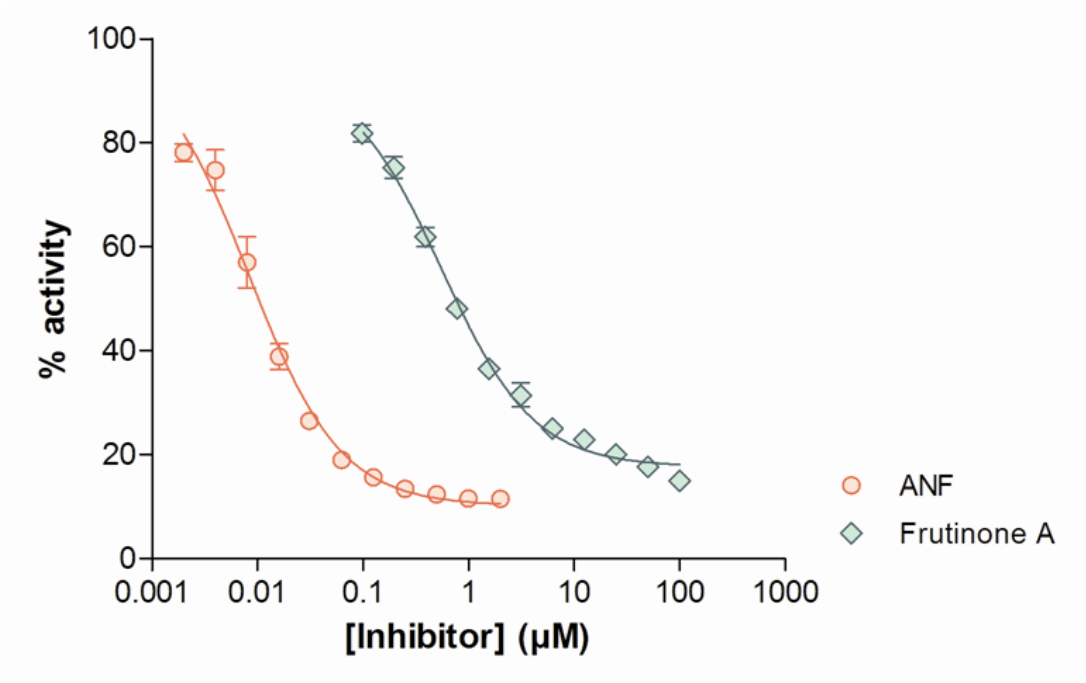

Figure 4.32: Inhibition of CYP1A2 mediated 3-cyano-7-ethoxycoumarin metabolism by Frutinone A. α-Naphthoflavone was used as a positive control inhibitor. The IC_{50} for α-naphthoflavone and Frutinone A were 0.008μM and 0.56μM respectively.

The mode of inhibition by Frutinone A was determined to be mixed with CEC and competitive with ER (Figure 4.33). The **α** -naphthoflavone inhibited via mixed-type inhibition. The inhibition kinetic parameters for Frutinone A and **α** -naphthoflavone with each of the substrates are summarized in Table 4.14.

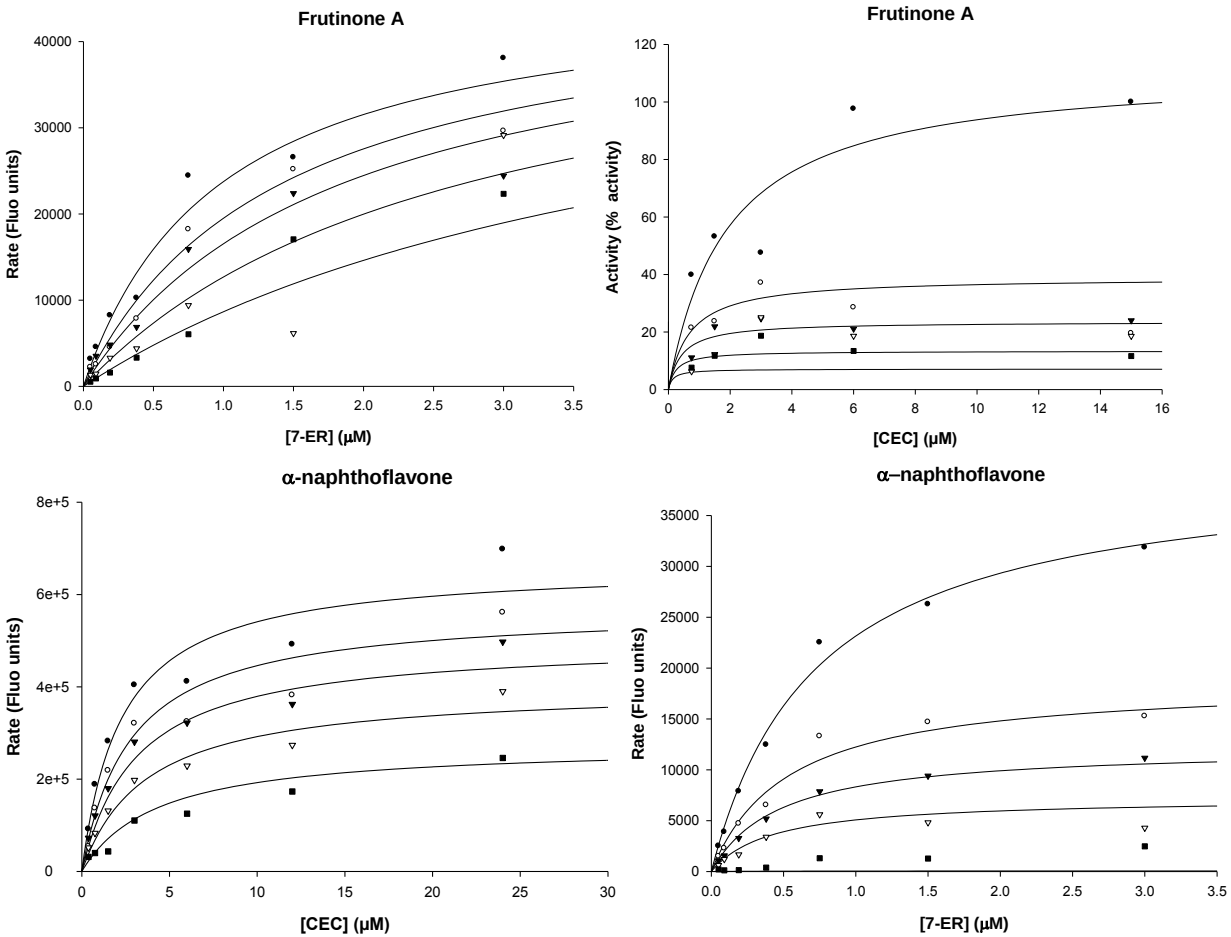

Figure 4.33: Enzyme kinetics for the inhibition of CYP1A2 by Frutinone A and α-naphthoflavone. Frutinone *A* inhibited CYP1A2 mediated *3-cyano-7-ethoxycoumarin* metabolism via a competitive mechanism and 7-*ethoxyresorufin* via *a* mixed mechanism. The control compound, α-naphthoflavone inhibited via a mixed mechanism in both substrates. Incubations were made at varying concentrations of substrates and inhibitor.

Table 4.14: Disappearance of Frutinone A from media in incubations with various enzymes

	CEC	ER
α-naphthoflavone		
Km	2.3μM	0.72
K_i	0.005μM	0.003
Mode of inhibition	Mixed	Mixed
R^2	0.94	0.98
Frutinone A		
Km	1.9	0.97
K_i	0.48	0.31
Mode of inhibition	Mixed	Competitive
R^2	0.95	0.93

The parameters were determined as described in the experimental section. The data was derived from fitted curves using non-linear regression (Fig 4.32) and were results of duplicate experiments

4.5.5 Docking studies for Frutinone A

To validate the accuracy of the docking software, the docking orientation of the docked α-naphthoflavone was compared to that of co-crystallized α -naphthoflavone. There was a clear overlay of the two structures when they were superimposed on top of each other as indicated in Figure 4.34. Also as previously described, α–naphthoflavone had a single preferred binding orientation. Frutinone A interacted with the amino acids in the active site in the same way as α-naphthoflavone with a similar binding orientation (Figure 4.35).

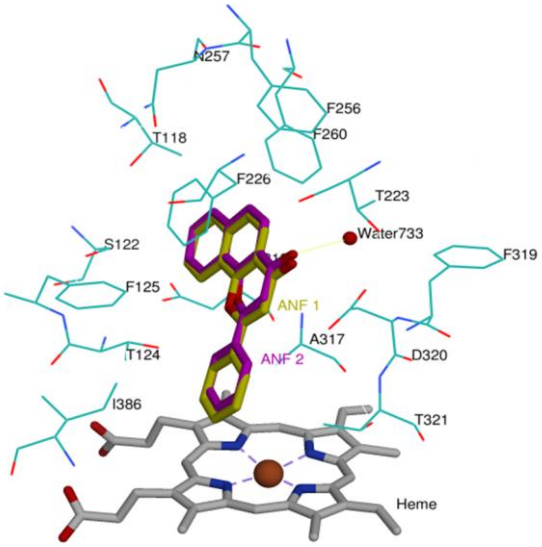

Figure 4.34: Validation of docking protocol. Orientations of the co-crystallised and docked α-naphthoflavone that were computed in Autodock Vina were superimposed and compared. The co-crystallised α-naphthoflavone (ANF 2 = purple), docked α-naphthoflavone (ANF 1 = yellow) and heme (grey) are depicted as sticks. The main amino in the active site (cyan) are depicted as wireframe. Other amino acids in the binding pocket have been left out for ease of visualization.

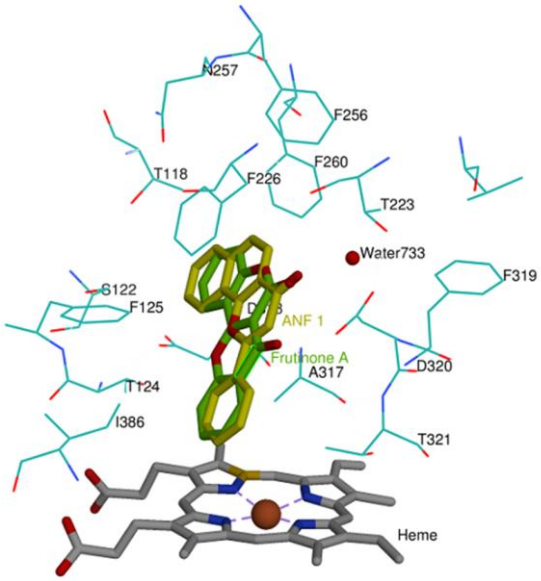

Figure 4.35: Comparison between binding orientation of α-naphthoflavone and Frutinone A Frutinone A and α-naphthoflavone were docked into the CYP1A2 active **site**. Frutinone A (green) and α-naphthoflavone (yellow) are depicted as sticks. The main amino acids in the binding pocket (cyan) are depicted as wireframe. Heme is shown as grey sticks. Other amino acids in the binding pocket have been left out for ease of visualisation

4.5.6 Binding orientations of Frutinone A compared to that of substrates

In an effort to explain the mixed inhibition we observed in the experiments, two software packages were used to dock Frutinone A, CEC and ER. Docking was also performed for **α**-naphthoflavone to control the experiment. Distances for the atoms nearest to the heme were measured to determine how likely metabolism could occur in those compounds. Distances measured with Autodock for CEC, ER, Frutinone A and **α**-naphthoflavone were 4.4, 4.0, 4.8 and 4.6 Å, respectively, with binding free energies of −7.0, −8.6, −13.3 and −14.5 kcal/mol. With this software, all the compounds were docking in the same binding orientation (Fig 4.36).

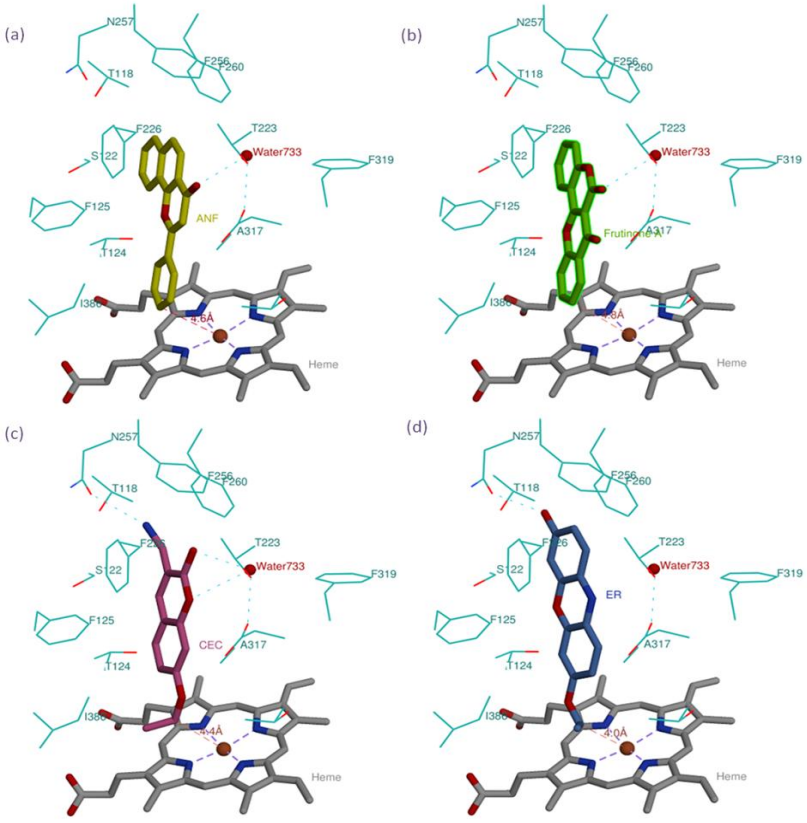

Figure 4.36: Binding of the various docked compounds in the active site of CYP1A2. The dockings were performed using the Autodock Vina software. The broken lines show hydrogen bonds between the docked concentrations of the compounds and the amino acids. Distances of the nearest atom to the heme are shown and indicated by the red broken lines.

However using FlexX, additional alternative binding orientations for substrates (Fig 4.37) were observed. The substrates bind below the hydrophobic pocket characterized by phenylalanines 226, 260 and 256. Distance of the metabolized sites for CEC and ER were 4.3 and 4.2 Å, respectively.

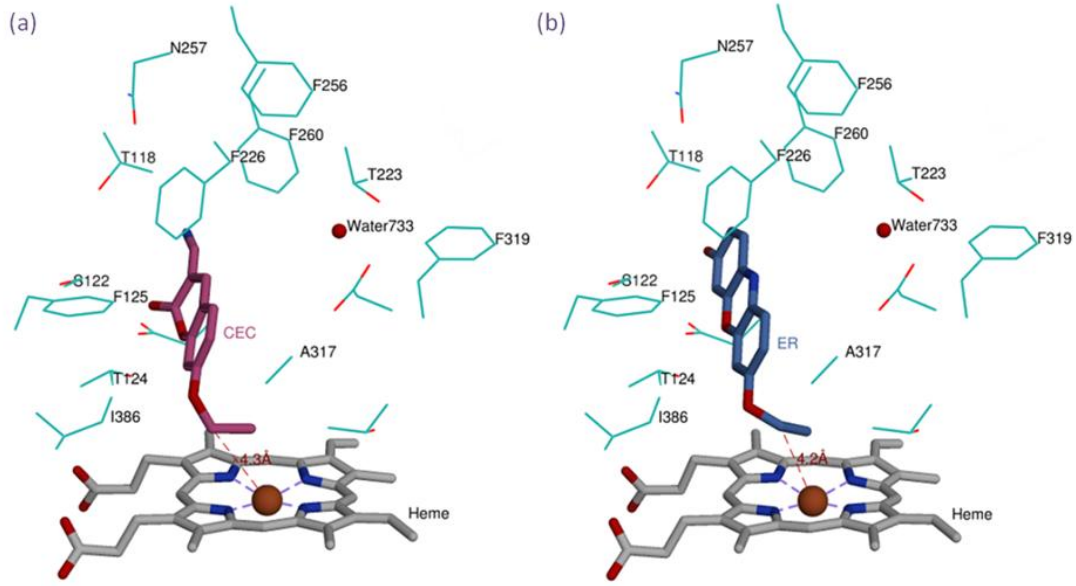

Figure 4.37: Binding orientations of CEC and ER in the active site of CYP1A2. The dockings were performed using the FlexX software. The active site was mapped using the co-crystallised α-naphthoflavone.

5 DISCUSSION

5.1 PART I: Setting up of the ADME/PK platform

Prior to the screening of the compounds for ADME/PK liabilities the various biochemical assays were setup and validated. Although the assays are used routinely in many drug discovery settings in developed countries, this is the first time to our knowledge an attempt has been made in Africa to come up with a facility that supports ADME studies for newly synthesized compounds in medicinal chemistry.

Most drug discovery efforts in Africa have traditionally been driven by both synthetic chemistry and natural products coupled to *in vitro* and *in vivo* pharmacological screens for potency. *In vivo* PK studies have also been done in a few cases in support of these drug discovery initiatives. The integration of ADME/PK in the drug discovery value chain from hit identification through to candidate selection has been shown to reduce attrition rates of NCEs due to PK liabilities from 40 to 10% (Kola and Landis, 2004). Successfully setting up the ADME/PK assays in our laboratory will therefore provide support to our projects and other drug discovery scientists in Africa. This will help in integrating this science in the drug discovery value chain, thus promote productive collaboration among medicinal chemists, ADME and pharmacology. In this project the approach was implemented in the lead identification for compounds with anti-malarial activities as illustrated in Fig 1.7.

In this project, we applied the ADME/PK platform in the characterization of existing and newly synthesized compounds with potential to be used as antiparasitic drugs. We also used the platform to screen for potential interactions between herbal/traditional medicines and drug metabolizing enzymes and the implications of their use with substrates of those compounds. Given that herbal/traditional medicines are widely used in Africa for treating various ailments including parasitic infections such as malaria and TB, it is important to explore the risk of concomitant administration of conventional medicines and herbal remedies. Drug-herb interactions have been studied with common examples being induction of CYP3A by St John's Wort (Moore *et al.*, 2000; Madabushi *et al.*, 2006) and inhibition of CYP3A by constituents of grapefruit juice (Bailey *et al.*, 1995; Bailey *et al.*, 1998; Fuhr, 1998; Kiani and Imam, 2007).

The setting up of this ADMET platform is also consistent with the increasing efforts to promote drug discovery and development initiatives in Africa through organizations such as the African Network for Drug and Diagnostics Innovation (ANDi), WHO-TDR, MMV, and others organizations. The platform we have setup is already supporting projects from some R&D based pharmaceutical companies in Africa, some university drug discovery research groups and other related biomedical and pharmaceutical R&D institutions.

As an example of validation, known time- and non-time dependent inhibitors of CYP2C9 were used to validate the time dependent assay. The validation set for CYP2C9 included tienilic acid (control), methimazole, cimetidine,

hydrastine, silibinin, fluvoxamine, fluoxetine and sulfaphenazole (control). Fluvoxamine and sulfaphenazole, which were non-TDI compounds (Atkinson *et al.*, 2005), were not picked by the assay. Silibinin and methimazole were not picked because they require very high concentration to show the inhibitory effects and this is consistent with literature (Zuber *et al.*, 2002; Guo *et al.*, 1997). Cimetidine has previously been reported as a weak inhibitor (Furuta *et al.*, 2001) and our observations were consistent with this. Parameters were also within range for the other isoforms.

Assays for metabolic stability, reaction phenotyping, metabolite identification, inhibition screening and for physicochemical profiling were successfully set up and used to screen the various compounds in the study. It was clearly demonstrated that the platform can be utilized to screen for liabilities in newly synthesized compounds as well as in drugs that are currently in use. The K_m values for CYP marker reactions were within the range of reported literature values (Ghosal *et al.*, 2003; Naritomi *et al.*, 2004; Crespi *et al.*, 1997) hence validating the assays.

5.2 PART II: Identification of ADME/PK liabilities of 3,4-HPO-4-amino-7-chloroquinolinyl hybrid compounds with antiplasmodial activity

Malaria still relies on chemotherapy for treatment. However there have been challenges associated with chemotherapy. Resistance and toxicity are some of the major challenges. There is continuous need to develop drugs that have efficacy and good safety profiles. Towards this aim, compounds with potential to have efficacy against resistant strains of P. falciparum were synthesized. Although the aim of this project was to evaluate ADME/PK liabilities in the compounds, the work was run in parallel with pharmacology screens as well as modifications of the potential compounds in medicinal chemistry.

The compounds were shown to have good activity against the CQR and CQS *P. falciparum* strains. The mechanism of action was unexpectedly shown to be β-haematin inhibition especially in the sensitive strain. The strong β-haematin inhibition activity was shown to translate into strong antiplasmodial activity more in the sensitive 3D7 than in the resistant K1 strain. This could have been as a result of the mutant *Pf*CRT in the resistant strain exporting test compounds out of the food vacuole resulting in the lowering of drug concentrations at the target site. However, it should be noted that the β-haematin inhibition and antiplasmodial activities were determined in cell free and cell based media respectively. Therefore good β-haematin inhibition activity may not necessarily translate into good antiplasmodial activity because the effect entirely depends on ability of the compounds to access the intracellular target.

The disease and the expected route of delivery, which was oral for this study, determined the choice of physicochemical properties to be studied. Properties allowing absorption by the human host as well as the parasite were preferred. The compounds were predicted to be drug like and all the other properties were within acceptable ranges; clogP (2.6 - 4.5), experimental logD (3 -5) and solubility (>20 μg/ml) with the exception of a few compounds (Table 4.5). Benzylated analogues had higher solubility besides them being the most lipophilic.

Lipophilicity was the main physicochemical property driving the antiplasmodial activity, β-haematin inhibition activity and CYP inhibition. The lipophilicity seemed to be driven by the N-1 alkyl group, which is the same group thought to affect antiplasmodial activity. Significant correlations between lipophilicity and antiplasmodial activity were observed for the W2 strain in the deprotected analogues (R^2 = 0.41) and benzylated analogues (R^2 = 0.88). Correlations were also strong for β-haematin inhibition with the benzylated analogues having an R^2 of 0.59 and the deprotected analogues with R^2 of 0.76. Lipophilicity also played a significant role in cytotoxicity From the CYP inhibition screens, it was observed that CYP3A4 inhibition was driven by lipophilicity, with the greatest inhibition being observed in the benzylated analogues (Table 4.9).

However there were instances where it was observed that lipophilicity was not the only factor driving biological activity. There was no correlation between lipophilicity and antiplasmodial activity in the hybrids in which the methyl

group replaced the benzyl group. This led to the postulation that other mechanisms were at play. The 3,4-HPO-chelator moiety may be enhancing the selectivity for the resistant strains possibly via some favourable interactions with the unprotected 3-OH group. The benzyl group may also be participating in π-π interactions with the heme porphyrin. This coupled with high lipophilicity could explain better β-haematin and antiplasmodial activity of the benzylated analogues compared to the methoxylated ones. Blocking the chelator group by benzylation or methoxylation (Table 4.3 and 4.4) led to a decrease in activity. However, data from the N-alkyl-3 HPOs indicate the chelator by itself is not enough to cause significant antiplasmodial activity as shown by the poor activity in these compounds (Table 4.3).

Prediction studies for intestinal absorption indicated that the synthesized analogues will be well absorbed (Table 4.5). Predictions for CNS penetration were indicative of good permeation. This property, if not optimal, could be a limiting factor in the capacity of the drug to access malaria parasites in the brain in the case of cerebral malaria. ADME studies were performed to access the safety of the compounds if they were to be used in humans.

From the CYP inhibition studies the compounds were shown to be potent inhibitors of CYP3A4 and CYP2D6. The mode of inhibition in CYP3A4 was mainly non-competitive in most of the compounds. This is very difficult to model, as the site of interaction between the ligand and the enzyme is relatively unknown. The IC_{50} and K_i for both CYP2D6 and CYP3A4 suggested the compounds carry an intermediate risk of interaction with substrates of the

enzymes. Since CYP3A4 and CYP2D6 metabolize about 70% of drugs currently on the market, the interactions may be a cause of concern. There was, however, no trend between lipophilicity and CYP2D6 inhibition.

Hepatocytes cleared the compounds faster than the microsomes. This could be due to the fact that hepatocytes have the full complement of drug metabolizing enzymes compared to microsomes. The mainly fast and intermediate clearance observed could be an indication that the compounds would need to be dosed more than once a day in the prophylaxis /treatment of malaria. Should these compounds be pursued as leads, a strategy for designing more metabolically stable compounds should be developed.

Biotransformation studies in hepatocytes indicated that the synthesised analogues were extensively metabolised to various primary and secondary metabolites (Appendix A).The primary metabolism mainly involved the formation of the **M1** metabolite and an intermediate metabolite which proceeds to form mainly metabolite **M5** (Fig 4.10). The analogues also undergo metabolism to **M2** metabolite through N-dealkylation and to an aldehydic intermediate metabolite that mainly proceeds to form the **M3** and/or **M4** metabolites. Given this metabolic stability status, efforts to stabilise the compounds with respect to metabolic clearance, should involve changes to substituents on the carbon adjacent to the aromatic ring of **M1** such that hydrogen abstraction at this site is difficult or impossible. Similarly, to block the formation of the second most common metabolite, **M3**, substitutions on the carbon adjacent to the NH of the quinoline moiety is recommended. The

substitutions at the carbons can be with halogens such as Cl or Br whose electron withdrawing effects inhibit CYP-mediated metabolism

Hot spots on the molecules were revealed to be N-dealkylation to **M1** and formation of a carbonyl intermediate, which subsequently gives rise to metabolites **M8** and **M5**. A strategy to stabilize these analogues could involve the substitutions of hydrogen on C-1'carbon next the pyridinone N, with halogens such as chloro or bromo groups. These electron-withdrawing atoms could reduce the reactivity of this molecule. The second major metabolite involves the cleavage of the molecule at a site adjacent to the quinoline moiety. A strategy to stabilize the molecule at this site could also include substitution of hydrogens with halogen. The resulting analogues should be retested for metabolic stability since instability could be introduced at other parts of the molecule. It is also necessary to retest for antiplasmodial activity, as properties of the linker chain that we propose to modify are associated with antiplasmodial effects.

5.3 PART III: Identification of ADME/PK liabilities in artemisinin-chloroquinoline hybrids

The artemisinin hybrid compounds were synthesized with the aim of creating a conjugate, which borrows good characteristics from both chloroquine and artemisinin. Artemisinin has a very short half life of 1 hour (World Health Organisation, 2010a) but is very effective against both sexual and asexual stages of *P. falciparum*. Chloroquine has a long half-life and has been the drug of choice for treating malaria before the parasite developed resistance to the drug. The hypothesis is that the hybrid compound will have both features, therefore effective against all stages of the parasite and the resistant strains.

From previous studies the artemisinin-chloroquinoline hybrids were shown to have good antiplasmodial activity in both the CQR and CQS(Feng *et al.*, 2011). One of the liabilities that was noted was cytotoxicity. In this work the compounds were characterized to determine if they possessed any further ADME liabilities. From metabolic stability studies the compounds were found to have intermediate stability in both hepatocytes and HLM with greater than 70% of the compound being detected intact.

The hybrids of chloroquine and artemisinin were hypothesized to result in pharmacokinetic properties influenced by those of the individual components where chloroquine is known to have a long half-life and artemisinin to have a very short half life. In the study, we observed the *in vitro* metabolic clearance of artemisinin-chloroquine hybrids to be predictive of moderate *in vivo* hepatic clearance. *In vitro* to *in vivo* extrapolations of clearance of chloroquine and its

derivatives is however confounded by the fact that the *in vivo* half-life of chloroquine is affected by volume of distribution ($t_{1/2}$ = (In2.Vd)/CL) which is very high as chloroquine binds to various tissues including melanin containing tissues. Recent studies on the metabolic stability of many chloroquine analogues also showed variable metabolic stabilities that did not correlated with *in vivo* half-lives (Ray et al., 2010) that make it difficult to make simplicity prediction of likely *in vivo* half-life properties of chloroquine-artemisinin based on the *in vitro* metabolic stability data.

The compounds however were shown to be potent inhibitors of CYP3A4, CYP2C9 and CYP2C19. Given the inhibition by CYP3A4 and the good antiplasmodial activity, it could be postulated that lipophilicity is playing a role as the two are mainly driven by lipophilicity. The same is true for the cytotoxicity. Lipophilicity has been demonstrated to be associated with good interaction with biological membranes and enzymes. However there may be a challenge as if activity and liabilities are both being driven by the same properties. Changing groups associated with liabilities may lead to loss of activity.

For CYP3A4 both the hybrids and the intermediates demonstrated potent inhibition. Intermediate **3.6** showed potent inhibition in all the isoforms tested except CYP2D6. It can be assumed that if any changes are to be made on the molecules then this moiety would need to be prioritized.

5.4 PART IV: Molecular Mechanism of CYP1A2 inhibition by TBZ

This study was performed using TBZ, a broad spectrum anthelminthic used to treat parasitic infections in humans (Brown *et al.*, 1961; Hennekeuser *et al.*, 1969; Walton *et al.*, 1999). It has also been used as an agricultural fungicide for pre and post harvest treatment of fruit and vegetables and as a preservative in many consumer food products (Szeto *et al.*, 1993; Arenas and Johnson, 1994; Groten *et al.*, 2000; Walton *et al.*, 1999). From earlier studies TBZ had been shown to be extensively metabolized in humans (Tocco *et al.*, 1966b). It has also been shown to inhibit CYP1A2 (Bapiro *et al.*, 2005)and to induce members of the CYP1A and CYP2B family in rats (Price *et al.*, 2004; Aix *et al.*, 1994).

In this study we investigated the potential for TBZ and its metabolite to be a TDI of CYP1A2. TBZ was picked as a potent TDI for CYP1A2 from a screen of antiparasitic drugs against CYP1A2, 2C9 and 3A4. Its metabolite 5OH-TBZ was also picked as a weak TDI of the enzyme. TDI has been linked to some clinically important toxicity which has resulted in some drugs being withdrawn (tienilic acid) from the market and some having restrictions in their usage (ticlopidine) (Riley *et al.*, 2007). The inactivation of CYP1A2 by TBZ and 5OH-TBZ was concentration-, time- and NADPH dependent (Fig 4.21), an indication that the inactivation occurred via a catalytic process.

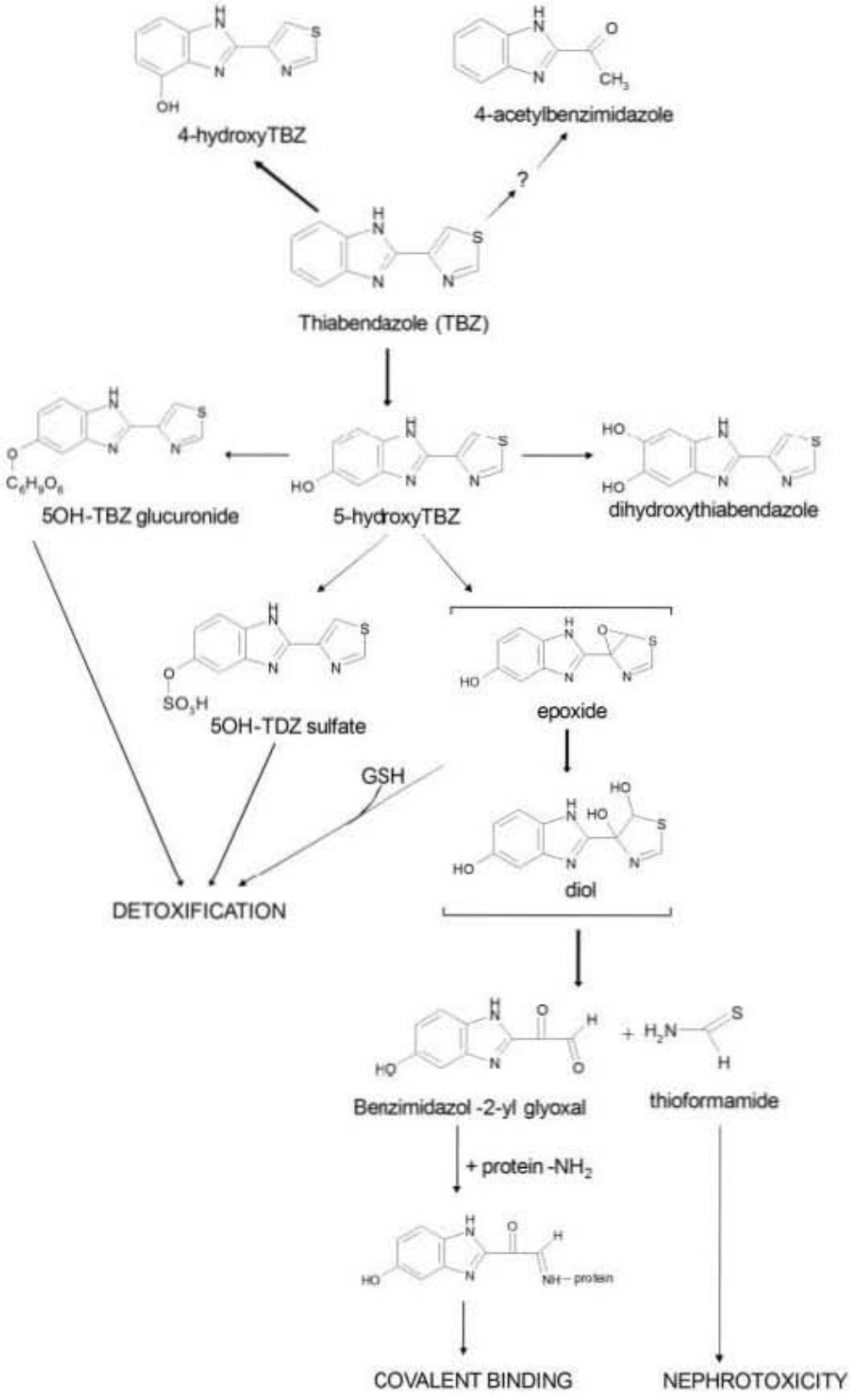

Figure 5.1: Proposed biotransformation of thiabendazole (its elimination and bioactivation) (Coulet *et al.*, 2000; Fujitani *et al.*, 1991; Dalvie *et al.*, 2006; Mizutani *et al.*, 1994)

The K_I determined for TBZ (1.4μM) was lower than the total plasma concentrations the drug is capable of reaching (19μM) (Bapiro *et al.*, 2005). The k_{inact} of 0.08min^{-1} is relatively high such that the resulting k_{inact}/K_I of 0.05μM/min is predictive of likely significant enzyme inactivation. In the treatment of strongyloidiasis in humans, the drug is given over 3 days at 25mg/kg/day (Satoh and Kokaze, 2004; Merck, 1999) thus providing the time component during which CYP1A2 will progressively be inactivated. In a chronic exposure study to TBZ (50mg/kg/day), the pharmacokinetic studies did not, however, show accumulation of TBZ (Bauer *et al.*, 1982)

TBZ showed much lower potency when preincubated in the absence (IC_{50} = 84.5μM) compared to the presence of NADPH (IC_{50} = 2.8μM) (Fig 4.22). This shift in the IC_{50} further suggests that TBZ is a likely TDI. It should be noted, however, that the high value (84.5μM) cannot be compared to the low IC_{50}s (1.2 and 0.83μM) obtained in the reversible inhibition assay (Bapiro *et al.*, 2001) since the inhibitor is diluted ten-fold before the inhibition is allowed to occur. A high substrate concentration was used to minimize competitive inhibition, hence the high IC_{50} value in our study.

There was no protection of CYP1A2 from inactivation by TBZ in the presence of the nucleophilic trapping agent, glutathione, an indication that reactive intermediates were not escaping the active site prior to inactivation. This is one of the characteristics that differentiate irreversible inhibitors from the reversible ones. In the case of irreversible inhibitors glutathione will have no effect in preventing inactivation since reactive species formed during the

enzymatic reaction react rapidly with amino acids in the active site rather than diffuse out.

Dialysis experiments were conducted to further confirm the mechanism of CYP1A2 TDI by TBZ and 5-OH TBZ. Approximately 20% of CYP1A2 activity was restored after dialysis following inactivation by TBZ (Fig 4.23) suggesting the mixed mode of inhibition. There was no restoration of activity when furafylline, a positive control MBI was used to inhibit CYP1A2. Activity was restored for the reversible inhibitor, fluvoxamine. Significant recovery was demonstrated for 5OH TBZ suggesting the generation of reversible inhibitory metabolite(s) *in vitro.* The results also confirm that 5OH-TBZ is a weak TDI and TBZ a true MBI. This has important implications for the proposed bioactivation path (Fig 5.1) where the route of TDI associated metabolism might not go through 5-OH TBZ but directly from TBZ as proposed in Fig 5.2.

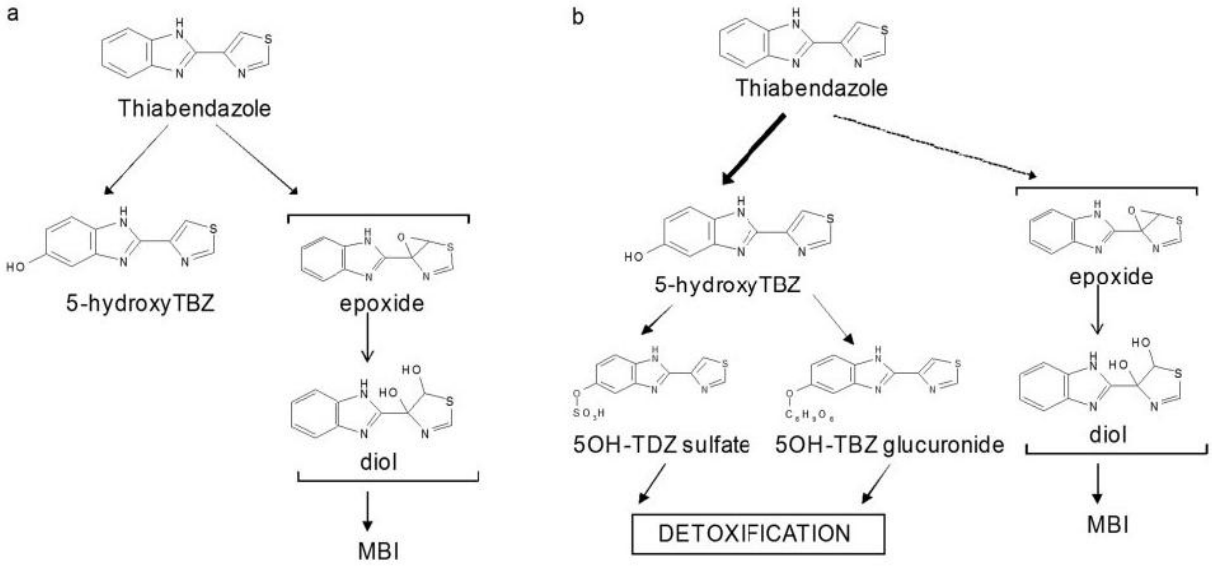

Figure 5.2: Proposed routes by which thiabendazole is metabolized in vitro (a) and *in vivo* (b).

In silico results were consistent each other and with observations from

literature. The first ranked site of metabolism was on the 5C of the benzene ring, a site where metabolism has been shown to take place (Coulet *et al.*, 1998). All three docking poses in GOLD and three of 10 docking poses in GLUE showed the site at a favorable distance to the heme catalytic center. The thiazole group was predicted as the likely site of metabolism by both MetaSite, and five of 10 docking poses in GLUE had the group close to the heme. In the other two docking poses, both predicted sites of metabolism were too far away from the catalytic center.TBZ has been reported to be a potent and mixed inhibitor of CYP1A2 both *in vitro* and *in vivo* (Bapiro *et al.*, 2005; Bapiro *et al.*, 2001).

The docking results could explain the observed results. When the compound is docked with the benzyl moiety oriented toward the heme (Fig 4.27a), hydroxylation to 5-hydroxythiabendazole, which is the main route of metabolism, is favored. The docking solution could explain the competitive inhibitory effects of thiabendazole on CYP1A2. When the thiazole moiety docks close to the heme (Fig 4.27b), bioactivation of thiabendazole could likely result in TDI. When TBZ docks in the active site cavity but far away from the reactive center (Fig. 4.27c), noncompetitive inhibition could result from allosteric binding. Therefore, it can be assumed that depending on the conditions *in vivo* and conformation of the active site, any of these types of inhibition can occur, giving a possible explanation to the observed mixed type inhibition in vitro (Bapiro *et al.*, 2001). The docking results also indicate that the observed TDI could arise from various mechanisms involving epoxidation of TBZ on the thiazole and benzyl rings. Further studies are therefore required

to explore these potential biotransformations, results of which could result in modification of the metabolism scheme proposed in Fig 5.1.

Assuming competitive inhibitory effects of TBZ on CYP1A2, Simcyp version 8.1 was used in the prediction of -fold increase in exposure of theophylline and caffeine (Table 4.11). Our result of 1.82-fold decrease in steady-state clearance of theophylline after TBZ therapy assuming competitive enzyme inhibition is in agreement with previously published clinical trial data (Schneider *et al.*, 1990). Theophylline infusion was started 37h after TBZ oral therapy, and a 2.91-fold decrease in theophylline clearance was observed. From pharmacokinetic principles (Lin and Pearson, 2002), the same magnitude in increase in drug exposure is anticipated.

These findings are particularly important in the use of theophylline, a narrow therapeutic index drug, in which a small change in plasma concentrations can result in serious side effects (Schneider *et al.*, 1990). In light of this published data and our findings, a dose reduction that is dependent on the route of administration and time of initiating the affected drug is recommended. The results for the effect of thiabendazole on caffeine are comparable with what has been found clinically for single doses of these two co-ingested drugs (Bapiro *et al.*, 2005) for which an increase in AUC of 1.6 was observed.

Results from simulations of TDI effects on itself and those of theophylline and caffeine indicated that TBZ would inhibit its own clearance, resulting in >20-fold increase in exposure after only 3 days of administration (Table 4.11). The

TBZ effects on theophylline and caffeine were predicted to result in 5.65 and 11.4 increases in exposure. These simulation results imply accumulation of TBZ with possible MBI activity on CYP1A2. The great impact of TBZ on its own elimination could partly be explained by it potentially being solely metabolized by CYP1A2 (fm_{1A2}=1.0), whereas the drugs theophylline (fm_{1A2} =0.85) (Monks *et al.*, 1979)and caffeine (fm_{1A2}=0.98) (Karjalainen *et al.*, 2006) could be eliminated by other pathways.

Our MBI simulation results (Table 4.11) are contrary to some clinical reports that indicate that TBZ does not accumulate upon chronic administration (Schneider *et al.*, 1990). Our *in vitro* results might offer an explanation for this poor *in vitro* to *in vivo* prediction of MBI-based DDI. *In vitro* studies using recombinant CYP1A2 clearly shows that TBZ is an MBI and that 5-OH TBZ is a weak inhibitor. The proposed pathway *in vivo* indicates the involvement of conjugation reactions that clear the 5OH-TBZ. We propose that in the *in vitro* system, in which there are no phase 2 reactions, 5OH-TBZ accumulates and feedback inhibits this route. This leaves more TBZ available and increases the probability of the substrate docking (Fig. 4.27) mode associated with bioactivation to metabolites, which are MBI (Fig. 5.2). This could explain why no MBI is observed in vivo because the MBI we observe is an *in vitro* artifact because of the simplicity of the system devoid of other enzymes involved in TBZ metabolism and disposition. This could also be explained by the inherent differences between recombinant enzymes and human liver microsomes (Polasek and Miners, 2007).

5.5 PART V: Drug-herb interaction by evaluating the ADMET/PK of the active ingredient natural product, Frutinone A

Herbal/traditional medicines have been widely used in the treatment of many illnesses including inflammation, pain, colds and as immune boosters. Many of the remedies have been widely used together with conventional medicines posing the risk of drug-drug interactions. This is particularly of concern especially with drugs with narrow therapeutic indices such as warfarin and digoxin. The study of the level of drug-herb interaction therefore is of great importance. Effects of herbal/traditional medicines on drug metabolizing enzymes including their role in causing interaction have been studied and reviewed (Zhou *et al.*, 2003; Chavez *et al.*, 2006; Saxena *et al.*, 2003; Izzo and Ernst, 2009; Tarirai *et al.*, 2010).

Extracts from the *polygala fruticosa* herb have been widely used in different parts of Africa. In South Africa *P. fruticosa* has been widely used to dropsy, scrofula and as a part of a decoction for tuberculosis treatment (Watt Jm, 1962). In Zimbabwe the herb is used to treat abdominal pains and venereal diseases (Gelfand M, 1985). Experiments have also shown the extract to have antifungal activity (Bergeron C, 1997; Paolo *et al.*, 1989; Hostettmann *et al.*, 2000). Among the extracts isolated Frutinone A was the most active, with the other 2 chromonocoumarins (Frutinone B and C) being inactive (Hostettmann *et al.*, 2000). The Frutinones are differentiated from each other by hydroxyl and methoxy substitutions (Fig 5.1), and it is these substitutions that have been linked to lack of activity in Frutinone B and C. In this study the interaction of Frutinone A, a purified compound from a herbal extract with CYP1A2 was pursued.

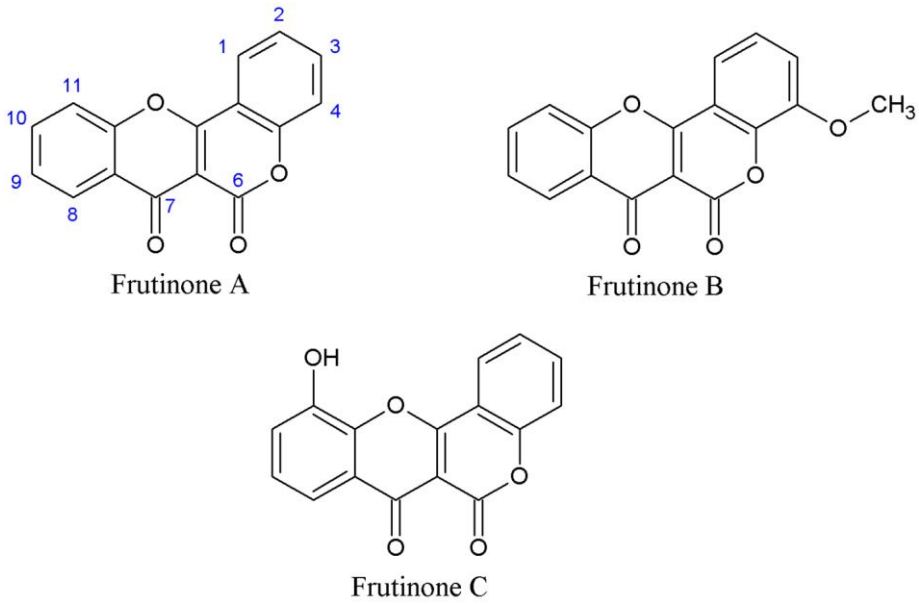

Figure 5.3: Chemical structures of Frutinone A, B, and C. The three chromonocoumarins were isolated from polygala fruticosa Berg (Paolo, 1989).

Frutinone A is a chromonocoumarin isolated from *polygala fruticosa Berg*, a herb growing in the Cape and Natal provinces of South Africa. The natural product was isolated from the lipophilic extract of the shrub (Paolo *et al.*, 1989) and from the roots and aerial parts of two other African species , *P. gazensis* Bak and *P. teretofolia L*. (Bergeron C, 1997). From our investigation of metabolic properties of the pure compound, the data suggest that Frutinone A is metabolically stable and only minute amounts of a by-product presumably resulting from enzymatic or non-enzymatic hydrolysis-mediated lactone ring opening were identified after incubation with human hepatocytes. From the reaction phenotyping studies Frutinone A was not metabolized by CYP1A2.

In vitro screening for metabolic interactions across 5 major human drug metabolizing enzymes, CYP1A2, 2C9, 2C19, 2D6 and 3A4 showed Frutinone A to be a very potent inhibitor of CYP1A2. Molecular modeling investigations provide a mechanistic rational for Frutinone A-CYP1A2 active site interactions

predictive of metabolic stability and potent competitive enzyme inhibition. These findings could have implications in the safe use of herbal remedies containing Frutinone A and the potential development of Frutinone A and/or related structures as conventional drugs.

To our knowledge no studies on potential interactions of various extracts with drug metabolising enzymes have been reported. Although toxicity studies using crude extract of the plant in rats have shown the extracts to be safe (Mukinda et al. 2010), there is need to conduct further studies with human drug metabolising enzymes for insights into possible safety issues when used in humans and in combination with other drugs. Although there have also been no reports of Frutinone A being used in its pure form, we speculate that its presence in the extract may cause interactions with drug metabolising enzymes.

Metabolism of the compound in hepatocytes is very minor, with only one minor by-product (4% of the parent compound) being identified in our study (Fig 4.28 and 4.29) which could not be attributed to any CYP reaction as indicated by the reaction phenotyping assay. The compound was also predicted to have low clearance. We therefore predict that Frutinone A has the potential to be circulated unchanged in the system for long periods.

Frutinone A inhibited all the 5 major drug metabolising CYPs tested (1A2, 2C9, 2C19, 2D6 and 3A4) with the most potent inhibition observed for CYP1A2. Inhibition K_is of 0.48 and 0.31μM are indicative of a high likelihood

of metabolic drug-drug interactions (DDI) where Frutinone A could inhibit the elimination of CYP1A2 substrate drugs. The actual extent of DDI is, however, difficult to establish since there is no data on *in vivo* Frutinone A exposure levels. Nevertheless the metabolic stability of the compound also alludes to likely extended DDI should Frutinone A attain systemic exposure levels associated with a risk for DDI.

As already mentioned *in vivo* studies in rats have shown no toxic effects of Frutinone A containing herbal extracts (Mukinda et al. 2010). Further studies on the potential risk of direct toxicity of Frutinone A or extracts that contain this compound need to be done in *in vitro* human systems since animal studies cannot always easily be extrapolated to humans. At this juncture it is noteworthy that the safety studies in literature (Mukinda et al. 2010) were also not evaluating safety issues related to DDI.

Given the inhibitory potency of Frutinone A on CYP1A2, an enzyme produced from an orthologus gene CYP1A2 found in both humans and rats, our studies lend support to the possibility of conducting *in vivo* DDI studies in rats which could be extrapolated to humans. Such studies could be conducted using both Frutinone A and Frutinone A-containing extracts in formulations used in a treatment setting. Although no further studies were done on CYP2D6, CYP2C9, 2C19 and CYP3A4, the possibility of interactions with these enzymes cannot be completely ruled out.

The potency of Frutinone A on CYP1A2 could be explained by its pharmacophoric similarity with compounds known to be substrates/inhibitors of CYP1A2. *In silico* experiments were conducted to explain the low metabolic stability of Frutinone A, the lack of time dependent inhibition (Fig 4.31) and the observed potent reversible inhibition of CYP1A2 (Table 4.13). From our docking studies, many similarities in the way Frutinone A and α-naphthoflavone, which is a known reversible inhibitor of CYP1A2, interact with the CYP1A2 active site space and chemistry were observed.

The compounds both show a good fit into the active site of CYP1A2 driven by direct hydrophobic interactions with side chains of phenylalanines 226, 260 and 125. These interactions and close fit have been associated with tight binding of α-naphthoflavone in the CYP1A2 active site (Mukinda et al. 2010). The distance of the nearest atom of Frutinone A to the heme was 4.6Å with Autodock and 5.04Å with FlexX. This distance has been earlier described to be too long for productive formation of metabolites via direct π-attack (Sansen et al. 2007). This may also help to explain why there was no significant formation of oxidative metabolites from the metabolism of Frutinone A by human hepatocytes.

Our docking studies may also help to explain the mechanism by which Frutinone A and α-naphthoflavone inhibit CYP1A2. Our control compound α-naphthoflavone inhibited via a mixed-type mechanism with both CEC and ER. Earlier studies have demonstrated α-naphthoflavone to be a competitive inhibitor of CYP1A2 with ER (de Visser, 2003) contrary to our mixed inhibition.

A study by another group has also shown α-naphthoflavone to be a mixed mode inhibitor (Cho et al. 2003). In our study the best fit favored the mixed-type inhibition with competitive inhibition having a greater contribution in the mixed type inhibition when compared to the non-competitive inhibition.

Frutinone A demonstrated mixed inhibition with CEC and competitive inhibition with ER. On the inhibition of CEC the greater contribution was from non-competitive inhibition, substrate-dependent mode (competitive versus non-competitive) and potency of inhibition of CYP1A2 by alpha naphthoflavone was previously postulated to be due to the nature of substrate and inhibitor binding modes in the CYP1A2 active site where those for the α-naphthoflavone/ER pair favoured competitive inhibition and that of alpha-naphthoflavone/EC favoured non-competitive inhibition (Shimada et al. 1998). They postulated that the structures of the substrates, ER and EC influenced these outcomes.

Docking simulations from the two software used in this study showed two binding modes for substrates. Docking simulations in Autodock Vina (Fig 4.36) show the substrates CEC (4.36c) and ER (4.36d) binding in the same pocket as the inhibitors Frutinone A (4.36b) and α-naphthoflavone (4.36a) which could explain the competitive inhibition. Docking simulations in FlexX (Fig 4.37) show an alternative binding mode where the substrates bind just below the hydrophobic pocket created by side chains of phenylalanines 226, 260 and 259. We propose that this binding orientation allows both the substrate and inhibitor to bind in the binding pocket resulting in non-

competitive inhibition. The existence of several binding modes in the active sites of CYPs has been observed for CYP2C9 and CYP3A4 and could explain both regio-selective metabolism of compounds and mode of inhibition as postulated in this study.

In this study we have therefore shown the potential for Frutinone A, a natural product extracted from a plant to interact with CYPs especially CYP1A2. The compound has also demonstrated behaviour very similar to α-naphthoflavone, which is a known potent inhibitor of CYP1A2. We have also suggested that there might be an alternative binding site in the active site of CYP1A2, which may help explain differential inhibition patterns when different substrates are used.

6 CONCLUSIONS

- An ADME/PK platform was successfully setup in this study. The tool can be used in an integrated manner with medicinal chemistry and pharmacology in support of drug discovery projects in Africa. In this study, this has been demonstrated by applying it in the identification of ADMET/PK liabilities of new chemical entities with antimalarial activity and drugs on the market used for the treatment of parasitic diseases.

- The 3,4-HPO-4-amino-7-chloroquinolinyl hybrids were predicted to pose drug-drug interaction risks if given together with other drugs, which depend on CYP2D6 and CYP3A4 for elimination. Whilst the efficacy of the compounds is promising and have good physicochemical profiles, they carry potentially limiting liability of CYP inhibition especially against CYP3A4.

- The artemisinin-chloroquinoline hybrids were metabolically stable and remained intact in the presence of drug-metabolizing enzymes. They therefore have potential to reach the target site. However they still need to be optimized to remove the liability of cytotoxicity and CYP inhibition. More work needs to be done to determine structure activity relationships. This is to further investigate if the liabilities are affected by the same properties that are responsible for the efficacy.

- The thiabendazole study was able to show that TBZ is a potent MBI ofCYP1A2. Although the use of computational methods as prediction

tools for likelihood of TDI still needs to be validated, the study demonstrated they could be useful in both predicting and explaining observed characteristics in both *in vivo* and *in vitro* experiments. Future MBI studies will therefore be done using hepatocytes with proven UDP-glucuronosyl transferase and sulfanotransferase activity to verify our current hypothesis in explaining why no clinical MBI-based DDI have been observed.

- The study on the interactions of Frutinone A with CYP1A2 study offers mechanistic insights into CYP1A2-substrate/inhibitor active site interactions. Inhibitory effects of Frutinone A may be attributed to its pharmacophoric similarity with CYP1A2 substrates/inhibitors. The potent CYP1A2 inhibition by Frutinone A could be predictive of the potential drug-herb interaction risk if the compound is co-administered with low therapeutic index CYP1A2 substrate drugs such as theophylline.

- Future work on the compounds will therefore need to take into account the role of absorption and transporters in predicting the fate of these compounds. There is also need to do detailed structure activity relationships which include multivariate analysis to determine if desired and non-desired properties fall in the same chemical space. Detailed metabolite profiling studies will also need to be done as some side effects observed for some compounds such as amodiaquine are as a result of reactive metabolites.

APPENDICES

Appendix A: Proposed biotransformation routes in hepatocytes for ,4-HPO-4-amino-7-chloroquinolinyl hybrids

1) Biotransformation of compound 3.1a in hepatocytes

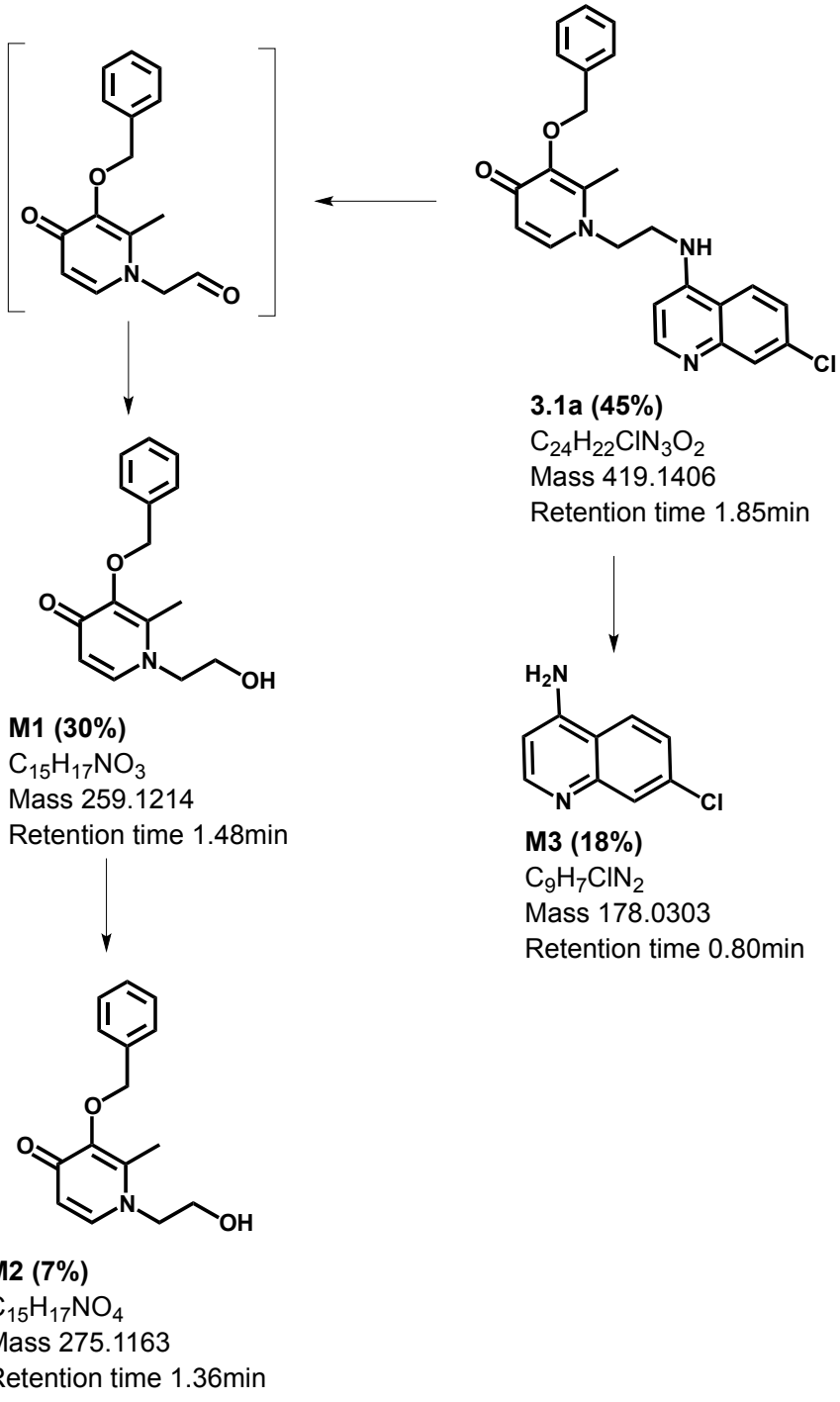

3.1a (45%)
$C_{24}H_{22}ClN_3O_2$
Mass 419.1406
Retention time 1.85min

M1 (30%)
$C_{15}H_{17}NO_3$
Mass 259.1214
Retention time 1.48min

M3 (18%)
$C_9H_7ClN_2$
Mass 178.0303
Retention time 0.80min

M2 (7%)
$C_{15}H_{17}NO_4$
Mass 275.1163
Retention time 1.36min

2) Biotransformation of compound 3.1b in hepatocytes

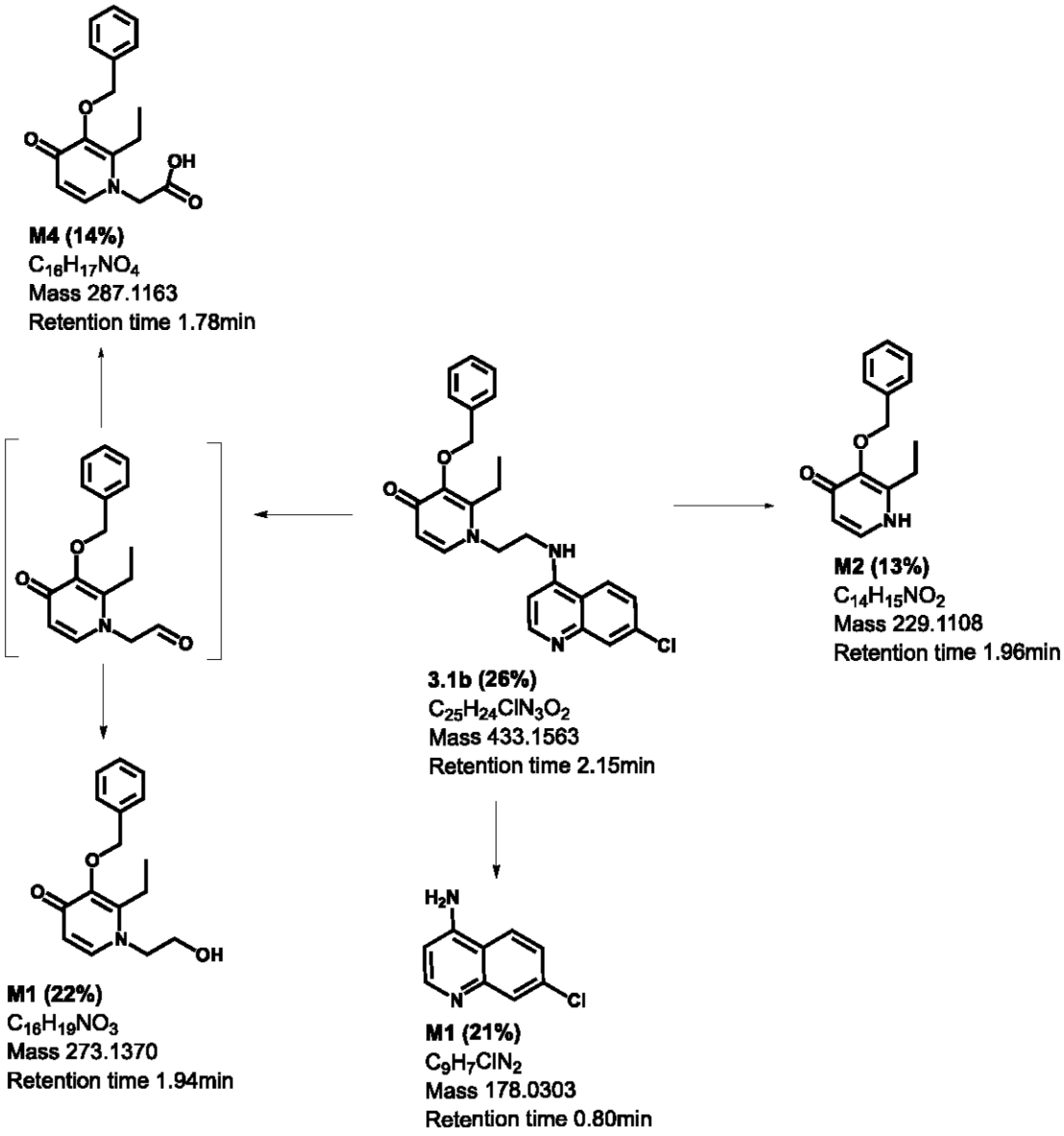

3) Biotransformation of compound 3.2a in hepatocytes

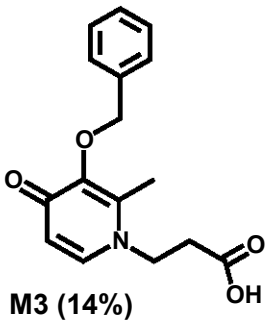

M3 (14%)
$C_{16}H_{17}NO_4$
Mass 287.1163
Retention time 1.65min

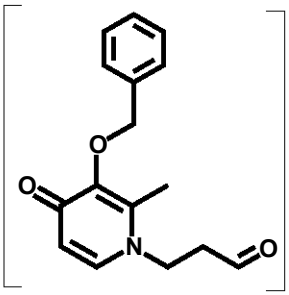

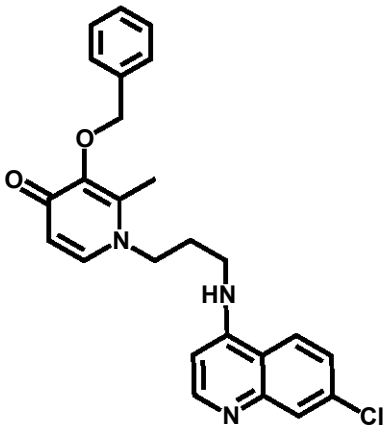

3.2a (68%)
$C_{25}H_{24}ClN_3O_2$
Mass 433.1562
Retention time 2.02min

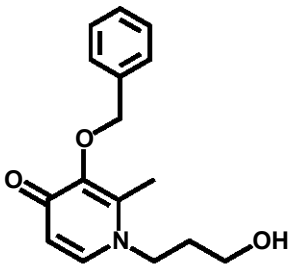

M2 (2%)
$C_{16}H_{19}NO_3$
Mass 273.1370
Retention time 1.61min

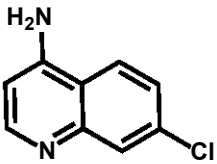

M1 (17%)
$C_9H_7ClN_2$
Mass 178.0303
Retention time 0.80min

4) Biotransformation of compound 3.2b in hepatocytes

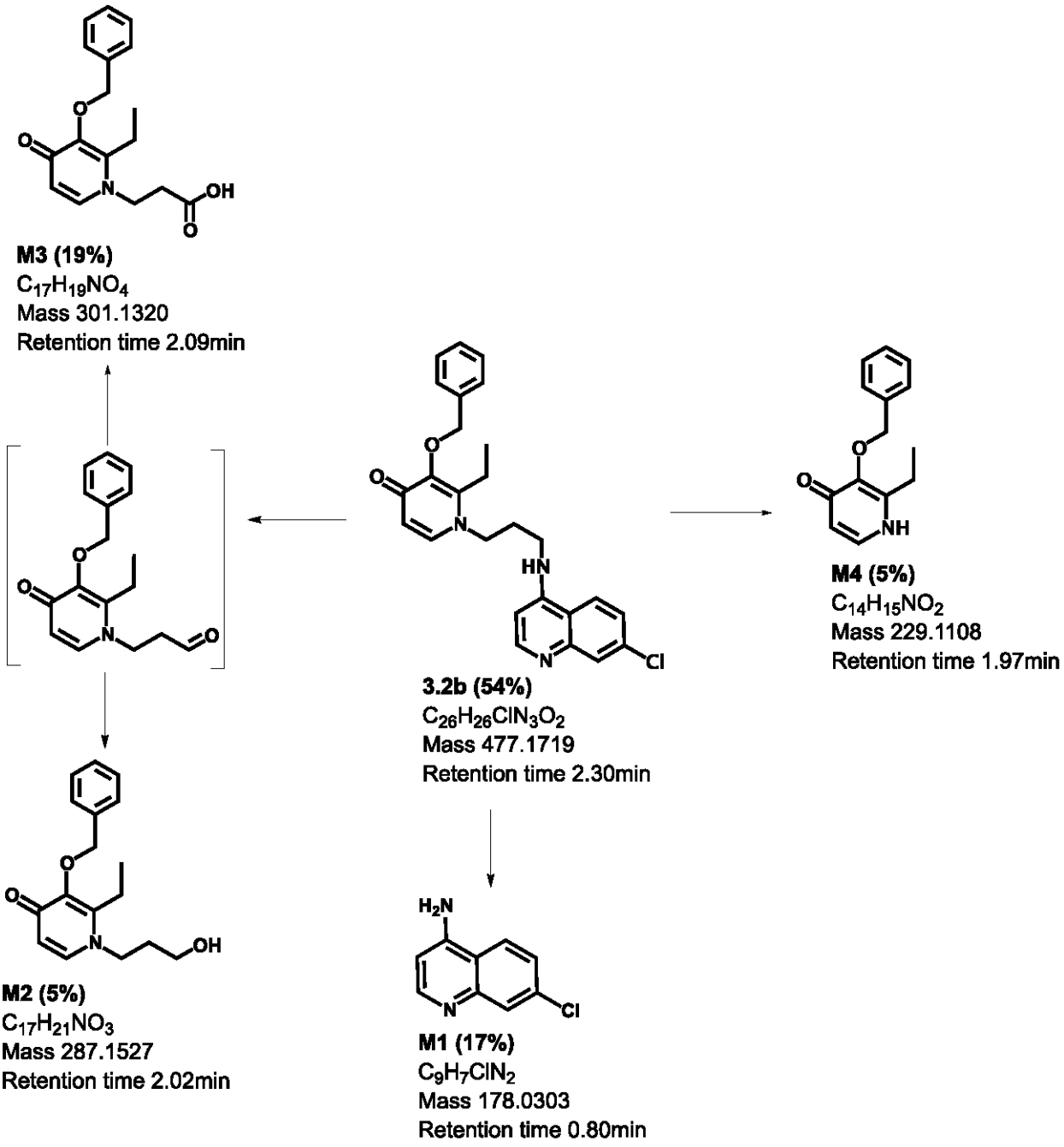

5) Biotransformation of compound 3.1c in hepatocytes

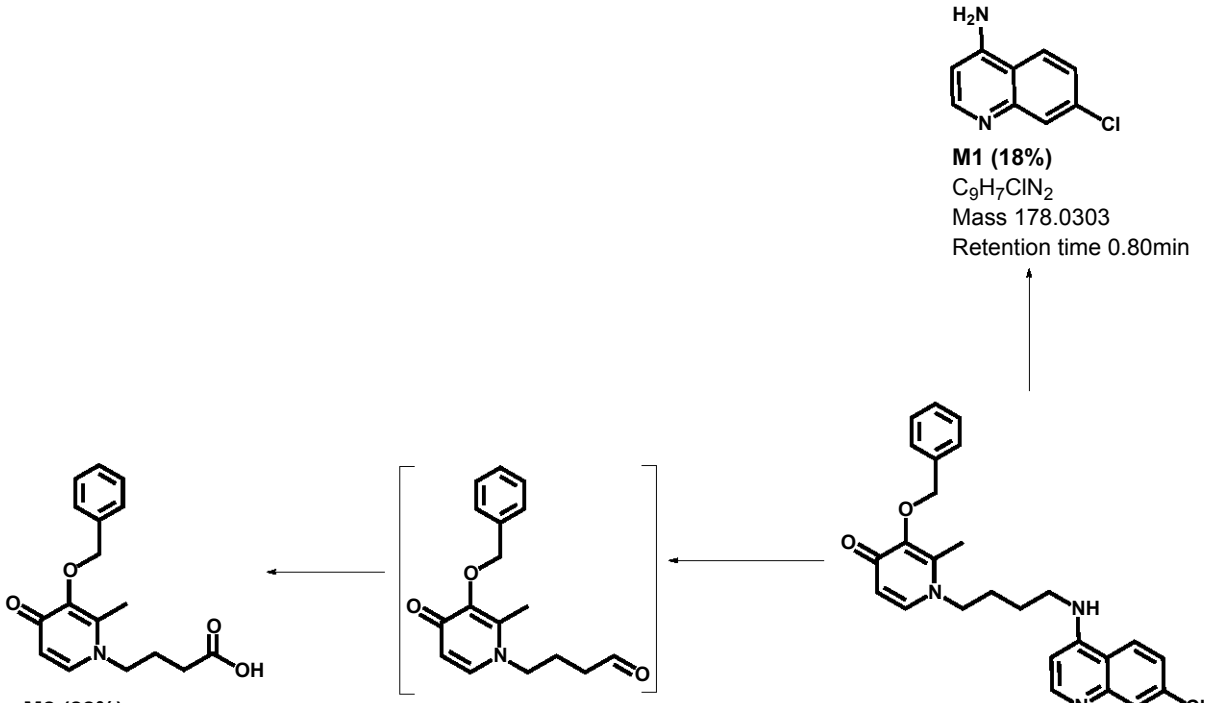

6) Biotransformation of compound 3.2c in hepatocytes

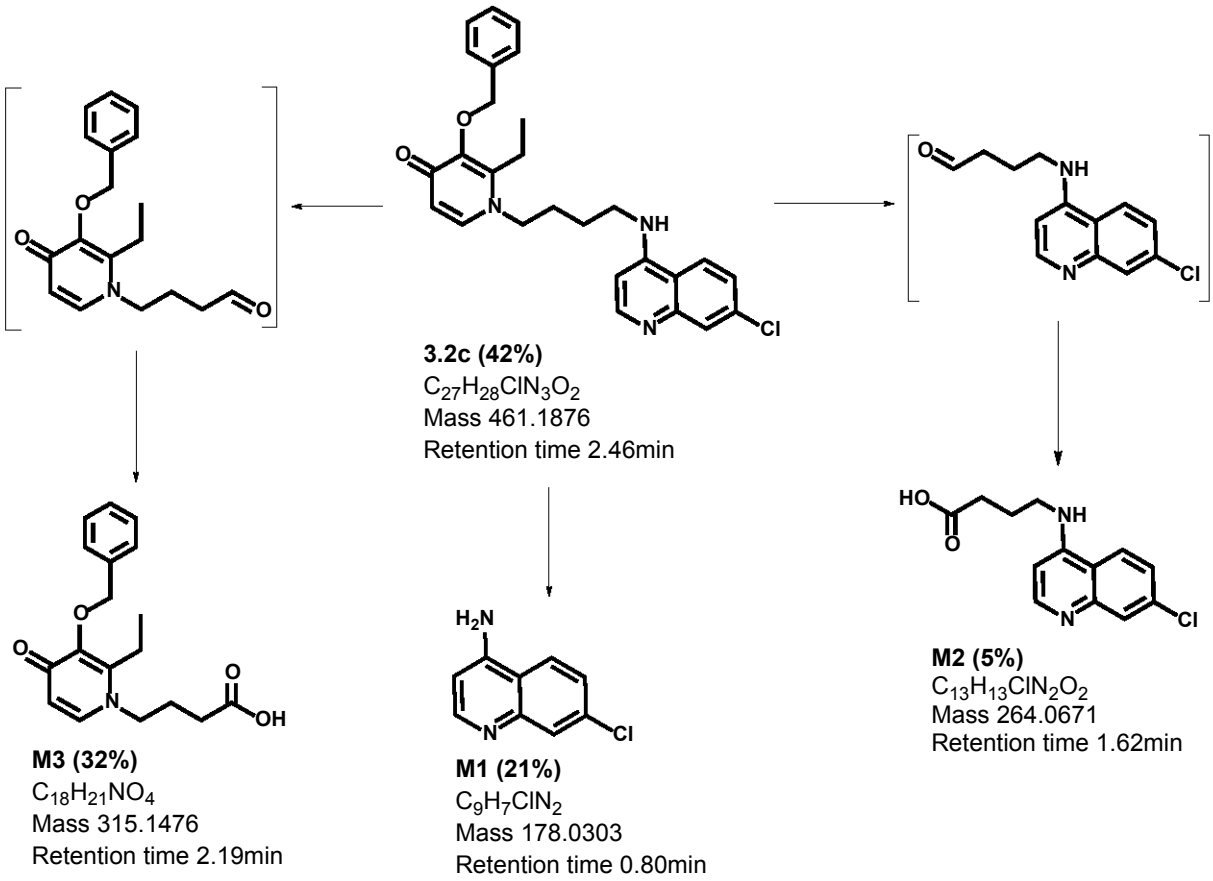

7) Biotransformation of compound 3.1d in hepatocytes

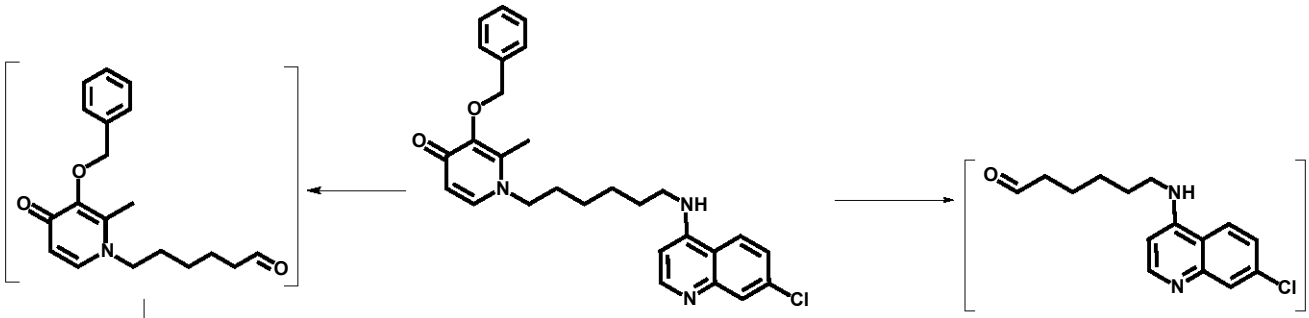

3.1d (41%)
$C_{28}H_{30}ClN_3O_2$
Mass 475.2032
Retention time 2.56min

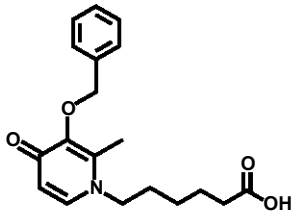

M3 (9%)
$C_{19}H_{23}NO_4$
Mass 329.1633
Retention time 2.23min

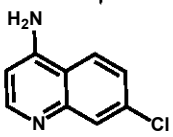

M1 (15%)
$C_9H_7ClN_2$
Mass 178.0303
Retention time 0.80min

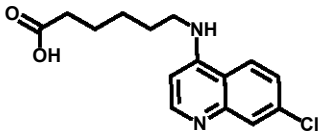

M2 (17%)
$C_{15}H_{17}N_2O_2$
Mass 292.0984
Retention time 1.62min

8) Biotransformation of compound 3.2d in hepatocytes

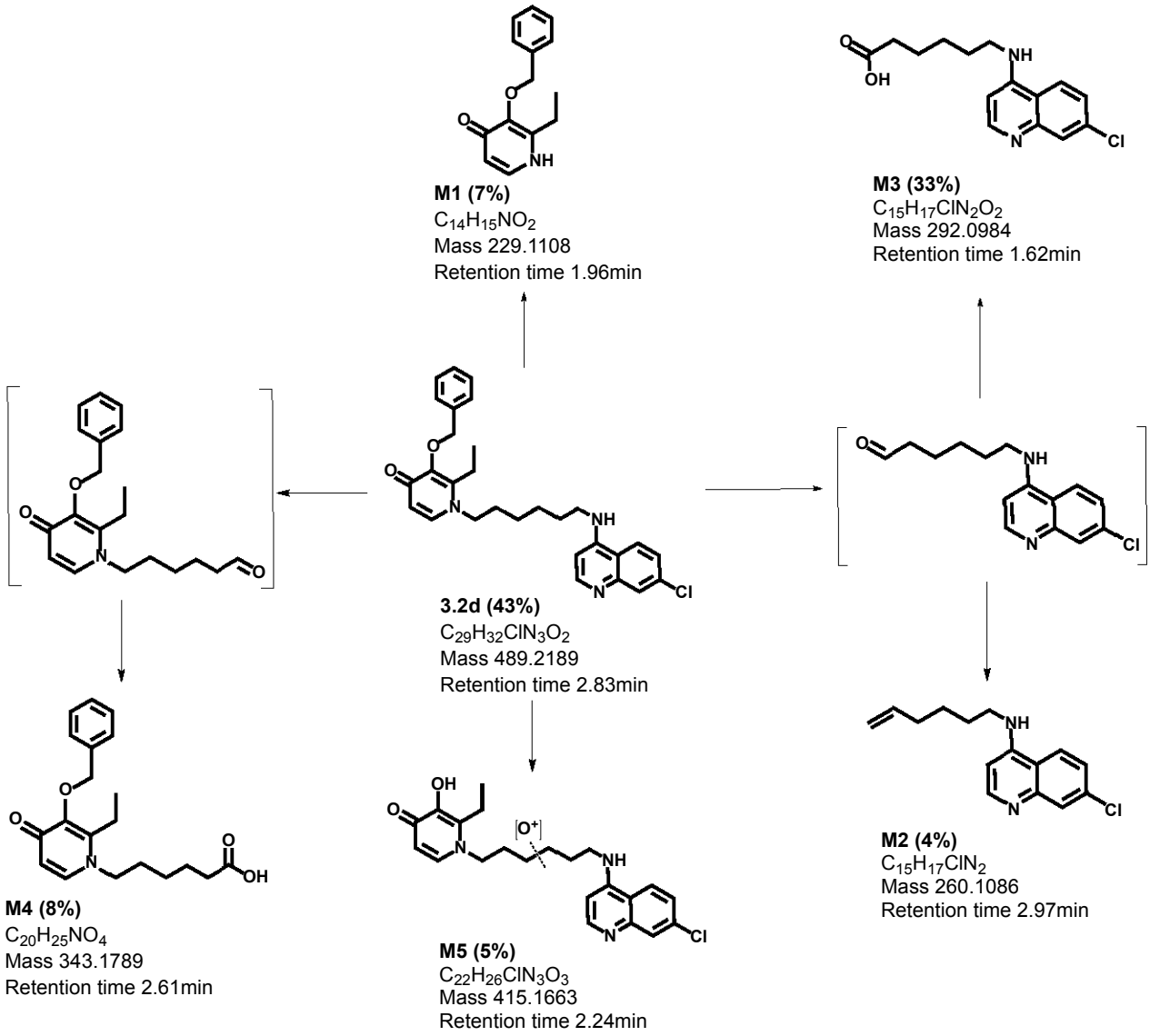

9) Biotransformation of compound 3.4a in hepatocytes

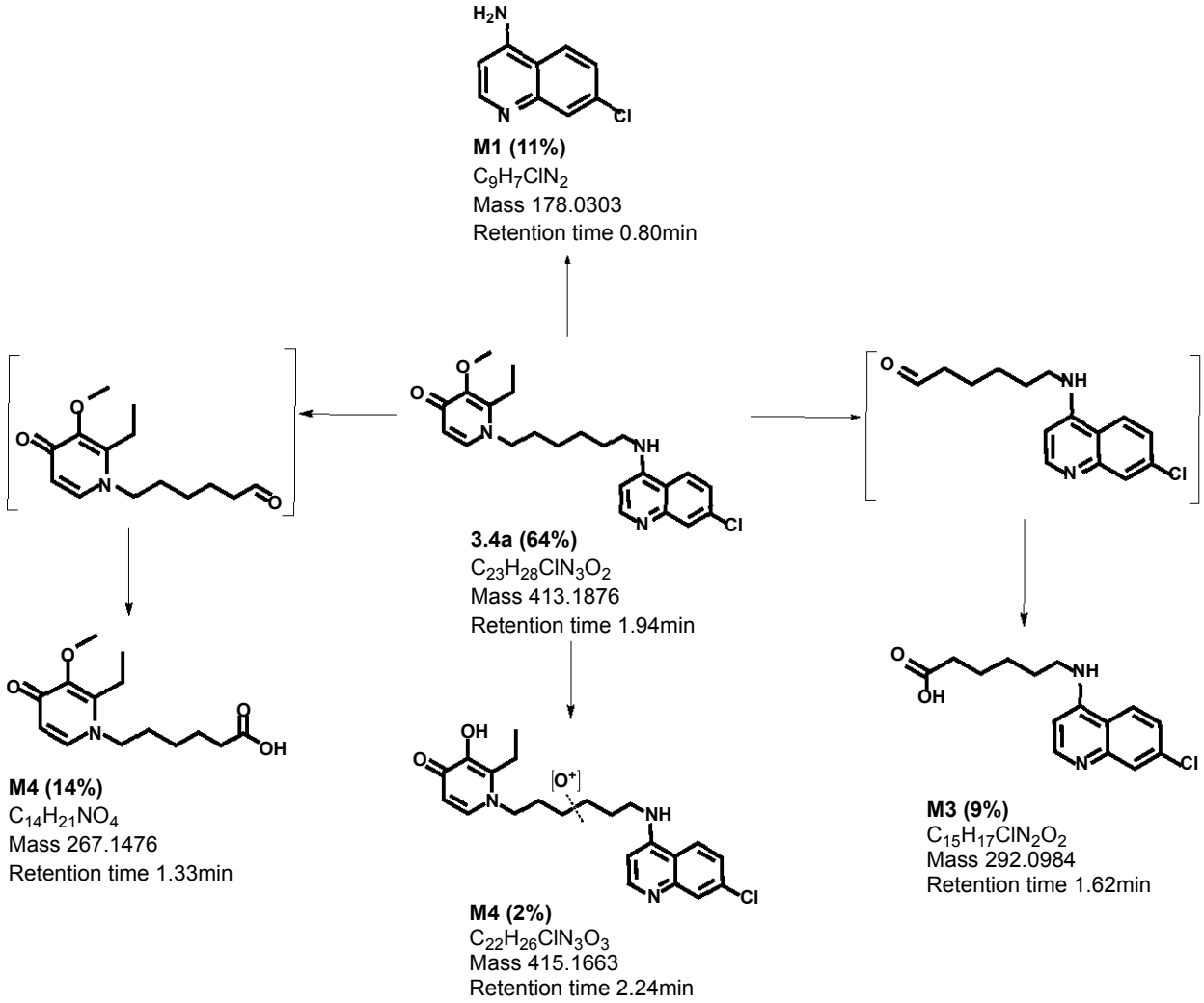

10) Biotransformation of compound 3.1h in hepatocytes

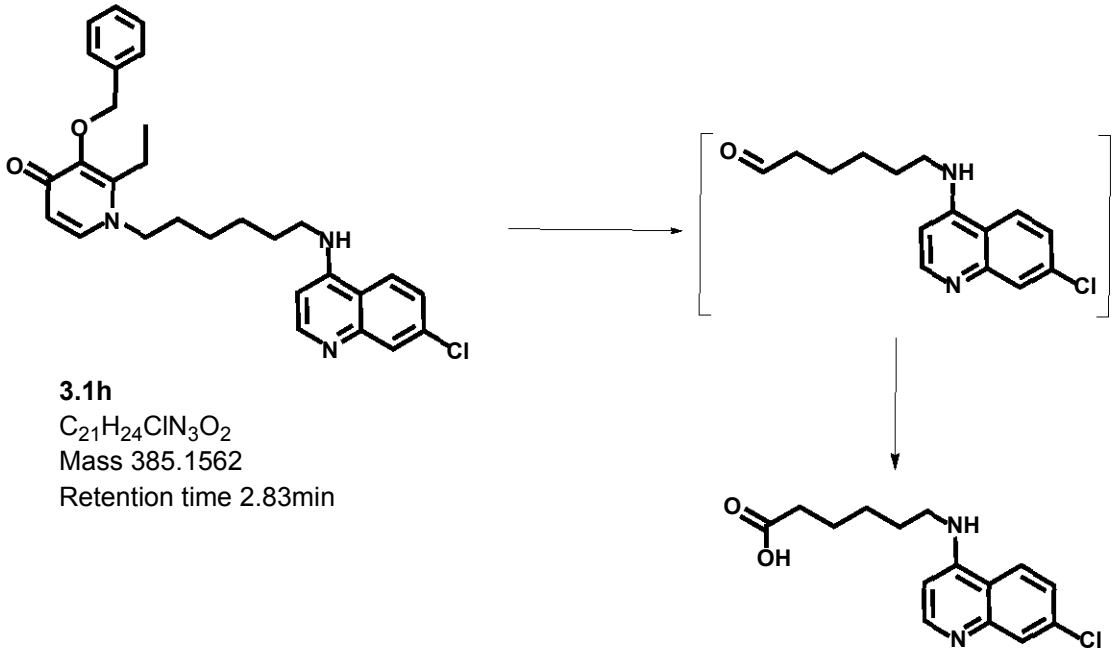

3.1h
$C_{21}H_{24}ClN_3O_2$
Mass 385.1562
Retention time 2.83min

M1
$C_{15}H_{17}ClN_2O_2$
Mass 292.0984
Retention time1.62min

REFERENCES

1. Aix, L., Reygrobellet, X., Larrieu, G., Lesca, P. &Galtier, P. (1994). Thiabendazole Is an Inducer of Cytochrome P4501A1 in Cultured Rabbit Hepatocytes. *Biochemical and Biophysical Research Communications* 202(3): 1483.

2. Ajibade, P. &Kolawole, G. (2008). Synthesis, characterization and antiprotozoal studies of some metal complexes of antimalarial drugs. *Transition Metal Chemistry* 33(4): 493-497.

3. Alsenz, J. &Kansy, M. (2007). High throughput solubility measurement in drug discovery and development. *Advanced Drug Delivery Reviews. Drug Solubility: How to Measure it, How to Improve it* 59(7): 546-567.

4. Angulo-Barturen, I., Jiménez-Díaz, M. B., Mulet, T., Rullas, J., Herreros, E., Ferrer, S., Jiménez, E., Mendoza, A., Regadera, J., Rosenthal, P. J., Bathurst, I., Pompliano, D. L., Gómez de las Heras, F. &Gargallo-Viola, D. (2008). A Murine Model of falciparum-Malaria by In Vivo Selection of Competent Strains in Non-Myelodepleted Mice Engrafted with Human Erythrocytes. *PLoS ONE* 3(5): e2252.

5. Arenas, R. V. &Johnson, N. A. (1994). Liquid chromatographic fluorescence method for the determination of thiabendazole residues in green bananas and banana pulp. *Journal of AOAC International.* 77: 710–713.

6. Artursson, P., Palm, K. &Luthman, K. (2001). Caco-2 monolayers in experimental and theoretical predictions of drug transport. *Advanced Drug Delivery Reviews* 46(1-3): 27-43.

7. Atkinson, A., Kenny, J. R. &Grime, K. (2005). Automated assessment of time dependent inhibition of human cytochrome P450 enzymes using liquid chromatography-tandem mass spectrometry analysis. *Drug Metabolism and Disposition* 33(11): 1637-1647.

8. Avdeef, A. (1993). pH-metric log P. II: Refinement of partition coefficients and Ionization constants of multiprotic substances. *Journal of Pharmaceutical Sciences* 82(2): 183-190.

9. Avdeef, A. (2001). Physicochemical Profiling (Solubility, Permeability and Charge State). *Current Topics in Medicinal Chemistry* 1(4): 277.

10. Avdeef, A. (2007).High-Throughput Measurements of Solubility Profiles. In *Pharmacokinetic Optimization in Drug Research*, 305-325: Verlag Helvetica Chimica Acta.

11. Bailey, D., Arnold, J. M. O., Bend, J. R., Tran, L. T. &Spence, J. D. (1995). Grapefruit juice-felodipine interaction: reproducibility and characterization with the extended release drug formulation. *British Journal of Clinical Pharmacology* 40: 135-140.

12. Bailey, D. G., Malcolm, J., Arnold, O. &David Spence, J. (1998). Grapefruit juice–drug interactions. *British Journal of Clinical Pharmacology* 46(2): 101-110.

13. Bapiro, T., Andersson, T., Otter, C., Hasler, J. &Masimirembwa, C. (2002). Cytochrome P450 1A1/2 induction by antiparasitic drugs: dose-dependent increase in ethoxyresorufin O-deethylase activity and mRNA caused by quinine, primaquine and albendazole in HepG2 cells. *European Journal of Clinical Pharmacology* 58(8): 537.

14. Bapiro, T., Sayi, J., Hasler, J. A., Jande, M., Rimoy, G., Masselle, A. &Masimirembwa, C. (2005). Artemisinin and thiabendazole are potent inhibitors of cytochrome P450 1A2 (CYP1A2) activity in humans. *European Journal of Clinical Pharmacology* 61(10): 755.

15. Bapiro, T. E., Egnell, A.-C., Hasler, J. A. &Masimirembwa, C. M. (2001). Application of Higher Throughput Screening (HTS) Inhibition Assays to Evaluate the Interaction of Antiparasitic Drugs with Cytochrome P450s. *Drug Metaboilsm Disposition* 29(1): 30-35.

16. Bard, B., Martel, S. &Carrupt, P.-A. (2008). High throughput UV method for the estimation of thermodynamic solubility and the determination of the solubility in biorelevant media. *European Journal of Pharmaceutical Sciences* 33(3): 230-240.

17. Barter, Z., Bayliss, M., Beaune, P., Boobis, A., Carlile, D., Edwards, R., Houston, J., Lake, B., Lipscomb, J., Pelkonen, O., Tucker, G. &Rostami-Hodjegan, A. (2007). Scaling factors for the extrapolation of in vivo metabolic drug clearance from in vitro data: reaching a consensus on values of human microsomal protein and hepatocellularity per gram of liver. *Current Drug Metabolism* 8: 33–45.

18. Bauer, L., Raisys, V., Watts, M. &Ballinger, J. (1982). The pharmacokinetics of thiabendazole and its metabolites in an anephric patient undergoing hemodialysis and hemoperfusion. *Journal of Clinical Pharmacol* 22: 276–280.

19. Bellot, F., Coslédan, F., Vendier, L., Brocard, J., Meunier, B. &Robert, A. (2010). Trioxaferroquines as New Hybrid Antimalarial Drugs. *Journal of Medicinal Chemistry* 53(10): 4103-4109.

20. Bergeron, C., Marston, A., Wolfender, J. L., Mavi, S., Rogers, C., Hostettmann., K. (1997). Isolation of Polyphenols from Polygala gazensisand Liquid Chromatography and Mass Spectrometry of Related African Polygala Species. *Phytochemical Analysis* 8: 32-36.

21. Berman, J. (2005). Recent developments in Leishmaniasis: Epidemiology, diagnosis, and treatment. *Current Infectious Disease Reports* 7(1): 33-38.

22. Bevan, C. D. &Lloyd, R. S. (2000). A High-Throughput Screening Method for the Determination of Aqueous Drug Solubility Using Laser Nephelometry in Microtiter Plates. *Analytical Chemistry* 72(8): 1781-1787.

23. Biot, C., Glorian, G., Maciejewski, L. A., Brocard, J. S., Domarle, O., Blampain, G., Millet, P., Georges, A. J., Abessolo, H., Dive, D. &Lebibi, J. (1997). Synthesis and Antimalarial Activity in Vitro and in Vivo of a New Ferrocene-Chloroquine Analogue. *Journal of Medicinal Chemistry* 40(23): 3715-3718.

24. Birkett, D. J., Rees, D., Andersson, T., Gonzalez, F. J., Miners, J. O. &Veronese, M. E. (1994). In vitro proguanil activation to cycloguanil by human

liver microsomes is mediated by CYP3A isoforms as well as by S-mephenytoin hydroxylase. *British Journal of Clinical Pharmacology* 37(5): 413-420.

25. Brown, H. D., Matzuk, A. R., Ilves, I. R. K., Peterson, L. H., Harris, S. A., Sarett, L. H., Egerton, J. R., Yakstis, J. J., Campbell, W. C. &Cuckler, A. C. (1961). Antiparasitic drugs. IV. 2-(4´-thiazolyl)benzimidazole, a new anthelminthic. *Journal of American Chemical Society.* 83: 1764.

26. Bruce-Chwatt, L. J. (1987). Quinine and the mystery of blackwater fever. *Acta Leiden* 55: 181-196.

27. Bu, H.-Z., Knuth, K., Magis, L. &Teitelbaum, P. (2000). High-throughput cytochrome P450 inhibition screening via cassette probe-dosing strategy. IV. Validation of a direct injection on-line guard cartridge extraction/tandem mass spectrometry method for simultaneous CYP3A4, 2D6 and 2E1 inhibition assessment. *Rapid Communications in Mass Spectrometry* 14(20): 1943-1948.

28. Burri, C. &Brun, R. (2003). Eflornithine for the treatment of human African trypanosomiasis. *Parasitology Research* 90(0): S49-S52.

29. Burton, P. S., Goodwin, J. T., Vidmar, T. J. &Amore, B. M. (2002). Predicting Drug Absorption: How Nature Made It a Difficult Problem. *Journal of Pharmacology and Experimental Therapeutics* 303(3): 889-895.

30. Caffrey, C. R. (2007). Chemotherapy of schistosomiasis: present and future. *Current Opinion in Chemical Biology* 11(4): 433-439.

31. Chan, H. O. &Stewart, B. H. (1996). Physicochemical and drug-delivery considerations for oral drug bioavailability. *Drug Discovery Today* 1(11): 461-473.

32. Chaudhary, A. &Willett, K. L. (2006). Inhibition of human cytochrome CYP1 enzymes by flavonoids of St. John's wort. *Toxicology* 217(2-3): 194-205.

33. Chavez, M. L., Jordan, M. A. &Chavez, P. I. (2006).Evidence-based drug-herbal interactions.*Life Science* 78: 2146-2157.

34. Clark, D. E. (1999). Rapid calculation of polar molecular surface area and its application to the prediction of transport phenomena. 1. Prediction of intestinal absorption. *Journal of Pharmaceutical Sciences* 88(8): 807-814.

35. Cleveland Jr, J. A., Benko, M. H., Gluck, S. J. &Walbroehl, Y. M. (1993). Automated pKa determination at low solute concentrations by capillary electrophoresis. *Journal of Chromatography A* 652(2): 301-308.

36. Coslédan, F., Fraisse, L., Pellet, A., Guillou, F., Mordmüller, B., Kremsner, P. G., Moreno, A., Mazier, D., Maffrand, J.-P. &Meunier, B. (2008). Selection of a trioxaquine as an antimalarial drug candidate. *Proceedings of the National Academy of Sciences* 105(45): 17579-17584.

37. Coulet, M., Eeckhoutte, C., Larrieu, G., Sutra, J.-F., Alvinerie, M., Mace, K., Pfeifer, A., Zucco, F., Laura Stammati, A., De Angelis, I., Vignoli, A. L. &Galtier, P. (2000). Evidence for cytochrome P4501A2-mediated protein covalent binding of thiabendazole and for its passive intestinal transport: use

of human and rabbit derived cells. *Chemico-Biological Interactions* 127(2): 109.

38. Coulet, M., Eeckhoutte, C., Larrieu, G., Sutra, J.-F., Hoogenboom, L. A. P., Huveneers-Oorsprong, M. B. M., Kuiper, H. A., Castell, J. V., Alvinerie, M. &Galtier, P. (1998). Comparative Metabolism of Thiabendazole in Cultured Hepatocytes from Rats, Rabbits, Calves, Pigs, and Sheep, Including the Formation of Protein-Bound Residues. *Journal of Agriculture and Food Chem.* 46(2): 742-748.

39. Crespi, C. L., Gonzalez, F. J., Steimel, D. T., Turner, T. R., Gelboin, H. V., Penman, B. W. &Langenbach, R. (1991). A metabolically competent human cell line expressing five cDNAs encoding procarcinogen-activating enzymes: application to mutagenicity testing. *Chemical Reseasrch in Toxicology* 4(5): 566-572.

40. Crespi, C. L., Miller, V. P. &Penman, W. (1997). Assays for cytochrome P450 inhibition. *Analytical Biochemistry* 248: 188-190.

41. Crivori, P., Cruciani, G., Carrupt, P.-A. &Testa, B. (2000). Predicting Blood-Brain Barrier Permeation from Three-Dimensional Molecular Structure. *Journal of Medicinal Chemistry* 43(11): 2204-2216.

42. Crivori, P., Zamora, I., Speed, B., Orrenius, C. &Poggesi, I. (2004). Model based on GRID-derived descriptors for estimating CYP3A4 enzyme stability of potential drug candidates. *Journal of Computer-Aided Molecular Design* 18(3): 155-166.

43. Croft, S. L., Barrett, M. P. &Urbina, J. A. (2005). Chemotherapy of trypanosomiases and leishmaniasis. *Trends in Parasitology* 21(11): 508-512.

44. Cruciani, G., Carosati, E., De Boeck, B., Ethirajulu, K., Mackie, C., Howe, T. &Vianello, R. (2005). MetaSite: Understanding Metabolism in Human Cytochromes from the Perspective of the Chemist. *Journal of Medicinal Chemistry* 48: 6970-6979.

45. Cruciani, G., Pastor, M. &Guba, W. (2000). VolSurf: a new tool for the pharmacokinetic optimization of lead compounds. *European Journal of Pharmaceutical Sciences* 11(Supplement 2): S29.

46. Dalvie, D., Smith, E., Deese, A. &Bowlin, S. (2006). In vitro metabolic activation of thiabendazole via 5-hydroxythiabendazole : Identification of a glutathione conjugate of 5-hydroxythiabendazole. *Drug Metabolism and Disposition* 34(4): 709-717.

47. Daniels, N., Hunnisett, A. &Morris, P. (1984). Interaction between cyclosporin and rifampicin. *Lancet* II: 639.

48. Davis, T. M. E., Hung, T.-Y., Sim, I.-K., Karunajeewa, H. A. &Ilett, K. F. (2005). Piperaquine: A Resurgent Antimalarial Drug. *Drugs* 65(1): 75-87.

49. de Aquino Ribeiro, J. A., de Campos, L. M. M., Alves, R. J., Lages, G. P. &Pianetti, G. A. (2007). Efavirenz related compounds preparation by hydrolysis procedure: Setting reference standards for chromatographic purity analysis. *Journal of Pharmaceutical and Biomedical Analysis* 43(1): 298-303.

50. De, D., Krogstad, F. M., Cogswell, F. B. &Krogstad, D. J. (1996). Aminoquinolines That Circumvent Resistance in Plasmodium falciparum in Vitro. *The American Journal of Tropical Medicine and Hygiene* 55(6): 579-583.

51. De Graaf , C., Vermeulen, P. E. &Feenstra, A. K. (2005). Cytochrome P450 in Silico: An Intergrated modelling Approach. *Journal of Medicinal Chemistry* 48(8): 2725-2755.

52. Dechy-Cabaret, O., Benoit-Vical, F., Loup, C., Robert, A., Gornitzka, H., Bonhoure, A., Vial, H., Magnaval, J.-F., Séguéla, J.-P. &Meunier, B. (2004). Synthesis and Antimalarial Activity of Trioxaquine Derivatives. *Chemistry – A European Journal* 10(7): 1625-1636.

53. DeLano, W. L. (2002). The PyMOL molecular graphics system. http://www.pymol.org.

54. Delespaux, V. &de Koning, H. P. (2007). Drugs and drug resistance in African trypanosomiasis. *Drug Resistance Updates* 10(1-2): 30-50.

55. Dierks, E. A., Stams, K. R., Lim, H.-K., Cornelius, G., Zhang, H. &Ball, S. E. (2001). A Method for the Simultaneous Evaluation of the Activities of Seven Major Human Drug-Metabolizing Cytochrome P450s Using an in Vitro Cocktail of Probe Substrates and Fast Gradient Liquid Chromatography Tandem Mass Spectrometry. *Drug Metabolism and Disposition.* 29(1): 23-29.

56. Donahue, S. R., Flockhart, D. A., Abernethy, D. R. &Ko, J.-W. (1997). Ticlopidine inhibition of phenytoin metabolism mediated by potent inhibition of CYP2C19[ast]. *Clinical Pharmacology and Therapeutics* 62(5): 572-577.

57. Dondorp, A. M., Fairhurst, R. M., Slutsker, L., MacArthur, J. R., M.D., J. G. B., Guerin, P. J., Wellems, T. E., Ringwald, P., Newman, R. D. &Plowe, C. V. (2011). The Threat of Artemisinin-Resistant Malaria. *New England Journal of Medicine* 365(12): 1073-1075.

58. Dondorp, A. M., Nosten, F. o., Yi, P., Das, D., Phyo, A. P., Tarning, J., Lwin, K. M., Ariey, F., Hanpithakpong, W., Lee, S. J., Ringwald, P., Silamut, K., Imwong, M., Chotivanich, K., Lim, P., Herdman, T., An, S. S., Yeung, S., Singhasivanon, P., Day, N. P. J., Lindegardh, N., Socheat, D. &White, N. J. (2009). Artemisinin Resistance in Plasmodium falciparum Malaria. *New England Journal of Medicine* 361(5): 455-467.

59. Dong, H., Haining, R. L., Thummel, K. E., Rettie, A. E. &Nelson, S. D. (2000). Involvement of Human Cytochrome P450 2D6 in the Bioactivation of Acetaminophen. *Drug Metabolism and Disposition* 28(12): 1397-1400.

60. Evans, W. E. &Relling, M. V. (1999). Pharmacogenomics: Translating Functional Genomics into Rational Therapeutics. *Science* 286(5439): 487-491.

61. Fairlamb, A. H. (2003). Chemotherapy of human African trypanosomiasis: current and future prospects. *Trends in Parasitology* 19(11): 488-494.

62. Feng, M. R. (2002). Assessment of Blood-Brain Barrier Penetration: In Silico, In Vitro and In Vivo. *Current Drug Metabolism* 3(6): 647-657.

63. Feng, T.-S., Guantai, E. M., Nell, M., van Rensburg, C. E. J., Ncokazi, K., Egan, T. J., Hoppe, H. C. &Chibale, K. (2011). Effects of highly active novel artemisinin-chloroquinoline hybrid compounds on β-hematin formation, parasite morphology and endocytosis in Plasmodium falciparum. *Biochemical Pharmacology* 82(3): 236-247.

64. Fenwick, A., Savioli, L., Engels, D., Robert Bergquist, N. &Todd, M. H. (2003). Drugs for the control of parasitic diseases: current status and development in schistosomiasis. *Trends in Parasitology* 19(11): 509-515.

65. Fidock, D. A., Nomura, T., Talley, A. K., Cooper, R. A., Dzekunov, S. M., Ferdig, M. T., Ursos, L. M. B., Sidhu, A. b. S., Naude´, B., Deitsch, K. W., Su, X.-z., Wootton, J. C., Roepe, P. D. &Wellems, T. E. (2000). Mutations in the P. falciparum Digestive Vacuole Transmembrane Protein PfCRT and Evidence for Their Role in Chloroquine Resistance. *Molecular Cell* 6(4): 861-871.

66. Fidock, D. A., Rosenthal, P. J., Croft, S. L., Brun, R. &Nwaka, S. (2004). Antimalarial drug discovery: efficacy models for compound screening. *Nature Reviews in Drug Discovery* 3(6): 509-520.

67. Fitch, C. D. (1969). Chloroquine resistance in malaria: A deficence of chloroquine binding *Proceedings of the National Academy of Sciences* 64(4): 1181-1187.

68. Fontana , E., Dansette , P. M. &Poli , S. M. (2005). Cytochrome P450 Enzymes Mechanism Based Inhibitors: Common Sub-Structures and Reactivity. *Current Drug Metabolism* 6: 413-454.

69. Fugh-Berman, A. &Ernst, E. (2001). Herb–drug interactions: Review and assessment of report reliability. *British Journal of Clinical Pharmacology* 52(5): 587-595.

70. Fuhr, U. (1998). Drug Interactions with Grapefruit Juice: Extent, Probable Mechanism and Clinical Relevance. *Drug Safety* 18(4): 251-272.

71. Fujitani, T., Yoneyama, M., Ogata, A., Ueta, T., Mori, K. &Ichikawa, H. (1991). New metabolites of thiabendazole and the metabolism of thiabendazole by mouse embryo in vivo and in vitro. *Food and Chemical Toxicology* 29(4): 265.

72. Furuta, S., Kamada, E., Suzuki, T., Sugimoto, T., Kawabata, Y., Shinozaki, Y. &Sano, H. (2001). Inhibition of drug metabolism in human liver microsomes by nizatidine, cimetidine and omeprazole. *Xenobiotica* 31(1): 1.

73. Gelfand M, M. S. D. R. B. N. B. (1985). *The Traditional Medical Practitioner in Zimbabwe.* Gweru: Mambo Press.

74. Ghosal, A., Hapangama, N., Yuan, Y., Lu, X., Horne, D., Patrick, J. E. &Zbaida, S. (2003). Rapid determination of enzyme activities of recombinant human cytochromes P450, human liver microsomes and hepatocytes. *Biopharmaceutics & Drug Disposition* 24(9): 375-384.

75. Gibaldi, M. &Perrier, D. (1975). *Pharmacokinetics.* New York: Marcel and Dekker.

76. Groten, J. P., Butler, W., Feron, V. J., Kozianowski, G., Renwick, A. G. &Walker, R. (2000). An Analysis of the Possibility for Health Implications of Joint Actions and Interactions between Food Additives. *Regulatory Toxicology and Pharmacology* 31(1): 77.

77. Guengerich, F. P. (1995). *Cytochrome P450: Structure, Mechanism, and Biochemistry.* New York: Plenum Press.

78. Guo, Z., Raeissi, S., White, R. B. &Stevens, J. C. (1997). Orphenadrine and Methimazole Inhibit Multiple Cytochrome P450 Enzymes in Human Liver Microsomes. *Drug Metabolism and Disposition* 25(3): 390-393.

79. Hann, M. M. &Oprea, T. I. (2004). Pursuing the leadlikeness concept in pharmaceutical research. *Current Opinion in Chemical Biology* 8(3): 255-263.

80. Hayeshi, R., Masimirembwa, C., Mukanganyama, S. &Ungell, A.-L. B. (2006). The potential inhibitory effect of antiparasitic drugs and natural products on P-glycoprotein mediated efflux. *European Journal of Pharmaceutical Sciences* 29: 70-81.

81. Hennekeuser, H. H., Pabst, K., Poeplau, W. &Gerok, W. (1969). Thiabendazole for the treatment of trichinosis in humans. *Texas Reports on Biology and Medicine* 27 (Suppl. 2): 581-596.

82. Hoet, S., Opperdoes, F., Brun, R. &Quetin-Leclercq, J. (2004). Natural products active against African trypanosomes: a step towards new drugs. *Natural Product Reports* 21(3): 353-364.

83. Hostettmann, K., Marston, A., Ndjoko, K. &Wolfender, J. L. (2000). The Potential of African Plants as a Source of Drugs. *Current Organic Chemistry* 4: 973-1010.

84. Houston, B. J. &Carlile, D. J. (1997). Prediction of Hepatic Clearance from Microsomes, Hepatocytes, and Liver Slices. *Drug Metabolism Reviews* 29(4): 891-922.

85. http://dndi.org/portfolio/asaq.html.

86. Hyde, J. E. (2005). Drug-resistant malaria. *Trends in Parasitology* 21(11): 494-498.

87. Irvine, J. D., Takahashi, L., Lockhart, K., Cheong, J., Tolan, J. W., Selick, H. E. &Grove, J. R. (1999). MDCK (Madin–Darby canine kidney) cells: A tool for membrane permeability screening. *Journal of pharmaceutical Sciences* 88(1): 28-33.

88. Izzo, A. A. (2005). Herb and drug interactions: an overview of the clinical evidence. *Fundamental & Clinical Pharmacology* 19(1): 1-16.

89. Izzo, A. A. &Ernst, E. (2009). Interactions Between Herbal Medicines and Prescribed Drugs: An Updated Systematic Review. *Drugs* 69(13): 1777-1798.

90. Kansy, M., Senner, F. &Gubernator, K. (1998). Physicochemical High Throughput Screening:‚Äâ Parallel Artificial Membrane Permeation Assay in

the Description of Passive Absorption Processes. *Journal of Medicinal Chemistry* 41(7): 1007-1010.

91. Karjalainen, M. J., Neuvonen, P. J. &Backman, J. T. (2006). Rofecoxib Is a Potent, Metabolism-Dependent Inhibitor of CYP1A2: Implications for in Vitro Prediction of Drug Interactions. *Drug Metabolism and Disposition* 34(12): 2091-2096.

92. Kelly, J. X., Smilkstein, M. J., Cooper, R. A., Lane, K. D., Johnson, R. A., Janowsky, A., Dodean, R. A., Hinrichs, D. J., Winter, R. &Riscoe, M. (2007). Design, Synthesis, and Evaluation of 10-N-Substituted Acridones as Novel Chemosensitizers in Plasmodium falciparum. *Antimicrobial Agents and Chemotherapy* 51(11): 4133-4140.

93. Kerns, E. H. &Di, L. (2008a).Chapter 7 - Solubility. In *Drug-like Properties: Concepts, Structure Design and Methods*, 56-85 San Diego: Academic Press.

94. Kerns, E. H. &Di, L. (2008b). *Drug Like Properties: Concepts, Structure Design Methods From ADME To Toxicity Optimization.* London: Elsevier Academic Press.

95. Kerns, E. H. &Li, D. (2008). *Drug-like Properties: Concepts, Structure Design and Methods.* San Diego: Academic Press.

96. Kiani, J. &Imam, S. (2007). Medicinal importance of grapefruit juice and its interaction with various drugs. *Nutrition Journal* 6(1): 33-33.

97. Kola, I. &Landis, J. (2004). Can the pharmaceutical industry reduce attrition rates? *Nature Reviews in Drug Discovery* 3(8): 711-716.

98. Krishna, S. &White, N. J. (1996). Pharmacokinetics of Quinine, Chloroquine and Amodiaquine: Clinical Implications. *Clinical Pharmacokinetics* 30(4): 263-299.

99. Kutt, H. (1975). Interactions of Antiepileptic Drugs. *Epilepsia* 16(2): 393-402.

100. Laine, J. E., Auriola, S., Pasanen, M. &Juvonen, R. O. (2009). Acetaminophen bioactivation by human cytochrome P450 enzymes and animal microsomes. *Xenobiotica* 39(1): 11-21.

101. Langhorne, J., Buffet, P., Galinski, M., Good, M., Harty, J., Leroy, D., Mota, M., Pasini, E., Renia, L., Riley, E., Stins, M. &Duffy, P. (2011). The relevance of non-human primate and rodent malaria models for humans. *Malaria Journal* 10(1): 23.

102. Larrey, D., Castot, A., Pessayre, D., Merigot, P., Machayekhy, J.-P., Feldmann, G., Lenoir, A., Rueff, B. &Benhamou, J.-P. (1986). Amodiaquine-Induced Hepatitis. *Annals of Internal Medicine* 104(6): 801-803.

103. Laufer, M. K., Takala-Harrison, S., Dzinjalamala, F. K., Stine, O. C., Taylor, T. E. &Plowe, C. V. (2010). Return of Chloroquine-Susceptible Falciparum Malaria in Malawi Was a Reexpansion of Diverse Susceptible Parasites. *Journal of Infectious Diseases* 202(5): 801-808.

104. Lin , J. H. &Lu, A. Y. H. (1998). Inhibition and Induction of Cytochrome P450 and the clinical Implications. *Clinical Pharmacokinetics* 35(5): 361-390.

105. Lipinski, C. A., Lombardo, F., Dominy, B. W. &Feeney, P. J. (2001). Experimental and computational approaches to estimate solubility and permeability in drug discovery and development settings. *Advanced Drug Delivery Reviews* 46(1-3): 3-26.

106. Lombardino, J. G. &Lowe, J. A. (2004). The role of the medicinal chemist in drug discovery - then and now. *Nature Reviews in Drug Discovery* 3(10): 853-862.

107. Lu, A. H., Shu, Y., Huang, S. L., Wang, W. R., Ou-Yang, D. S. &Zhou, H. H. (2000). In vitro proguanil activation to cycloguanil is mediated by CYP2C19 and CYP3A4in adult Chinese liver microsomes. *Acta Pharmacology Sinica* 21(8): 747-752.

108. Madabushi, R., Frank, B., Drewelow, B., Derendorf, H. &Butterweck, V. (2006). Hyperforin in St. John‚Äôs wort drug interactions. *European Journal of Clinical Pharmacology* 62(3): 225-233.

109. Makler, M. T. &Hinrichs, D. J. (1993). Measurement of the Lactate Dehydrogenase Activity of Plasmodium falciparum as an Assessment of Parasitemia. *The American Journal of Tropical Medicine and Hygiene* 48(2): 205-210.

110. Makler, M. T., Ries, J. M., Williams, J. A., Bancroft, J. E., Piper, R. C., Gibbins, B. L. &Hinrichs, D. J. (1993). Parasite Lactate Dehydrogenase as an Assay for Plasmodium falciparum Drug Sensitivity. *The American Journal of Tropical Medicine and Hygiene* 48(6): 739-741.

111. Masimirembwa, C., Bredberg, U. &Andersson, T. (2003). Metabolic stability for drug discovery and development: pharmacokinetic and biochemical challenges. *Clinical Pharmacokinetics* 42: 515–528.

112. Masimirembwa, C., Thompson, R. &Andersson, T. (2001). In vitro high throughput screening of compounds for favourable metabolic properties in drug discovery. *Combinatorial Chemistry and High Throughput Screening* 4: 245–263.

113. Masimirembwa, C. M. &Hasler, J. A. (1994). Characterisation of praziquantel metabolism by rat liver microsomes using cytochrome P450 inhibitors. *Biochemical Pharmacology* 48(9): 1779-1783.

114. Masimirembwa, C. M., Hasler, J. A. &Johansson, I. (1995). Inhibitory effects of antiparasitic drugs on cytochrome P450 2D6. *European Journal of Clinical Pharmacology* 48(35-38).

115. Masimirembwa, C. M., Otter, C., Berg, M., Jönsson, M., Leidvik, B., Jonsson, E., Johansson, T., Bäckman, A., Edlund, A. &Andersson, T. B. (1999). Heterologous Expression and Kinetic Characterization of Human Cytochromes P-450: Validation of a Pharmaceutical Tool for Drug Metabolism Research. *Drug Metabolism and Disposition* 27(10): 1117-1122.

116. Mathews, J. M., Etheridge, A. S. &Black, S. R. (2002). Inhibition of human cytochrome P450 activities by kava extract and kavalactones. *Drug Metabolism and Disposition* 30(22): 1153–1115.

117. Meier, H. &Blaschke, G. (2001). Investigation of Praziquantel metabolism in isolated rat hepatocytes. *Journal of Pharmaceutical and Biomedical Analysis* 26(3): 409-415.

118. Merck (1999). Parasitic infections. In: Beers MH, Berkow R, eds. In *The Merck Manual of Diagnosis and Therapy*, Vol. 17th ed., 1237-1275: Rhahway, NJ: Merk Research Laboratories.

119. Mizutani, T., Yoshida, K. &Kawazoe, S. (1994). Formation of toxic metabolites from thiabendazole and other thiazoles in mice: Identification of Thioamides as Ring Cleavage Products. *Drug Metabolism and Disposition* 55(2): 750-755.

120. Moddry, D. L., Stinson, E. B., Dyer, P. E., Jamielson, S. W., Baldwin, J. C. &Shumway, N. E. (1985). Acute Rejection and Massive Cyclosporine Requirements in Heart Transplant Recipients Treated With Rifampin. *Transplantation* 39(3): 313-314.

121. Monks, T., Caldwell, J. &Smith, R. (1979). Influence of methylxanthine-containing foods on theophylline metabolism and kinetics. *Clinical Pharmacology Ther* 26: 513–524.

122. Moody, G. C., Griffin, S. J., Mather, A. N., McGinnity, D. F. &Riley, R. J. (1999). Fully automated analysis of activities catalysed by the major human liver cytochrome P450 (CYP) enzymes: assessment of human CYP inhibition potential. *Xenobiotica* 29(1): 53-75.

123. Moore, L. B., Goodwin, B., Jones, S. A., Wisely, G. B., Serabjit-Singh, C. J., Willson, T. M., Collins, J. L. &Kliewer, S. A. (2000). St. John's wort induces hepatic drug metabolism through activation of the pregnane X receptor. *Proceedings of the National Academy of Sciences of the United States of America* 97(13): 7500-7502.

124. Na-Bangchang, K., Doua, F., Konsil, J., Hanpitakpong, W., Kamanikom, B. &Kuzoe, F. (2004). The pharmacokinetics of eflornithine (a-difluoromethylornithine) in patients with late-stage T.b. gambiense sleeping sickness. *European Journal of Clinical Pharmacology* 60(4): 269-278.

125. Naritomi, Y., Teramura, Y., Terashita, S. &Kagayama, A. (2004). Utility of Microtiter Plate Assays for Human Cytochrome P450 Inhibition Studies in Drug Discovery: Application of Simple Method for Detecting Quasi-irreversible and Irreversible Inhibitors. *Drug Metabolism and Pharmacokinetics* 19(1): 55-61.

126. Navarro, M., Pe´rez, H. &Sa´nchez-Delgado, R. A. (1997). Toward a Novel Metal-Based Chemotherapy against Tropical Diseases. 3. Synthesis and Antimalarial Activity in Vitro and in Vivo of the New Gold-Chloroquine Complex [Au(PPh3)(CQ)]PF6. *Journal of Medicinal Chemistry* 40(12): 1937-1939.

127. Ncokazi, K. K. &Egan, T. J. (2005). A Colorimetric High-Throughput Beta-Hematin Inhibition Screening Assay For Use In The Search For Antimalarial Compounds. *Annals of Biochemistry* 338(2): 306-306.

128. Noedl, H., Se, Y., Schaecher, K., Smith, B. L., Socheat, D. &Fukuda, M. M. (2008). Evidence of Artemisinin-Resistant Malaria in Western Cambodia. *New England Journal of Medicine* 359(24): 2619-2620.

129. Nok, A. J. (2003). Arsenicals (melarsoprol), pentamidine and suramin in the treatment of human African trypanosomiasis. *Parasitology Research* 90(1): 71-79.

130. Nzila, A., Ma, Z. &Chibale, K. (2011). Drug repositioning in the treatment of malaria and TB. *Future Medicinal Chemistry* 3(11): 1413-1426.

131. O'Neill, P. M., Mukhtar, A., Stocks, P. A., Randle, L. E., Hindley, S., Ward, S. A., Storr, R. C., Bickley, J. F., O'Neil, I. A., Maggs, J. L., Hughes, R. H., Winstanley, P. A., Bray, P. G. &Park, B. K. (2003). Isoquine and Related Amodiaquine Analogues: A New Generation of Improved 4-Aminoquinoline Antimalarials. *Journal of Medicinal Chemistry* 46(23): 4933-4945.

132. O'Neill, P. M., Park, B. K., Shone, A. E., Maggs, J. L., Roberts, P., Stocks, P. A., Biagini, G. A., Bray, P. G., Gibbons, P., Berry, N., Winstanley, P. A., Mukhtar, A., Bonar-Law, R., Hindley, S., Bambal, R. B., Davis, C. B., Bates, M., Hart, T. K., Gresham, S. L., Lawrence, R. M., Brigandi, R. A., Gomez-delas-Heras, F. M., Gargallo, D. V. &Ward, S. A. (2009). Candidate Selection and Preclinical Evaluation of N-tert-Butyl Isoquine (GSK369796), An Affordable and Effective 4-Aminoquinoline Antimalarial for the 21st Century. *Journal of Medicinal Chemistry* 52(5): 1408-1415.

133. O'Neill, P. M., Stocks, P. A., Pugh, M. D., Araujo, N. C., Korshin, E. E., Bickley, J. F., Ward, S. A., Bray, P. G., Pasini, E., Davies, J., Verissimo, E. &Bachi, M. D. (2004). Design and Synthesis of Endoperoxide Antimalarial Prodrug Models. *Angewandte Chemie* 116(32): 4289-4293.

134. O'Neill, P. M., Shone, A. E., Stanford, D., Nixon, G., Asadollahy, E., Park, B. K., Maggs, J. L., Roberts, P., Stocks, P. A., Biagini, G., Bray, P. G., Davies, J., Berry, N., Hall, C., Rimmer, K., Winstanley, P. A., Hindley, S., Bambal, R. B., Davis, C. B., Bates, M., Gresham, S. L., Brigandi, R. A., Gomez-de-las-Heras, F. M., Gargallo, D. V., Parapini, S., Vivas, L., Lander, H., Taramelli, D. &Ward, S. A. (2009). Synthesis, Antimalarial Activity, and Preclinical Pharmacology of a Novel Series of 4'-Fluoro and 4'-Chloro Analogues of Amodiaquine. Identification of a Suitable "Back-Up" Compound for N-tert-Butyl Isoquine. *Journal of Medicinal Chemistry* 52(7): 1828-1844.

135. Obach, R. S. (1999). Prediction of Human Clearance of Twenty-Nine Drugs from Hepatic Microsomal Intrinsic Clearance Data: An Examination of In Vitro Half-Life Approach and Nonspecific Binding to Microsomes. *Drug Metabolism and Disposition* 27(11): 1350-1359.

136. Obach, R. S. (2000). Inhibition of Human Cytochrome P450 Enzymes by Constituents of St. John's Wort, an Herbal Preparation Used in the Treatment of Depression. *Journal of Pharmacology and Experimental Therapeutics* 294(1): 88-95.

137. Oprea, T. (2002a). Current trends in lead discovery: Are we looking for the appropriate properties? *Journal of Computer-Aided Molecular Design* 16(5): 325-334.

138. Oprea, T. I. (2002b). Chemical space navigation in lead discovery. *Current Opinion in Chemical Biology* 6(3): 384-389.

139. Oprea, T. I., Davis, A. M., Teague, S. J. &Leeson, P. D. (2001). Is There a Difference between Leads and Drugs? A Historical Perspective. *Journal of Chemical Information and Computer Sciences* 41(5): 1308-1315.

140. Opsenica, I., Opsenica, D., Jadranin, M., Smith, K., Milhous, W. K., Stratakis, M. &Šolaja, B. (2007). On peroxide antimalarials. *Journal of the Serbian Chemical Society* 72(12): 1181-1190.

141. Opsenica, I., Opsenica, D., Lanteri, C. A., Anova, L., Milhous, W. K., Smith, K. S. &SÃåolaja, B. A. (2008). New Chimeric Antimalarials with 4-Aminoquinoline Moiety Linked to a Tetraoxane Skeleton(1). *Journal of Medicinal Chemistry* 51(19): 6216-6219.

142. Pajouhesh, H. &Lenz, G. (2005). Medicinal chemical properties of successful central nervous system drugs. *Neurotherapeutics* 2(4): 541-553.

143. Palm, K., Stenberg, P., Luthman, K. &Artursson, P. (1997). Polar Molecular Surface Properties Predict the Intestinal Absorption of Drugs in Humans. *Pharmaceutical Research* 14(5): 568-571.

144. Paolo, E. R. D., Hamburger, M., Stoeckli-Evans, H., Rogers, C. &Hostettmann, K. (1989). New Chromonocoumarin (= 6H,7H-[1]Benzopyrano[4,3-b][1]benzopyran-6,7-dione) Derivatives from Polygala fruticosa BERG. *Helvetica Chimica Acta* 72: 1455-1462.

145. Pardridge, W. M. (1995). Transport of small molecules through the blood-brain barrier: biology and methodology. *Advanced Drug Delivery Reviews* 15(1,Äì3): 5-36.

146. Pardridge, W. M. (1998). CNS Drug Design Based on Principles of Blood-Brain Barrier Transport. *Journal of Neurochemistry* 70(5): 1781-1792.

147. Patel, P., Osechinskiy, S., Koehler, J., Zhang, L., Vajjhala, S., Philips, C. &Hobbs, S. (2004). Micro parallel liquid chromatography for high-throughput compound purity analysis and early ADMET profiling. *Journal of the Association for Laboratory Automation* 9(3): 185-191.

148. Paul, S. M., Mytelka, D. S., Dunwiddie, C. T., Persinger, C. C., Munos, B. H., Lindborg, S. R. &Schacht, A. L. (2010). How to improve R&D productivity: the pharmaceutical industry's grand challenge. *Nature Reviews in Drug Discovery* 9(3): 203-214.

149. Pink, R., Hudson, A., Mouries, M.-A. &Bendig, M. (2005). Opportunities and Challenges in Antiparasitic Drug Discovery. *Nature Reviews in Drug Discovery* 4(9): 727-740.

150. Polasek, T. M., Elliot, D. J., Somogyi, A. A., Gillam, E. M. J., Lewis, B. C. &Miners, J. O. (2006). An evaluation of potential mechanism-based inactivation of human drug metabolizing cytochromes P450 by monoamine oxidase inhibitors, including isoniazid. *British Journal of Clinical Pharmacology* 61(5): 570-584.

151. Polasek, T. M. &Miners, J. O. (2007). In vitro approaches to investigate mechanism-based inactivation of CYP enzymes. *Expert Opinion on Drug Metabolism & Toxicology* 3(3): 321-329.

152. Polonio, T. &Efferth, T. (2008). Leishmaniasis: Drug resistance and natural products *International Journal of Molecular Medicine* 22: 277-286.

153. Poole, S. K., Durham, D. &Kibbey, C. (2000). Rapid method for estimating the octanol-water partition coefficient (log Pow) by microemulsion electrokinetic chromatography. *Journal of Chromatography B: Biomedical Sciences and Applications* 745(1): 117-126.

154. Price, R. J., Scott, M. P., Walters, D. G., Stierum, R. H., Groten, J. P., Meredith, C. &Lake, B. G. (2004). Effect of thiabendazole on some rat hepatic xenobiotic metabolising enzymes. *Food and Chemical Toxicology* 42(6): 899-899.

155. Rasoanaivo, P., Wright, C., Willcox, M. &Gilbert, B. (2011). Whole plant extracts versus single compounds for the treatment of malaria: synergy and positive interactions. *Malaria Journal* 10(Suppl 1): S4.

156. Raucy, J., Warfe, L., Yueh, M.-F. &Allen, S. W. (2002). A Cell-Based Reporter Gene Assay for Determining Induction of CYP3A4 in a High-Volume System. *Journal of Pharmacology and Experimental Therapeutics* 303(1): 412-423.

157. Ray, S., Madrid, P.B., Catz, P., LeValley, S.E., Furniss, M.J., Rausch, L.L., Gu, R.K., DeRisi, J.L, Iyer, L.V, Green, C.E., Mirsalis, J.C. (2010). Development of a new generation of 4-aminoquinoline antimalarial compounds using predictive pharmacokinetic and toxicology models. *Journal of Medicnal Chemistry*. 53 (9): 3685-95.Renslo, A. R. &McKerrow, J. H. (2006). Drug discovery and development for neglected parasitic diseases. *Nature Chemistry and Biology* 2(12): 701-710.

158. Riley, R. J., Grime, K. &Weaver, R. (2007). Time-dependent CYP inhibition. *Expert Opinion on Drug Metabolism & Toxicology* 3(1): 51-66.

159. Rottmann, M., McNamara, C., Yeung, B. K. S., Lee, M. C. S., Zou, B., Russell, B., Seitz, P., Plouffe, D. M., Dharia, N. V., Tan, J., Cohen, S. B., Spencer, K. R., González-Páez, G. E., Lakshminarayana, S. B., Goh, A., Suwanarusk, R., Jegla, T., Schmitt, E. K., Beck, H.-P., Brun, R., Nosten, F., Renia, L., Dartois, V., Keller, T. H., Fidock, D. A., Winzeler, E. A. &Diagana, T. T. (2010). Spiroindolones, a Potent Compound Class for the Treatment of Malaria. *Science* 329(5996): 1175-1180.Rouveix, B., Coulombel, L., Aymard, J. P., Chau, F. &Abel, L. (1989). Amodiaquine-induced immune agranulocytosis. *British Journal of Haematology* 71(1): 7-11.

160. Sa´nchez-Delgado, R. A., Navarro, M., Pe´rez, H. &Urbina, J. A. (1996). Toward a Novel Metal-Based Chemotherapy against Tropical Diseases. 2. Synthesis and Antimalarial Activity in Vitro and in Vivo of New Ruthenium- and Rhodium-Chloroquine Complexes. *Journal of Medicinal Chemistry* 39(5): 1095-1099.

161. Sai, Y., Dai, R., Yang, T. J., Krausz, K. W., Gonzalez, F. J., Gelboin, H. V. &Shou, M. (2000). Assessment of specificity of eight chemical inhibitors using cDNA-expressed cytochromes P450. *Xenobiotica* 30(4): 327-343.

162. Sansen, S., Yano, J. K., Reynald, R. L., Schoch, G. A., Griffin, K. J., Stout, C. D. &Johnson, E. F. (2007). Adaptations for the Oxidation of Polycyclic Aromatic Hydrocarbons Exhibited by the Structure of Human P450 1A2. *Journal of Biological Chemistry* 282(19): 14348-14355.

163. Satoh, M. &Kokaze, A. (2004). Treatment strategies in controlling strongyloidiasis. *Expert Opinion on Pharmacotherapy* 5(11): 2293-2301.

164. Saxena, S., Pant, N., Jain, D. C. &Bhakuni, R. S. (2003). Antimalarial agents from plant sources. *Current Science* 85(9): 1314-1329.

165. Schneider, D., Gannon, R., Sweeney, K. &Shore, E. (1990). Theophylline and antiparasitic drug interactions. A case report and study of the influence of thiabendazole and mebendazole on theophylline pharmacokinetics in adults. *Chest* 97(1): 84-87.

166. Sereno, D., Cordeiro da Silva, A., Mathieu-Daude, F. &Ouaissi, A. (2007). Advances and perspectives in Leishmania cell based drug-screening procedures. *Parasitology International* 56(1): 3-7.

167. Shimada, H., Eto, M., Ohtaguro, M., Ohtsubo, M., Mizukami, Y., Ide, T. &Imamura, Y. (2010). Differential mechanisms for the inhibition of human cytochrome P450 1A2 by apigenin and genistein. *Journal of Biochemical and Molecular Toxicology* 24(4): 230-234.

168. Silverman, R. B. (1988). *Mechanism-Based Enzyme Inactivation.* CRC Press: Boca Raton.

169. Simooya, O. O., Sijumbil, G., Lennard, M. S. &Tucker, G. T. (1998). Halofantrine and chloroquine inhibit CYP2D6 activity in healthy Zambians. *British Journal of Clinical Pharmacology* 45(3): 315-317.

170. Sowunmi, A., Falade, C. O., Oduola, A. M. J., Ogundahunsi, O. A. T., Fehintola, F. A., Gbotosho, G. O., Larcier, P. &Salako, L. A. (1998). Cardiac effects of halofantrine in children suffering from acute uncomplicated falciparum malaria. *Transactions of the Royal Society of Tropical Medicine and Hygiene* 92(4): 446-448.

171. Sudsakorn, S., Skell, J., Williams, D. A., O'Shea, T. J. &Liu, H. (2007). Evaluation of 3-O-Methylfluorescein as a Selective Fluorometric Substrate for CYP2C19 in Human Liver Microsomes. *Drug Metabolism and Disposition* 35(6): 841-847.

172. Szeto, S. Y., Joshi, V., Price, P. M. &Holley, J. (1993). Persistence and efficacy of thiabendazole on potatoes for control of silver scurf. *Journal of Agriculture and Food Chemistry* 41: 2156–2159.

173. Tarirai, C., Viljoen, A. M. &Hamman, J. H. (2010). Herb,Äìdrug pharmacokinetic interactions reviewed. *Expert Opinion on Drug Metabolism & Toxicology* 6(12): 1515-1538.

174. Taylor, W. R. J. &White, N. J. (2004). Antimalarial Drug Toxicity: A Review. *Drug Safety* 27(1): 25-61.

175. Teng-Man Chen, L., Hong, S. &Chegnyue Zhu, L. (2002). Evaluation of a Method for High Throughput Solubility Determination using a Multi-wavelength UV Plate Reader. *Combinatorial Chemistry & High Throughput Screening* 5(7): 575.

176. Thompson, T. (2000). Early ADME in support of drug discovery: the role of metabolic stability studies. *Current Drug Metabolism* 1: 215–241.

177. Tocco, D., Rosenblum, C., Martin, C. &Robinson, H. (1966a). Absorption, metabolism and excretion of thiabendazole in man and laboratory animals. . *Toxicology and Applied Pharmacology* 9: 31–39.

178. Tocco, D. J., Rosenblum, C., Martin, C. M. &Robinson, H. J. (1966b). Absorption, metabolism and excretion of thiabendazole in man and laboratory animals. *Toxicology andApplied Pharmacology* 9: 31–39.

179. Trager, W. &Jensen, J. (1976). Human malaria parasites in continuous culture. *Science* 193(4254): 673-675.

180. Trott, O. &Olson, A. J. (2010). AutoDock Vina: Improving the speed and accuracy of docking with a new scoring function, efficient optimization, and multithreading. *Journal of Computational Chemistry* 31(2): 455-461.

181. van de Waterbeemd, H., Camenisch, G., Folkers, G., Chretien, J. R. &Raevsky, O. A. (1998). Estimation of Blood-Brain Barrier Crossing of Drugs Using Molecular Size and Shape, and H-Bonding Descriptors. *Journal of Drug Targeting* 6(2): 151-165.

182. Van Laethem, Y. &Lopes, C. (1996). Treatment of Onchocerciasis. *Drugs* 52(6): 861-869.

183. van Schalkwyk, D. A. &Egan, T. J. (2006). Quinoline-resistance reversing agents for the malaria parasite Plasmodium falciparum. *Drug Resistance Updates* 9(4,Äì5): 211-226.

184. Varma, M. V. S., Obach, R. S., Rotter, C., Miller, H. R., Chang, G., Steyn, S. J., El-Kattan, A. &Troutman, M. D. (2010). Physicochemical Space for Optimum Oral Bioavailability: Contribution of Human Intestinal Absorption and First-Pass Elimination. *Journal of Medicinal Chemistry* 53(3): 1098-1108.

185. Veber, D. F., Johnson, S. R., Cheng, H.-Y., Smith, B. R., Ward, K. W. &Kopple, K. D. (2002). Molecular Properties That Influence the Oral Bioavailability of Drug Candidates. *Journal of Medicinal Chemistry* 45(12): 2615-2623.

186. Venkatakrishnan , K., L., v. M. L., Obach, R. S. &Greenblatt , D. J. (2003). Drug Metabolism and Drug Interactions: Application and Clinical Value of In Vitro Models. *Current Drug Metabolism* 4: 423-459.

187. Vennerstrom, J. L., Arbe-Barnes, S., Brun, R., Charman, S. A., Chiu, F. C. K., Chollet, J., Dong, Y., Dorn, A., Hunziker, D., Matile, H., McIntosh, K., Padmanilayam, M., Santo Tomas, J., Scheurer, C., Scorneaux, B., Tang, Y., Urwyler, H., Wittlin, S. &Charman, W. N. (2004). Identification of an antimalarial synthetic trioxolane drug development candidate. *Nature* 430(7002): 900-904.

188. Walsh, J. J. &Bell, A. (2009). Hybrid Drugs for Malaria. *Current Pharmaceutical Design* 15(25): 2970-2985.

189. Walton, K., Walker, R., van de Sandt, J. J. M., Castell, J. V., Knapp, A. G. A. A., Kozianowski, G., Roberfroid, M. &Schilter, B. (1999). The application of in vitro data in the derivation of the Acceptable Daily Intake of food additives. *Food and Chemical Toxicology* 37(12): 1175.

190. Waterman, M. R. (1994). Heterologous expression of mammalian P450 enzymes. *Advances in Enzymology and Related Areas Molecular Biology.* 68: 37-66.

191. Watkins, B. M. (2003). Drugs for the control of parasitic diseases: current status and development. *Trends in Parasitology* 19(11): 477-478.

192. Watt Jm, B.-B. M. G. (1962). *The Medicinal and Poisonous Plants of Southern and Eastern Africa.*

193. Weaver, R., Graham, K. S., Beattie, I. G. &Riley, R. J. (2003). Cytochrome P450 inhibition using recombinant proteins and mass spectrometry/multipe reaction monitoring technology in a cassette incubation. *Drug Metabolism and Disposition* 31(7): 955-966.

194. Weisman, J. L., Liou, A. P., Shelat, A. A., Cohen, F. E., Kiplin Guy, R. &DeRisi, J. L. (2006). Searching for New Antimalarial Therapeutics amongst Known Drugs. *Chemical Biology & Drug Design* 67(6): 409-416.

195. Wilson, Z., Rostami-Hodjegan, A., Burn, J., Tooley, A., Boyle, J., Ellis, S. &Tucker, G. (2003). Inter-individual variability in levels of human microsomal protein and hepatocellularity per gram of liver.*British Journal of Clinical Pharmacology* 56: 433–440.

196. World Health Organisation (2004). *The global burden of disease: 2004 update.* Geneva, Switzerland: http://www.who.int/healthinfo/global_burden_disease/2004_report_update/en/index.html.

197. World Health Organisation (2006). Human African trypanosomiasis (sleeping sickness): epidemiological update. *Weekly Epidemiological Record* (81): 69–80.

198. World Health Organisation (2010a). *Guidelines for the treatment of malaria* Geneva, Switzerland: http://whqlibdoc.who.int/publications/2010/9789241547925_eng.pdf.

199. World Health Organisation (2010b). *Working to overcome the global impact of neglected tropical diseases.* Geneva, Switzerland: http://whqlibdoc.who.int/publications/2010/9789241564090_eng.pdf.

200. World Health Organisation (2011). *World Malaria Report 2011.* Geneva, Switzerland: http://www.who.int/malaria/world_malaria_report_2011/en/.

201. Xie, Y., Jiang, Z.-H., Zhou, H., Cai, X., Wong, Y.-F., Liu, Z.-Q., Bian, Z.-X., Xu, H.-X. &Liu, L. (2007). Combinative method using HPLC quantitative and qualitative analyses for quality consistency assessment of a herbal medicinal preparation. *Journal of Pharmaceutical and Biomedical Analysis* 43(1): 204-212.

202. Yin, H., Racha, J., Li, S.-Y., Olejnik, N., Satoh, H. &Moore, D. (2000). Automated high throughput human CYP isoform activity assay using SPE-LC/MS method: application in CYP inhibition evaluation. *Xenobiotica* 30(2): 141-154.

203. Zeruesenay, D., Soukhova, N. V. &Flockhart, D. A. (2001). Inhibition of Cytochrome P450 (CYP450) Isoforms by Isoniazid: Potent inhibition of CYP2C19 and CYP3A. *Antimicrobial Agents and Chemotherapy* 45(2): 382-392.

204. Zhang, J., Zhou, F., Lu, M., Ji, W., Niu, F., Zha, W., Wu, X., Hao, H. &Wang, G. (2012). Pharmacokinetics-Pharmacology Disconnection of Herbal Medicines and its Potential Solutions with Cellular Pharmacokinetic-Pharmacodynamic Strategy. *Current Drug Metabolism* 13(5): 558-576.

205. Zhou, S., Gao, Y., Jiang, W., Huang, M., Xu, A. &Paxton, J. W. (2003). Interactions of Herbs with Cytochrome P450. *Drug Metabolism Reviews* 35(1): 35-98.

206. Zuber, R., Modrianský, M., Dvořák, Z., Rohovský, P., Ulrichová, J., Simánek, V. &Anzenbacher, P. (2002). Effect of Silybin and its congeners on human liver microsomal cytochrome P450 activities. *Phytotherapy Research* 16(7): 632-638.